TOWARDS THE NON-ERGODIC GROUND MOTION MODELS OF TURKEY: ASSESSMENT OF SYSTEMATIC SITE, SOURCE AND PATH EFFECTS

A THESIS SUBMITTED TO
THE GRADUATE SCHOOL OF NATURAL AND APPLIED SCIENCES
OF
MIDDLE EAST TECHNICAL UNIVERSITY

BY

FATİH MEHMET ÖNDER

IN PARTIAL FULFILLMENT OF THE REQUIREMENTS
FOR
THE DEGREE OF MASTER OF SCIENCE
IN
CIVIL ENGINEERING

AUGUST 2022

Approval of the thesis:

TOWARDS THE NON-ERGODIC GROUND MOTION MODELS OF TURKEY: ASSESSMENT OF SYSTEMATIC SITE, SOURCE AND PATH EFFECTS

submitted by **FATİH MEHMET ÖNDER** in partial fulfillment of the requirements for the degree of **Master of Science** i**n Civil Engineering, Middle East Technical University** by,

Prof. Dr. Halil Kalıpçılar
Dean, Graduate School of **Natural and Applied Sciences** _____

Prof. Dr. Erdem Canbay
Head of the Department, **Civil Engineering** _____

Prof. Dr. Zeynep Gülerce
Supervisor, **Civil Engineering, METU** _____

Assoc. Prof. Dr. A. Arda Özacar
Co-Supervisor, **Geological Engineering, METU** _____

Examining Committee Members:

Prof. Dr. Kemal Önder Çetin
Civil Engineering, METU _____

Prof. Dr. Zeynep Gülerce
Civil Engineering, METU _____

Assoc. Prof. Dr. Onur Pekcan
Civil Engineering, METU _____

Assoc. Prof. Dr. A. Arda Özacar
Geological Engineering, METU _____

Assoc. Prof. Dr. M. Abdullah Sandıkkaya
Civil Engineering, Hacettepe University _____

Date: 26.08.2022

I hereby declare that all information in this document has been obtained and presented in accordance with academic rules and ethical conduct. I also declare that, as required by these rules and conduct, I have fully cited and referenced all material and results that are not original to this work.

Name Last name : Fatih Mehmet Önder

Signature :

ABSTRACT

TOWARDS THE NON-ERGODIC GROUND MOTION MODELS OF TURKEY: ASSESSMENT OF SYSTEMATIC SITE, SOURCE AND PATH EFFECTS

Önder, Fatih Mehmet
Master of Science, Civil Engineering
Supervisor: Prof. Dr. Zeynep Gülerce
Co-Supervisor: Assoc. Prof. Dr. A. Arda Özacar

August 2022, 128 pages

Ground Motion Models (GMMs) and their standard deviations (σ) are the most significant contributors of the median ground motions and their variability that are estimated in Probabilistic Seismic Hazard Analysis (PSHA). Most of the GMMs used in the current practice were derived from the datasets that include recordings from multiple sites attenuating from different seismic sources; therefore, the standard deviation of these GMMs includes the spatial and temporal variability of ground motions based on the ergodic assumption. In the last decade, several attempts were made to decompose the sigma of GMMs into different components such as site-to-site, path-to-path and source-to-source variability in regions with well-established ground motion datasets. The primary objective of this study is to evaluate the systematic site, source and path effects in the Turkish strong motion dataset in order to provide the necessary tools to develop a fully non-ergodic GMM for Turkey. To this end, the updated Turkish Strong Motion Database (N-TSMD, Akbaş et al., 2022) that contains 23019 recordings from 743 earthquakes recorded at 904 stations is utilized. The site terms ($\delta S2S$) and the related standard deviations ($\varphi_{ss,s}$) for the

state-of-the-art NGA-West2 GMMs are calculated for each station in the N-TSMD and ≈15% reduction in total sigma is achieved, which is consistent with the previous studies in literature for other regions. Spatial distribution of calculated site terms are assessed to identify regional differences and underlying reasons such as basin effects and uncertainities in shear wave velocity profile. In addition to the systematic site effects, repeatable source effects mapped into the event terms are also investigated, which may result in a further reduction in total sigma for selected regions. Finally, the site and source corrected within-event terms (δWS_{es}) are examined for systematic path effects on a site-specific basis to observe any remaining bias.

Keywords: Ground motion models, non-ergodic GMMs, Turkey-adjusted GMMs, single station sigma

ÖZ

TÜRKİYE İÇİN ERGODİK OLMAYAN YER HAREKETİ MODELLERİNE DOĞRU: SAHADAN SAHAYA, KAYNAKTAN KAYNAĞA VE ROTADAN ROTAYA SİSTEMATİK DEĞİŞKENLİKLERİN DEĞERLENDİRMESİ

Önder, Fatih Mehmet
Yüksek Lisans, İnşaat Mühendisliği
Tez Yöneticisi: Prof. Dr. Zeynep Gülerce
Ortak Tez Yöneticisi: Doç. Dr. A. Arda Özacar

Ağustos 2022, 128 sayfa

Yer hareketi modelleri ve bu modellere ait standart sapmalar (σ) Olasılıksal Sismik Tehlike Analizinden (OSTA) elde edilen medyan yer hareketleri ve onların değişkenliğine en çok katkı sağlayanlardan bazılarıdır. Güncel uygulamadaki yer hareketi modellerinin çoğu, birden fazla sahaya ait, farklı sismik kaynaklar nedeniyle oluşmuş kayıtları içeren veri tabanlarından türetilmiştir; dolayısıyla bu yer hareketi modellerinin standart sapmaları, ergodik varsayıma istinaden yer hareketlerinin uzamsal ve geçici değişkenliğini içermektedir. Son on yılda, gelişmiş yer hareketi veri setleri kullanılarak yer hareketlerine ait toplam Sigma'yı sahadan sahaya, kaynaktan kaynağa ve rotadan rotaya sistematik değişkenlik gibi farklı bileşenlerine ayırmak için birçok girişimde bulunulmuştur. Bu çalışmanın temel katkısı, Türkiye'ye özel ve tamamen ergodik olmayan yer hareketi modelleri oluşturmak için gerekli araçları sağlamak amacıyla, Türkiye'deki kuvvetli yer hareketi istasyonları için sahadan sahaya, kaynaktan kaynağa ve rotadan rotaya değişkenliğin ölçülmesidir. Bu amaçla, 23019 kayıt, 743 deprem ve 904 istasyon içeren güncellenmiş Türkiye Kuvvetli Yer Hareketi Veritabanı (N-TSMD, Akbaş vd.,

2022) kullanılmıştır. Saha terimleri ($\delta S2S$) ve ilgili standard sapmalar ($\varphi_{ss,s}$) en güncel NGA-West2 yer hareketi modelleri için hesaplanmış olup, sigma'daki yaklaşık %15 azalma, literatürde mevcut olan diğer bölgelere özel çalışmalar ile uyumlu bulunmuştur. Hesaplanan saha terimlerinin uzamsal dağılımı, bölgesel farklılıkları ve bu farklılıkların basen etkileri ve kayma dalgası hızı profilindeki belirsizlikler gibi muhtemel sebeplerini belirlemek için incelenmiştir. Sahadan sahaya sistematik değişkenliğe ek olarak, seçilen bölgelerde toplam Sigma'da daha da azalmaya yol açabilecek olan ve deprem terimleriyle eşleştirilen tekrarlı kaynak etkileri belirlenmiştir. Son olarak, saha ve kaynak düzeltmesi yapılmış kayıtlar arası terimler (δWS_{es}) sistematik rota etkileri özelinde, kalan eğilimi gözlemlemek için incelenmiştir.

Anahtar Kelimeler: Yer hareketi modelleri, ergodic olmayan yer hareketi modelleri, Türkiye'ye uyarlanmış yer hareketi modelleri, istasyona özel sigma

ACKNOWLEDGMENTS

I would like to express my sincere thanks to my supervisors Prof. Dr. Zeynep Gülerce and Assoc. Prof. Dr. A. Arda Özacar for their guidance, patience, and effort especially at struggling times during pandemics.

I would like to thank Norman Abrahamson for being able to use hazard code. I would like also to thank Burak Akbaş for his enormous effort and the cooperation for the Turkish strong motion database, which enabled this study. I also acknowledge the contribution of Fatma Begüm Kaya for helping me to automatize the dataset preparation and for her guidance during my master studies.

I am grateful to the faculty members of Middle East Technical University Civil Engineering Department for the knowledge and experience I have gained through their lectures.

My special thanks belong to my family, who supported me for my whole education life.

Finally, I would like to thank Bersu Çelikkol for her support and encouragement from the beginning till the last day.

TABLE OF CONTENTS

LIST OF TABLES

TABLES

LIST OF FIGURES

FIGURES

CHAPTER 1

INTRODUCTION

Standard deviations of ground motion models (GMMs) are one of the most important parameters that affect the results of probabilistic seismic hazard assessment (PSHA). The contribution of standard deviations to PSHA is especially crucial for long return periods, which correspond to seismic design levels of nuclear power plants and other important structures. Following the ergodic assumption, most of the available GMMs in the current literature provide a stable estimate for median but inherit the standard deviations related to the recordings from multiple global sites and seismic sources. In other words, they do not provide a site or source specific standard deviation model and assume that the standard deviation does not spatially vary for a specific earthquake scenario. As a result of the ergodic assumption, the global GMMs that were developed using recordings from different host regions that have high standard deviations and their standard deviation models may not be suitable for every target region.

Thanks to the availability of extensive and well-established strong motion datasets, an effective way of reducing the standard deviation of a GMM is found by relaxing the ergodic assumption by removing the systematic site, source and path effects and treating them as epistemic uncertainty instead of aleatory variability. Several attempts were made in the last decade to develop partially (where only systematic site effects are separated) and fully non-ergodic GMMs for different regions around the world.

Moving from ergodic to partially or fully non-ergodic GMMs requires expertise in ground motion modelling and unfortunately does not guarantee a reduction in the estimated ground shaking levels (e.g., Lanzano et al., 2017 and Abrahamson et al., 2019). Moreover, despite the numerous attempts, substantial

computational efforts are necessary to integrate fully non-ergodic GMMs into PSHA applications, due to the complexity of implementation of spatially changing path terms and standard deviations. Nevertheless, the ground motion modelling practice is moving towards this direction and the non-ergodic GMMs will possibly be the industry-standard in the next decade.

1.1 Research Statement

Systematic site, source and path characteristics in emprical ground motion datasets were studied and partially or fully non-ergodic GMMs were developed for Western United States (e.g., Atkinson, 2006 for Los Angeles; Villani and Abrahamson, 2015 and Abrahamson et al., 2019 for Southern California), Japan (Rodriguez-Marek et al., 2011 and Morikawa et al., 2008), Taiwan (Lin et al., 2011), Europe (e.g., Luzi et al., 2014 and Lanzano et al., 2017 for Italy; Ktenidou et al., 2018 for EUROSEISTEST in Greece), and Iran (Zafarani and Soghrat, 2017). Other than the ground motion characterization studies for nuclear site evaluation projects, scientific publications on ground motion non-ergodicity are quite limited for Turkey. Gulerce et al. (2016) had developed the first partially non-ergodic median GMMs for Turkey by adding Turkey-specific small magnitude, large distance, and stiff site terms to the Next Generation Attenuation West 1 GMMs. Douglas and Aochi (2016) had focused on the systematic path effects for Marmara Sea Region using a simulated ground motion dataset. Çağnan and Akkar (2019) have complemented the Gulerce et al. (2015) study by adding event-corrected single-station standard deviation and source-corrected between-event standard deviation models to the median GMMs developed for Turkey.

The Turkish ground motion datasets used in these previous efforts were quite limited as described in numerous publications by Akkar et al. (2010), Akkar et al. (2014), Kale et al. (2015), Gulerce et al. (2015), Sandikkaya (2017), and Alipour et al. (2019). Substantial increase in the strong motion recordings after 2017, especially with two M≈7 events occurred 2020 underlined the need for a substantial evaluation

and update of the Turkish Strong Motion Database (TSDM) that complies with international standards. The New-TSMD provided by Akbaş et al. (2022) includes more than 23,000 recordings from 743 earthquakes recorded at 904 stations and is suitable for an in-depth assessment of the systematic source, site and path effects for Turkish ground motions. These systematic characteristics and the limitations of the dataset should be thoroughly evaluated to move towards developing fully non-ergodic ground motion models for Turkey.

The objective of this study is to develop partially non-ergodic median GMMs for Turkey that include the repeatable source and site terms in the aletory variability model using N-TSMD. For this purpose, a statistically stable subset of N-TSMD and the state-of-the-practice NGA-West2 GMMs are utilized. The bias in the depth scaling and constant terms of two GMMs developed by Abrahamson et al. (2014) and Chiou and Youngs (2014) are corrected by the selected subset of ground motions. These partially non-ergodic median GMMs may be utilized in ground motion characterization studies of Turkey along with Turkey-specific between-event variability model. In addition, non-ergodic between-event variability models are developed for Marmara, Western and Southwestern Turkey, East Anatolian Platoue, and Maras-Hatay Block. For each ground motion recording station in the dataset, the site-to-site variability and its standard deviation (a.k.a. the single-station sigma) are calculated. These results are used for developing partially non-ergodic within-event variability models for Turkey. Another important contribution of this study is the discussion on the spatial distribution of high-frequency site-to-site variability and its relation with surface geology and site stiffness. Finally, a preliminary evaluation of repetable path effects in site corrected within-event residuals are provided for selected stations to deliver valuable guidance for fully non-ergodic GMM development attempts for Turkey.

1.2 Organization of Thesis

Chapter 2 describes the ergodic assumption, clarifies the terminology used in the fully and partially non-ergodic approach in ground motion modelling and summarizes the previous attempts to develop fully and partially non-ergodic GMMs that are available in the literature.

Chapter 3 presents the Turkish strong ground motion dataset used in the regression analysis. Four candidate GMMs are selected, their predictive performances are tested and necessary pieces of two selected models are modified to make sure that the average event terms are unbiased. Details of this regionalization process and the partially non-ergodic median GMMs are given in Chapter 3. This chapter also discusses the systematic source effects mapped into the event terms and provides the non-ergodic between-event variability model for Turkey.

Systematic site and path effects observed in the within-event residuals are discussed within the scope of Chapter 4. Site-to-site variability and the single-station sigma values are calculated and presented for each station in the Turkish strong ground motion dataset. Spatial distribution of the site terms and single station sigma values for high frequencies, their possible correlation with site geology and shear wave velocity profile is examined in this chapter.

Finally, the conclusions of this study are presented, and possible future works are addressed in Chapter 5. This chapter also provides a couple application examples to underline the findings of this study.

CHAPTER 2

DEFINITION AND EVALUATION OF NON-ERGODIC APPROACH IN GROUND MOTION MODELLING

Ground Motion Models (GMMs) and their standard deviations (also known as the sigma or total sigma) are the biggest contributors of the estimated design ground motions in Probabilistic Seismic Hazard Analysis (PSHA) (e.g. Strasser, 2009; Kuehn & Abrahamson, 2019). State-of-the-practice global GMMs were developed using large global datasets that include recordings from multiple sites, attenuating from different seismic sources (e.g., the Next Generation Attenuation – NGA models - https://peer.berkeley.edu/nga-west or the Pan-European GMMs developed for the RESORCE project - https://www.resorce-portal.eu/). Therefore, the standard deviations of these GMMs include the spatial and temporal variability of ground motions due to the ergodic assumption. Ergodic assumption was defined by Anderson & Brune (1999) as a "random process where the distribution of a random variable in space equals to the distribution of the same variable at a single point when sampled as a function of time'. Global GMMs rely on the ergodic assumption by assuming that the standard deviation of the ground motion predictions from a particular earthquake scenario does not vary spatially (or from region to region). Consequently, the global ergodic GMMs have statistically stable estimates of the median ground motion, but they are penalized with a high variability (or a large total sigma). This substantial total sigma value significantly influences the PSHA results, especially for long return periods which correspond to the hazard levels for important structures such as nuclear power plants (e.g., Bommer & Abrahamson (2006)).

Several alternative approaches were proposed, and many attempts were made to reduce the standard deviations of ergodic GMMs. A relatively straight-forward way of reducing the variability is to use local or regional ground motion datasets. A decrease in total sigma is expected, assuming that the "repeatable" path and site effects are more accurately modelled in local datasets (reduction in the aleatory variability), but the reduction in total sigma may also be achieved due to the smaller size of the dataset (decrease in the epistemic uncertainty). Regional GMMs typically have smaller standard deviations (e.g. Scherbaum et al., 2009); however, these models are developed using a limited ground motion database that usually suffer from the lack of near-field recordings from large magnitude events. Thus, the magnitude and distance scaling of the regional GMMs are typically less established and the median estimates of the GMM are statistically less stable.

2.1 Repeatable Site Effects and Partially Non-Ergodic Ground Motion Models

Another promising approach followed over the last decade is developing **fully or partially non-ergodic** GMMs using large regional or global datasets. Utilizing non-ergodic terms decreases the aleatory variability in the ergodic GMMs by removing the systematic site, path, and source effects and treating them as epistemic uncertainty (Al Atik et al., 2010). This approach leads to a GMM with smaller aleatory variability in general, but the epistemic uncertainty would be large in regions with sparse data, and it would be small where recordings from past earthquakes are available.

2.1.1 Theoretical Background

Following the notation commonly used in the literature, a GMM may be expressed by using the following form:

$$\ln(Y) = f(X_{es}, \theta) + \Delta \quad (2.1)$$

where Y is the actual recording of the ground motion parameter of interest, $f(X_{es}, \theta)$ is the estimation of GMM using the model coefficients (θ) and predictive parameters (X_{es}), and Δ is the residual of the GMM for these set of predictive parameters. In other words, Δ represents the misfit between the actual ground motion and the model's median estimation.

It is possible to decompose this misfit, a.k.a. the residual, into between-event (or inter-event) and within-event (or intra-event) terms:

$$\Delta_{es} = \delta B_e + \delta W_{es} \quad (2.2)$$

where Δ_{es} is the residual belongs to the earthquake e at site s, δB_e is between-event residual associated with earthquake e and δW_{es} is within-event residual for earthquake e and site s. As shown in Figure 2.1, between-event residual (δB_e) represents the average difference between the actual recordings associated with that earthquake and the median estimates from the GMM. On the other hand, within-event residual (δW_{es}) is the misfit between actual recording related to a specific site and event-corrected median estimate from the GMM. In the ergodic GMMs, the total standard deviation is calculated as follows:

$$\sigma = \sqrt{\varphi^2 + \tau^2} \quad (2.3)$$

where φ is the standard deviation of the within-event residuals (δW_{es}) and τ is the standard deviation of between-event residuals (δB_e).

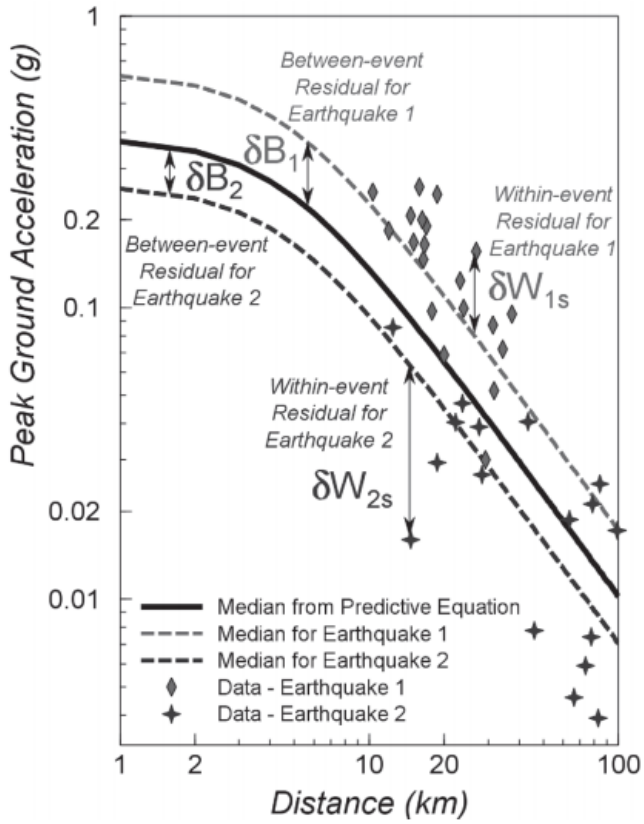

Figure 2.1. Illustration of between-event (δB_e) and within-event (δW_{es}) residuals for two earthquake case (Al Atik et. al., 2010)

To separate systematic site effects, average within-event residual for each station may be calculated as shown below:

$$\delta S2S_s = \frac{1}{NE_s}\sum_{e=1}^{NE_s}\delta W_{es} \qquad (2.4)$$

where $\delta S2S_s$ (the site term, hereafter) is the average of the within-event residuals (δW_{es}) at the station s and NE_s is the total number of recordings at the station s. The standard deviation of the site term ($\delta S2S_s$) is φ_{S2S} and it is a measure of the site-to-site variability that cannot be explained by the GMM (Luzi et al., 2014). Using the site term, the site-corrected within-event residual is calculated as:

$$\delta WS_{es} = \delta W_{es} - \delta S2S_s \quad (2.5)$$

The associated standard deviation of the site-corrected within-event residual for a single-station is given in Eq. (2.6) and the total sigma for site-corrected within-event residuals is shown in Eq. (2.7), where NS is the number of stations:

$$\varphi_{SS,s} = \sqrt{\frac{\sum_{e=1}^{NE_s} \delta WS_{es}^2}{NE_s - 1}} \quad (2.6)$$

$$\varphi_{SS} = \sqrt{\frac{\sum_{s=1}^{NS} \sum_{e=1}^{NE_s} \delta WS_{es}^2}{\sum_{s=1}^{NS} NE_s - 1}} \quad (2.7)$$

Finally, the so-called single station sigma, or single station standard deviation is computed, in a similar manner to Eq. (2.3) as:

$$\sigma_{SS} = \sqrt{\varphi_{SS}^2 + \tau^2} \quad (2.8)$$

The above explained process is visualized in Ktenidou et al. (2018) for a dataset that includes relatively small number of stations (Figure 2.2). The top figure shows the distribution of within-event residuals and their standard deviation ($\varphi = 0.473$) for this particular dataset, the middle figure presents the site term for each station ($\delta S2S_s$) and their standard deviation (φ_{S2S}), and the bottom figure shows the distribution of site-corrected within-event residuals and their standard deviation ($\varphi_{SS} = 0.331$). It should be underlined that the single station sigma (σ_{SS}) calculated by φ_{SS} represents the partially non-ergodic case, where only **the systematic site effects are taken into consideration** and the systematic source and path effects are not evaluated.

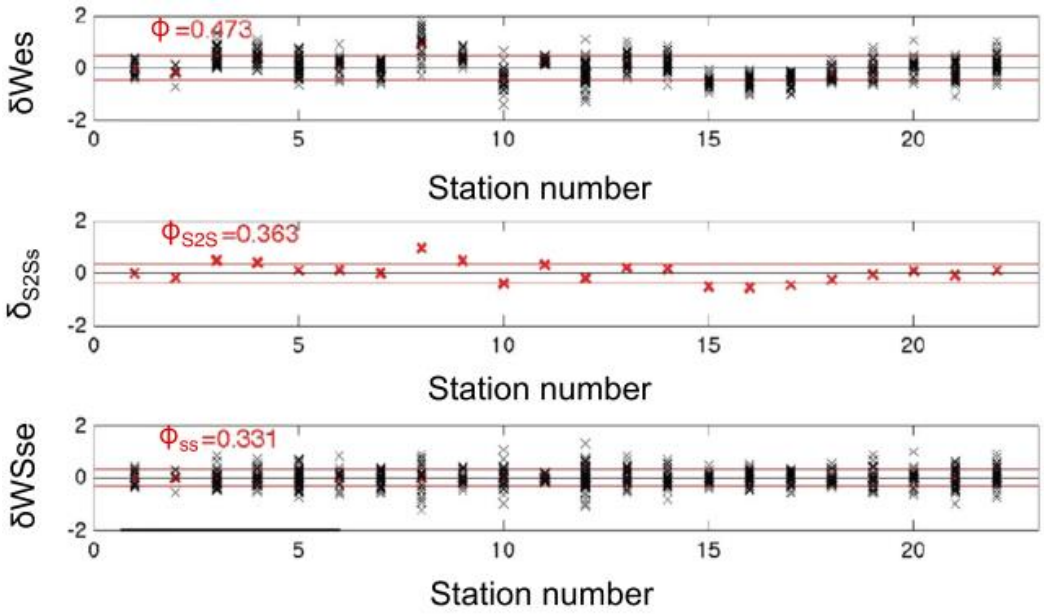

Figure 2.2. Calculation of site-corrected within-event residuals and their standard deviations (taken from Ktenidou et al., 2018)

2.1.2 Ground Motion Models with Systematic Site Effects

The first step towards the fully non-ergodic GMMs was the development of partially non-ergodic GMMs that remove the systematic site-specific effects from the aleatory variability without changing the median. Atkinson (2006) proposed that the sigma for individual recording stations was less than the overall sigma of the GMM by using 21 stations in Los Angeles area with measured V_{S30} values (Figure 2.3). In this pioneering work, Atkinson (2006) suggested that the site-specific sigma can be taken as approximately 90% of the total sigma of the GMM, when the site amplification of a specific site has been estimated based on either an empirical correction or V_{S30}.

After 2006, several attempts were made to estimate the single station sigma values for different regions around the world and these studies generally included a complementary site amplification analysis. Rodriguez-Marek et al. (2011) estimated the single station sigma values using a subset of the Japanese KiK-net database and

proposed 16% reduction in total sigma. An important feature of the KiK-net database is the availability of two recording instruments, one at the surface and the other at depths of 100-200 m, for every recording station. The difference in the single station sigma values estimated at the ground surface and within the borehole was found to be significantly smaller than the difference obtained from the ergodic approach, underlining the poor representation of site amplification effects in the ergodic GMMs. The availability of two separate recordings at the same site enabled the authors to investigate the site amplification effects and to decompose the single site variability. In the analysis, the between-event terms were forced to be same at both levels for each station so that source-related variability is not included in single site standard deviation. Analysis results showed that the reduction in the total standard deviation corresponds to only 10% when the amplification was predicted using a site-response analysis.

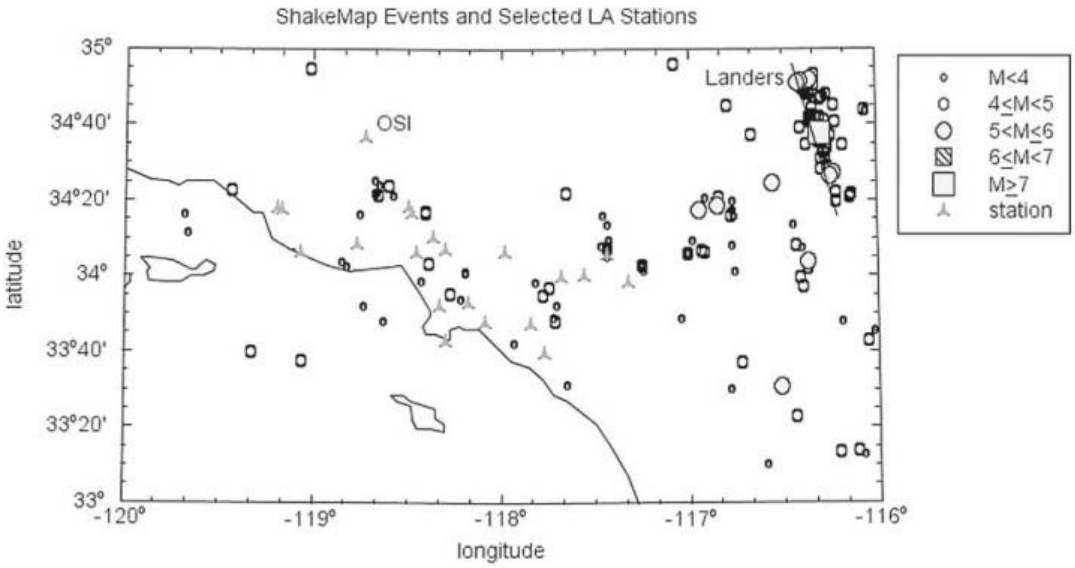

Figure 2.3. Earthquakes and stations in LA that were analyzed in Atkinson (2006)

Studies performed after 2011 have suggested similar single-station sigma values for different tectonic regimes. For example, Lin et al. (2011) have used a dataset derived from the recording stations in Taiwan and estimated 9-14% reduction in the total sigma at different spectral periods. Luzi et al. (2014) have utilized three different datasets from Italy, largest one including 2805 recordings from 658 events

recorded at 254 stations. The authors proposed that it is possible to decrease the total standard deviation by 15%, when the ergodic assumption is relaxed by removing the repeatable site effects. The reduction in sigma for three different datasets after removing the ergodic assumption partially is shown in Figure 2.4. In Figure 2.4, black dots represent the total standard deviation with the ergodic assumption and black triangles represent the standard deviation after the removal of systematic site effects. Additionally, white dots correspond to within-event and gray dots between-event standard deviation. On the other hand, results of the study showed that the total standard deviation may decrease further (up to 30%) when a comparably smaller area that includes only one seismic source was examined.

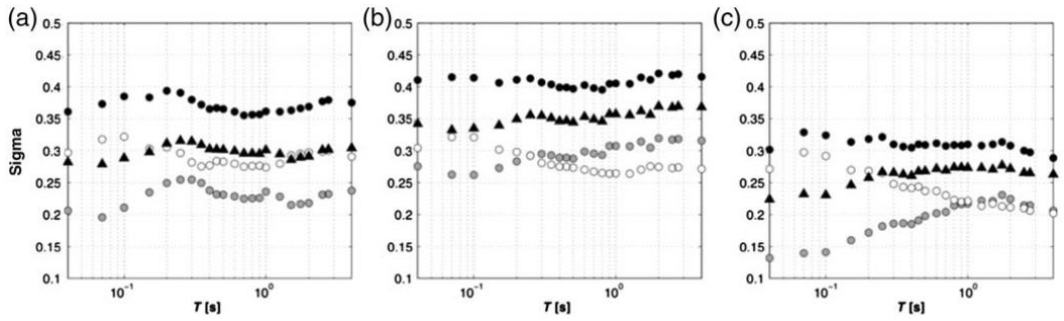

Figure 2.4. Reduction in sigma by the separation of site terms using three different datasets (taken from Luzi et al. (2014))

Zafarani & Soghrat (2017) have estimated the single station sigma values using the Iranian strong motion stations. Their dataset consists of 1837 recordings from 374 earthquakes recorded at 370 stations. Six GMMs were used in this study and 15% decrease in total standard deviation was reported. Figure 2.5 shows that the ratio of single station sigma to sigma (total standard deviation with ergodic assumption) varies between 0.86-0.89 for different GMMs for Iranian dataset.

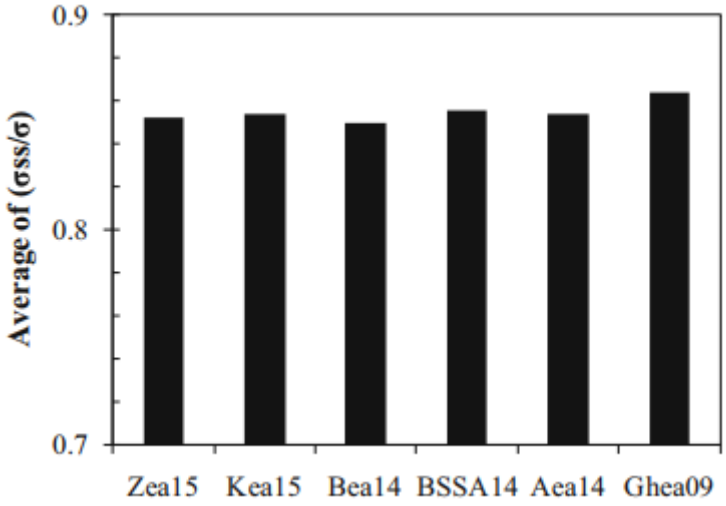

Figure 2.5. The ratio of single station sigma and sigma in different GMMs (each bar represents a different GMM – e.g. Aea14 is for Akkar et al. (2014) model).

The studies specific to Turkey are limited to the scientific publications by Çağnan & Akkar (2019) and Douglas & Aochi (2016), in addition to the ground motion characterization studies of ongoing NPP projects. Çağnan & Akkar (2019) had developed event-corrected single-station standard deviation and source-corrected between-event standard deviation models that are specific to Turkey. For this purpose, they decomposed the residuals from 11 global and regional GMMs, which were assumed to be applicable to Turkey, and derived separate standard deviation models for each component. This study had utilized the strong motion dataset developed for the EMME Project (Akkar et al, 2014) with 1190 recordings from 203 events recorded at 304 stations. However, the number of data points was reduced further in regression, due to the inclusion of a recording threshold (minimum 5 recordings per station) (Figure 2.6). The authors have also proposed an approximately 15% reduction in sigma, when the systematic site effects are taken into consideration.

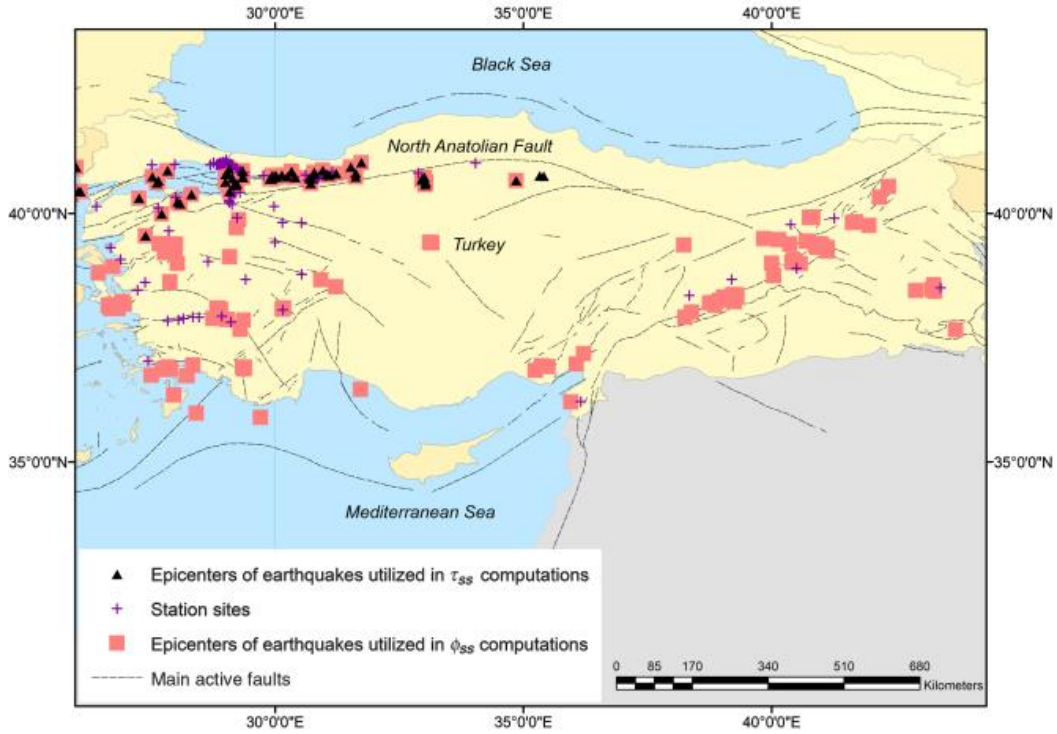

Figure 2.6. Geographical distribution of events and stations used in Çağnan & Akkar (2019)

2.2 Repeatable Path Effects and Source-to-Site Variability

In addition to the repeatable site effects that are removed from the within-event residuals in partially non-ergodic GMMs, repeatable source and path effects are also considered in **fully non-ergodic** GMMs.

2.2.1 Theoretical Background

Like the separation of systematic site effects from the within-event residuals (δW_{es}), systematic source effects can be isolated from the between-event residuals as shown in Eq. (2.9):

$$\delta L2L_r = \frac{1}{NE_r}\sum_{e=1}^{NE_s}\delta B_{er} \quad (2.9)$$

where $\delta L2L_r$ (the location term hereafter) is the average of between-event residuals at Region r (δB_{er}) and NE_r is the total number of earthquakes at Region r. The standard deviation of the location term ($\delta L2L_r$) is τ_{L2L} and it is a measure of the location-to-location variability that cannot be explained by the source parameters in the GMM. Using $\delta L2L_r$, the location-corrected between-event residual is calculated as shown below.

$$\delta B_{0,er} = \delta B_{er} - \delta L2L_r \quad (2.10)$$

The standard deviation of the location-corrected between-event residual for each region is given in Eq. (2.11) and the total sigma for location-corrected between-event residuals is shown in Eq. (2.12), where NR is the number of source regions in the dataset:

$$\tau_{0,r} = \sqrt{\frac{\sum_{e=1}^{NE_r}\delta B_{0,er}^2}{NE_r - 1}} \quad (2.11)$$

$$\tau_0 = \sqrt{\frac{\sum_{r=1}^{NR}\sum_{e=1}^{NE_r}\delta B_{0,er}^2}{\sum_{r=1}^{NR} NE_r - 1}} \quad (2.12)$$

The final step of developing the non-ergodic GMMs is the separation of systematic path effects as follows:

$$\delta P2P_{sr} = \frac{1}{NE_{sr}}\sum_{e=1}^{NE_{sr}}\delta WS_{esr} \quad (2.13)$$

where NE_{sr} is the number of recordings from site s and region r and $\delta P2P_{sr}$ (the path term hereafter) is the average of site-corrected within-event residual at a travel path (δWS_{esr}), which is a representation of how travel path characteristics differ

from the median predictions of the GMM (Lanzano et al., 2017). Hence, path- and site-corrected within-event residual is calculated as

$$\delta W_{0,esr} = \delta WS_{esr} - \delta P2P_{sr} \qquad (2.14)$$

The associated standard deviation with path- and site-corrected within-event residuals is:

$$\varphi_{0,sr} = \sqrt{\frac{\sum_{e=1}^{NE_{sr}} \delta W_{0,sr}^2}{NE_{sr} - 1}} \qquad (2.15)$$

Subsequently, for the whole dataset, the standard deviation with path- and site-corrected within-event residuals is given by:

$$\varphi_0 = \sqrt{\frac{\sum_{s=1}^{NS} \sum_{r=1}^{NR} \sum_{e=1}^{NE_{sr}} \delta W_{0,sr}^2}{\sum_{s=1}^{NS} \sum_{r=1}^{NR} NE_{sr} - 1}} \qquad (2.16)$$

Finally, the fully non-ergodic standard deviation is calculated as follows:

$$\sigma_0 = \sqrt{\varphi_0^2 + \tau_0^2} \qquad (2.17)$$

2.2.2 Ground Motion Models with Systematic Location and Path Effects

In a ground motion database, there exist many site/path pairs from different source-to-site azimuths, which leads to an exhausting number of parameters for evaluating the repeatable location and path effects. One way to overcome this problem is to define broad source regions based on the geometry of the seismic sources and to calculate the residuals for ray paths that originate from one source region and end at a particular site. The pioneering study by Atkinson (2006) also investigated the repeatable path effects for a relatively limited dataset. Sigma at a particular station due to a specific seismic source was evaluated and it was concluded that around 40% of the total sigma of the ergodic GMMs is associated with

systematic site and source/path effects. This observation indicates that systematic path effects contribute more to the total sigma than the repeatable site effects.

Another study was conducted by Morikawa et al. (2008) using the K-NET and KiK-net records to investigate the effects of magnitude, distance, and amplitude on the uncertainty. They identified six areas, smaller than 50 km x 50 km, with at least five earthquakes per area. Then, the "source-area site factors" for ground motions recorded at individual stations coming from each specific source area were calculated. It should be noted that the estimated source-area site factors were specific to the station and depended on the source area. Aleatory variability was reduced by approximately 50% by averaging the source-area site factors at each station. Çağnan & Akkar (2019) attempted to evaluate the location term by limiting the database to the events originating from North Anatolian Fault Zone (NAFZ). Due to the lack of extensive source-site pairs, repeatable path effects were not included in the scope by Çağnan and Akkar (2019). However, standard deviations were further reduced by 15% in some period ranges, by only considering the earthquakes from NAFZ.

A more robust way for modelling the repeatable site effects is to use the "**region-less**" approach. As the name suggests, it is not necessary to define broad source regions in this approach. Instead, the non-ergodic site, source and path effects are captured by imposing spatial correlation between these terms. The region-less approach was mostly adapted in the development of non-ergodic GMMs built in the last decade.

An introductory application of the region-less approach was presented in Lin et al. (2011) for Taiwan. Their dataset consists of 4756 recordings from 64 events recorded at 285 stations after limiting the rupture distance as 200 km and restricting ground motion recording stations to the ones with more than 10 recordings. In this study, the non-ergodic source and path terms were assumed to be spatially correlated, and the site terms were assumed as site-specific; although, it was mentioned that they are also likely to be spatially correlated. The spatial correlation between the site-source pairs was parametrized by a closeness index, which is a measure of the

closeness of site-source pairs. The equation of the closeness index and its components is shown in Figure 2.7.

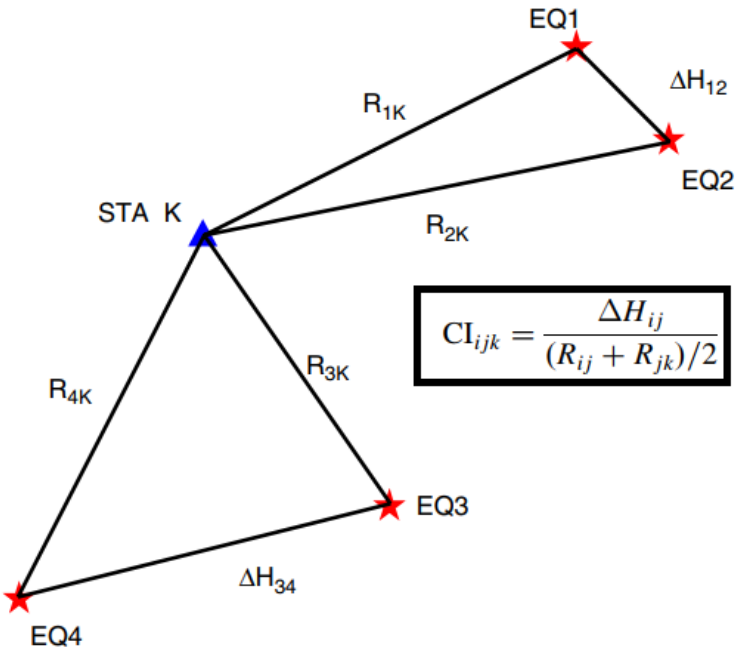

Figure 2.7. Components and the equation of the closeness index defined by Lin et al. (2009)

Considering the closeness index ensures that the correlation between closer paths is stronger in comparison to farther apart paths. At the end, rather than developing a non-ergodic GMM, the authors investigated the reduction in the standard deviation by removing systematic site, source and path components. The results revealed that it is possible to reduce the total standard deviation by 9% - 14% for a single site using the single station sigma, and by 39 - 47% for a single site-path combination.

Villani & Abrahamson (2015) have studied repeatable site and path effects using the empirical residual dataset from Abrahamson et al. (2014) GMM and a synthetic set of ground motions generated by CyberShake simulations. The study was performed only for 3 second spectral accelerations, due to the frequency limitation of simulations. In the case of the site terms, the results from both datasets were generally consistent, while the variability resulted from the synthetic data was

bigger. Path effects were evaluated using two methods: the first method defined grid-based source regions all over California and the latter was the region-less approach proposed by Lin et al. (2011). Unlike the site terms, empirical data and CyberShake simulations had a negative correlation for more than half of the sites. This study also questioned the applicability of the path terms determined from moderate-magnitude earthquakes to larger magnitude events. The results indicated that it is possible to apply these path terms to $M_w < 7.5$ events, however for very large magnitude events ($M_w > 8$) other factors also should be considered.

Douglas & Aochi (2016) was the only study that examined the systematic path effects in GMMs for Turkey. The assessment focused on the Marmara Sea Region, where İstanbul is located. In this study, simulated ground motions resulting from 156 events (all $M_w = 5$), that were simulated at 70 stations in the Marmara Sea Region (200 x 120 km^2), totaling to 10,920 ground motion time histories were used to derive a GMM for PGV. Calculated residuals were portioned into site, source and path components using the methodology presented in Lin et al. (2011). They have found comparably lower standard deviations for between-event and within-event components, probably due to the use of simulated ground motions. Sub-regional findings for Marmara Sea Region (in addition to Istanbul) were also discussed and edges of the Marmara Sea and islands within found to produce ground motions higher than the average.

Lanzano et al. (2017) separated the residuals of a regional GMM for Northern Italy into systematic site-specific, location-specific and path-specific components using both region-based (Figure 2.8) and region-less approach following the methodology introduced by Lin et al. (2011). Their analysis included 2241 recordings from 88 events recorded at 168 sites. As 90 stations in their dataset had recordings from only one source region, almost half of the stations were not included in the region-based analysis. The results from two methods showed similar trends despite the use of different datasets. The lowest contribution to the total sigma was found to come from the location-to-location term, since the dataset is dominated by

a single seismic sequence. Average reduction with respect to total standard deviation was 37% for the region-dependent approach and 40% for the region-less approach, while the maximum reduction was 60% at 0.1 s period. Moreover, a fully non-ergodic PSHA for three sites based on the results of the region-dependent approach was conducted. However, the epistemic uncertainty related to the non-ergodic adjustment terms was not accounted for in the PSHA.

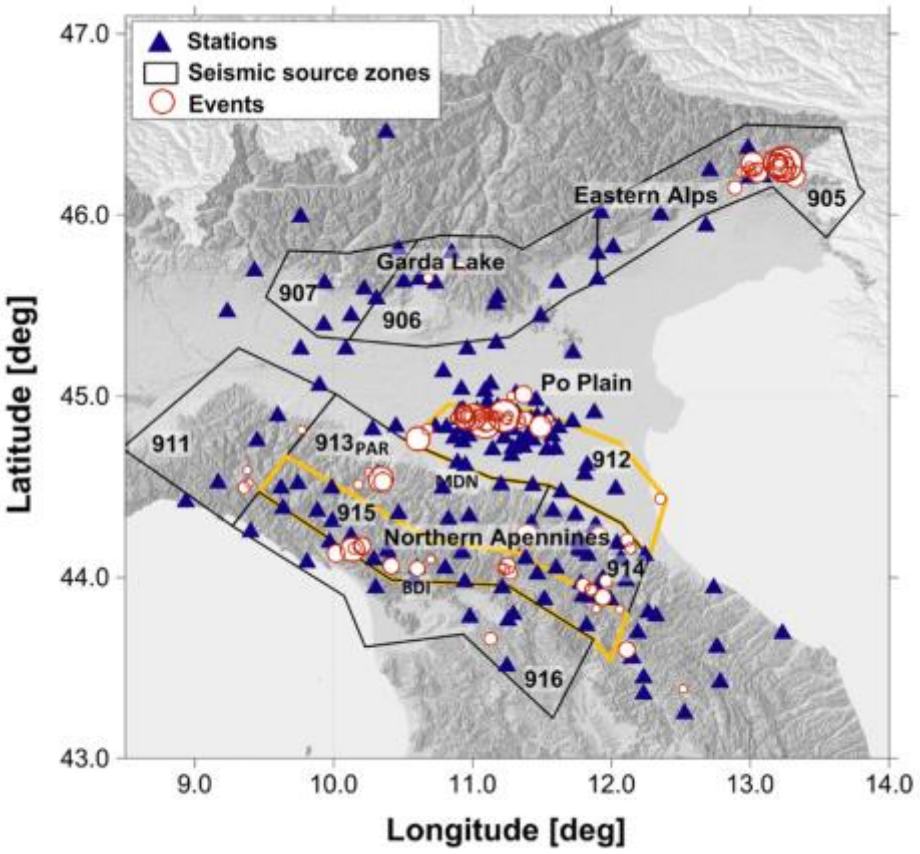

Figure 2.8. Events, stations and regions used in the study by Lanzano et al. (2017)

Abrahamson et al. (2019) developed a non-ergodic GMM for California that considers the systematic effects explicitly. A fully non-ergodic PSHA was carried out including the uncertainty associated with systematic effects. 100 realizations for the base (and ergodic) GMMs were derived from five NGA-West2 GMMs to incorporate epistemic uncertainty in PSHA by placing each one of them in the logic tree. Adjustment terms, that added on top of the ergodic base GMMs, were taken

from two previous studies. In addition to the adjustment terms taken from Landwehr et al. (2016), an additional path term, anelastic attenuation term, which was calculated similar to Dawood & Rodriguez-Marek (2013) and Kuehn et al. (2019), was included in this study. The newly developed non-ergodic GMM was tested with the 2016 South Napa earthquake, which was not included in the database. The model fitted the data better than NGA-West2 GMMs at all distance ranges. Moreover, the results of the PSHA calculations, that were performed in three different locations in California, one of them having very limited ground motion data and another having relatively larger dataset, suggested important conclusions. For the sites where the number of observed ground motion data is sparse, the uncertainty associated with the hazard may be even larger than ergodic models. Therefore, moving from ergodic GMMs to non-ergodic ones does not ensure a decrease in the hazard. A further conclusion or recommendation regarding the use of non-ergodic GMMs in PSHA, is the inclusion of the epistemic uncertainty in non-ergodic GMMs. One of the possible improvements for the implementation of non-ergodic GMMs to PSHA, stated in the article was the use of integrated analysis instead of using the results of other studies. Besides, it was assumed that non-ergodic terms from small and moderate earthquakes also apply for larger magnitudes.

Another approach is to develop a non-ergodic GMM from scratch, i.e., without a backbone model. Landwehr et al. (2016) developed a non-ergodic GMM using a subset of the NGA-West 2 database. In contrast to the aforementioned non-ergodic GMMs that added adjustment terms to the global models, in this study new model coefficients were developed to include site, source and path effects. The coefficients of this model varied smoothly with location, yet they were similar for nearby locations. The model was based on varying-coefficient model (VCM) regression, which assigns a Gaussian process (GP) prior to coefficients because there were not enough data in every location to constrain the coefficients. A drawback of this study was that the path effects were not directional: the coefficients including path effects represent only an average distance attenuation for each event. Based on the results and the validation with a global model, it was concluded that accounting

for spatial effects improves the prediction and VCM is a superior alternative for developing a non-ergodic GMM.

The non-ergodic GMMs discussed up to this point were developed for the response spectral acceleration (PSa) and were applicable for the common earthquake engineering applications. Recently, Lavrentiadis et al. (2021) developed a non-ergodic GMM for effective amplitude spectrum (EAS) for California. The motivation behind the study was interesting: unlike PSa, the scaling of EAS is not affected by the spectral shape, which enables the use of small magnitude records for the estimation of non-ergodic terms for large magnitudes (Lavrentiadis et al., 2021). The backbone model was selected as the Bayless & Abrahamson (2019) ergodic EAS GMM to profit from its relatively large database. Similar to Abrahamson et al. (2019), non-ergodic source and site terms were calculated following the methodology presented in Landwehr et al. (2016) and non-ergodic path term as cell-specific anelastic attenuation following Dawood & Rodriguez-Marek (2013) and Kuehn et al. (2019).

2.3 Application of Non-Ergodic GMMs in Hazard Calculations

Once the ergodic assumption in a GMM is relaxed, it is not possible to use the ergodic mean: the specific deviations belong to a particular site, source and path combination should be incorporated in hazard calculations (Lin et al., 2011). Relaxing the ergodic assumption does not necessarily lead to a reduction in the hazard, since not only sigma but also mean prediction is modified (Lanzano et al., 2017; Villani & Abrahamson, 2015). Lanzano et al. (2017) compared the results of PSHA for three sites in Northern Italy using ergodic, partially non-ergodic and fully non-ergodic GMMs. The analysis was conducted only for spectral accelerations at 0.2 and 2 s. As shown in Figure 2.9, the results exhibited a strong variation from one site to another. The shift from ergodic GMMs to the partially or fully non-ergodic GMMs resulted in a decrease in hazard values at short period spectral accelerations for all three sites. At longer spectral periods, the difference between three approaches

for two sites was very small. Unlike these two sites, in the case of the other site, the results of partially and fully non-ergodic approaches differed significantly. In general, moving to partially ergodic PSHA from ergodic one led to bigger changes in hazard curve than moving to fully non-ergodic PSHA from the partially non-ergodic one. However, an important drawback of this analysis is that epistemic uncertainty associated with the non-ergodic terms are not considered.

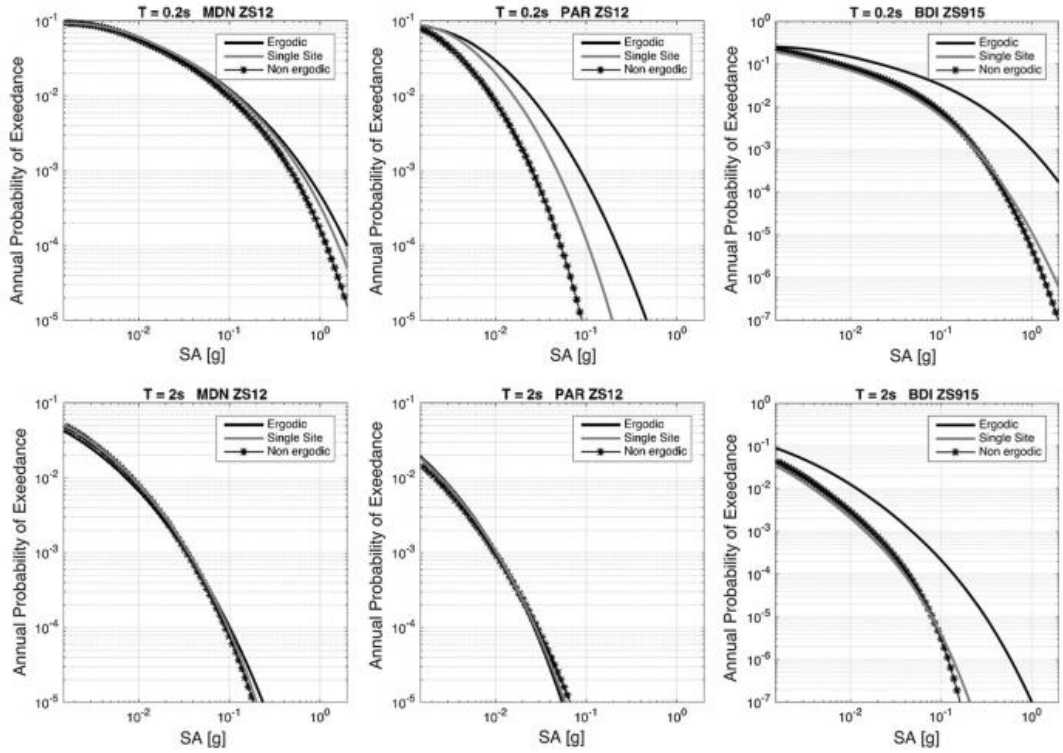

Figure 2.9. Comparison of PSHA results (Lanzano et al., 2017)

Abrahamson et al. (2019) implemented a logic tree with 100 branches (Figure 2.10) in PSHA in order to capture the epistemic uncertainty associated with the non-ergodic GMM. Applied logic tree included 100 branches such that each of them is an ergodic base GMM. The constants and coefficients of each GMM were derived from the original base GMM. Using this approach, the authors computed non-ergodic hazard for three sites for spectral period of $T = 2$s (Figure 2.11). The hazard results for NE California site, where the data is sparse showed only a small change because the high epistemic uncertainty eliminates the reduction in aleatory

variability. The other two sites exhibited hazard curves with steeper slopes, indicating the reduction in aleatory variability. Non-ergodic PSHA for San Luis Obispo site resulted in higher values for short return periods (Figure 2.11).

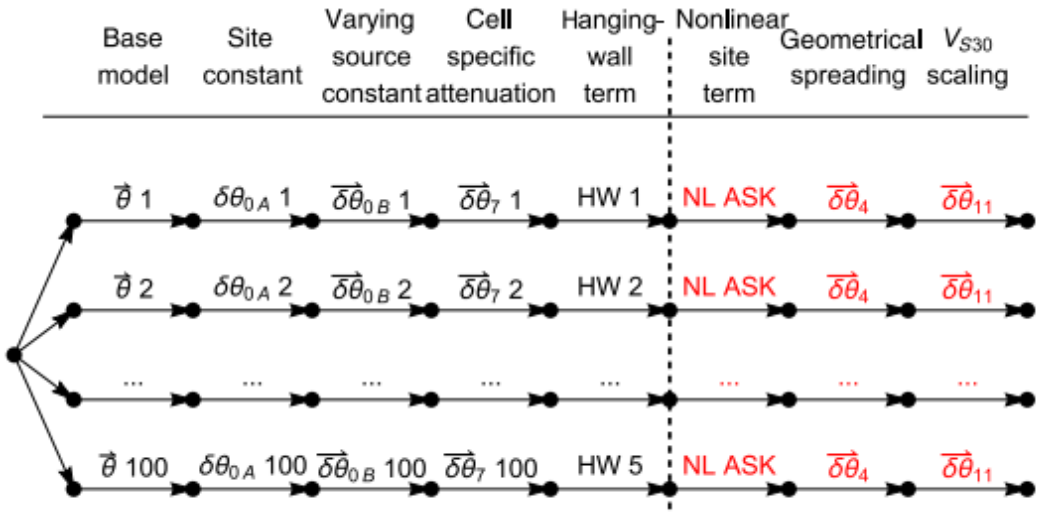

Figure 2.10. Logic tree in PSHA application (Abrahamson et al., 2019)

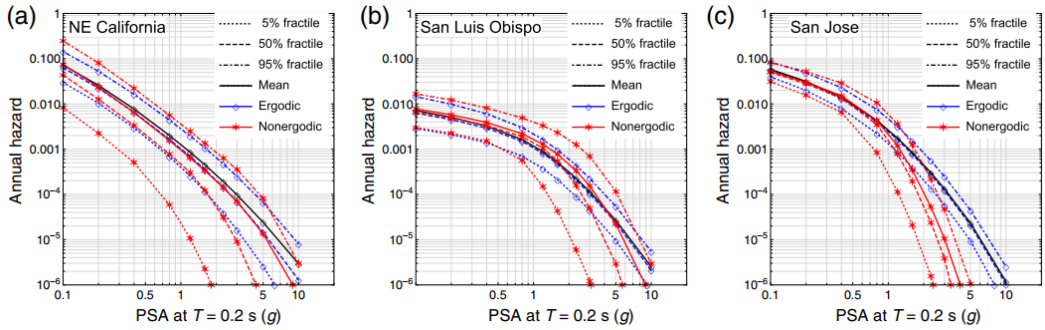

Figure 2.11. Ergodic and non-ergodic PSHA results for three sites (taken from Abrahamson et al., 2019)

CHAPTER 3

PARTIALLY NON-ERGODIC MEDIAN GROUND MOTION MODELS AND BETWEEN EVENT VARIABILITY MODEL FOR TURKEY

A well-established ground motion database with all necessary metadata is vital to develop fully or partially non-ergodic ground motion models. Therefore, the first part of this chapter briefly summarizes the new Turkish Strong Motion Database (N-TSMD) developed by Akbaş et al. (2022) and presents the subset of data used in this study. Ground motion datasets may be utilized **to develop a non-ergodic ground motion model** or **to add the non-ergodic terms to the median predictions and standard deviations of an existing model**. In this study, the second approach is preferred, four NGA-West2 GMMs (Bozorgnia et al., 2014) are selected as the candidate GMMs, their predictive performances are tested using the selected subset of Turkish ground motions, and relevant pieces of the models are adjusted to ensure unbiased median predictions. Second part of this chapter discusses this **"regionalization"** process, which should be considered as the first step of making these models **"partially non-ergodic"**. After the regionalization, the between-event residuals (hereafter the event terms) are re-calculated, and the spatial distribution of the event terms is analyzed in the last part of this chapter. Based on the analysis results, non-ergodic between-event standard deviations are provided for different seismo-tectonic regions of Turkey.

3.1 New Turkish Strong Motion Database (N-TSMD)

The N-TSMD, an extensive strong ground motion database, was developed by Akbaş et al. (2022) to be used in engineering seismology and earthquake engineering applications. N-TSMD includes 23,019 strong motions disseminated by Disaster and Emergency Management Presidency of Turkey (AFAD) through

https://tadas.afad.gov.tr/map (last accessed on Feb 1, 2022) that were recorded between 1983 and January 2021 and comply with the following criteria:

- Recordings from events of $M_w \geq 3.5$,
- Recordings from events with hypocentral depths shallower than 30 km,
- Recordings with epicentral distance (R_{EPI}) less than 200 km,
- Recordings from events that were recorded by at least 5 stations within $R_{EPI} \leq 200$ km.

Almost 85% of the 743 earthquakes included in N-TSMD may be considered as small magnitude events ($M_w < 5$); however, an important portion of these events are in the $4 \leq M_w < 5$ range. Approximately half of the earthquakes are classified as strike-slip (SS) and 30% are classified as normal (NM) events, whereas the style-of-faulting (SoF) of almost 16% of the earthquakes in the database is unknown. For accurate estimations of event location and depth, the information gathered from AFAD were compared to the relocated earthquake catalogue of International Seismological Center (ISC). This process resulted in the update of epicentral location and hypocentral depth information of 197 ($M_w < 6$) events. Further information on this database and compiled earthquake metadata may be found in Akbaş et al. (2022).

The $M_w \geq 6$ earthquakes (16 events in total) were evaluated case-by-case for the field observations of surface rupture, co-seismic slip distribution by waveform inversion or geodetic data, and the aftershock distribution to define the finite fault geometry. The source-to-site distance metrics such as rupture distance (R_{RUP}) and Joyner-Boore distance (R_{JB}) for $M_w \geq 6$ earthquakes were calculated based on the event-specific rupture planes determined by these evaluations. For $M_w < 6$ earthquakes, the source-to-site distance metrics were estimated by using the procedure given in Kaklamanos et al. (2011) and the average values for conjugate fault planes were provided in the database.

875 of 904 strong motion stations included in N-TSMD are operated by AFAD. For these stations, station coordinates and time-averaged shear wave velocity at the top 30 meters (V_{s30}) were compiled from AFAD's website. It should be noted

that the shear wave velocity profiles for most of AFAD's strong-motion stations are measured, well-documented and open to public at (https://tadas.afad.gov.tr/list-station); however, the site characterization is not yet performed for relatively new (located after 2017) stations. In addition to AFAD's strong-motion stations, several temporary stations that were operated by KOERI, İstanbul Technical University and other international organizations had recorded the 1999 Kocaeli and Düzce earthquakes. The site characterization for some of these stations was performed and the V_{s30} value is available; therefore, strong motion recordings (15 records for Kocaeli and 21 records for Düzce) from these 29 stations were added to N-TSMD. Approximately 71% of the 904 stations have measured V_s profiles, while the V_{s30} of the remaining stations are unknown.

Figure 3.1 (a) shows the spatial distribution of the strong motion stations included in N-TSMD with measured or unknown V_{s30} values. As expected, the network is quite dense in Marmara region, around the North Anatolian and East Anatolian Fault zones, and in western Turkey. Stations with unknown V_{s30} are generally concentrated around the Adapazari region. Number of stations in each site class defined by the new Turkish Building Earthquake Code (TBDY, 2019) is presented in Figure 3.1(b). Majority of the stations in the database are classified as site class ZB, ZC or ZD ($V_{s30} = 180 – 760$ m/s) and there are only a few stations in the site class ZA and ZE.

Only a subset of N-TSMD is utilized in this study since some events and recordings are eliminated due to different concerns. Recordings that did not pass the visual check of Akbaş et al. (2022) and the recordings from events with unknown SoF are removed. In addition, recordings from events of $3.5 < M_w < 4.0$ are removed because most of these earthquakes have incomplete (or estimated) event metadata that would result in a higher uncertainty in regression analysis. This elimination has reduced the number of recordings in the dataset to 17,584 and removed 54 stations. The number of recordings at the remaining 850 stations is presented in Figure 3.1(c). Almost half of the stations have less than 10 recordings;

therefore, a stable estimation of the systematic site effects may not be possible for these stations (Çağnan and Akkar, 2019; Lanzano et al., 2017; Lin et al., 2011). Because of this concern, stations with less than 10 recordings are excluded and the dataset is further reduced to 15,956 recordings from 445 strong motion recording stations associated with 538 earthquakes.

(a)

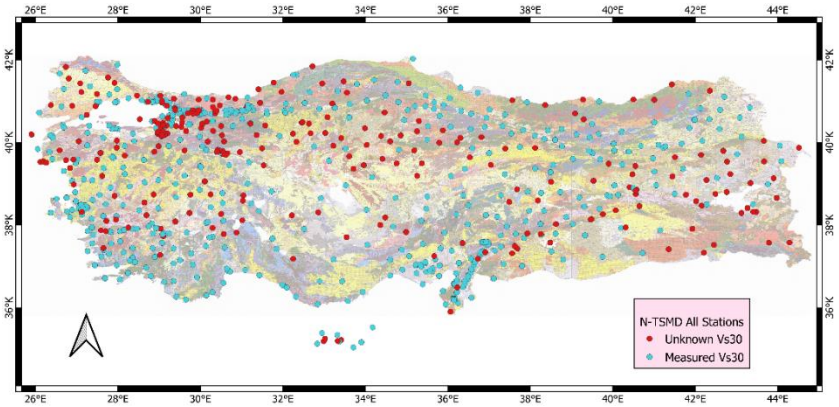

(b)

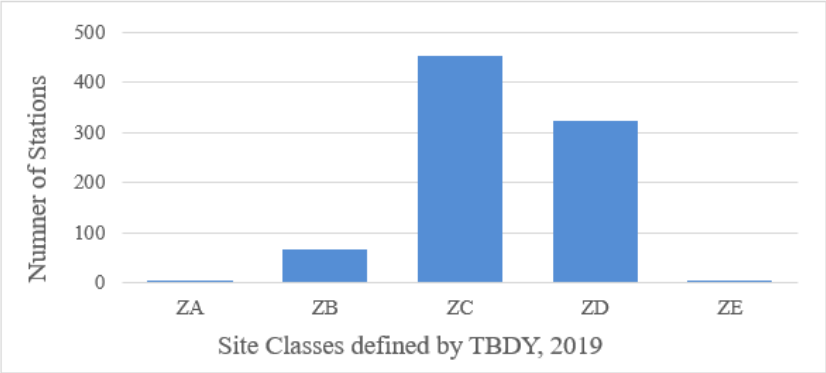

(c)

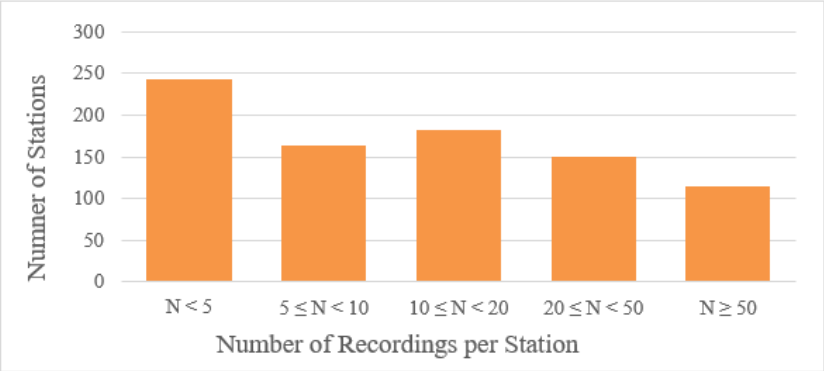

Figure 3.1: (a) Spatial distribution of strong motion stations in N-TSMD (with measured and unknown Vs profile), (b) the distribution of stations among site classes according to TBDY, 2019, and (c) number of recordings per station (N).

The final magnitude – distance (R_{RUP}) distribution of the study dataset is shown in Figure 3.2(a). Although the near-source recordings (R_{RUP}<10km) and large magnitude events are rare in the dataset, it is still very extensive, especially when it is compared with the datasets utilized in the similar studies. Akbas et al. (2022) has provided the minimum useable frequency values for each recording, based on the filter cut-offs used in data processing. In the regression analysis, this minimum usable frequency value is taken into consideration: a recording is only used in the regression for frequencies higher than the minimum useable frequency. Due to this limitation applied, the number of recordings in the regression analysis decreases sharply after 1s as shown in Figure 3.2(b) and the regression results are statistically less stable after 3s spectral periods.

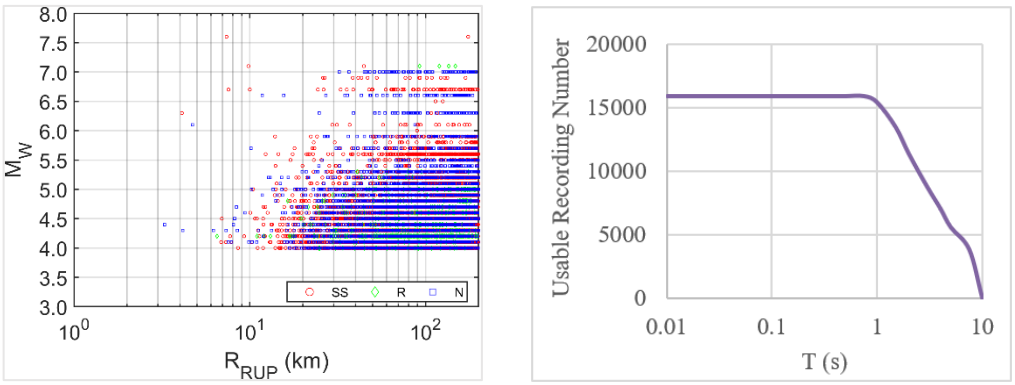

(a) (b)

Figure 3.2: (a) Magnitude – distance (R_{RUP}) distribution of the study dataset, (b) Number of usable recordings at each period

3.2 Regionalization of Selected GMMs for Turkey

Four NGA-West2 GMMs (Abrahamson et al., 2014; hereafter, ASK14), Boore et al., 2014; hereafter, BSSA14, Campbell and Bozorgnia, 2014; hereafter, CB14, and Chiou and Youngs, 2014; hereafter, CY14) are selected as candidate models for this study. Using the selected subset of ground motions from N-TSMD, the residuals of base GMMs are calculated and separated into between-event (δB_e) and within-event residuals (δW_{es}) (with reference to definitions given in Al-Atik et

al., 2010) by employing a single random-effects regression (Abrahamson and Youngs, 1992). Distribution of between-event residuals for the ASK14, BSSA14, CB14 and CY14 models with magnitude, depth to the top of the rupture (Z_{TOR}), and rake angle are presented in Figure 3.3 through Figure 3.14 for the spectral periods of 0.01s, 0.2s and 1s, respectively.

Figure 3.3 - Figure 3.14show that the event terms are generally negative (indicating over-prediction) at high frequencies (for T=0.01 and T=0.2s plots) as expected, while they are centered on the zero line at longer periods (T>0.75s). This significant over-prediction at high frequencies does not show a clear trend with magnitude and rake angle. The events terms are "less negative" compared to the analysis results of Gulerce et al. (2016) for NGA-W1 models, showing that the small-magnitude scaling implemented in NGA-West2 model fits better with the magnitude scaling on Turkish strong ground motions. A similar observation for NGA-West 2 GMMs was also stated in Cagnan and Akkar (2019). On the other hand, there is a strong trend in the distribution of event terms with Z_{TOR} for ASK14, CB14 and CY14 models. It should be noted that this trend is not visible in BSSA14 model that employs R_{JB} as the source-to-site-distance metric and does not have a separate Z_{TOR} term. The negative trend increases with Z_{TOR} up to 20km and then stabilizes as the Z_{TOR} scaling of shallow crustal models are typically capped at 20km.

This observation indicates that the Z_{TOR} scaling implemented in NGA-West 2 models is not compatible with the Z_{TOR} scaling in N-TSMD and the base models should be modified (or regionalized for Turkey) before analyzing the systematic source, site, and path effects. The underlying reason for this incompatibility is not clearly recognizable, however, might be related to the stress drop ($\Delta\tau$). The effect of $\Delta\tau$ on ground motion variability has gained increased attention in the last decade (e.g., Baltay et al., 2013; Cotton et al., 2013): recent studies relate the stress drop with the depth of the rupture area and between-event residuals (Satoh and Okazaki, 2016; Oth et al., 2017), finding a clear regional correlation between δB_e and $\Delta\tau$.

The Z_{TOR} scaling of the ASK14 model is given by:

$$f_6(Z_{TOR}) = \begin{cases} a_{15}(T)\left(\frac{Z_{TOR}}{20}\right) \; for \; Z_{TOR} < 20 \; km \\ a_{15}\,(T) for \; Z_{TOR} \; \geq 20 \; km \end{cases} \quad (3.1)$$

where $a_{15}\,(T)$ is the period-dependent regression coefficients and the period dependency of $a_{15}\,(T)$ is shown in Figure 3.15. A similar functional form is selected for the Z_{TOR} adjustment for Turkey as shown in Eq. (3.2) and the new regression coefficient ($a_{15,TR}\,(T)$) is estimated for 21 spectral periods varying between 0.01-10 sec. (please see Figure 3.15 (a) for an example fit at T=0.1 sec residuals of the ASK14 model). Estimated coefficients are smoothed to maintain a smooth spectral shape as shown in Figure 3.15 (b). Figure 3.15 (c) compares the original and estimated regression coefficients for the Z_{TOR} scaling. According to this figure, the $a_{15,TR}\,(T)$ coefficient tries to reverse the applied Z_{TOR} scaling for the ASK14 model and the total Z_{TOR} scaling of the model after the adjustment is very close to zero. In the light of this comparison, instead of adding Eq. (3.2) to the ASK14 model, the Z_{TOR} scaling implemented by the original model is removed completely.

$$f_{6,TR}(Z_{TOR}) = \begin{cases} Z_{TOR} \times a_{15,TR}\,(T) for \; Z_{TOR} < 20 \; km \\ 20 \times a_{15,TR}\,(T) for \; Z_{TOR} \; \geq 20 \; km \end{cases} \quad (3.2)$$

The Z_{TOR} scaling of the CY14 model has the following functional form:

$$\left\{c_7 + \frac{c_{7b}}{\cosh(2 \times \max(M_i - 4.5, 0))}\right\} \Delta Z_{TORi} \quad (3.3)$$

Unlike the ASK14 model, the Z_{TOR} and magnitude effects were not treated independently in regression for the CY14 model. Because the amount and linearity of the negative trend in the residual plots of ASK14 and CY14 models were quite comparable, the Z_{TOR} scaling implemented by the original CY14 model is also removed. After these modifications, the distribution of event terms with magnitude, Z_{TOR} and rake angle is re-plotted and presented in Figure 3.16 - Figure 3.21 for ASK14 and CY14 models. It should be noted that no corrections are applied to the BSS14 and CB14 models. For further analysis, the regionalized ASK14 and CY14 models will be used as the base GMMs.

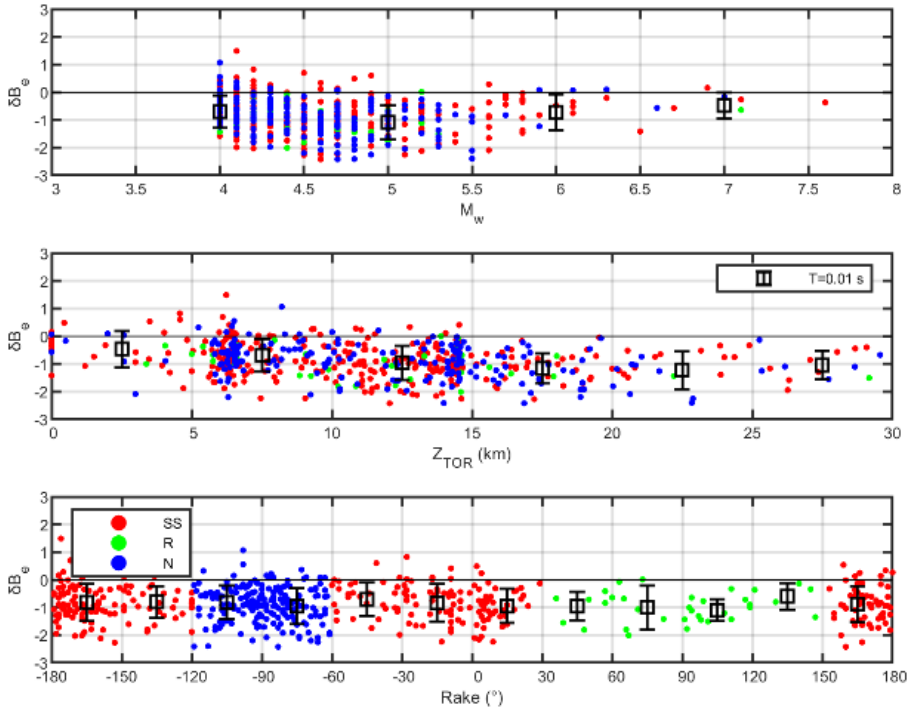

Figure 3.3: Distribution of event terms (δB_e) with moment magnitude (M_w), depth to the top of the rupture (Z_{TOR}) and rake angle for ASK14 at T= 0.01s

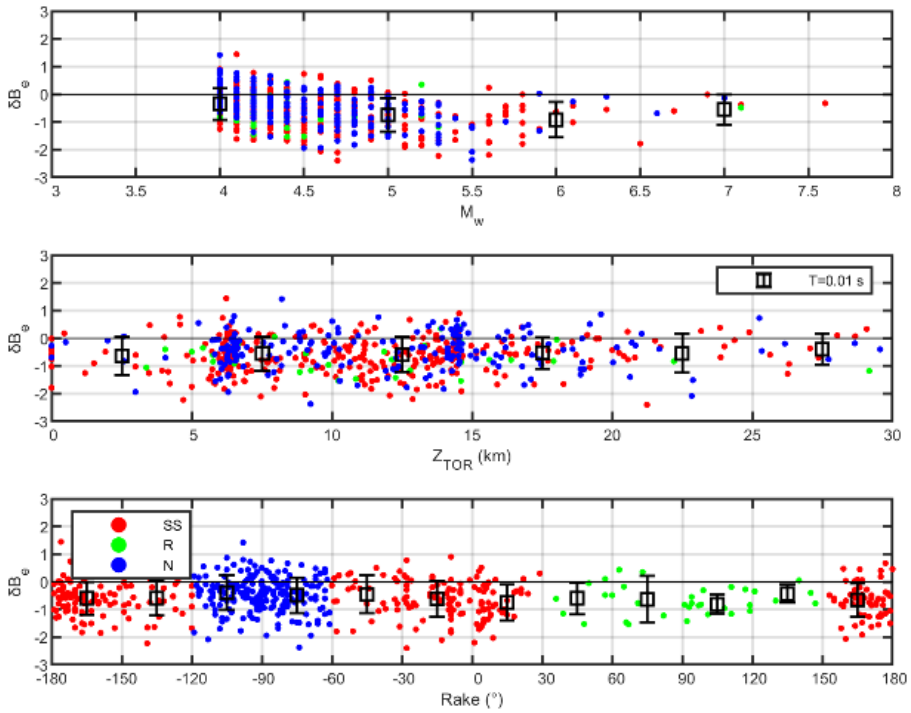

Figure 3.4: Distribution of event terms (δB_e) with moment magnitude (M_w), depth to the top of the rupture (Z_{TOR}) and rake angle for BSSA14 at T= 0.01s

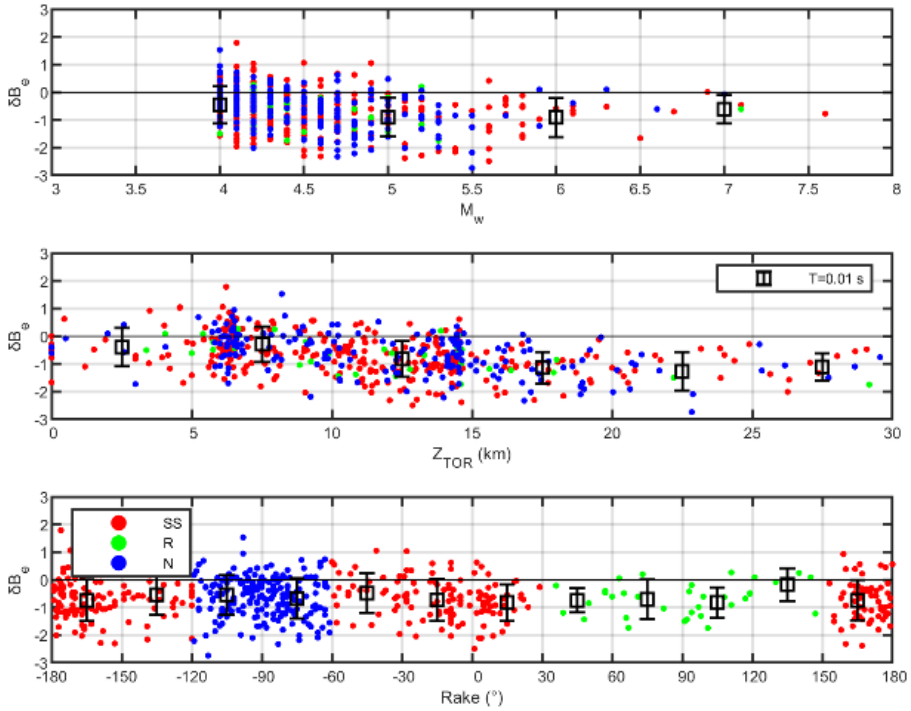

Figure 3.5: Distribution of event terms (δB_e) with moment magnitude (M_w), depth to the top of the rupture (Z_{TOR}) and rake angle for CB14 at T= 0.01s

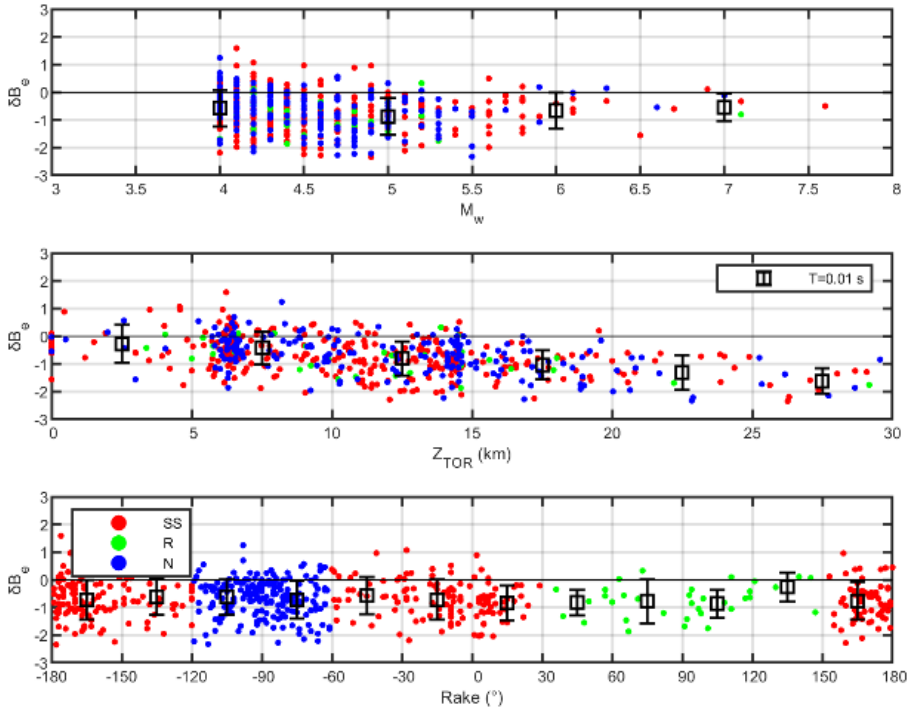

Figure 3.6: Distribution of event terms (δB_e) with moment magnitude (M_w), depth to the top of the rupture (Z_{TOR}) and rake angle for CY14 at T= 0.01s

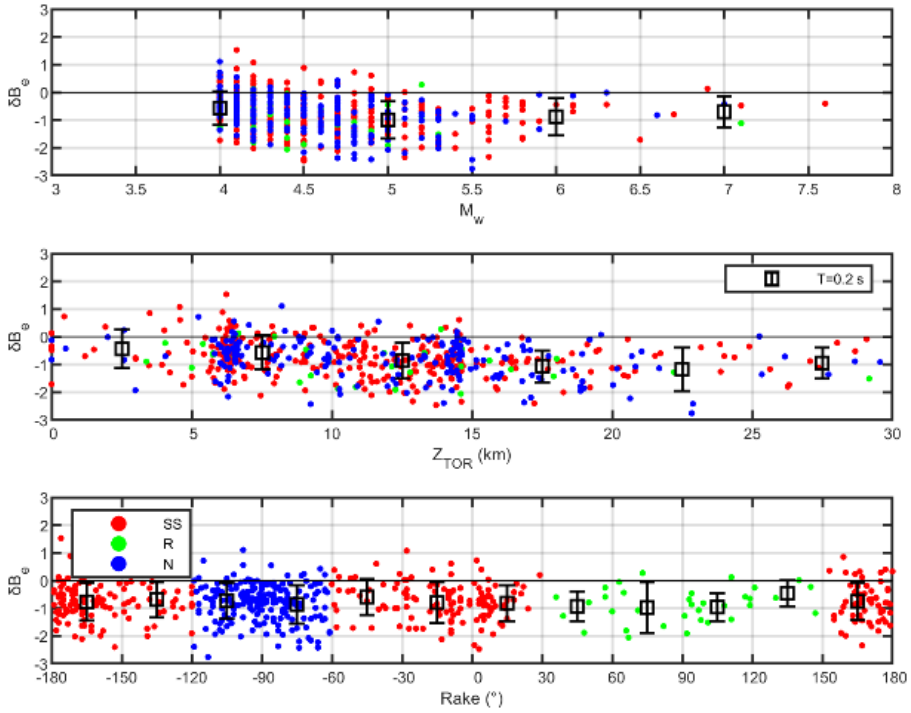

Figure 3.7: Distribution of event terms (δB_e) with moment magnitude (M_w), depth to the top of the rupture (Z_{TOR}) and rake angle for ASK14 at T= 0.2s

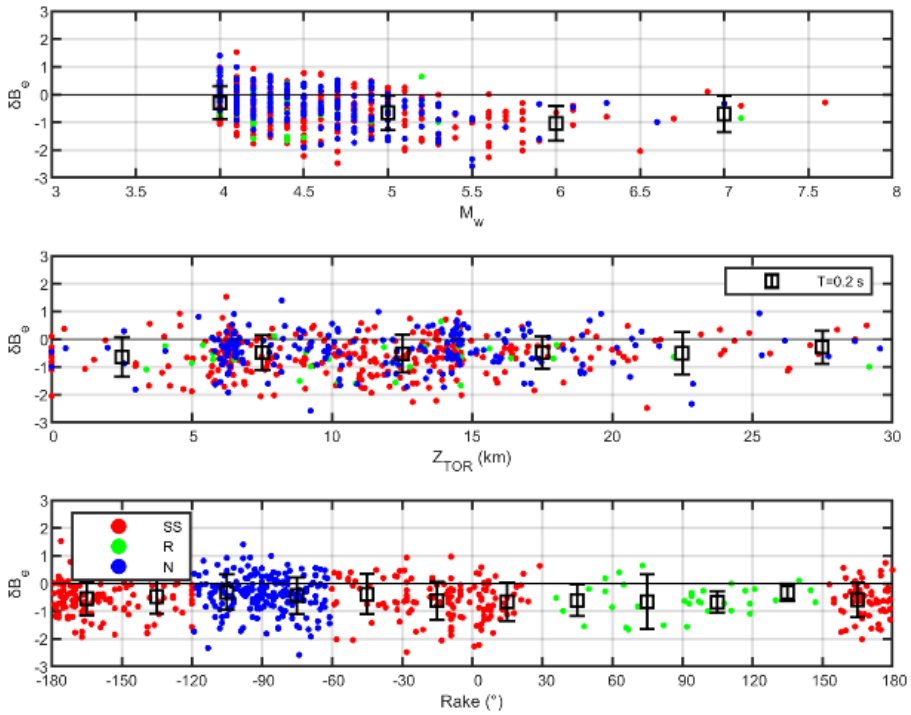

Figure 3.8: Distribution of event terms (δB_e) with moment magnitude (M_w), depth to the top of the rupture (Z_{TOR}) and rake angle for BSSA14 at T= 0.2s

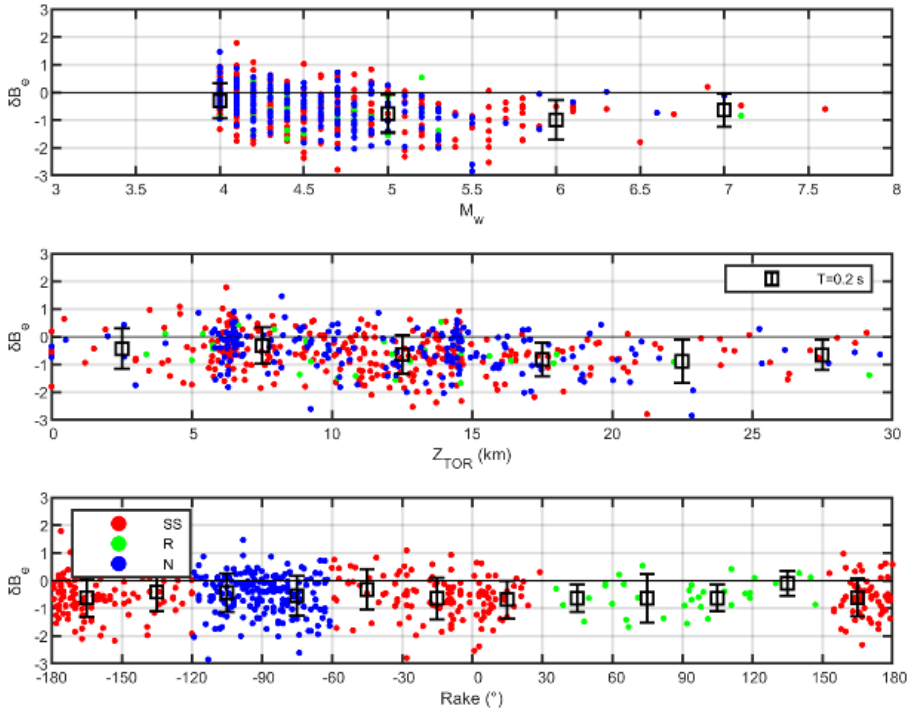

Figure 3.9: Distribution of event terms (δB_e) with moment magnitude (M_w), depth to the top of the rupture (Z_{TOR}) and rake angle for CB14 at T= 0.2s

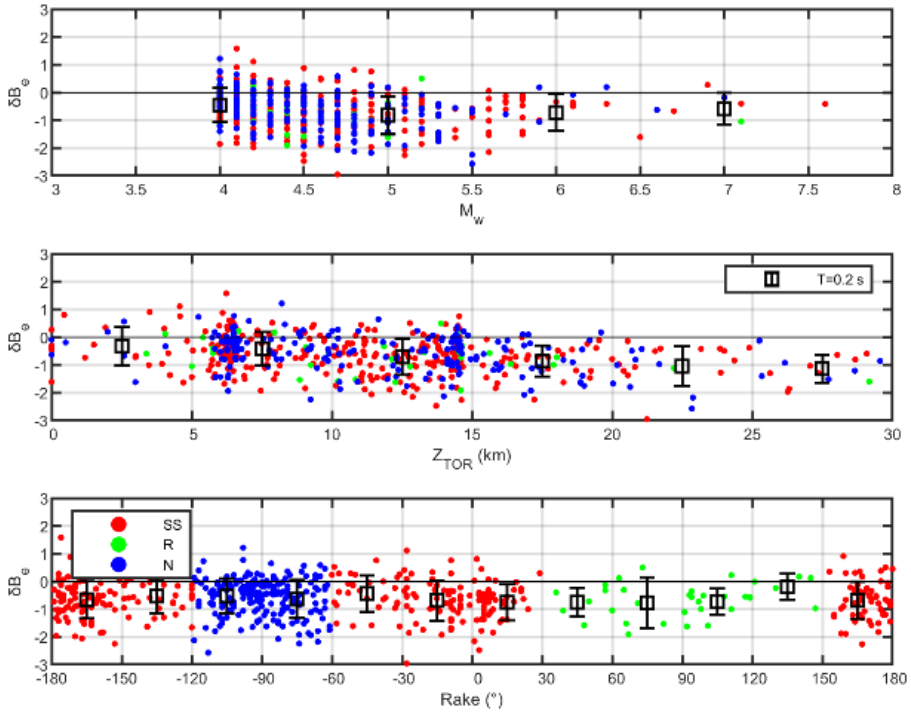

Figure 3.10: Distribution of event terms (δB_e) with moment magnitude (M_w), depth to the top of the rupture (Z_{TOR}) and rake angle for CY14 at T= 0.2s

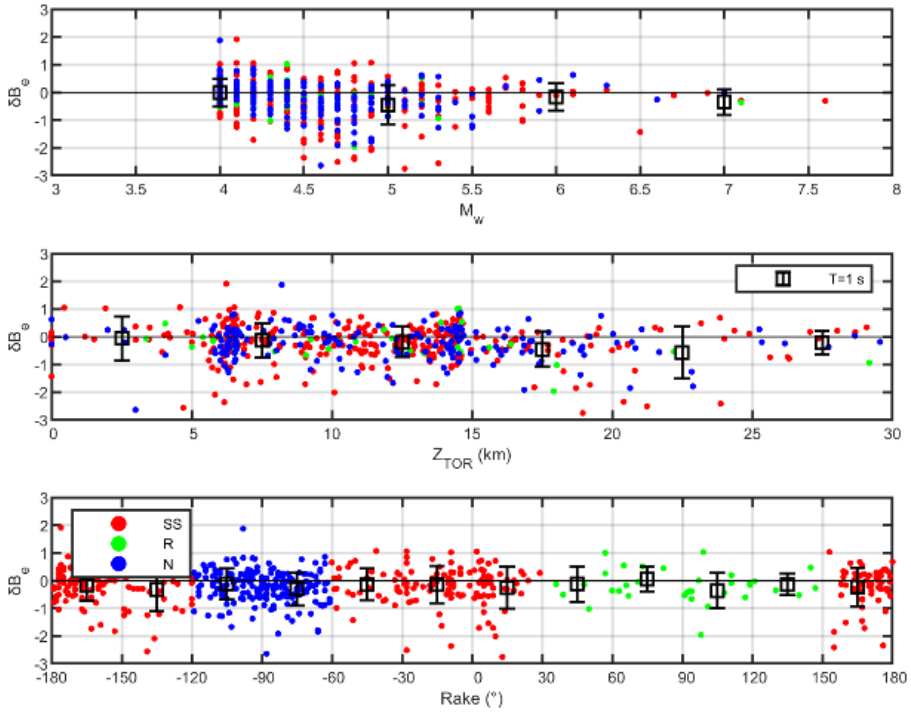

Figure 3.11: Distribution of event terms (δB_e) with moment magnitude (M_w), depth to the top of the rupture (Z_{TOR}) and rake angle for ASK14 at T= 1s

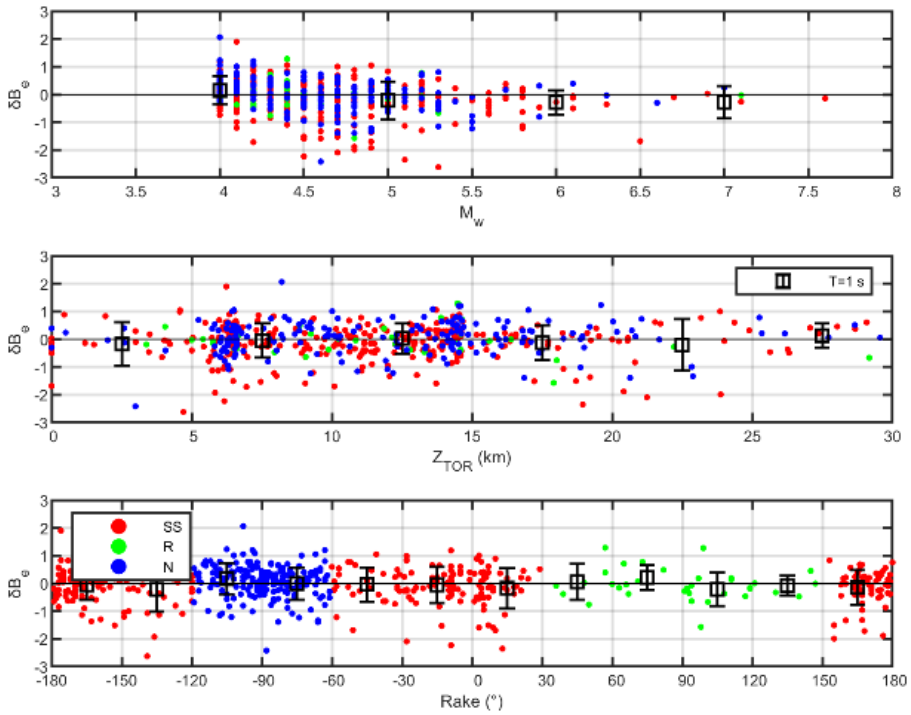

Figure 3.12: Distribution of event terms (δB_e) with moment magnitude (M_w), depth to the top of the rupture (Z_{TOR}) and rake angle for BSSA14 at T= 1s

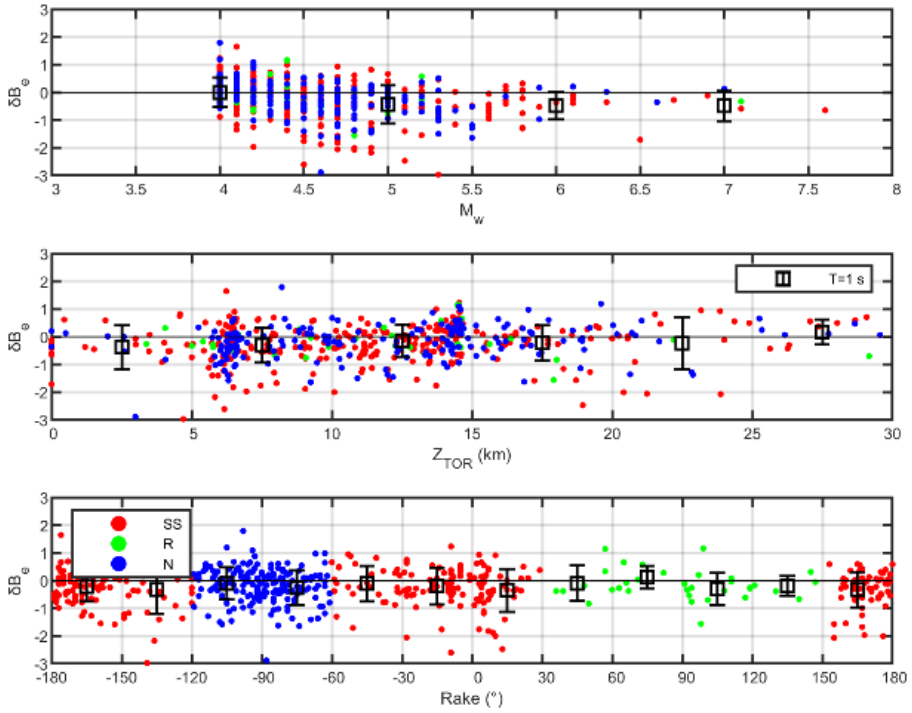

Figure 3.13: Distribution of event terms (δB_e) with moment magnitude (M_w), depth to the top of the rupture (Z_{TOR}) and rake angle for CB14 at T= 1s

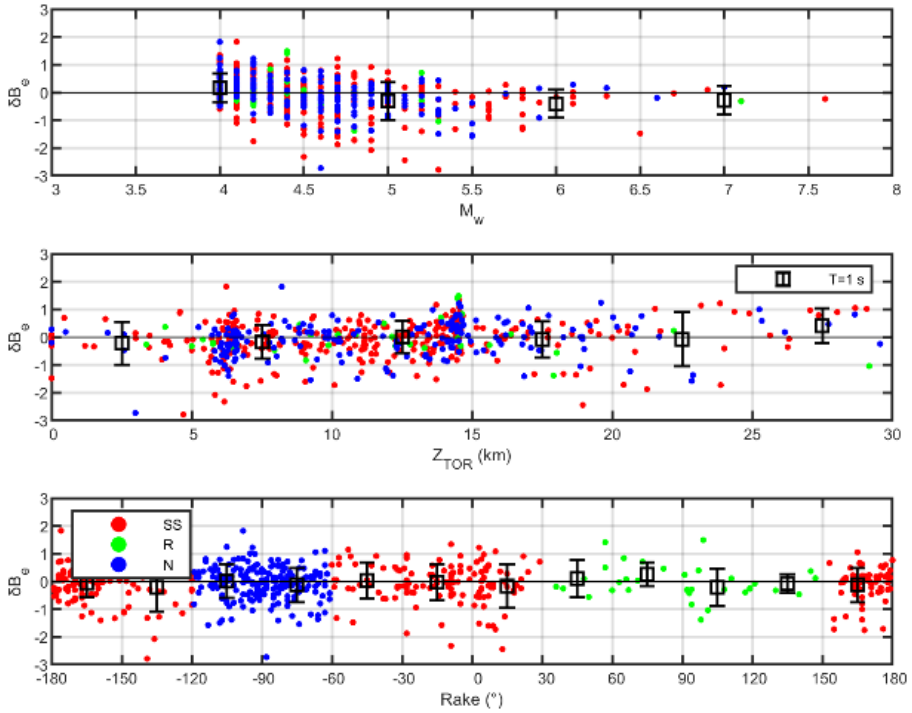

Figure 3.14: Distribution of event terms (δB_e) with moment magnitude (M_w), depth to the top of the rupture (Z_{TOR}) and rake angle for CY14 at T= 1s

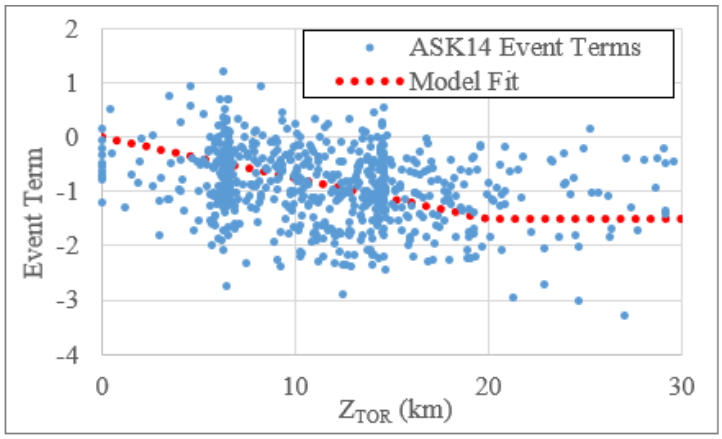

(a)

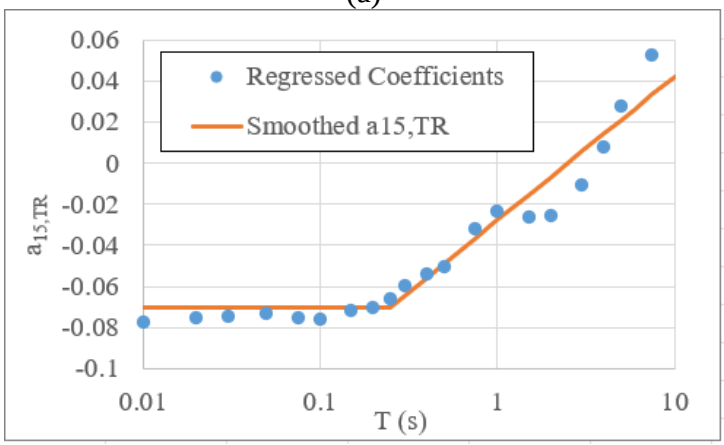

(b)

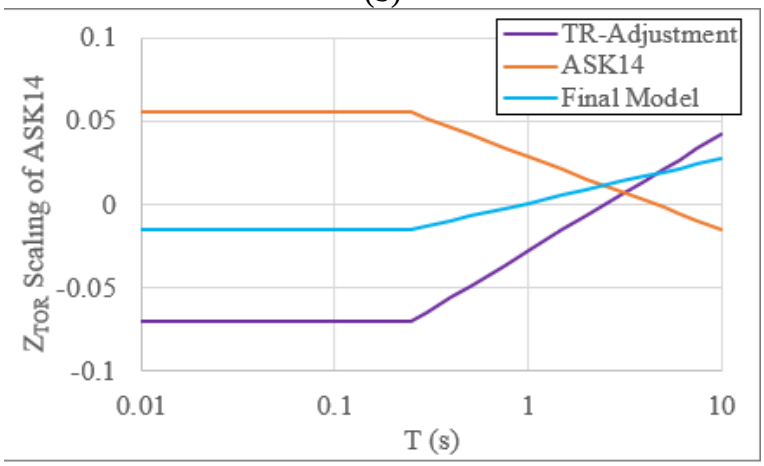

(c)

Figure 3.15: (a) The adjustment applied to the between event residuals of ASK14 model for T= 0.1s, the slope of the red line is $a_{15,TR}$, (b) smoothing applied to regressed $a_{15,TR}$ coefficients, (c) comparison of Z_{TOR} scaling of ASK14 model before and after the applied corrections.

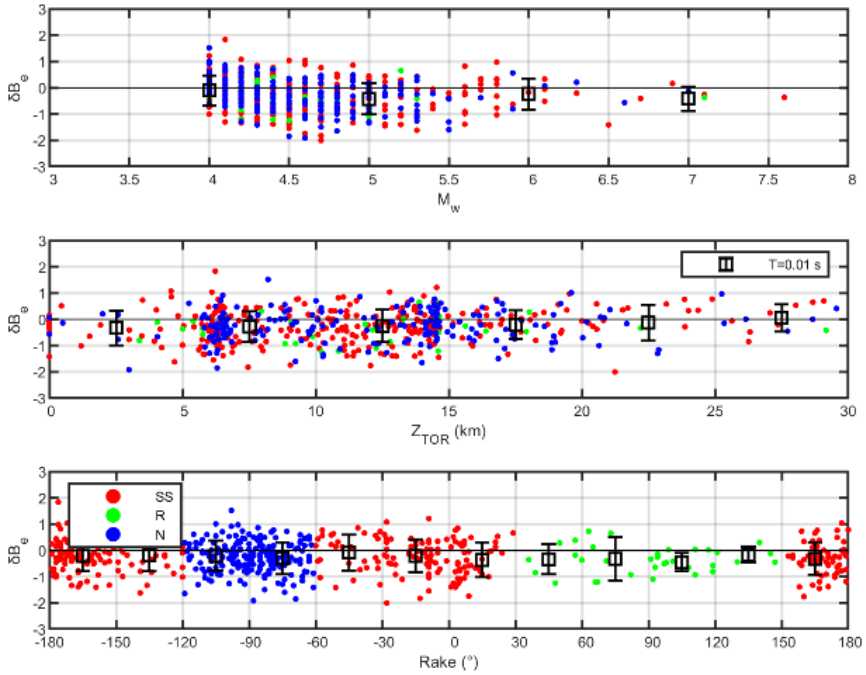

Figure 3.16: Distribution of event terms (δB_e) with moment magnitude (M_w), depth to the top of the rupture (Z_{TOR}) and rake angle for ASK14 at T= 0.01s after the Z_{TOR} correction

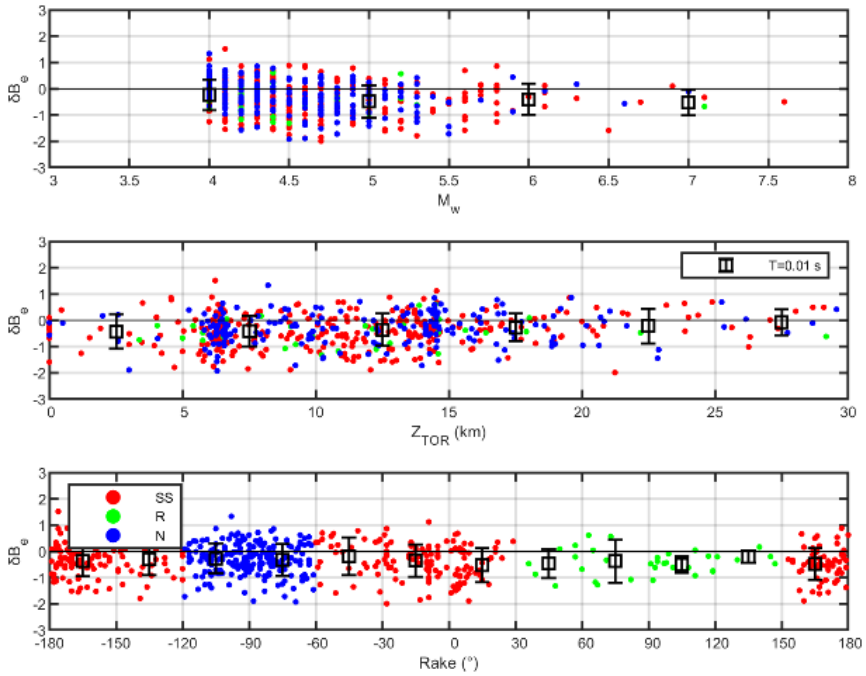

Figure 3.17: Distribution of event terms (δB_e) with moment magnitude (M_w), depth to the top of the rupture (Z_{TOR}) and rake angle for CY14 at T= 0.01s after the Z_{TOR} correction

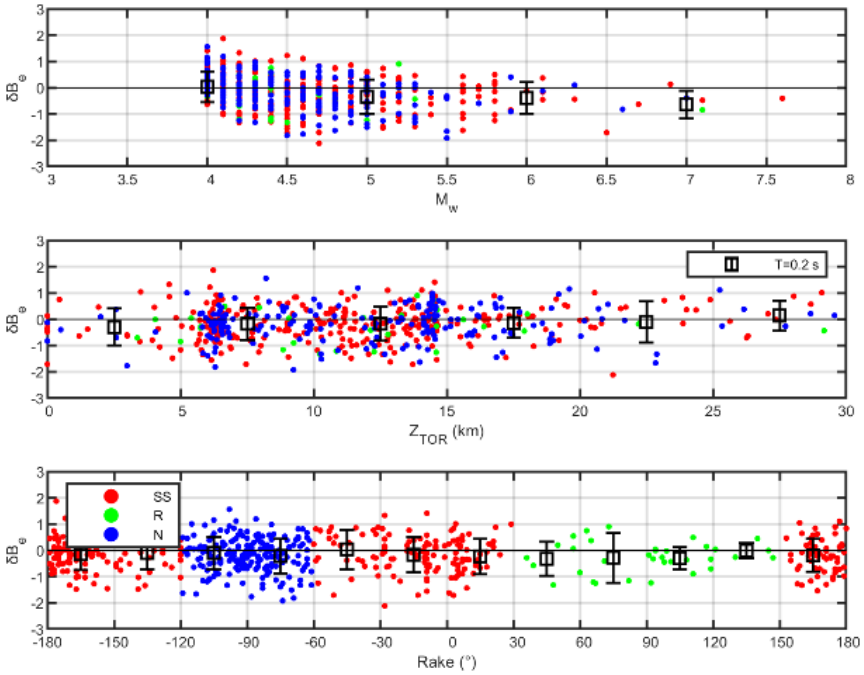

Figure 3.18: Distribution of event terms (δB_e) with moment magnitude (M_w), depth to the top of the rupture (Z_{TOR}) and rake angle for ASK14 at T= 0.2s after the Z_{TOR} correction

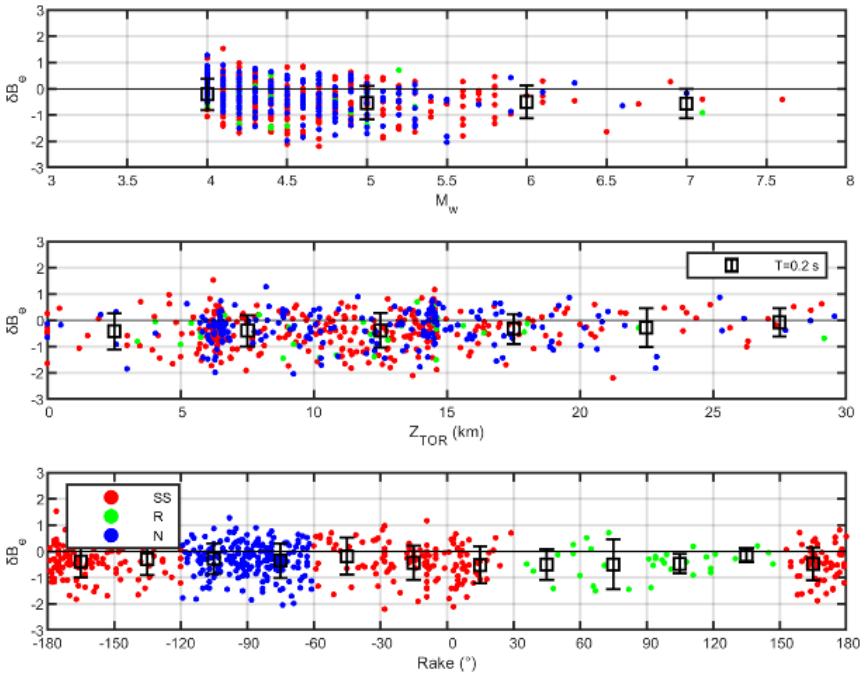

Figure 3.19: Distribution of event terms (δB_e) with moment magnitude (M_w), depth to the top of the rupture (Z_{TOR}) and rake angle for CY14 at T= 0.2s after the Z_{TOR} correction

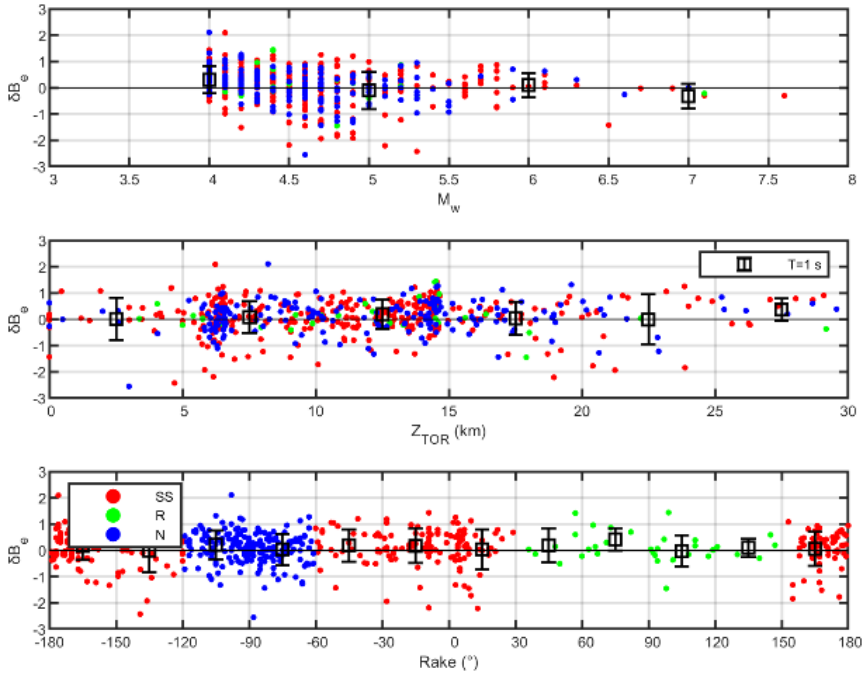

Figure 3.20: Distribution of event terms (δB_e) with moment magnitude (M_w), depth to the top of the rupture (Z_{TOR}) and rake angle for ASK14 at T= 1s after the Z_{TOR} correction

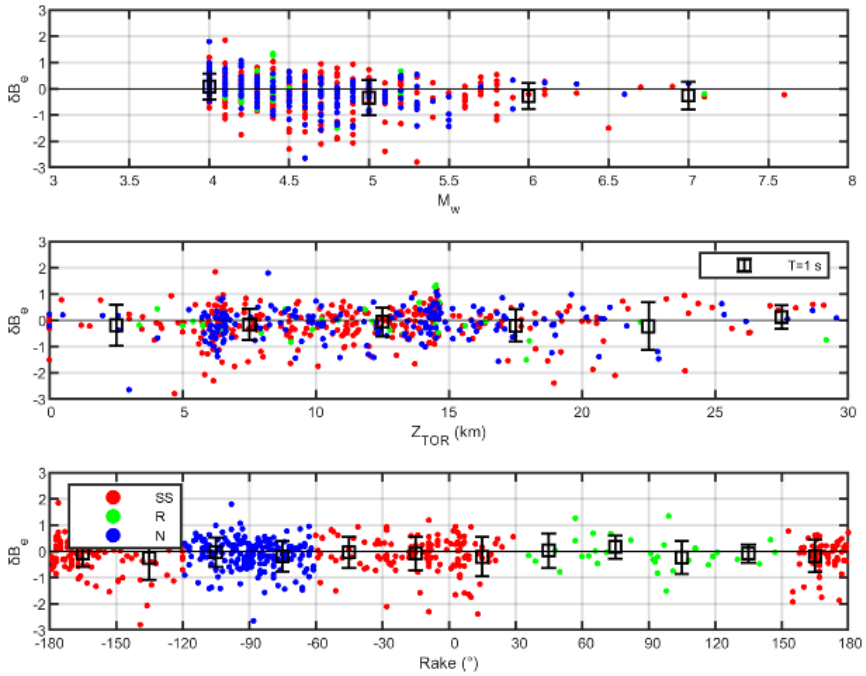

Figure 3.21: Distribution of event terms (δB_e) with moment magnitude (M_w), depth to the top of the rupture (Z_{TOR}) and rake angle for CY14 at T= 1s after the Z_{TOR} correction

According to Figure 3.16 - Figure 3.21, removing the Z_{TOR} scaling implemented in the original ASK14 and CY14 models resulted in a significant improvement in the negative trends in the residuals. The improvement is more visible at smaller periods where the effect of Z_{TOR} scaling is stronger. However, a slightly negative trend persists, especially for moderate to large magnitude events with relatively smaller Z_{TOR} values. This negative trend still seems to be independent of the style-of-faulting.

To ensure the unbiased distribution of the event terms, a small additional adjustment is applied to ASK14 and CY14 models in form of a slight shift in the model constants. This change in the model's constant coefficient is in principle similar to the regional constants applied to the NGA-West2 GMMs for regions other than Western US. For this adjustment, the average of the event terms (δB_e) are calculated for each period (blue dots in Figure 3.22) and smoothed as shown with the red lines of Figure 3.22. The positive values after T=3s are ignored as the number of recordings decreases significantly at these periods. After this final adjustment, the distribution of event terms of TR-adjusted ASK14 and CY14 GMMs are re-calculated and presented in Figure 3.23 through Figure 3.28, showing that the distribution of between event residuals with magnitude, Z_{TOR} and rake angle are now unbiased, especially for CY14 model. For ASK14 model, the residuals of small magnitude (and Z_{TOR} >20km) events are now slightly positive.

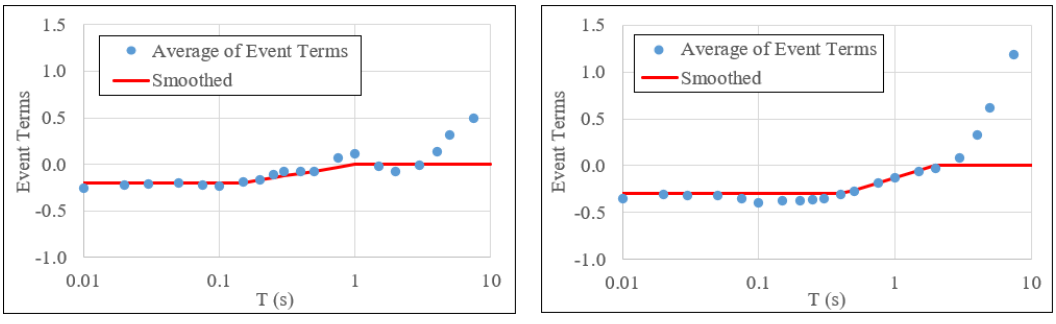

(a) (b)

Figure 3.22: The adjustment applied to the between event residuals of (a) ASK14, (b) CY14 models in form of a constant shift.

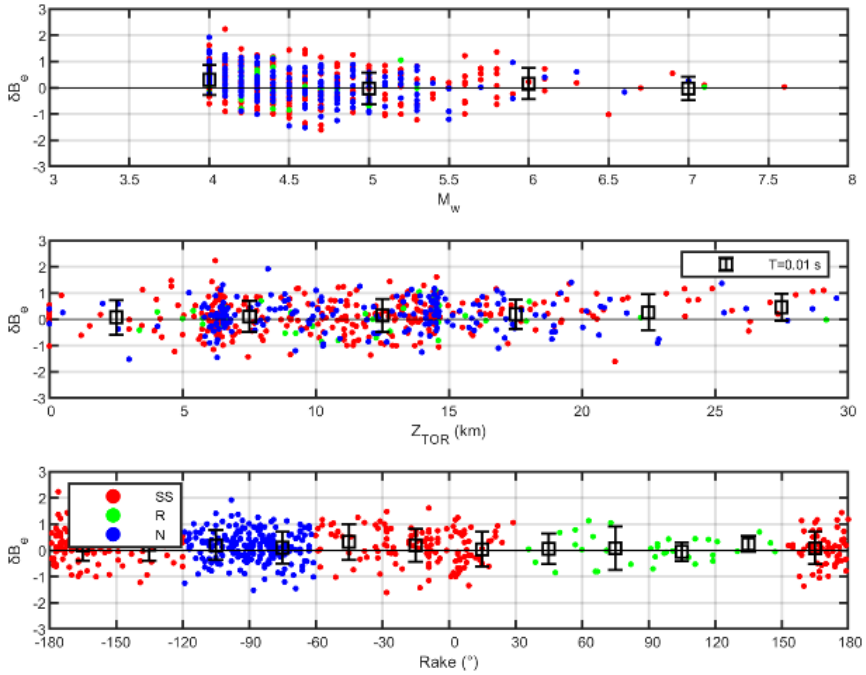

Figure 3.23: Distribution of event terms (δB_e) with moment magnitude (M_w), depth to the top of the rupture (Z_{TOR}) and rake angle for TR-Adjusted ASK14 at T= 0.01s

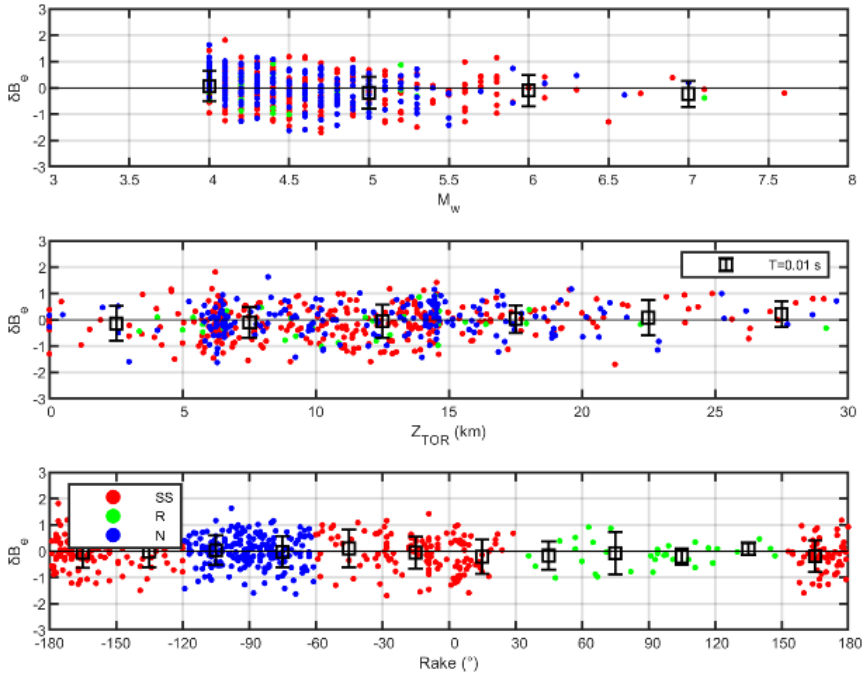

Figure 3.24: Distribution of event terms (δB_e) with moment magnitude (M_w), depth to the top of the rupture (Z_{TOR}) and rake angle for TR-Adjusted CY14 at T= 0.01s

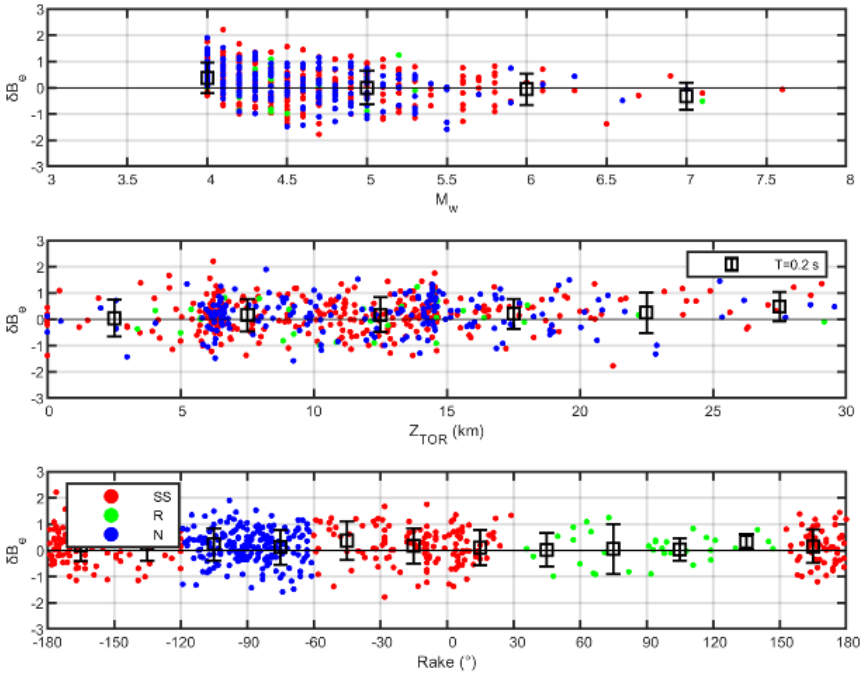

Figure 3.25: Distribution of event terms (δB_e) with moment magnitude (M_w), depth to the top of the rupture (Z_{TOR}) and rake angle for TR-Adjusted ASK14 at T= 0.2s

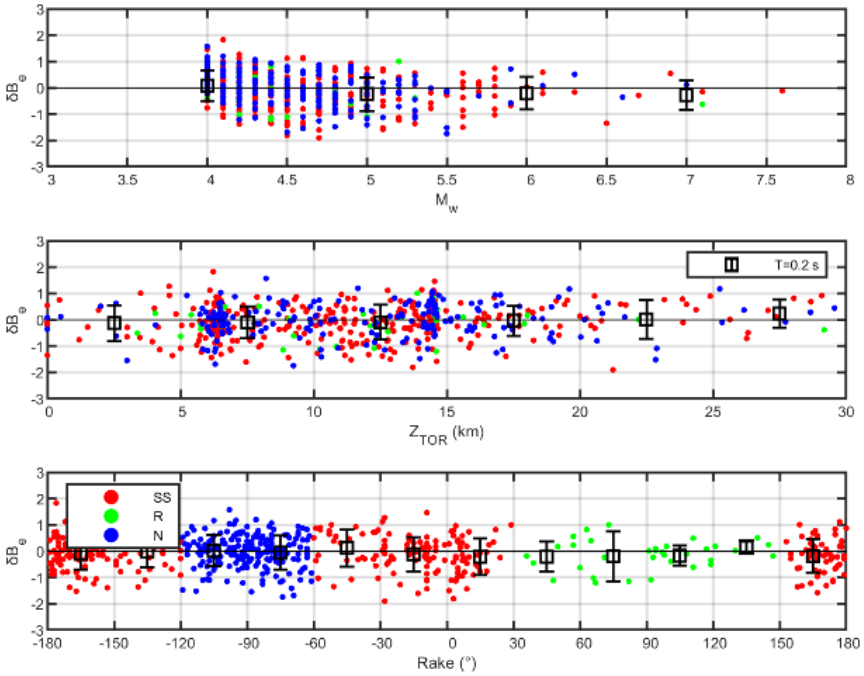

Figure 3.26: Distribution of event terms (δB_e) with moment magnitude (M_w), depth to the top of the rupture (Z_{TOR}) and rake angle for TR-Adjusted CY14 at T= 0.2s

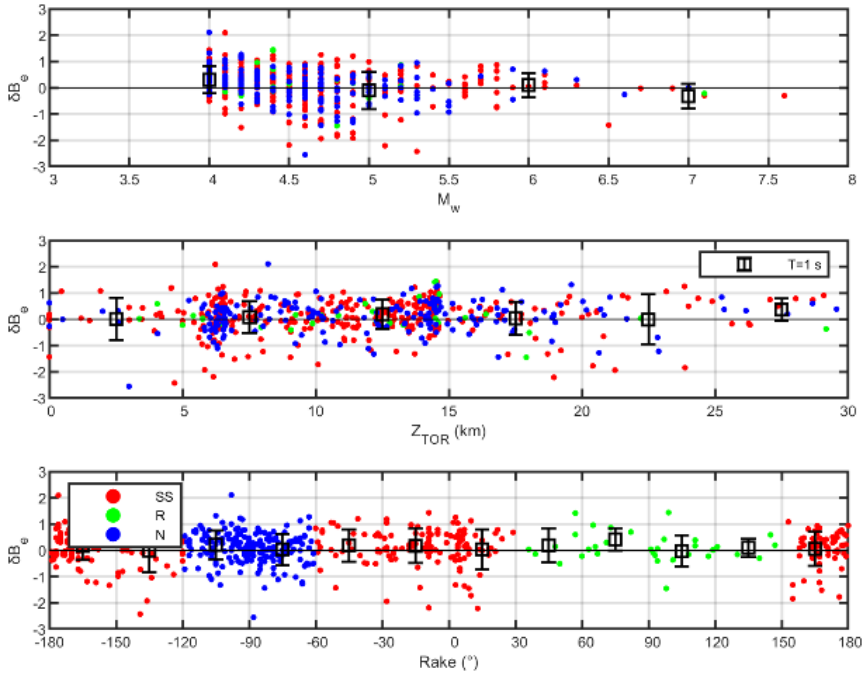

Figure 3.27: Distribution of event terms (δB_e) with moment magnitude (M_w), depth to the top of the rupture (Z_{TOR}) and rake angle for TR-Adjusted ASK14 at T= 1s

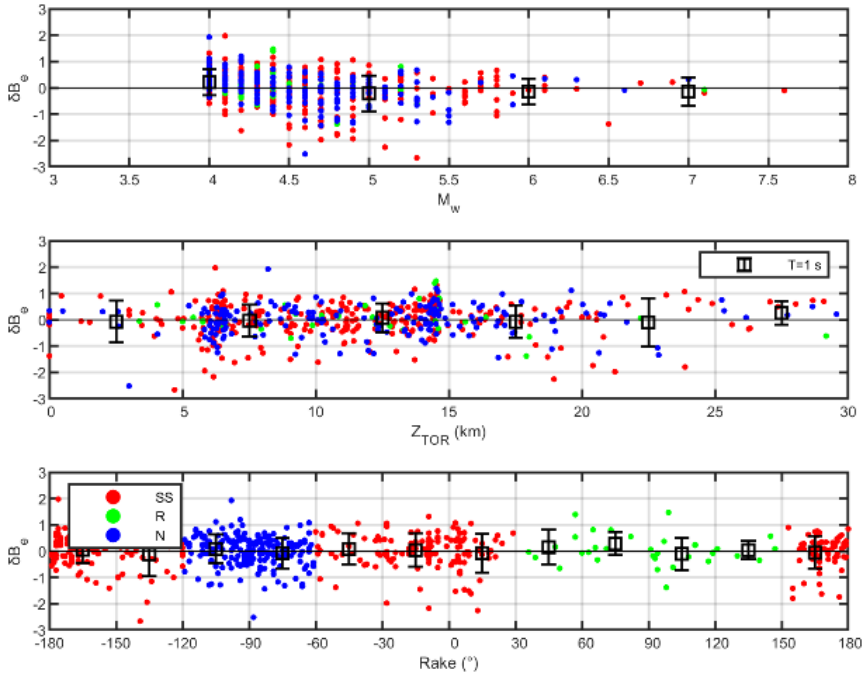

Figure 3.28: Distribution of event terms (δB_e) with moment magnitude (M_w), depth to the top of the rupture (Z_{TOR}) and rake angle for TR-Adjusted CY14 at T= 1s

3.3 Spatial Distribution of Event Terms and Between-Event Variability Model for Turkey

To analyze the location-to-location variability in regression that is captured by the between-event random-effects group, the color-coded event terms (δB_e) for the regionalized GMMs are plotted over geology constructed from 1/500.000 scaled geological maps of Turkey published by General Directorate of Mineral Exploration and Research (MTA). In Figure 3.29 through Figure 3.36, the spatial distribution of δB_e for TR-Adjusted ASK14 and TR-Adjusted CY14 models at four spectral periods (T=0.01s, 0.2s, 1s and 2s) are provided with warm colors showing positive (underestimation) and cool colors showing negative (over-estimation) event terms. According to these figures:

- The spatial distribution of event terms for regionalized ASK14 and CY14 models are very similar to each other for each spectral period, indicating that the applied adjustments to the original models remove the model-specific source scaling effects.
- Majority of the event terms lies between -0.25< δB_e <0.25 (in ln units, shown by green points) for longer periods (T=1 and 2 sec); while the number of δB_e values out of this range is significant at short periods. This observation is somehow in accordance with the physics behind the ground motion estimations: the source characteristics are more dominant at higher frequencies and not as controlling at longer periods.

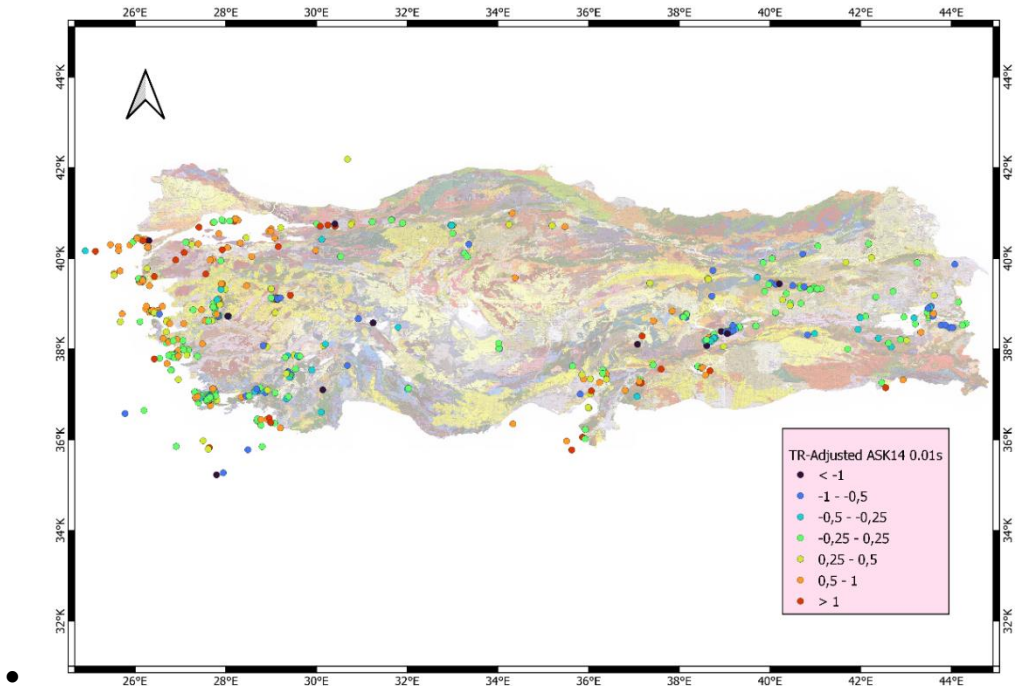

Figure 3.29: Spatial distribution of event terms (δB_e) for TR-Adjusted ASK14 at period 0.01s

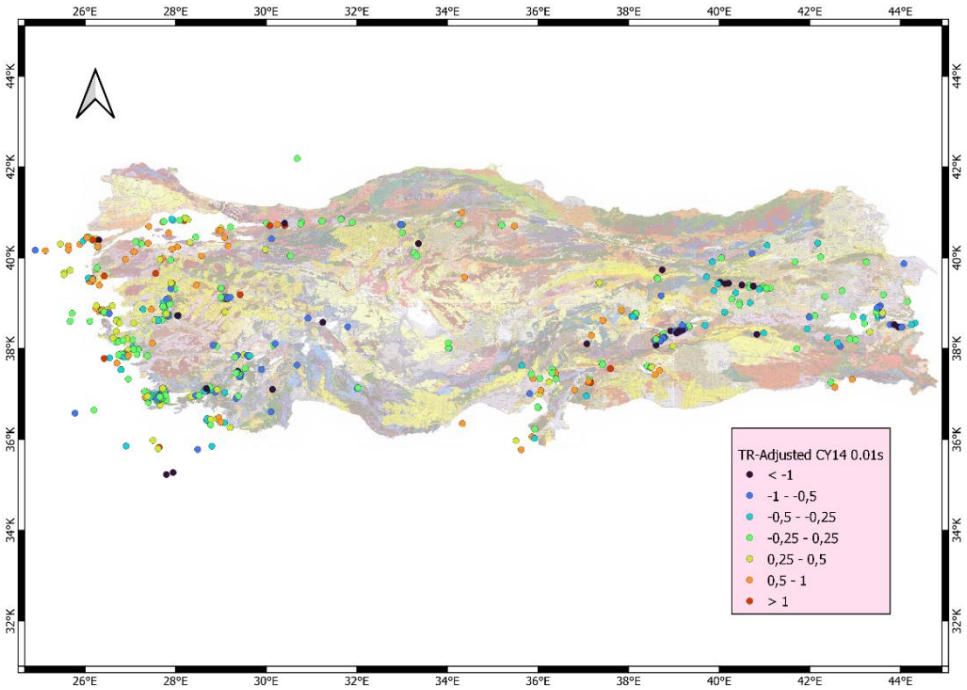

Figure 3.30: Spatial distribution of event terms (δB_e) for TR-Adjusted CY14 at period 0.01s

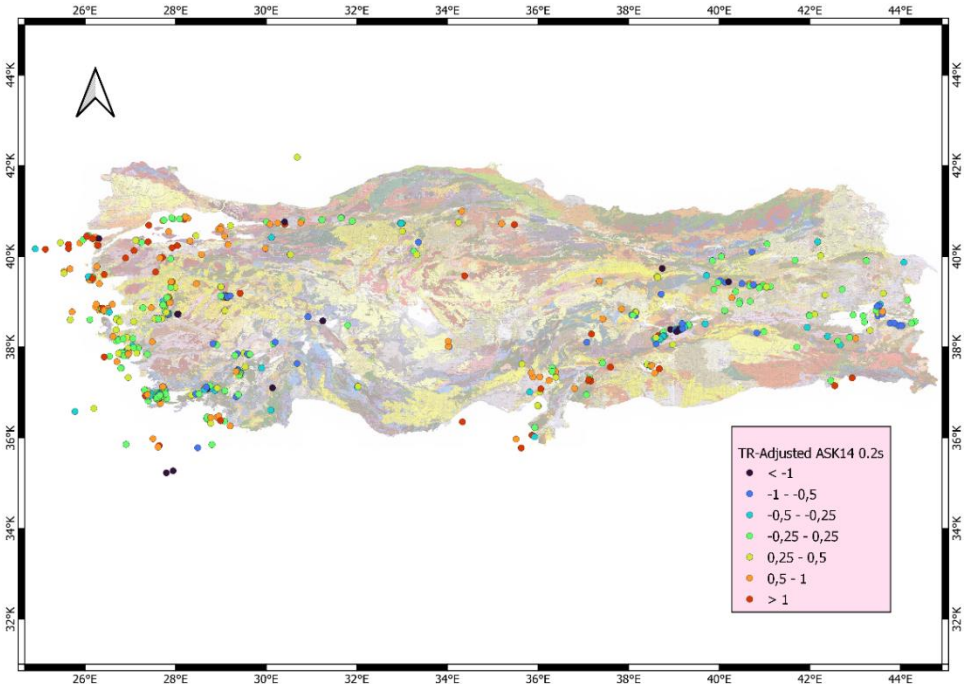

Figure 3.31: Spatial distribution of event terms (δB_e) for TR-Adjusted ASK14 at period 0.2s

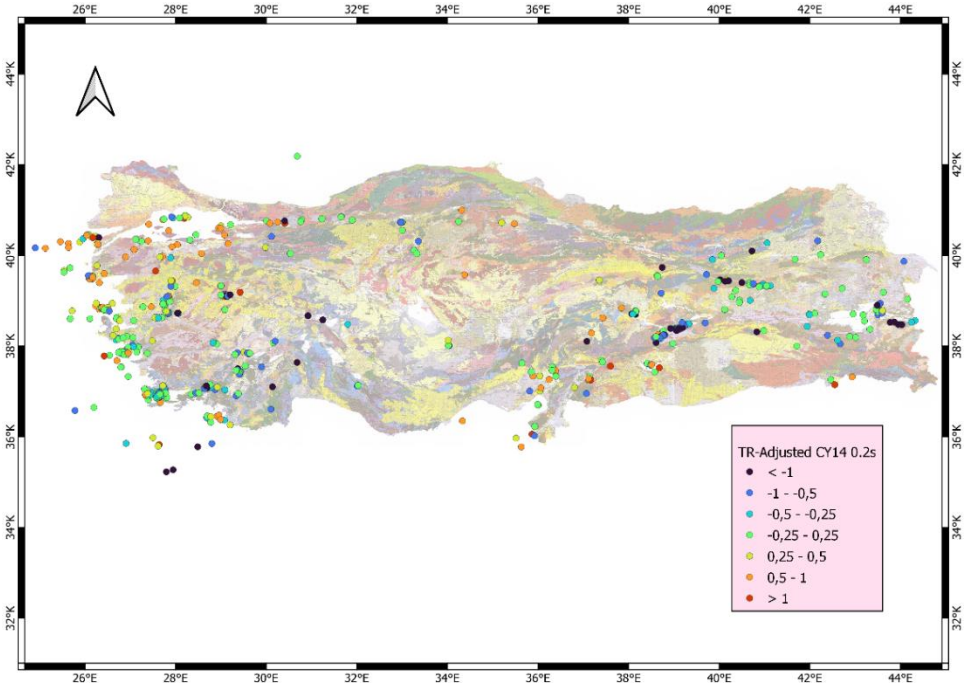

Figure 3.32: Spatial distribution of event terms (δB_e) for TR-Adjusted CY14 at period 0.2s

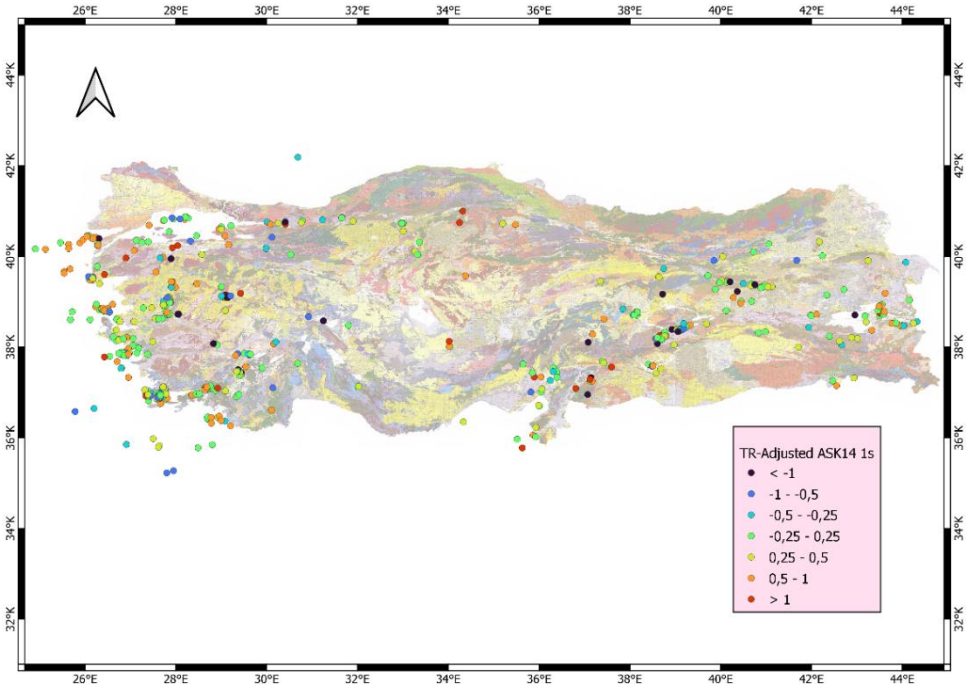

Figure 3.33: Spatial distribution of event terms (δB_e) for TR-Adjusted ASK14 at period 1s

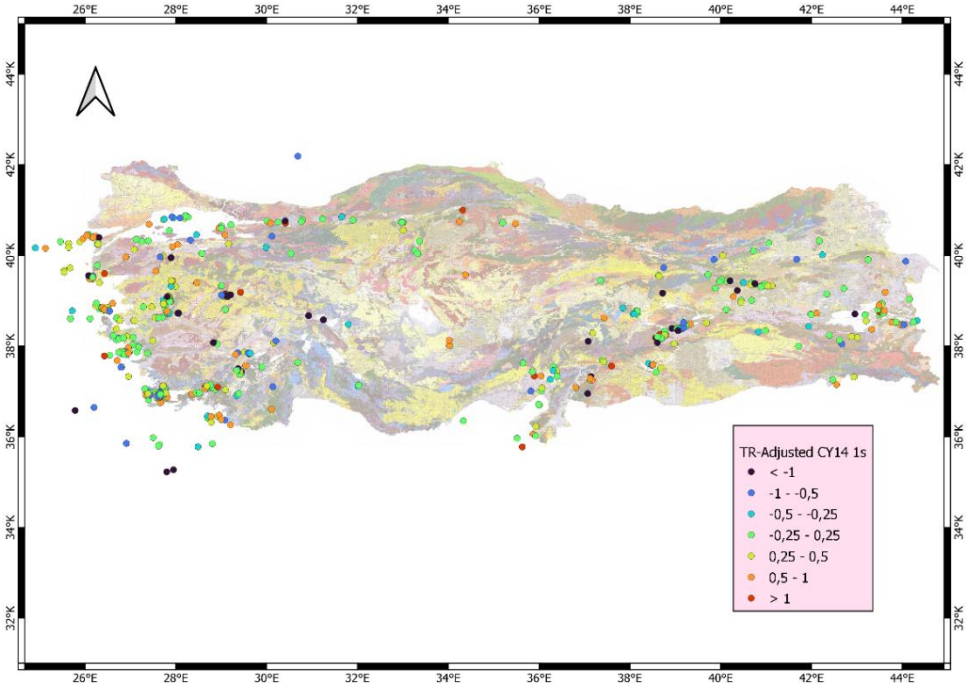

Figure 3.34: Spatial distribution of event terms (δB_e) for TR-Adjusted CY14 at period 1s

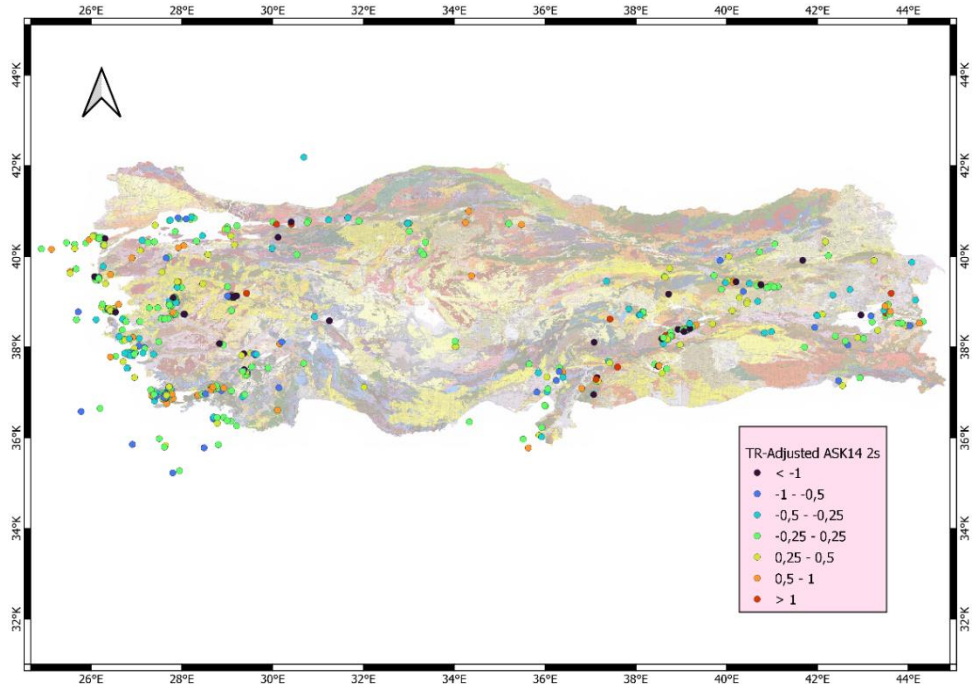

Figure 3.35: Spatial distribution of event terms (δB_e) for TR-Adjusted ASK14 at period 2s

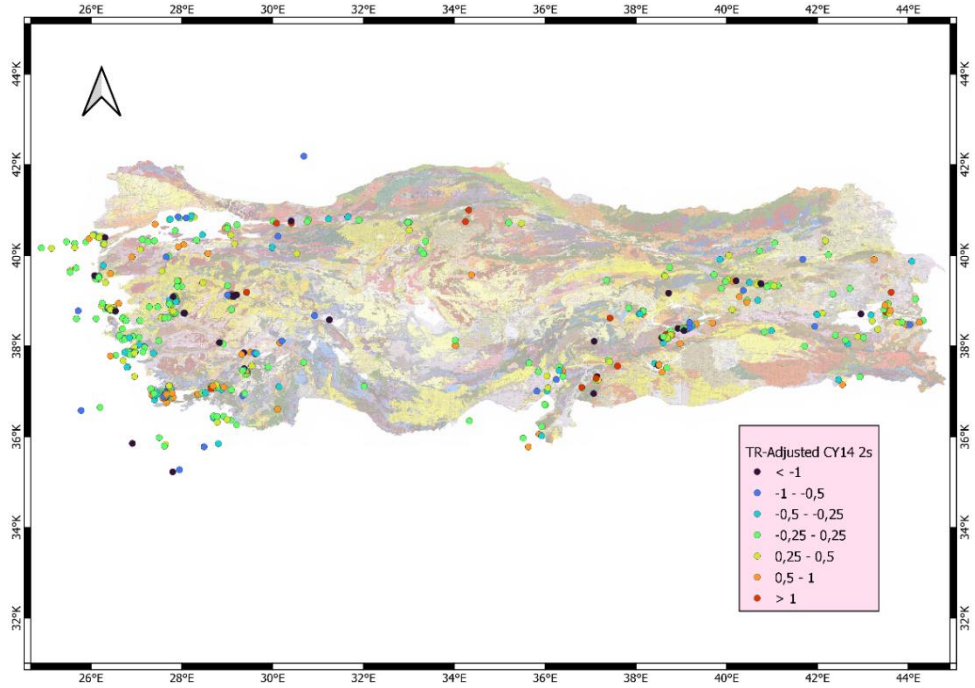

Figure 3.36: Spatial distribution of event terms (δB_e) for TR-Adjusted CY14 at period 2s

- Spatial distribution of short period event terms for both GMMs show some noticeable geographic correlations. Based on these observations, five main domains as Marmara, Western Anatolia, Southwestern Anatolia, East Anatolian Plateau, and the vicinity of Amanos and Maraş Blocks are defined (and numbered as Region #1,2,3,4 and 5, respectively) as shown in Figure 3.37. Due to the sparse distribution of events, no domains are defined for Central Anatolia and Black Sea blocks.
- Marmara region and East Anatolian Plateau dominated clearly by positive and negative event terms, respectively. Most of the earthquakes in the Marmara region are under-estimated (in average, independent of the station) by the TR-adjusted ASK14 and CY14 models, even if these models are unbiased for the complete Turkish dataset. Similarly, majority of the earthquakes occurred in the East Anatolian Plateau are over-estimated (in average, independent of the station) by the TR-adjusted ASK14 and CY14 models. In general, the event terms lean towards positive in the vicinity of Amanos and Maraş Blocks and across Western Anatolia and lean towards negative in Southwestern Anatolia.

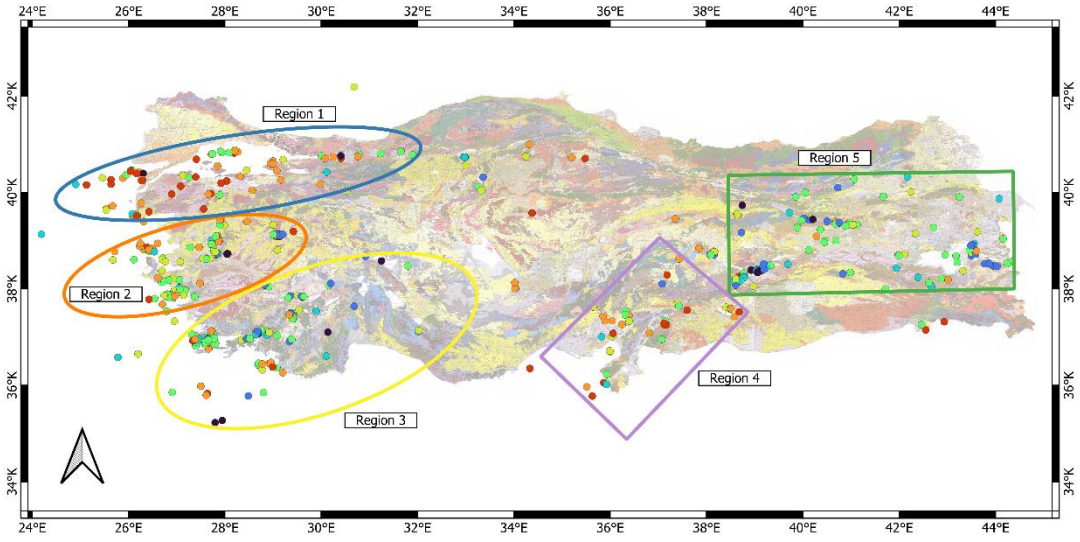

Figure 3.37: Main domains selected to represent the location-to-location variability in regionalized ASK14 and CY14 GMMs

- The average values of δB_e are calculated at 21 spectral periods for these five domains and presented in Figure 3.38(a) and Figure 3.39(a) for TR-adjusted ASK14 and CY14 models, respectively. Estimated averages are in good agreement with the visual interpretations. The average δB_e for Region#1 (Marmara) and Region#4 (Amanos-Maras Blocks) are quite positive at short-to-medium periods (T<1sec) and reaches to almost zero at longer periods. Region#2 (Western Anatolia) also has positive average δB_e values at shorter periods. For these regions, the ground motions will be underestimated if the regionalized TR-adjusted ASK14 and CY14 models are utilized in seismic hazard assessment. Theoretically, observed underestimations within these regions can be linked to high earthquake stress drops. It is worth to note that these regions interact widely with older geologic terranes such as metamorphic core complexes and ongoing deformations are highly partitioned by active fault systems which may explain the origin of high stress drop events.
- The average δB_e values for Region#3 (Southwestern Anatolia) and Region#5 (East Anatolian Plateau) are negative for short periods, reaching to zero after T>1sec. If the regionalized TR-adjusted ASK14 and CY14 models are utilized in seismic hazard assessment for these regions, the ground motions will be overestimated. Both East Anatolian Plateau and SW Anatolia are controlled by dynamic mantle processes including slap break-off and tearing that results in relatively hot and weak lithosphere displaying high seismic attenuation. Thus, observed overestimations in these regions can be linked to earthquakes with lower stress drops likely associated to reduced stress state.
- Comparing Figure 3.38(a) and Figure 3.39(a) shows that the average of positive domains (Regions 1, 2, and 4) are higher for TR-adjusted ASK14 when compared to TR-adjusted CY14. Similarly, the average of negative domains (Regions 3 and 5) is more negative for TR-adjusted CY14 when compared to TR-adjusted ASK14. This difference is related to the average

δB_e values for the whole dataset: due to the slightly positive residuals of regionalized ASK14 model in small magnitude events, the total average δB_e is not zero at shorter periods (broken black line in Figure 3.38(a)). This observation underlines the need for using multiple GMMs in hazard estimations to capture the epistemic uncertainty.

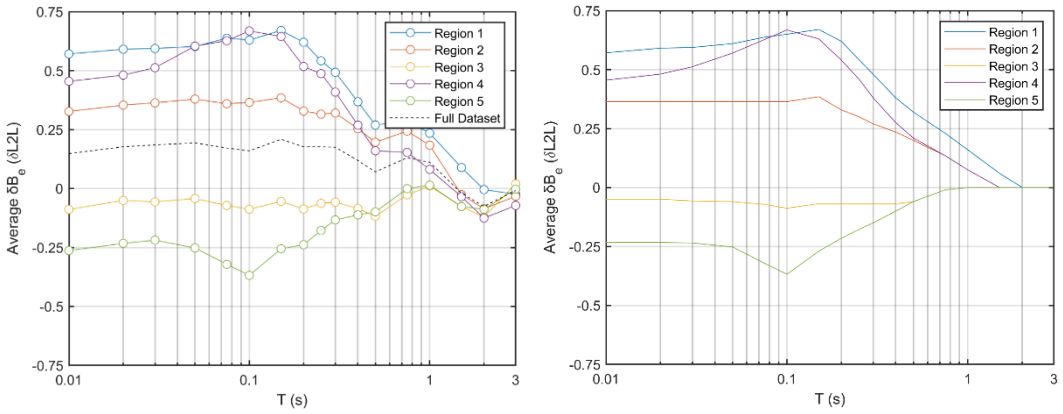

(a) (b)

Figure 3.38: Regional averages of event terms (δB_e) for TR-Adjusted ASK14

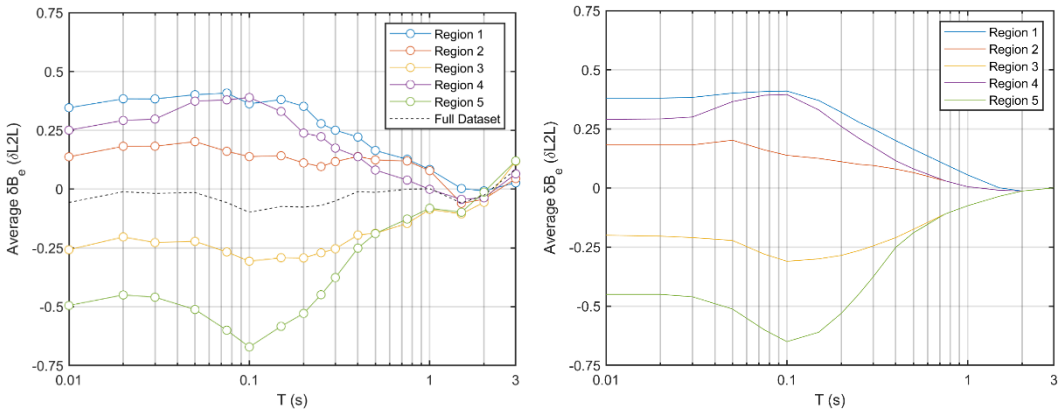

(a) (b)

Figure 3.39: Regional averages of event terms (δB_e) for TR-Adjusted CY14

Figure 3.40(a) and Figure 3.41(a) compares the between-event standard deviations (a.k.a the τ values) estimated from the N-TSMD with the between-event standard deviations of the original ASK14 and CY14 models. Both GMMs have magnitude dependent, linear and smoothed τ models with break points at M=5 and

M=7, therefore, the τ values for M>7 and M<5 earthquakes are provided in Figure 3.40(a) and Figure 3.41(a). The between-event standard deviations calculated from the full dataset (≈0.6 ln units) are significantly higher than the between-event variability embedded in the original models (varying between 0.3-0.5 ln units). An initial attempt of comparing the between-event variabilities was made by in Gulerce et al. (2016) for NGA-West1 GMMs using a relatively small Turkish strong motion dataset. Gulerce et al. (2016) had calculated the τ values varying between 0.6-0.8 (ln units) for four NGA-West1 models with no clear magnitude dependence and not applied any corrections to the τ values. Figure 3.40(a) also compares the estimated τ values with the between-event standard deviations of Kale et al. (2015) GMM (called hereafter KA15) (digitized from Cagnan and Akkar, 2019), showing that the new τ estimates are very similar to the τ estimates of Cagnan and Akkar (2019), especially at short periods. This reduction in the between-event variability over the last 6-7 years is related to the improvements in the compiled event metadata and the changes implemented in small magnitude scaling of NGA-West 2 GMMs. New estimates of τ do not have a clear magnitude dependence as well; however, stable enough for developing a between-event variability model for Turkey.

Figure 3.40 and Figure 3.41 shows an increase in the τ at short periods, which has also been observed in other datasets and has been called the ‘‘bump in τ’’ (Abrahamson and Gulerce, 2022). As discussed in detail in Abrahamson and Gulerce (2022), there is no clear physical reason for the between-event variability to have a large increase around T = 0.1s. It is more likely that regional site effects (e.g. differences in the high-frequency attenuation) manifest itself in the δB_e term. It should be noted that the ‘‘bump in τ’’ observed in Figure 3.40 and Figure 3.41 are much less prominent that the bump in the NGA-Subduction dataset. Following the simplification applied to the τ-model by Abrahamson and Gulerce (2022), a magnitude independent τ-model is proposed for TR-adjusted ASK14 and CY14 models as shown in Figure 3.40(a) and Figure 3.41(a) with the red line, which is applicable to Turkey in general.

In addition to the τ-model applicable to Turkey, region-specific magnitude-independent non-ergodic τ-models are developed for Regions 1-5 by smoothing the data points in Figure 3.40(b) and Figure 3.41(b) and presented in Figure 3.40(c) and Figure 3.41(c). Please note that the region-specific τ values are generally lower than the TR-specific τ values. The level of reduction in τ is different for every region: for example, Region 5 has up to 25% lower standard deviations at short periods as compared to the values from the TR-specific model. On the other hand, no reduction can be observed for Region 4 up to 0.1 s and due to the limited number of events in this region the values exhibit an abnormal behavior after 0.3s. Since the abnormal values are caused by the lack of sufficient number of events, these values are ignored at the smoothing step. As discussed in the previous section, the effect of source parameters become less prominent, which limits the extent of the τ reduction at long periods. The region specific τ values are equal to the TR-specific τ values after T=1s spectral periods for both models. The region-specific τ-model coefficients are summarized in Table 3.1.

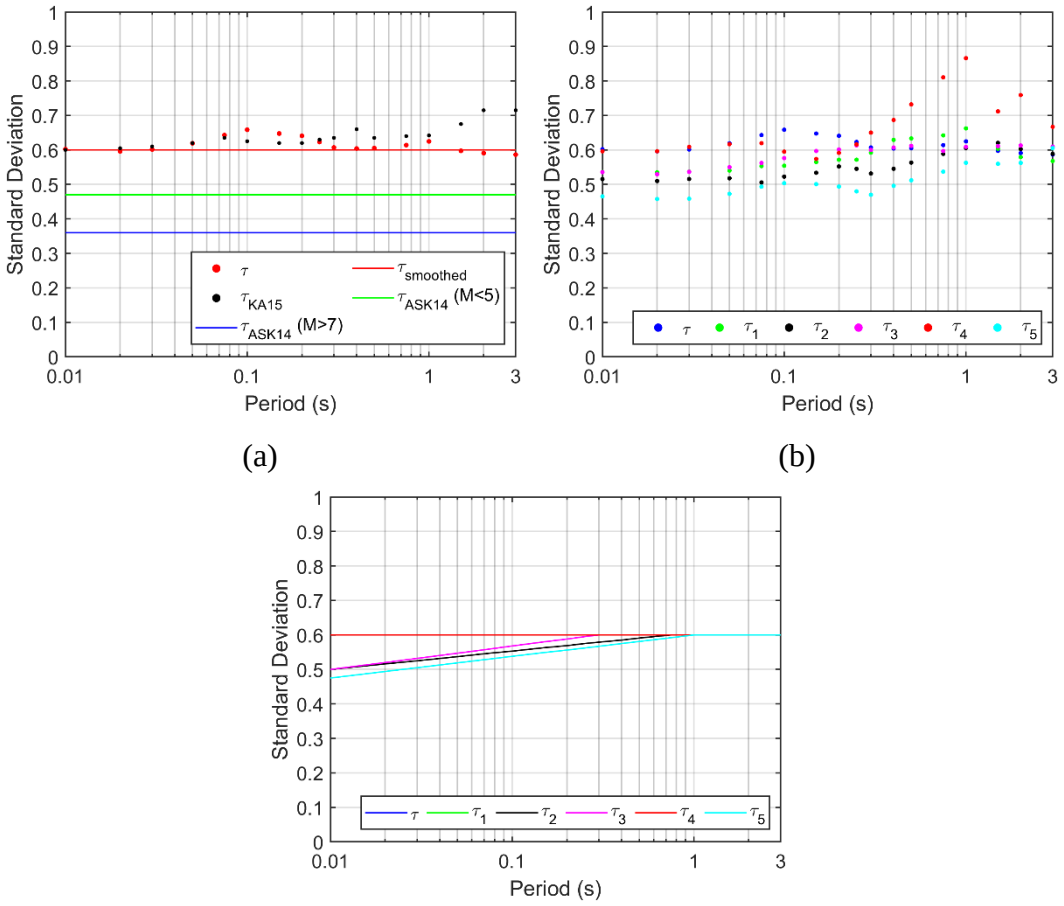

Figure 3.40: Standard deviation of between-event residuals (τ) (a) for the whole dataset before removing systematic source effects in comparison with the original ASK14, CY14 and KA15 models based on EMME dataset (digitized from Çağnan and Akkar, 2019) (b) for each defined region after removing systematic source effects (c) smoothed τ models for TR-Adjusted ASK14 model.

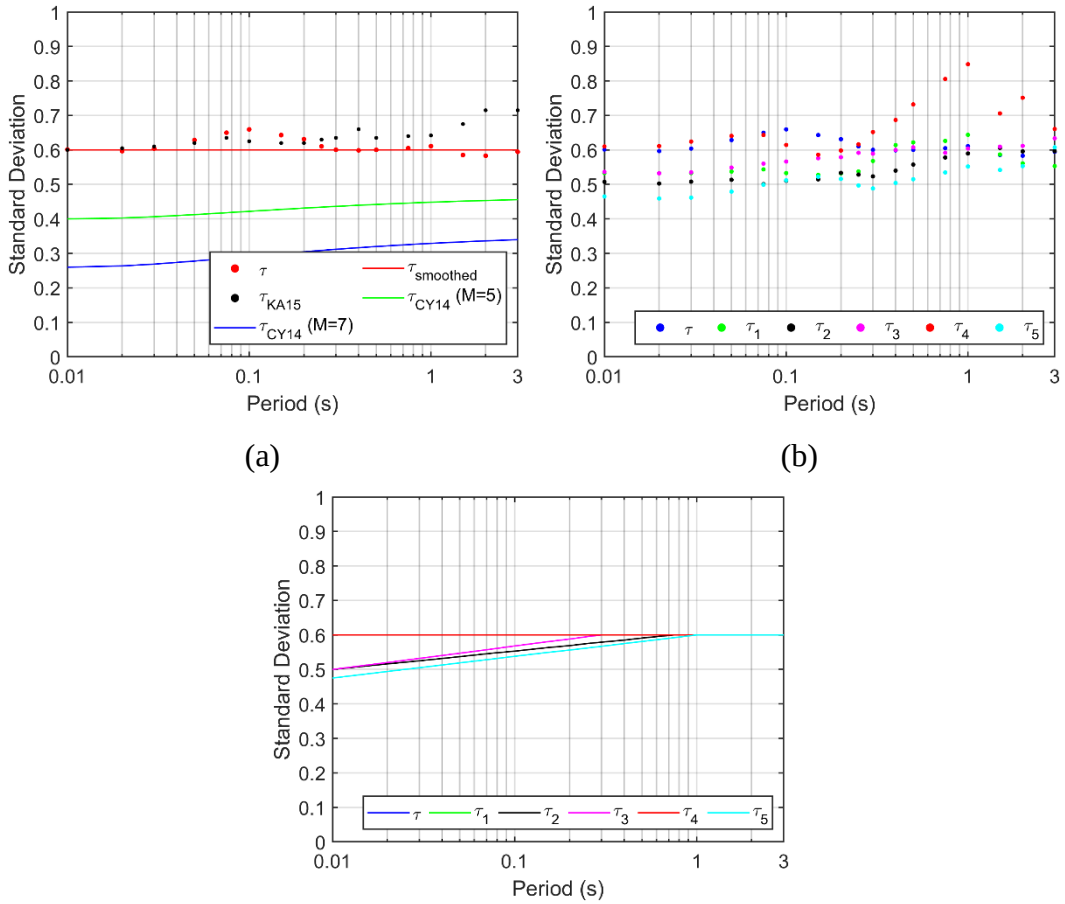

Figure 3.41: Standard deviation of between-event residuals (τ) (a) for the whole dataset before removing systematic source effects in comparison with the original ASK14, CY14 and KA15 models based on EMME dataset (digitized from Çağnan and Akkar, 2019) (b) for each defined region after removing systematic source effects (c) smoothed τ models for TR-Adjusted CY14 model.

Table 3.1 Coefficients of the location-to-location variability models for Turkey

Period	TR-adjusted ASK14 δL2L					TR-adjusted CY14 δL2L					TR-adjusted ASK14/CY14 τ					TR-specific τ
	Reg 1	Reg 2	Reg 3	Reg 4	Reg 5	Reg 1	Reg 2	Reg 3	Reg 4	Reg 5	Reg 1	Reg 2	Reg 3	Reg 4	Reg 5	
0.01	0.571	0.364	-0.050	0.455	-0.233	0.380	0.182	-0.200	0.290	-0.450	0.500	0.500	0.500	0.600	0.475	0.600
0.02	0.591	0.364	-0.050	0.481	-0.233	0.380	0.182	-0.204	0.292	-0.450	0.520	0.516	0.520	0.600	0.494	0.600
0.03	0.594	0.364	-0.057	0.512	-0.235	0.383	0.182	-0.210	0.300	-0.460	0.532	0.525	0.532	0.600	0.505	0.600
0.05	0.610	0.364	-0.060	0.570	-0.252	0.401	0.202	-0.222	0.365	-0.512	0.547	0.537	0.547	0.600	0.519	0.600
0.075	0.637	0.364	-0.072	0.627	-0.321	0.408	0.161	-0.280	0.392	-0.600	0.559	0.547	0.559	0.600	0.530	0.600
0.1	0.650	0.364	-0.088	0.668	-0.368	0.410	0.138	-0.310	0.395	-0.650	0.568	0.553	0.568	0.600	0.538	0.600
0.15	0.670	0.385	-0.069	0.630	-0.270	0.370	0.125	-0.300	0.330	-0.610	0.580	0.563	0.580	0.600	0.549	0.600
0.2	0.620	0.329	-0.069	0.540	-0.215	0.320	0.111	-0.285	0.260	-0.530	0.588	0.569	0.588	0.600	0.556	0.600
0.25	0.542	0.300	-0.069	0.460	-0.178	0.278	0.100	-0.265	0.210	-0.449	0.595	0.575	0.595	0.600	0.562	0.600
0.3	0.480	0.270	-0.069	0.380	-0.150	0.250	0.095	-0.245	0.174	-0.376	0.600	0.579	0.600	0.600	0.567	0.600
0.4	0.380	0.235	-0.069	0.275	-0.100	0.200	0.080	-0.210	0.115	-0.251	0.600	0.585	0.600	0.600	0.575	0.600
0.5	0.320	0.200	-0.060	0.210	-0.060	0.164	0.065	-0.175	0.081	-0.190	0.600	0.591	0.600	0.600	0.581	0.600
0.75	0.230	0.135	-0.010	0.135	-0.010	0.100	0.030	-0.110	0.030	-0.110	0.600	0.600	0.600	0.600	0.592	0.600
1	0.160	0.075	0.000	0.075	0.000	0.055	0.005	-0.075	0.005	-0.075	0.600	0.600	0.600	0.600	0.600	0.600
1.5	0.060	0.000	0.000	0.000	0.000	0.000	-0.010	-0.035	-0.010	-0.035	0.600	0.600	0.600	0.600	0.600	0.600
2	0.000	0.000	0.000	0.000	0.000	-0.013	-0.013	-0.013	-0.013	-0.013	0.600	0.600	0.600	0.600	0.600	0.600
3	0.000	0.000	0.000	0.000	0.000	0.000	0.000	0.000	0.000	0.000	0.600	0.600	0.600	0.600	0.600	0.600
4	0.000	0.000	0.000	0.000	0.000	0.000	0.000	0.000	0.000	0.000	0.600	0.600	0.600	0.600	0.600	0.600
5	0.000	0.000	0.000	0.000	0.000	0.000	0.000	0.000	0.000	0.000	0.600	0.600	0.600	0.600	0.600	0.600
7.5	0.000	0.000	0.000	0.000	0.000	0.000	0.000	0.000	0.000	0.000	0.600	0.600	0.600	0.600	0.600	0.600
10	0.000	0.000	0.000	0.000	0.000	0.000	0.000	0.000	0.000	0.000	0.600	0.600	0.600	0.600	0.600	0.600

CHAPTER 4

NON-ERGODIC GROUND MOTION MODELS FOR TURKEY - ASSESSMENT OF WITHIN-EVENT RESIDUALS

This chapter focuses on the analysis of the within-event residuals (δW_{es}) of TR-adjusted ASK14 and TR-adjusted CY14 models for systematic site and path effects. For this purpose, distribution of δW_{es} with V_{S30} before and after the separation of site terms ($\delta S2S_s$) is discussed, focusing on the availability of the measured V_{S30} value for the station. The standard deviation of site terms (a.k.a. the single station sigma) is calculated and compared with the findings of Cagnan and Akkar (2019). Proposed decrease in the standard deviation of within-event residuals, and consequently in total sigma (σ) due to the separation of systematic site effects is presented and discussed.

The dense strong motion station network in the study dataset enabled the evaluation of a possible relation between the estimated site terms and local geological conditions, which is provided in the second part of this chapter. Special attention is given to the regions with systematically positive or negative site terms. A susceptibility analysis for the identified regional trends in the site terms is conducted by assuming constant V_{S30} values for each station.

The final step through the development of a **"fully non-ergodic"** GMM is the analysis of systematic path effects. To capture the systematic path effects arising from particular seismic sources to closely spaced group of recording stations, the azimuthal distribution of the site-corrected within-event residuals (δWS_{es}) are evaluated with the help of rose diagrams. This chapter only includes a preliminary analysis of systematic path effects for selected set of stations in Turkey (a.k.a the Bodrum stations) and the cases where the site terms ($\delta S2S_s$) are significantly negative or positive. Due to the computational complexity and the lack of clear path

effects in most of the stations, it is not attempted to separate path effects from the site corrected within-event residuals (δWS_{es}) in this study.

4.1 Systematic Site Effects in the Within-Event Variability

The site term ($\delta S2S_s$), in simple words, is the average of the within-event residuals (δW_{es}) at a recording station. Therefore, $\delta S2S_s$ is a measure of the average misfit of the recordings at a specific station from the event-corrected median predictions of GMM. This misfit may be associated with the error in the site parameters that are included in the GMM (for this study, the error in V_{S30}), may be related to the site amplification scaling implemented in the model, or may indicate other local site characteristics that were not reflected in GMMs with simple predictive parameters like V_{S30}.

Out of the 445 recording stations in the dataset (see Chapter 3.1 for details), the shear wave velocity profile of 340 stations were measured by different geophysical surveys. For the remaining stations, the V_{S30} values were estimated from the topography using the "USGS V_{s30} Map Viewer" web-based tool (Wald and Allen, 2007) by Akbas et al. (2022). The site terms estimated from TR-Adjusted ASK14 and TR-Adjusted CY14 GMMs are plotted against V_{S30} for 10 different spectral periods and given in Figure 4.1 through Figure 4.4. The error in the estimated and measured V_{S30} values may be significantly different; therefore, the distribution of site terms with V_{S30} is evaluated separately in Figures 4.1-4.4. The left column in each figure belongs to the sites whose V_{S30} value was determined based on a measurement, whereas the sites at the right column have a V_{S30} estimate only.

The site terms, both for the stations with estimated and measured V_{S30}, do not exhibit a clear trend with V_{S30} within the comfort zone of the GMMs (≈230 m/s $> V_{S30} >$ 800 m/s). The site terms are slightly negative for $V_{S30} < 230\ m/s$, indicating overall (independent of magnitude and distance) overprediction at softer

sites and positive for V_{S30}>800 m/s, indicating overall underprediction for rock/hard rock sites. Trends on the rock/hard rock sites are persistent for both measured and estimated V_{S30} cases. V_{S30}>800 m/s is very close to the upper prediction limit of USGS V_{s30} Map Viewer web-based tool; therefore, it is not clear if the underprediction is related to an error in the V_{S30} estimate or not. On the other hand, trend in the site terms seems to increase almost linearly after T=0.5s for the sites with measured V_{S30}. It is possible that the V_{S30} scaling in the original ASK14 and CY14 models may be different than the V_{S30} scaling of the ground motions in N-TSMD. A similar inconsistency was observed by Gulerce et al. (2016), but towards overprediction for NGA-W1 models.

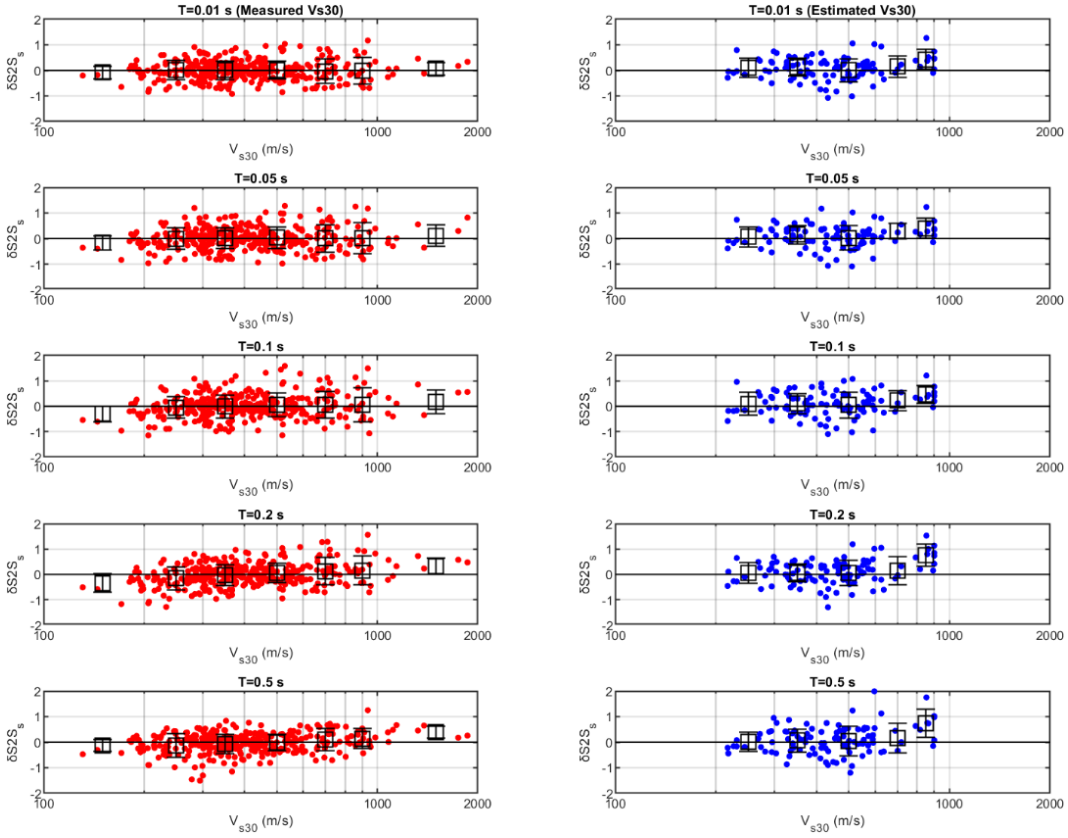

Figure 4.1: Distribution of site terms ($\delta S2S_s$) with $V_{s,30}$ for TR-Adjusted ASK14 at T= 0.01s, 0.05s, 0.1s, 0.2s and 0.5s

The picture changes completely once the systematic site effects are separated from the within-event residuals (δW_{es}) by simply subtracting the site term of the

corresponding station from the within-event residuals. The distribution of site-corrected within-event residuals (δWS_{es}) are compared with the within-event residuals before the site correction in Figure 4.5 through Figure 4.8. As shown in these figures, the slight bias that existed before the site correction is completely diminished after the systematic site effects are separated. It should be noted that the slight positive trend in within-event residuals (δW_{es}) vs V_{S30} graphs (Figure 4.5 and Figure 4.6) is identical with the one detected in the site terms ($\delta S2S_s$) vs V_{S30} graphs (Figure 4.1 through Figure 4.4).

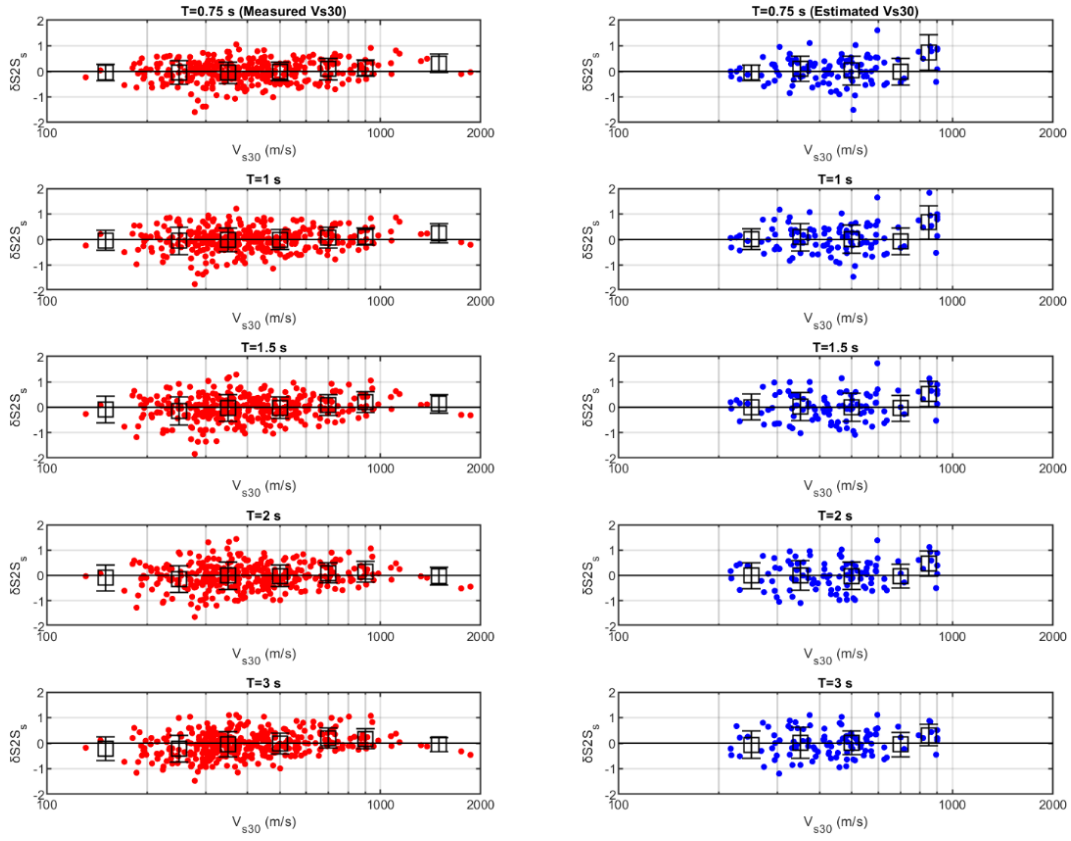

Figure 4.2: Distribution of site terms ($\delta S2S_s$) with $V_{s,30}$ for TR-Adjusted ASK14 at T=0.75s, 1s, 1.5s, 2s and 3s

Standard deviations of site-corrected within-event residuals (a.k.a. the single station sigma or $\varphi_{SS,s}$) are calculated at each station and provided in Appendix A for 4 spectral periods. Distribution of $\varphi_{SS,s}$ with V_{S30} is provided in Figure 4.9 through Figure 4.12 for different spectral periods and for two TR-adjusted GMMs. As shown

in these figures, $\varphi_{SS,s}$ is independent of the V_{S30} and almost constant (≈0.5), both for sites with estimated and measured V_{S30} values for both GMMs.

Figure 4.13(a) and Figure 4.14(a) compare the standard deviations of within-event residuals (φ) calculated in this study with the magnitude-dependent φ-models of the original GMMs. For the sake of comparison, only the linear φ-models of the original GMMs are used. The original ASK14 model has a magnitude and period dependent multi-linear φ-model with two break points at M=4 and M=6, whereas the CY14 GMM has a more complex form for the φ-model and two break points at M=5 and M=6.5. φ values calculated in this study (0.6-0.7 ln units) are larger than the φ values of original GMMs (Figures 4.13(a)-4.14(a)), as in the case of standard deviations of between-event residuals (τ) (Chapter 3). Like the between-event variability, the within-event variability estimated for TR-adjusted ASK14 and TR-adjusted CY14 models are very close to each other for N-TSMD. Estimated φ values for TR-adjusted ASK14 are close to the small magnitude φ values of the original GMM, while the estimated φ values for TR-adjusted CY14 model are significantly larger than the φ values of the original model.

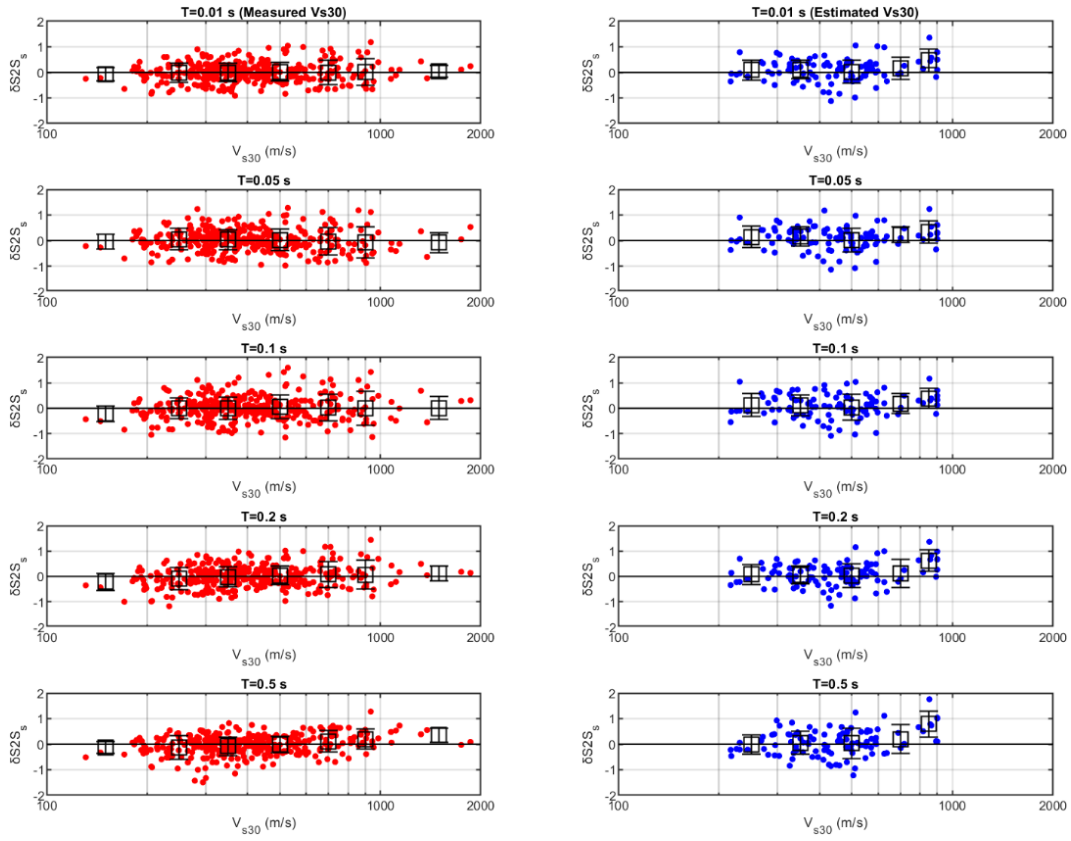

Figure 4.3: Distribution of site terms ($\delta S2S_s$) with $V_{s,30}$ for TR-Adjusted CY14 at T=0.01s, 0.05s, 0.1s, 0.2s and 0.5s

Cagnan and Akkar (2019) had also utilized ASK14 and CY14 models in their study to calculate the φ values (Figure 4.13(b) and Figure 4.14(b)) and the results from both studies are very similar, except for the contradicting trends after T=1s. There is a reduction in φ after T=1s in original models for small magnitudes as in the case of this study. On the other hand, for larger magnitudes, the φ values increase after T=1s similar to the findings of Cagnan and Akkar (2019). Since the study dataset includes mostly small magnitude events, the proportion of the large magnitude events is probably lower than the EMME dataset. This might be the underlying reason for the different trends in φ after T=1s.

It should be underlined that the separation of systematic site effects from the aleatory variability enabled a 20% reduction in φ at short periods and up to 30% reduction at longer periods, as shown in Figure 4.13(c) and Figure 4.14(c). φ_{ss} values

are presented solely for comparison purposes, as for the fully or partially non-ergodic GMM prediction, the site-specific within-event standard deviation $\varphi_{ss,s}$ should be used. The calculated φ_{ss} values are in good agreement with the findings of Cagnan and Akkar (2019).

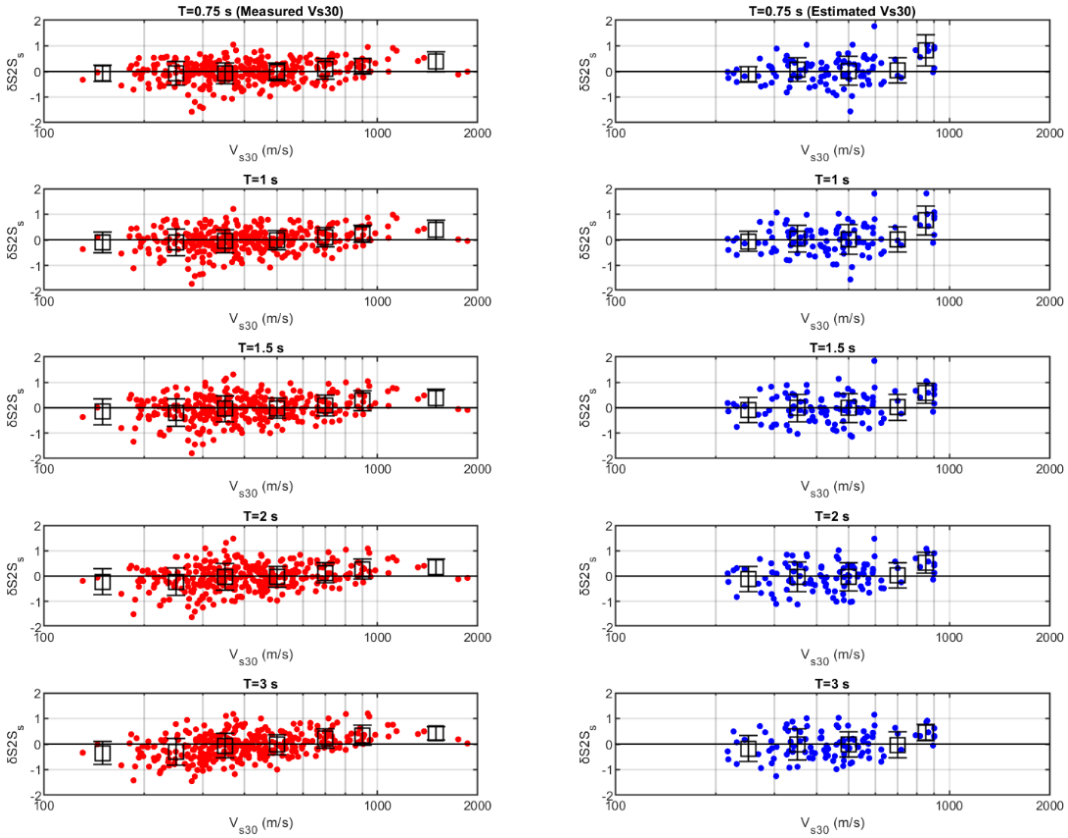

Figure 4.4: Distribution of site terms ($\delta S2S_s$) with $V_{s,30}$ for TR-Adjusted CY14 at T=0.75s, 1s, 1.5s, 2s and 3s

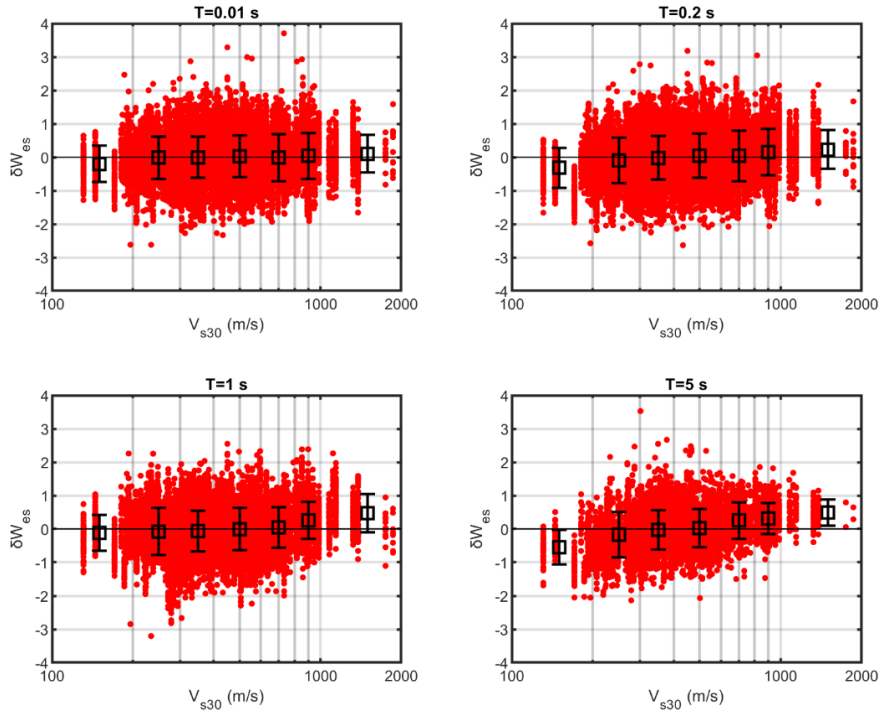

Figure 4.5: Before the site correction: Distribution of within-event residuals (δW_{es}) with $V_{s,30}$ for TR-Adjusted ASK14 at T=0.01s, 0.2s, 1s and 5s

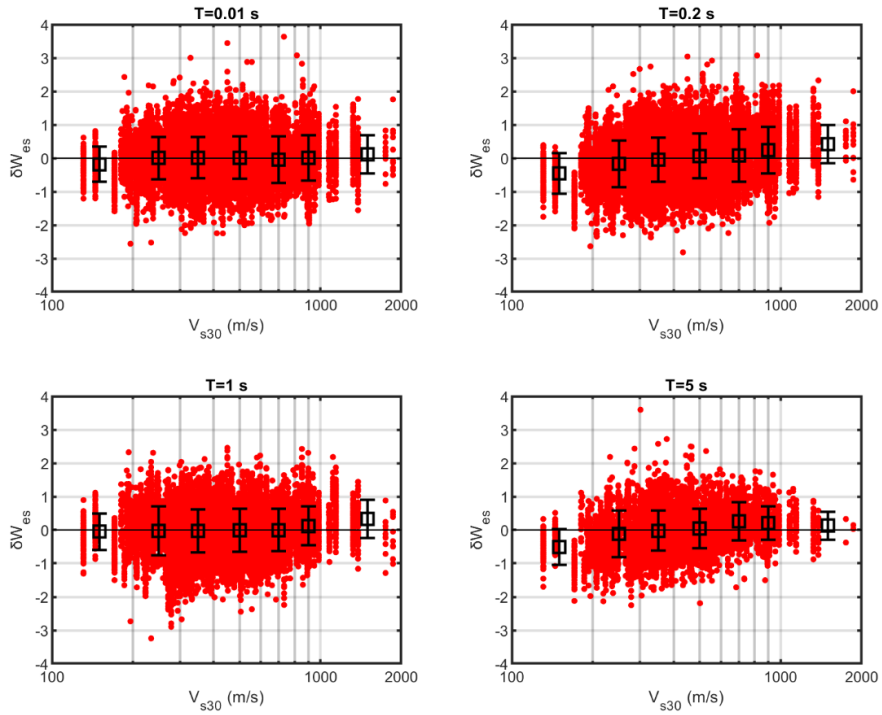

Figure 4.6: Before the site correction: Distribution of within-event residuals (δW_{es}) with $V_{s,30}$ for TR-Adjusted CY14 at T=0.01s, 0.2s, 1s and 5s

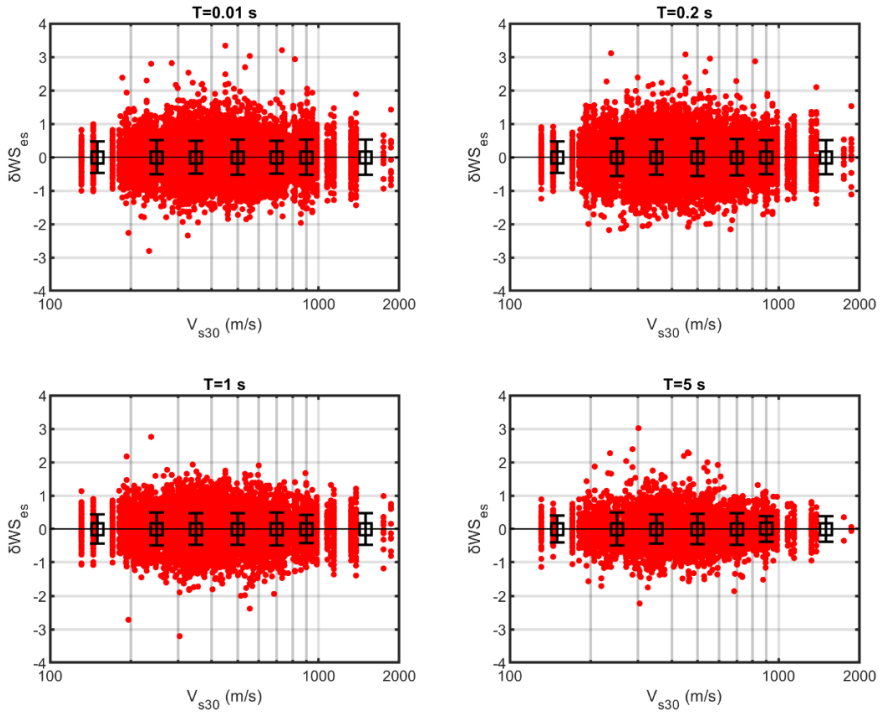

Figure 4.7: After the site correction: Distribution of site corrected within-event residuals (δWS_{es}) with $V_{s,30}$ for TR-Adjusted ASK14 at T=0.01s, 0.2s, 1s and 5s

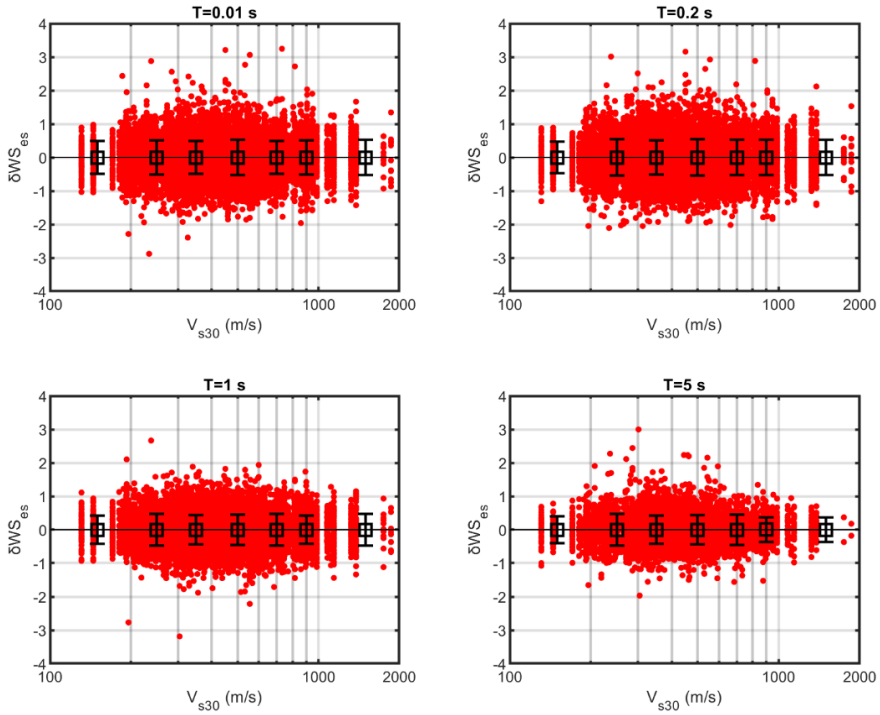

Figure 4.8: After the site correction: Distribution of site corrected within-event residuals (δWS_{es}) with $V_{s,30}$ for TR-Adjusted ASK14 at T=0.01s, 0.2s, 1s and 5s

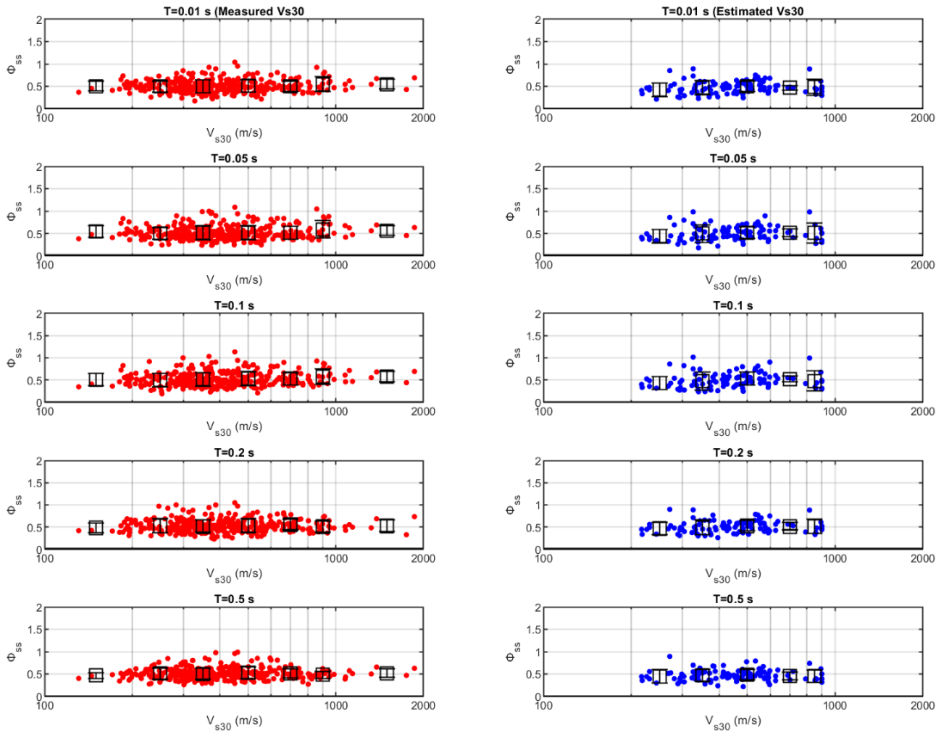

Figure 4.9: Distribution of site-corrected within-event residuals standard deviation ($\varphi_{SS,s}$) with $V_{s,30}$ for TR-Adjusted ASK14 at T=0.01s, 0.05s, 0.1s, 0.2s and 0.5s

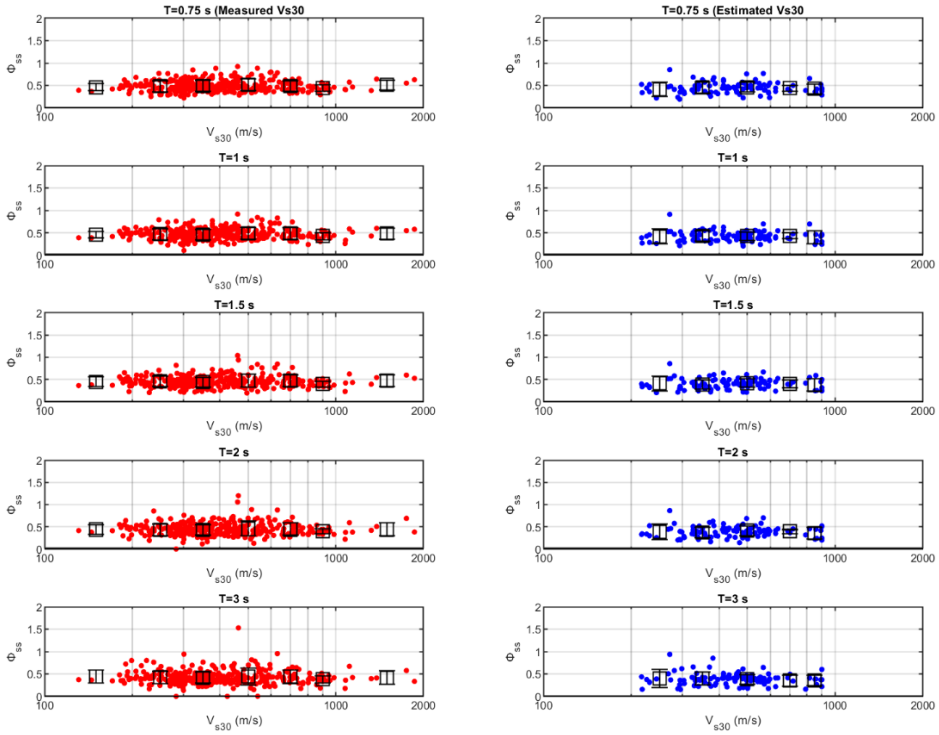

Figure 4.10: Distribution of site-corrected within-event residuals standard deviation ($\varphi_{SS,s}$) with $V_{s,30}$ for TR-Adjusted ASK14 at T=0.75s, 1s, 1.5s, 2 and 3s

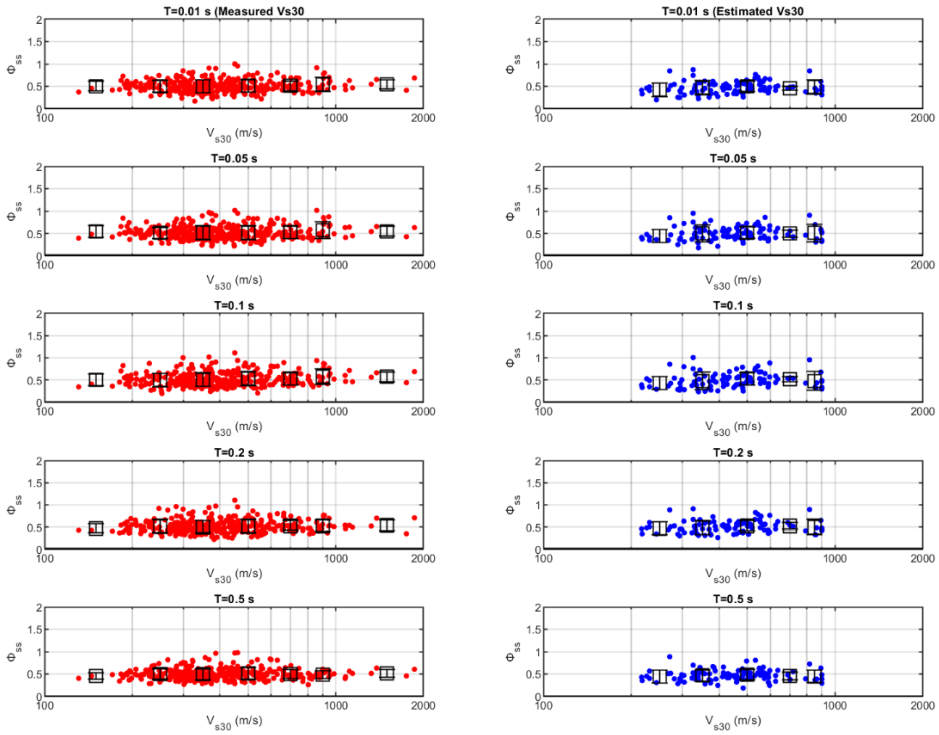

Figure 4.11: Distribution of site-corrected within-event residuals standard deviation ($\varphi_{SS,s}$) with $V_{s,30}$ for TR-Adjusted CY14 at T=0.01s, 0.05s, 0.1s, 0.2s and 0.5s

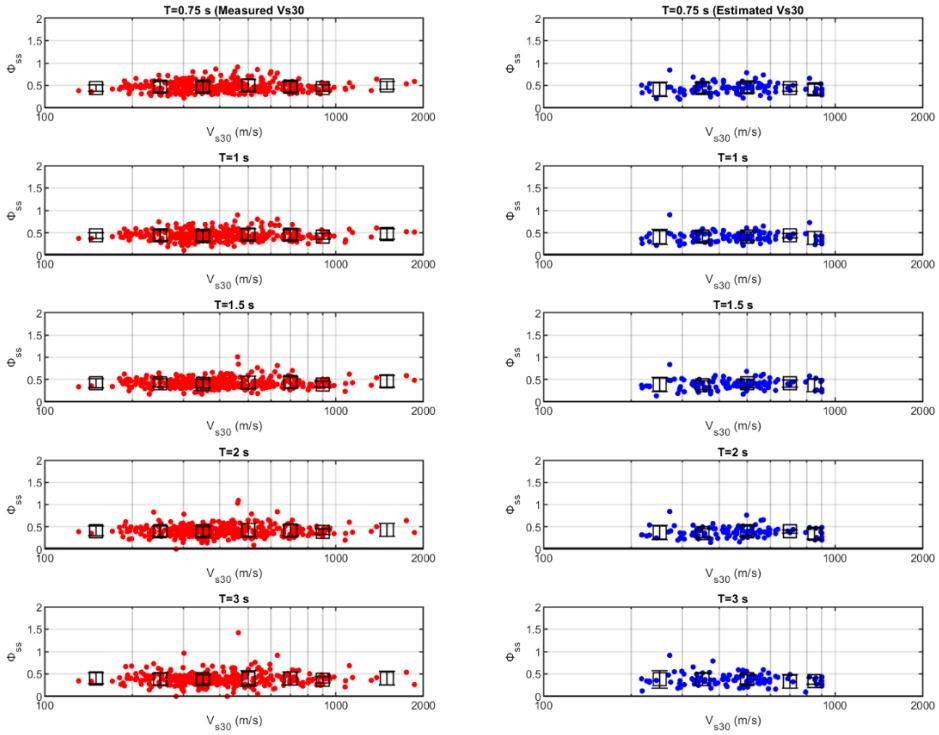

Figure 4.12: Distribution of site-corrected within-event residuals standard deviation ($\varphi_{SS,s}$) with $V_{s,30}$ for TR-Adjusted CY14 at T=0.75s, 1s, 1.5s, 2 and 3s

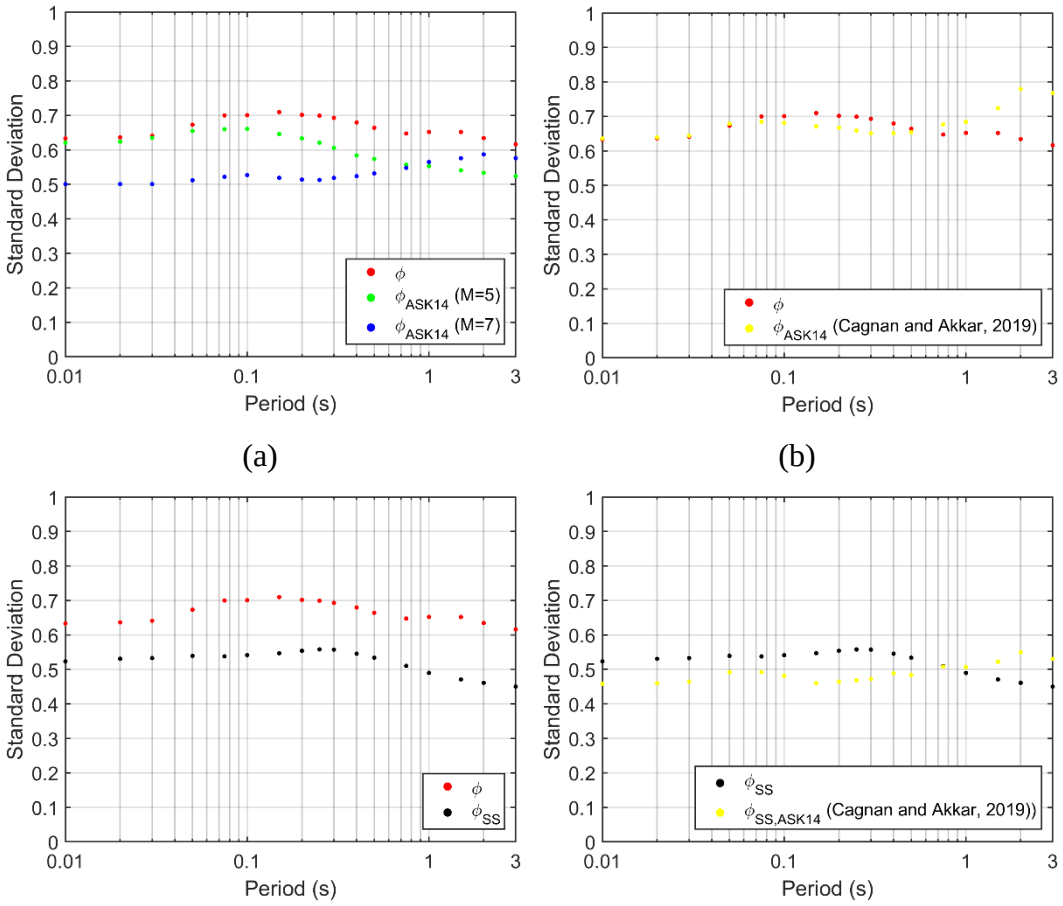

Figure 4.13: Within-event residuals standard deviations (φ) (a) in comparison with the original models (b) with Cagnan and Akkar (2019) (c) with site-corrected within-event residuals standard deviations (φ_{ss}) (d) comparison of site-corrected within-event residuals standard deviations (φ_{ss}) with Cagnan and Akkar (2019) for TR-Adjusted ASK14

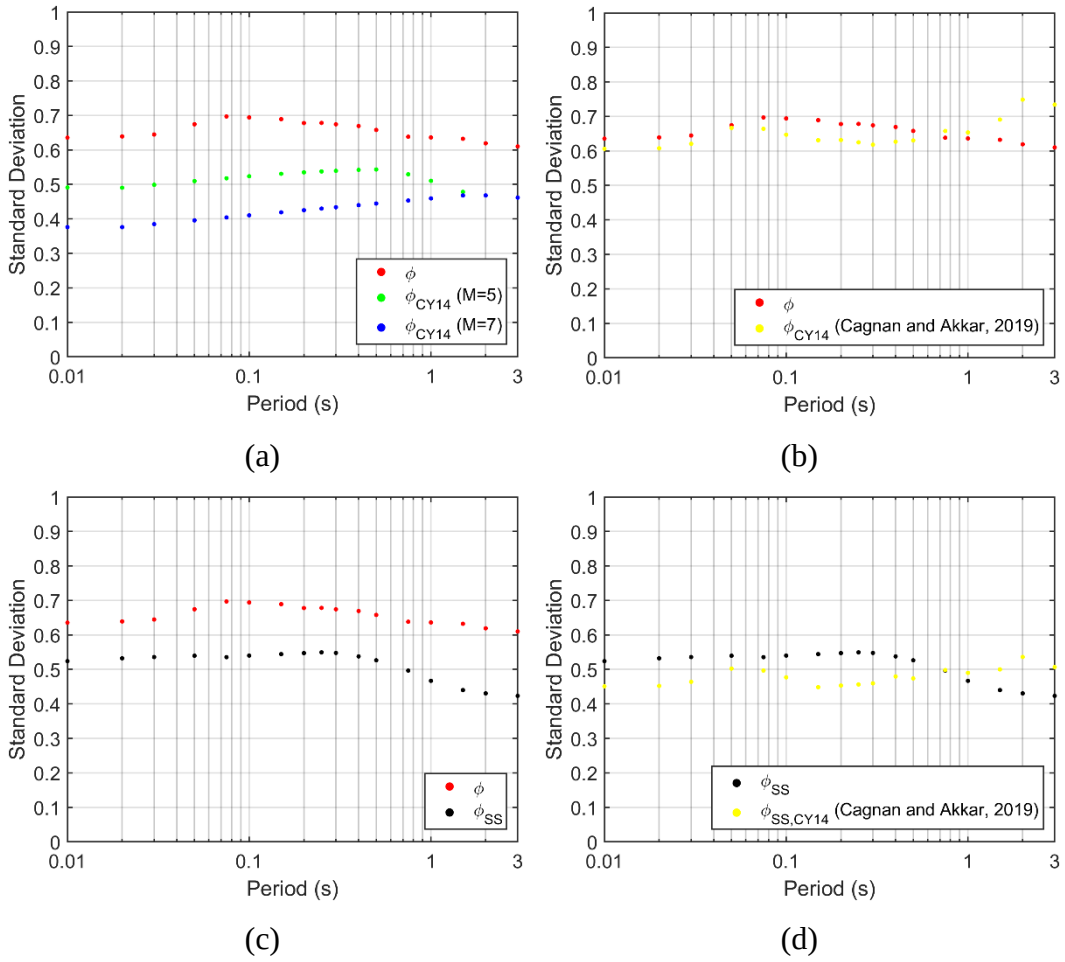

Figure 4.14: Within-event residuals standard deviations (φ) (a) in comparison with the original models (b) with Cagnan and Akkar (2019) (c) with site-corrected within-event residuals standard deviations (φ_{ss}) (d) comparison of site-corrected within-event residuals standard deviations (φ_{ss}) with Cagnan and Akkar (2019) for TR-Adjusted CY14

4.2 Spatial Distribution of Site Terms and Correlation with Local Geology

Spatial distribution of site terms ($\delta S2S_s$) are examined to evaluate the systematic regional effects and the correlation with local geology. The distribution of site terms over the 1/500.000 scaled geological map of Turkey (MTA, 2002) for both GMMs at four spectral periods (T=0.01s, 0.2s, 1s and 2s) are provided in Figure 4.15 through Figure 4.22. In these figures, the stations with positive site terms, i.e.,

the stations where actual ground motions are systematically underestimated, are marked with warm colors. The stations marked with white circles are the ones with a site term between -0.25 and 0.25. Finally, the cold colors represent the stations with negative site terms, i.e., with systematically overpredicted recordings. According to these figures:

- Unlike the event terms (δB_e) discussed in the previous chapter, the site terms seem to be spatially more uniformly distributed, independent of the GMM and spectral period, except for a few small regions. Majority of the site terms are close to zero for short periods, as shown by the domination of white colored stations in the Figures 4.15-4.18.
- The lack of regional trends was expected since the site terms are assumed to include only site-specific or near-site-specific characteristics that are not captured by the GMM. Any regional grouping in site terms would indicate a bias in the calculations.
- The spatial distribution the site terms estimated for both models is very similar for each spectral period, showing that the estimated site terms have captured the systematic effects related without being impaired by the choice of GMM. It is important to note that the TR-adjustments for these models, as discussed in the previous chapter, do not affect the within-event residuals, and consequently site terms, since the adjustments were included for only source related parameters.
- The number of stations marked with white decreases at larger periods as shown in Figure 4.21 and 4.22. This decrease could be explained by the fact that the site characteristics are more dominating at larger periods, as oppose of source effects.
- Although the site terms are mostly evenly distributed, there exists still a few groupings: The stations in South Marmara region, near Bursa, where a dense strong motion network is available, have generally positive site terms, their recordings are underestimated. This trend becomes stronger at larger periods.

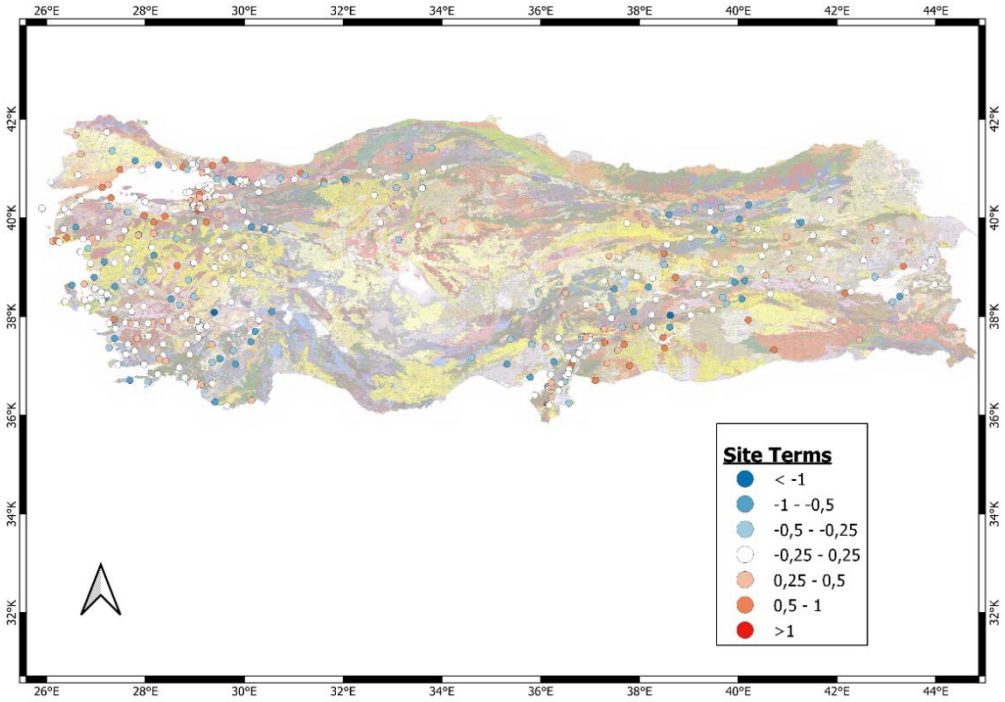

Figure 4.15: Spatial distribution of site terms ($\delta S2S_s$) at T=0.01s for TR-Adjusted ASK14

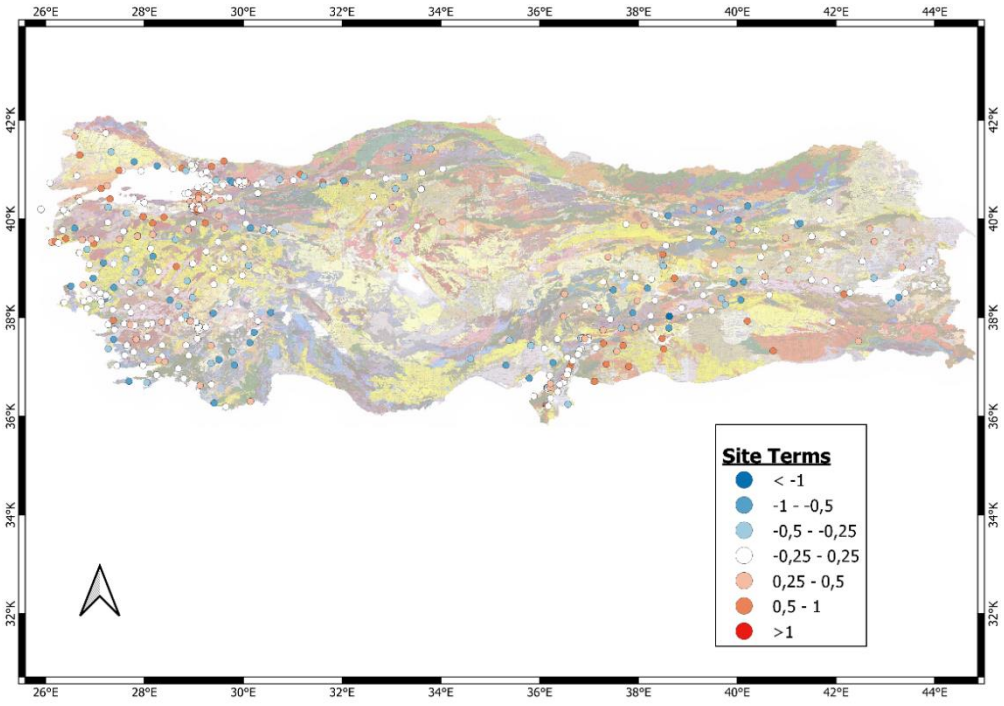

Figure 4.16: Spatial distribution of site terms ($\delta S2S_s$) at T=0.01s for TR-Adjusted CY14

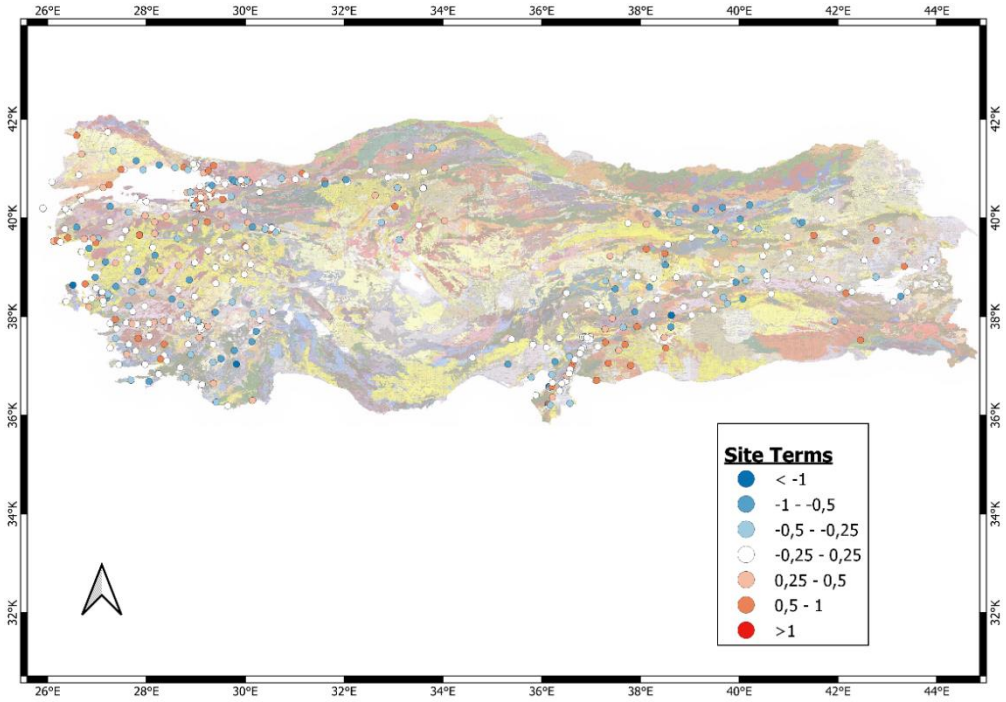

Figure 4.17: Spatial distribution of site terms ($\delta S2S_s$) at T=0.2s for TR-Adjusted ASK14

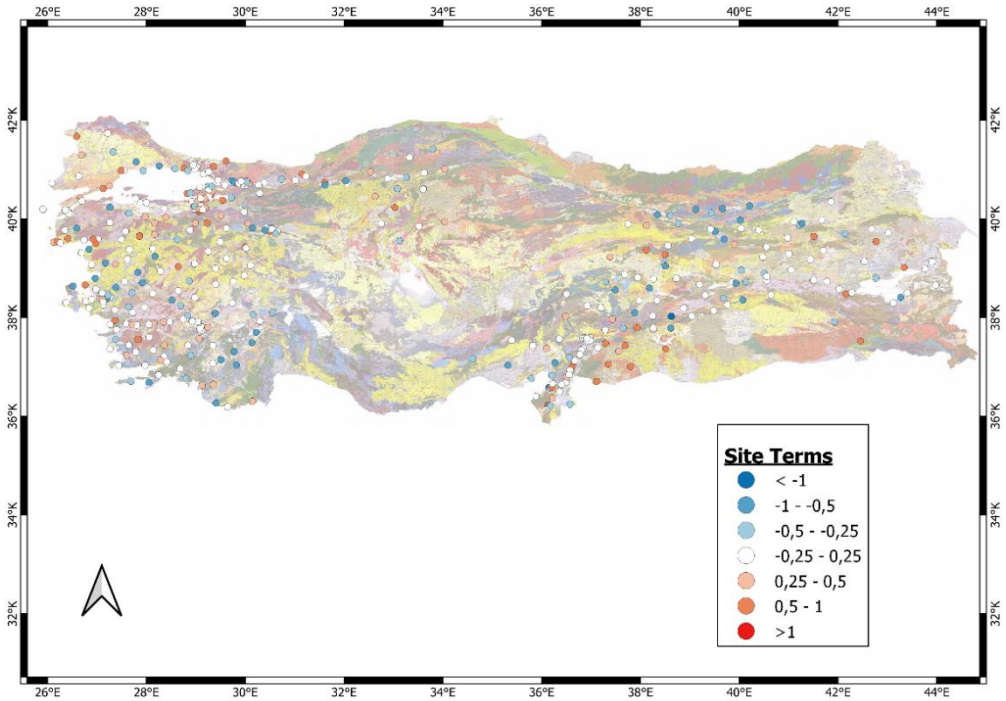

Figure 4.18: Spatial distribution of site terms ($\delta S2S_s$) at T=0.2s for TR-Adjusted CY14

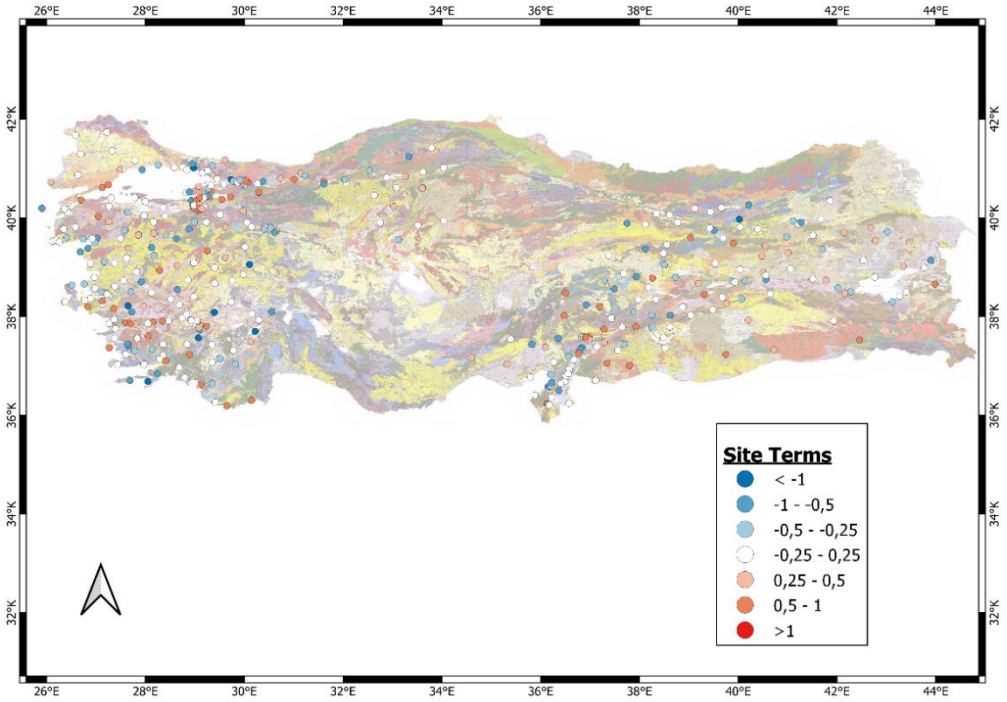

Figure 4.19: Spatial distribution of site terms ($\delta S2S_s$) at T=1s for TR-Adjusted ASK14

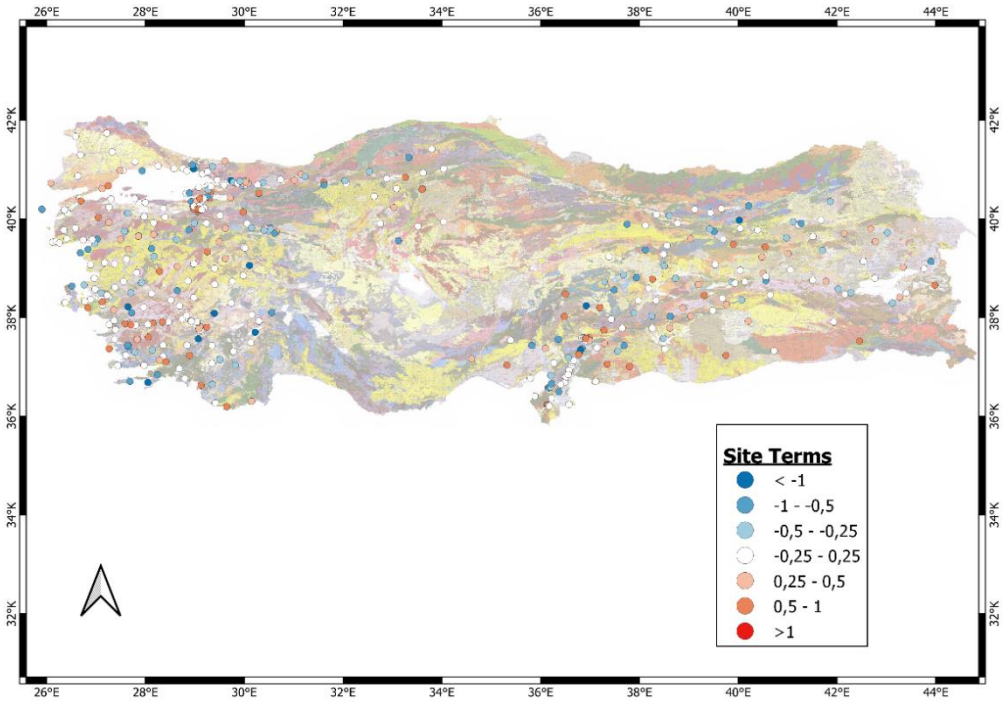

Figure 4.20: Spatial distribution of site terms ($\delta S2S_s$) at T=1s for TR-Adjusted CY14

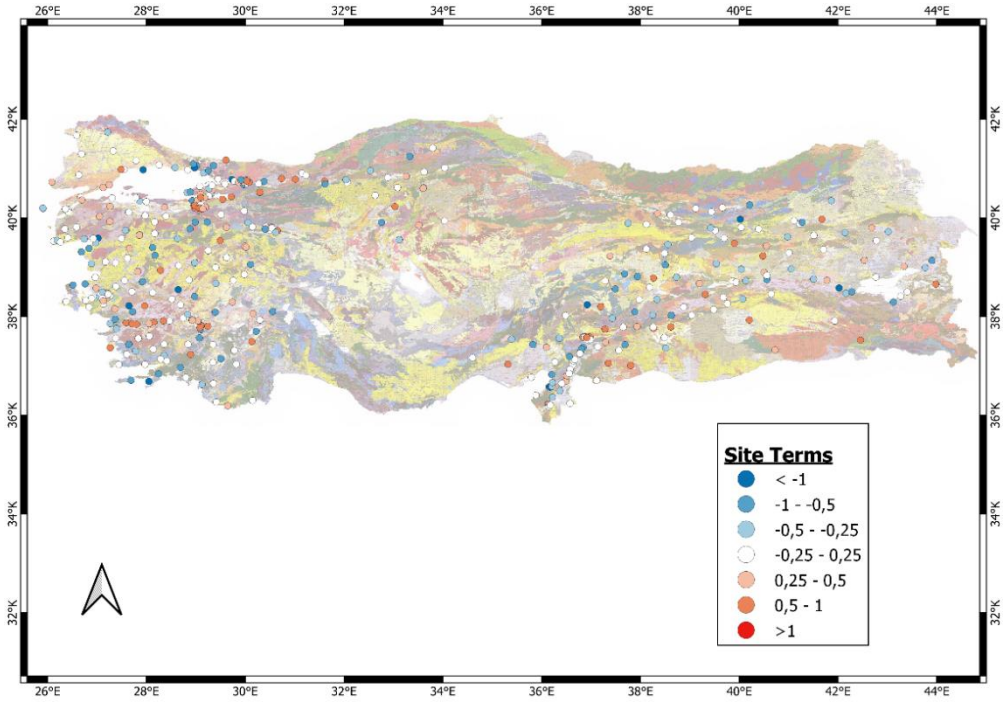

Figure 4.21: Spatial distribution of site terms ($\delta S2S_s$) at T=2s for TR-Adjusted ASK14

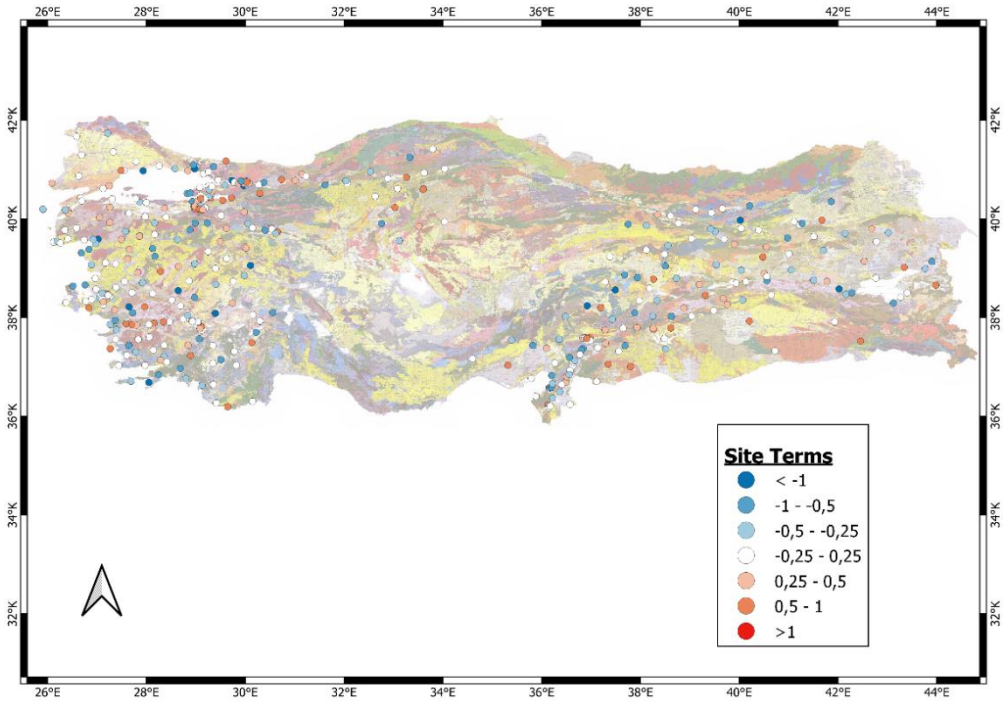

Figure 4.22: Spatial distribution of site terms ($\delta S2S_s$) at T=2s for TR-Adjusted CY14

4.3 Systematic Path Effects in the Within-Event Variability

The last step in the development of fully non-ergodic GMMs is the separation of systematic path effects from site-corrected within-event residuals (δWS_{es}). Theoretically, the path term ($\delta P2P_{sr}$) is the average of site-corrected within-event residuals (δWS_{es}) at the station $\boldsymbol{s}$ from the ray path $\mathbf{r}$. The most critical issue is the selection of ray paths, since not every station has enough records attenuating from a specific direction. Ray paths may be selected based on the location of seismic sources or by simply dividing the surrounding area into quadrants. For example, earthquakes located in 0-30° North of the station may be considered as a path or events occurring on North Anatolian Fault and their paths may be considered as a group.

A simple solution to the path selection problem would be the use of coordinate-based computation, like the varying-coefficient model (VCM) regression utilized by Lavrentiadis et al. (2021). The coordinate-based regression leads to the availability of path terms at every coordinate for any path. Moreover, it assumes that the nearly located paths (e.g., originating from the same seismic source) should have similar path terms. Before attempting to estimate the systematic path terms, the azimuthal distribution (rose) diagram for each station is prepared to observe the direction-based distribution of site-corrected within-event residuals (δWS_{es}). Due to the large number of stations, rose diagrams are presented only for TR-adjusted ASK14 GMM at T=0.01s in this chapter. The illustration of azimuthal distribution of within-event residuals is shown in Figure 4.23 for an example station located in İzmir. The diagram on the left shows the distribution of within-event residuals (δW_{es}) before the site correction and the right side shows the distribution of site-corrected within-event residuals. Residuals are color-coded and the continuous black line is the zero line. In this example, the within-event residuals are generally negative before the site correction: therefore, the estimated site term is negative. After the correction, the residuals are uniformly distributed around the zero-line. There are three clear groups: events from NW-N, events from NE-E and events from S-SE.

The within-event residuals in each group are negative before the correction: therefore a substantial path dependence is not observed.

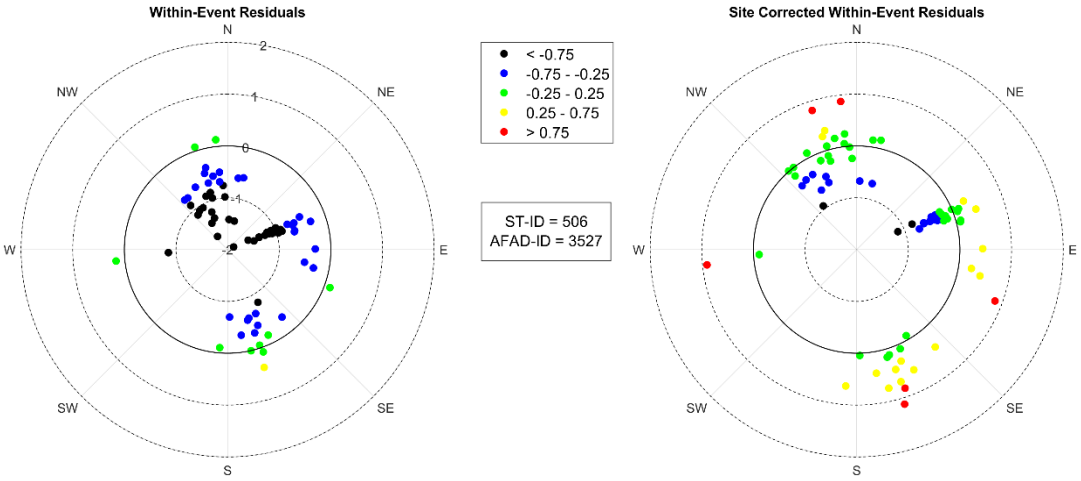

Figure 4.23: Rose diagram example from Station 3527

4.3.1 Example 1: Analysis of Stations in Bursa

To comprehend the possibility of selecting specific paths for systematic path effects, the rose diagrams of stations from the same region are examined together. A group of stations in South Marmara Region around Bursa (Stations 1627, 1650, 1651, 1645 and 1624) that are shown in Figure 4.24 is selected as an example case because the site terms in this region are systematically positive for short spectral periods (Figure 4.17).

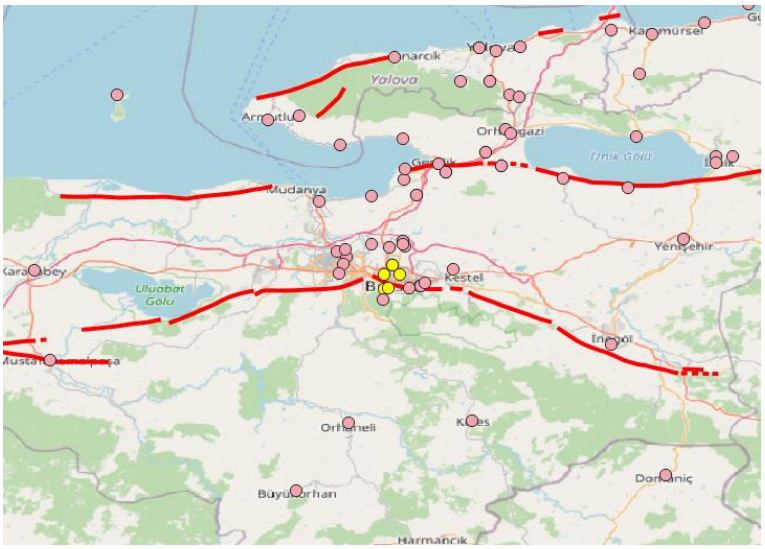

Figure 4.24: Selected stations in South Marmara - Bursa (Stations 1627, 1650, 1651, 1645 and 1624 from North to South, respectively)

The directional distribution of within- and site corrected within-event residuals for these stations are presented in Figure 4.25 through Figure 4.29. Figures 4-25-4.29 show that the recordings from southwest direction have clearly positive within-event residuals which may be attributed as a “path effect”. Because the site-terms are the calculated by using the average of all within-event residuals, this path has dominated the site term calculations and resulted in positive site terms for each station. On the other hand, there is not enough data in any of the other directions to analyze if this positive effect is path-specific or not.

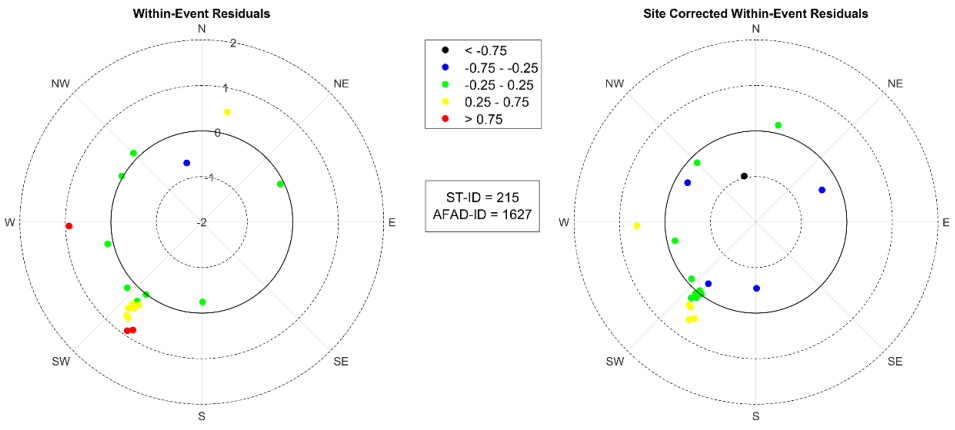

Figure 4.25: Directional distribution of within- and site-corrected within-event residuals for Station 1627

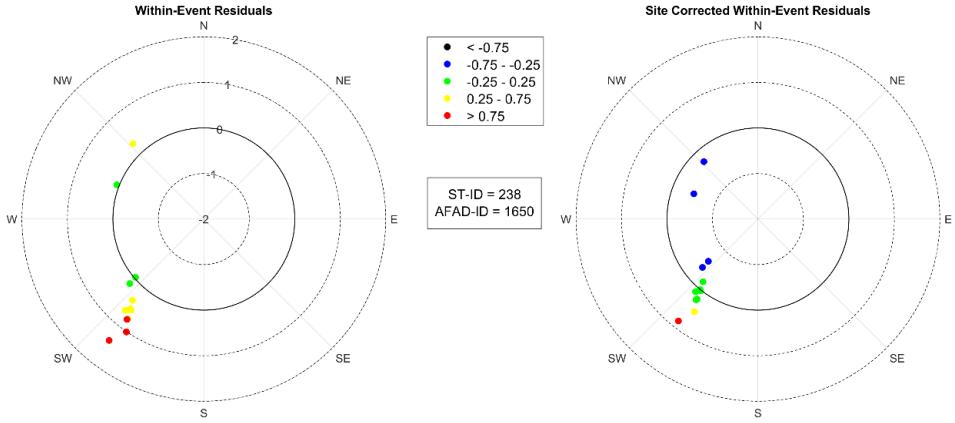

Figure 4.26: Directional distribution of within- and site-corrected within-event residuals for Station 1650

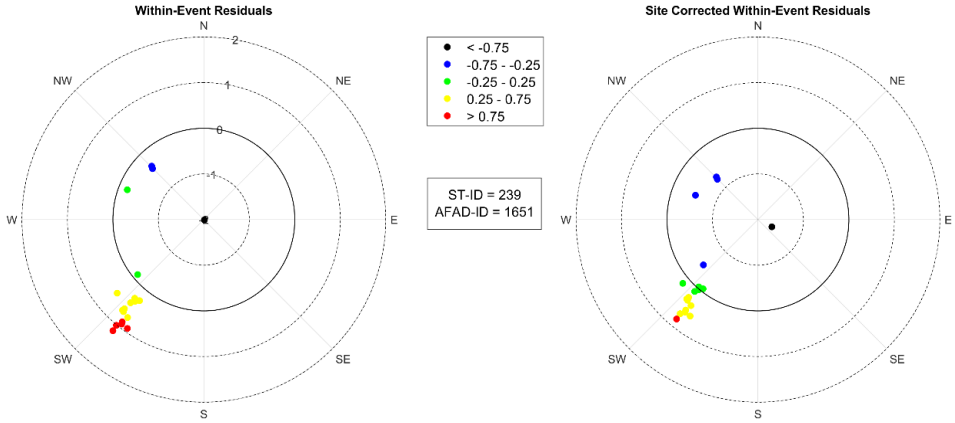

Figure 4.27: Directional distribution of within- and site-corrected within-event residuals for Station 1651

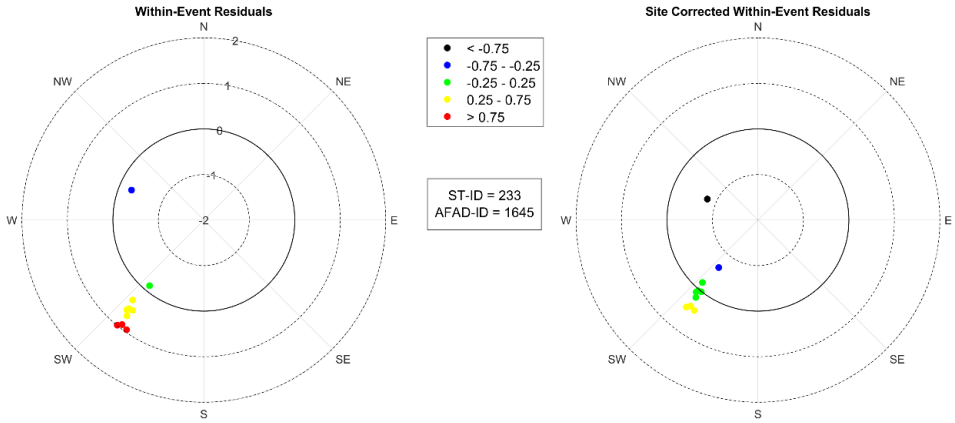

Figure 4.28: Directional distribution of within- and site-corrected within-event residuals for Station 1645

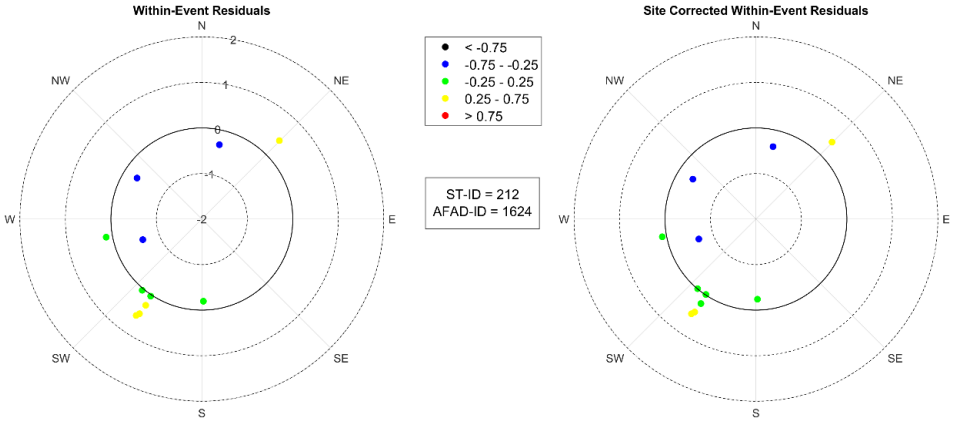

Figure 4.29: Directional distribution of within- and site-corrected within-event residuals for Station 1624

4.3.2 Example 2: Analysis of Stations in Izmir

The İzmir region has a dense strong motion recording network and the stations located here are rich in terms of the number of recordings (Figure 4.30). The stations in this region have neutral site terms (varying between -0.25 and 0.25), showing that the difference between the within-event and site corrected within-event residuals, and consequently between the distributions in rose diagrams is quite small. Five stations around the center of İzmir (Stations 3513, 3519, 3522, 3518 and 3512) are selected to analyze the systematic path effects in this region as shown in Figure 4.30. The rose diagrams for these stations are provided in Figure 4.31 through Figure 4.35. For all selected stations, the slight negative trend in the recordings attenuating from sources in Northwest and Northeast directions seems to be adjusted with the site correction. This overall correction resulted in a slight positive trend in the Southwest – South direction, but it is not possible to make a concrete conclusion as the trend is not significant in every station such as Station 3512 (Figure 4.35).

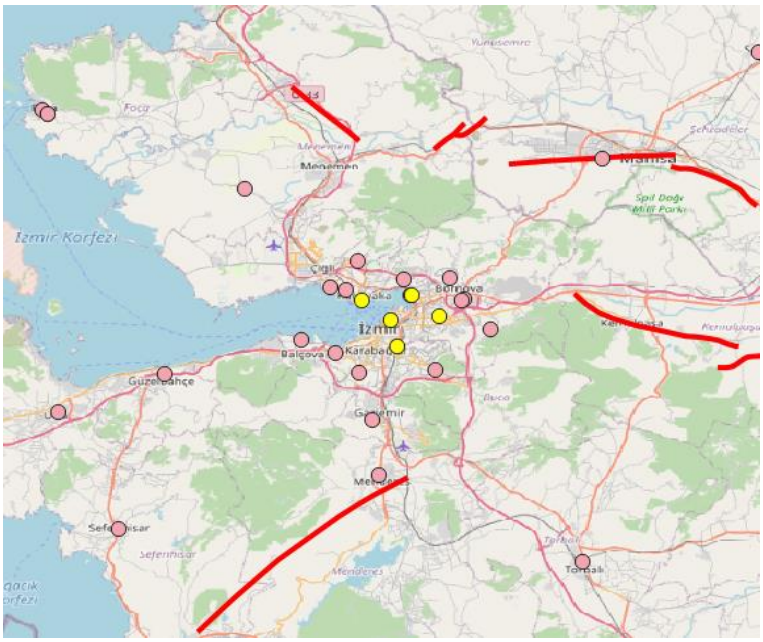

Figure 4.30: Selected stations in Izmir (Station 3513, 3519, 3522 (right), 3518 and 3512 from North to South respectively)

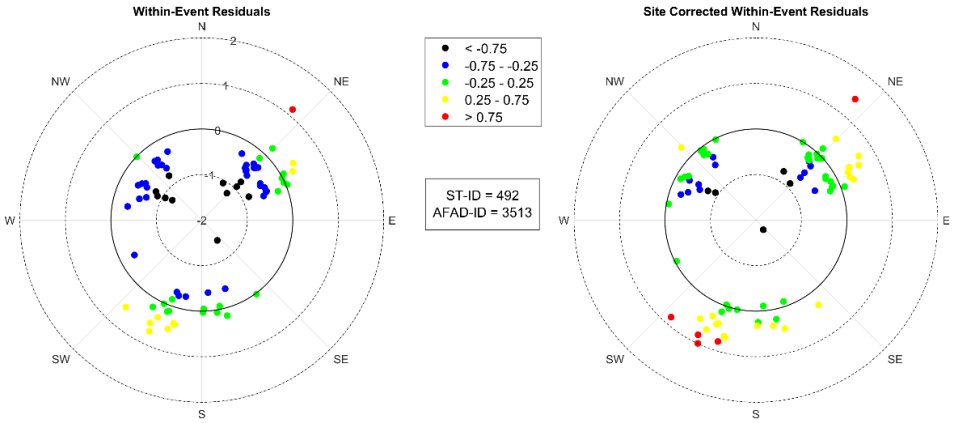

Figure 4.31: Directional distribution of within- and site-corrected within-event residuals for Station 3513

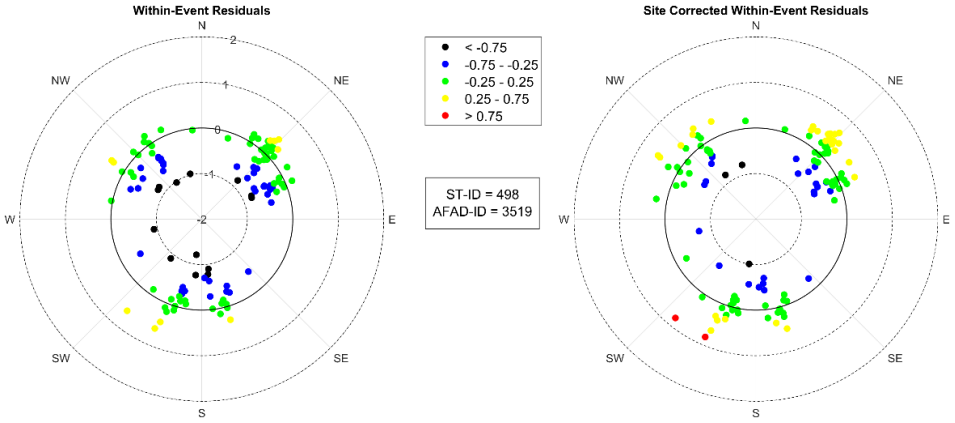

Figure 4.32: Directional distribution of within- and site-corrected within-event residuals for Station 3519

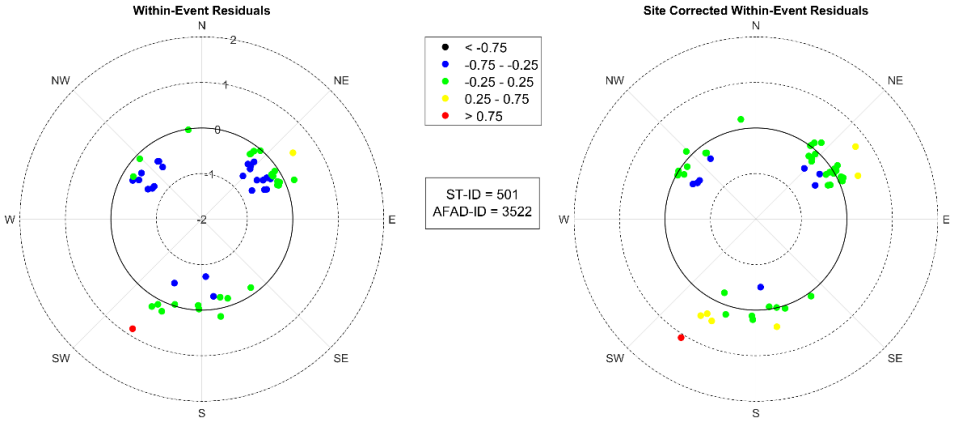

Figure 4.33: Directional distribution of within- and site-corrected within-event residuals for Station 3522

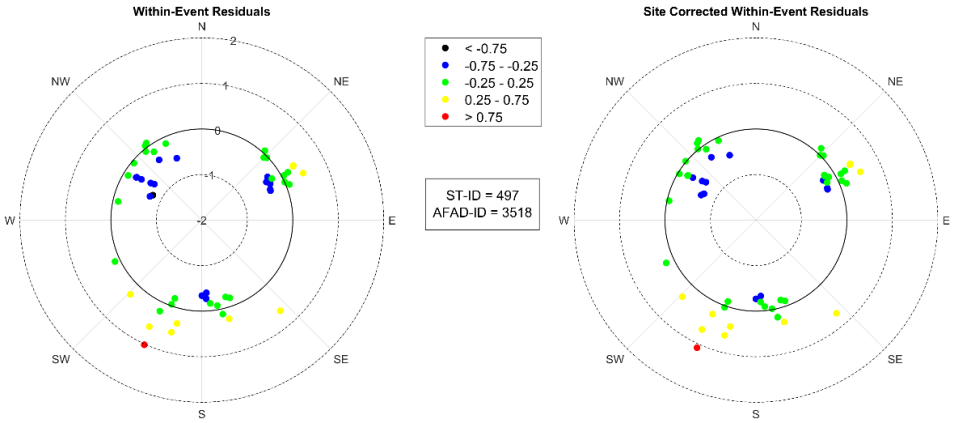

Figure 4.34: Directional distribution of within- and site-corrected within-event residuals for Station 3518

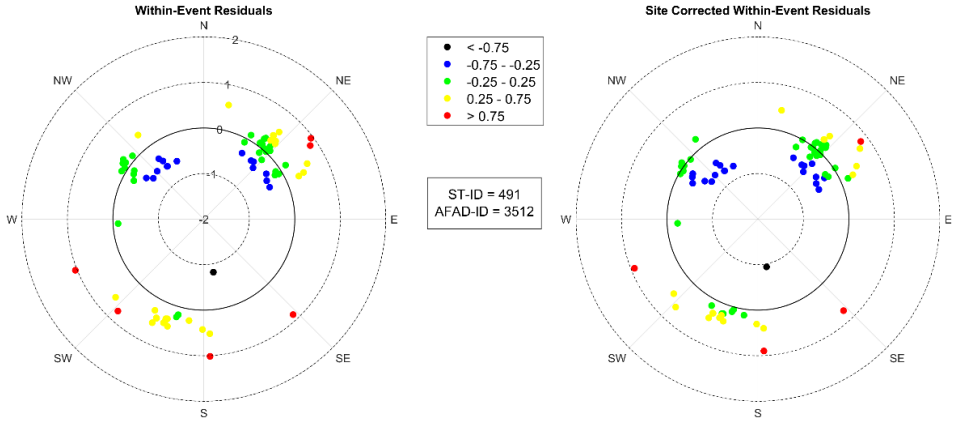

Figure 4.35: Directional distribution of within- and site-corrected within-event residuals for Station 3512

4.3.3 Example 3: Analysis of Stations in Bodrum

Bodrum-Mugla is another region where the strong ground motion recording network is dense and the number of recordings at several stations is significantly high. The preliminary evaluation of the directional distribution of within-event residuals in Bodrum stations pointed out that the trends in groups of events originating from certain paths are quite different; therefore, the path effects might be mapped into the estimated site terms. To demonstrate how the path effects may change the estimated site terms, nine stations on the north, south and east of the bay are selected as shown in Figure 4.36. In these stations, two particular groups of within-event residuals are selected: Group 1 represents the earthquakes originating from off-shore Datca Fault, which was ruptured in 2017 Bodrum-Kos earthquake (M_W=6.6, Karasözen et al., 2018) and Group 2 represents the earthquakes occurred on Oren Fault segments along the shoreline. The directional distribution of within-event residuals for these stations are presented in Figure 4.37 through Figure 4.39.

Figure 4.36: Selected stations in Bodrum (Group 1 - Stations 4801, 4808, 4821 (right), Group 2 – Stations 4806, 4809 and 4817 (left) and Group 3 – Stations 4810, 4812 and 4815)

The green rectangles on the rose diagrams show the recordings associated with Path 1 (Datca Fault) and orange rectangles show the recordings associated with Path 2 (Oren Fault). The path terms for each station and additionally for each group, i.e., the average of within-event residuals within each rectangle are calculated and tabulated in Table 4.1. Table 4.1 shows that the path terms from Path 1 are positive on the North and East of the bay and negative on the south of the bay. The path terms from Paths 1 and 2 are similar on the east and south on the bay, but quite different on the north of the bay. The path terms change significantly for each station, so it is not meaningful to group the path terms based on the location of the station and use the average of the stations as the average path term for that particular ray path.

Table 4.1: Path terms calculated for each station and region

	Station	Path 1	Path 2
Group 1	4801	0.003	0.018
	4808	0.673	0.683
	4821	0.289	0.392
	Whole	0.369	0.406
Group 2	4806	0.000	0.008
	4809	0.029	0.080
	4817	0.554	-0.202
	Whole	0.217	-0.024
Group 3	4810	-0.201	-0.370
	4812	-0.775	-0.429
	4815	-0.280	-0.992
	Whole	-0.445	-0.506

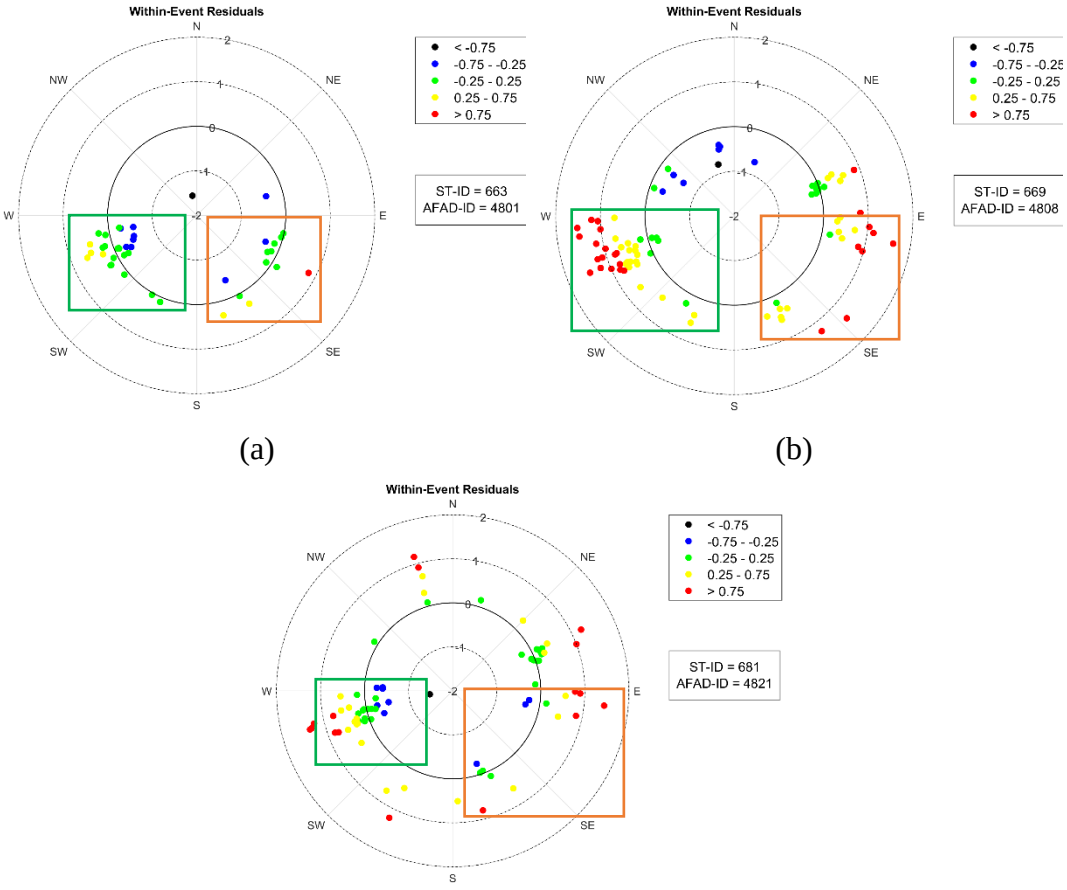

Figure 4.37: Directional distribution of within-event residuals and selected paths for Group 1 - Stations (a) 4801 (b) 4808 and (c) 4821

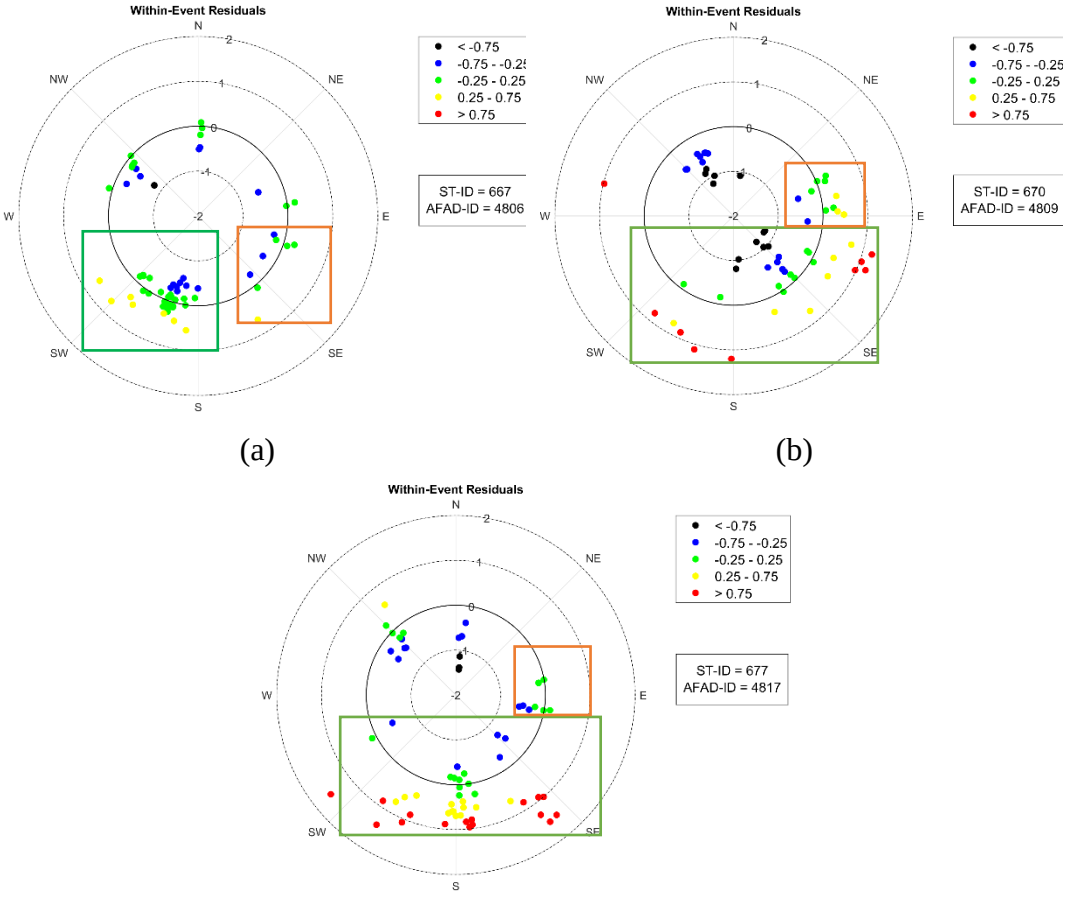

Figure 4.38: Directional distribution of within-event residuals and selected paths for Group 2 - Stations (a) 4806 (b) 4809 and (c) 4817

To demonstrate the effect of the path term on the site term, the within-event residuals are corrected using the calculated path terms. For the recordings, which do not fall into any of the selected paths no adjustment is made. The site terms are re-calculated by the path corrected within event terms and a comparison of the site terms before and after the separation of systematic path effects are given in Table 4.2. According to Table 4.2, separation of the path terms affected the site terms significantly. Significant site terms estimated for Station 4808, 4812 and 4815 are reduced substantially after the path effects are separated. The change is not that significant in some stations like Station 4801, 4806 and 4809. In general terms,

estimated site terms are near zero after the separation of the path effects, indicating that the site terms may be significantly affected by systematic path effects.

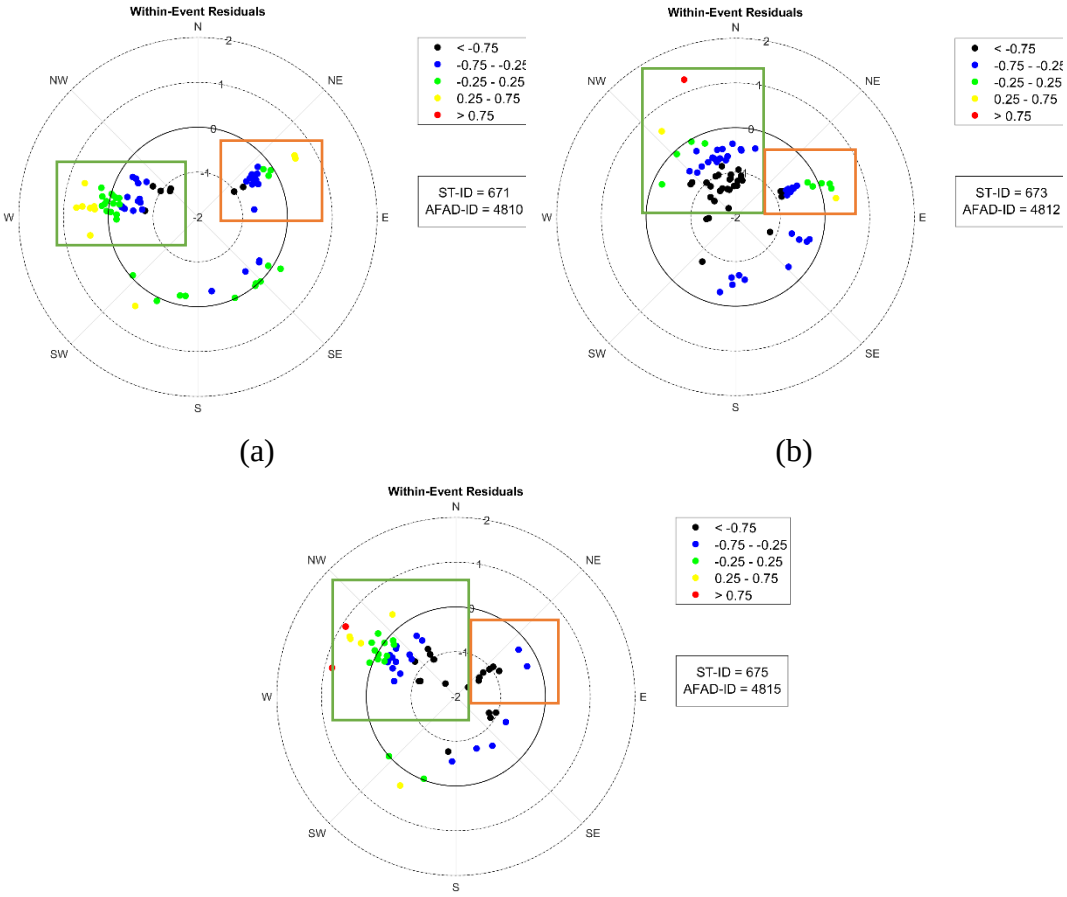

Figure 4.39: Directional distribution of within-event residuals and selected paths for Group 3 - Stations (a) 4810 (b) 4812 and (c) 4815

Table 4.2: Site terms before and after the separation of systematic path effects

	Station	Site Term	
Group#1		Before	After
	4801	-0.039	-0.047
	4808	0.460	-0.017
	4821	0.282	0.058
Group#2	Station	Site Term	
		Before	After
	4806	-0.057	-0.058
	4809	-0.099	-0.130
	4817	0.220	-0.110
Group#3	Station	Site Term	
		Before	After
	4810	-0.218	-0.017
	4812	-0.663	-0.085
	4815	-0.445	-0.108

Based on the Bodrum example, it can be concluded that the site terms provided in this study should be used with utmost care when the path effects are detectable. Finally, the directional distribution of within-event residuals after path and site adjustments are shown in Figure 4.40 through Figure 4.42.

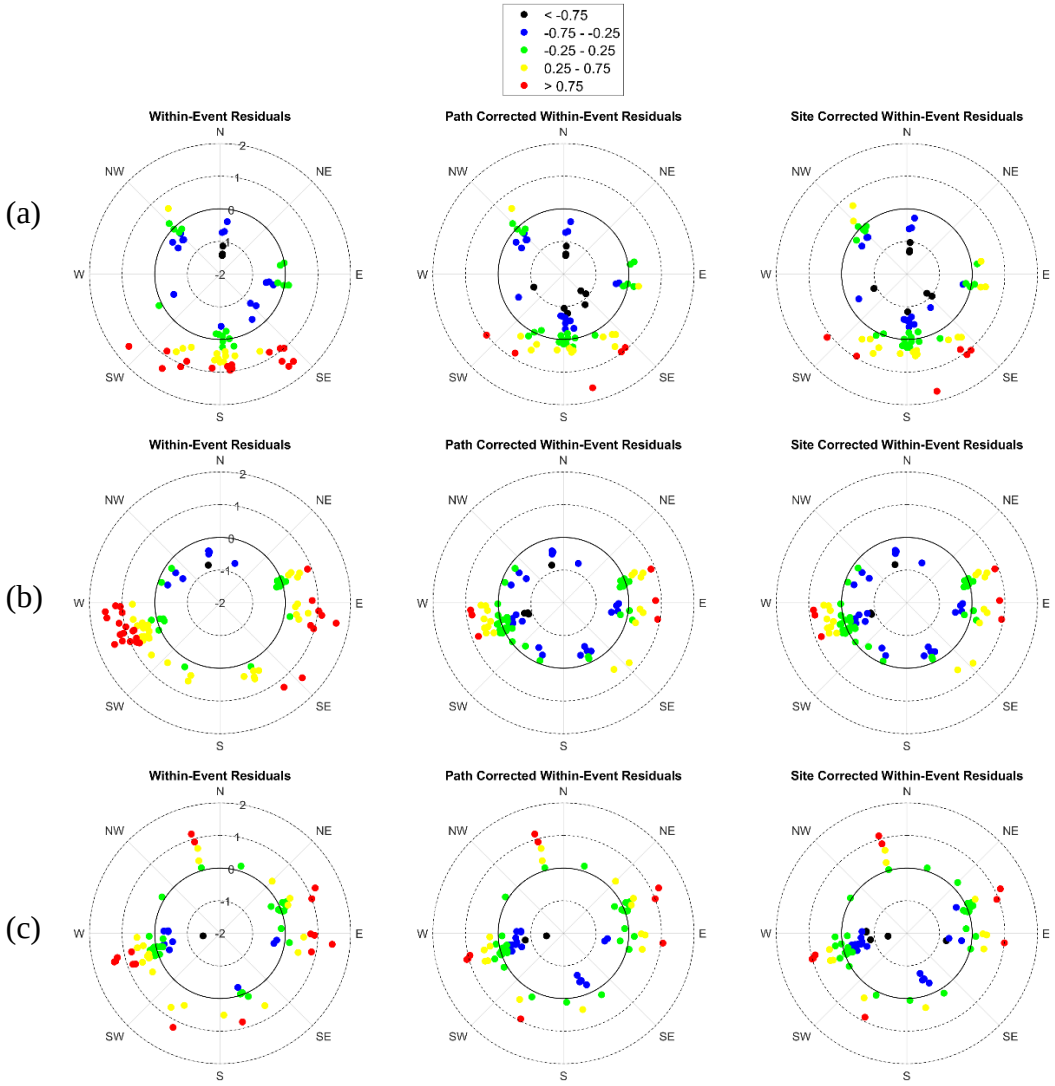

Figure 4.40: Directional distribution of within-event residuals and selected paths for Group 1 - Stations (a) 4801 (b) 4808 and (c) 4821

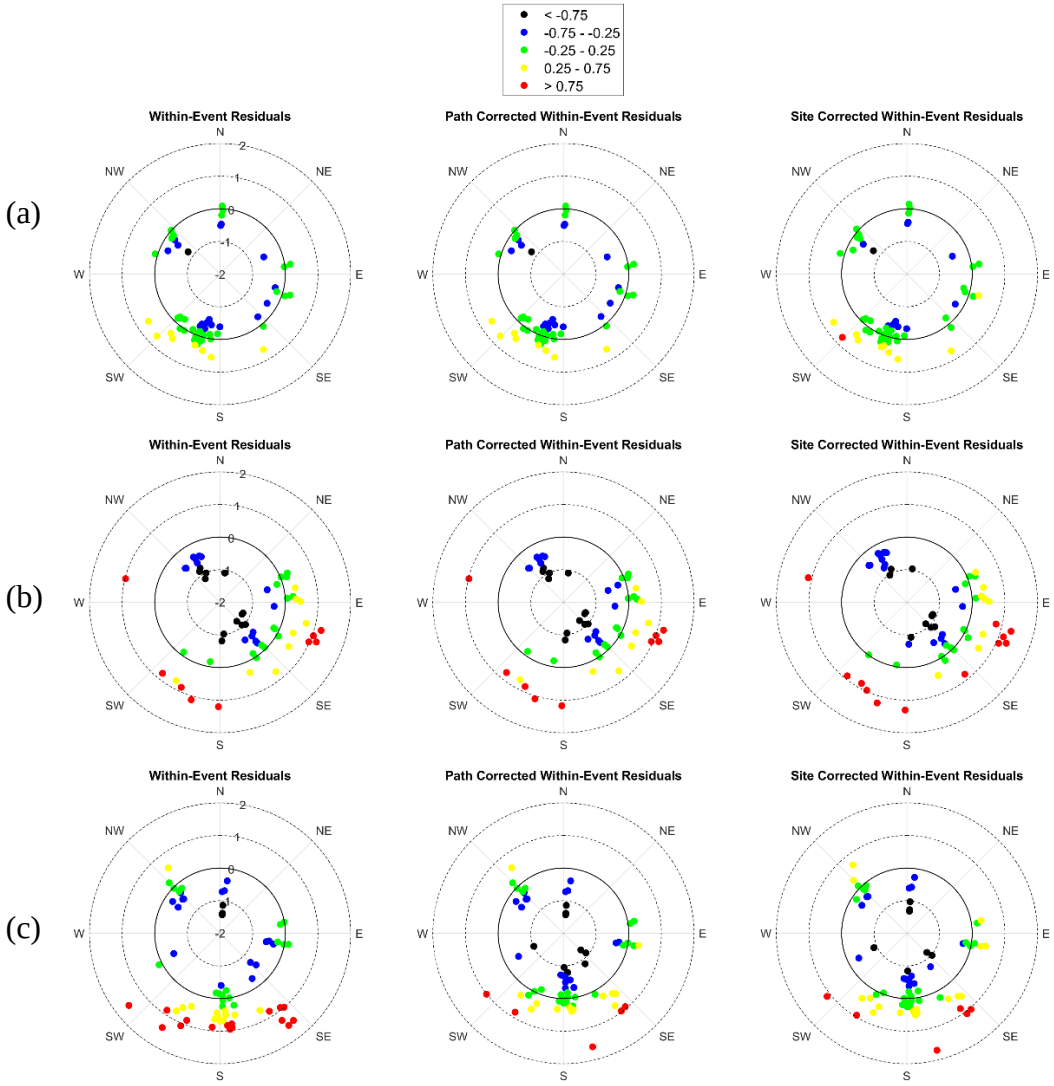

Figure 4.41: Directional distribution of within-event residuals and selected paths for Group 2 - Stations (a) 4806 (b) 4809 and (c) 4817

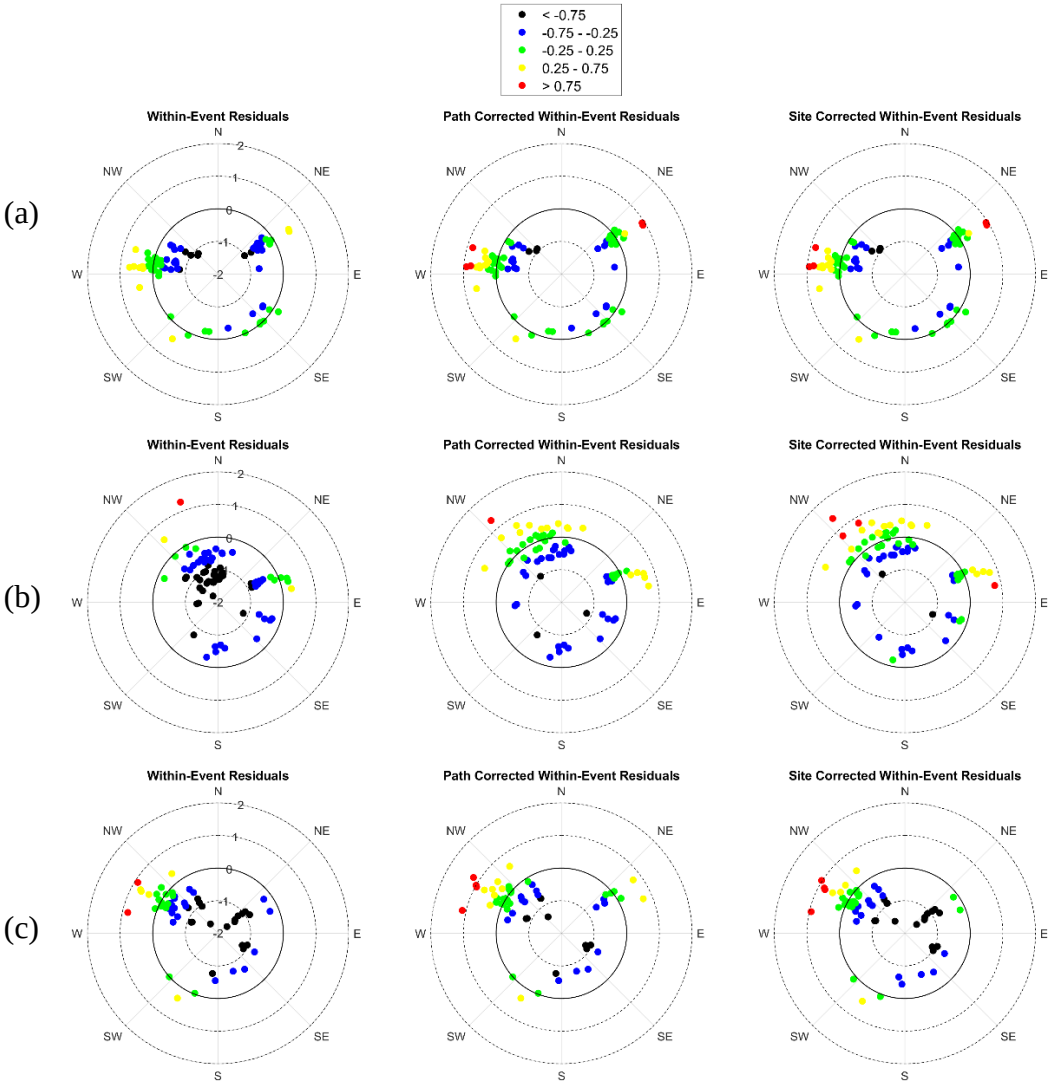

Figure 4.42: Directional distribution of within-event residuals and selected paths for Group 3 - Stations (a) 4810 (b) 4812 and (c) 4815

CHAPTER 5

APPLICATION EXAMPLES AND CONCLUSIONS

This study attempts to develop fully non-ergodic GMMs for Turkey by utilizing the well-established Turkish strong ground motion database (the N-TSMD developed by and explained in Akbas et al., 2022) based on two global GMMs proposed by Abrahamson et al. (2014 – ASK14) and Chiou and Youngs (2014 – CY14). Important aspects of the applied methodology and the main conclusions are as follows:

a. The NGA-West 2 GMMs are not utilized as base models in this study before checking their predictive performance with the N-TSMD for any possible bias in median predictions. **Residual analysis showed that all NGA-West 2 models are biased towards overprediction for applications in Turkey and should not be used in PSHA or engineering seismology applications without any modifications.** The overprediction bias in NGA-West 2 GMMs is smaller when compared to NGA-W1 models (Gulerce et al., 2016) but still quite large (≈1 ln units) to neglect.
b. **To correct for the bias**, **the Z_{TOR} scaling** of ASK14 and CY14 models were modified by removing the Z_{TOR} scaling implemented in the original models. This modification has improved the distribution of event terms significantly. It is not very straight-forward to understand the reason for the inconsistency in Z_{TOR} scaling of the N-TSMD and original NGA-West 2 models. The inconsistency is **clearly not related** to the **national estimates for focal depth** since the N-TSMD includes either case-by-case evaluations of the rupture plane (for M>6 events) or corrected focal depth estimated from ISC-EHB (for 5<M<6 events).
c. After the modification in Z_{TOR} scaling, the remaining bias in the ASK14 and CY14 models is further corrected by slight modification of models' constant

terms. This final modification created a small bias in TR-Adjusted ASK14 for small magnitudes towards underprediction. **Therefore, if a single GMMs will be utilised in calculations, the TR-Adjusted CY14 model should be preferred.** However, both models should be utilized in PSHA applications to cover the center, body and range of epistemic uncertainty.

d. Gulerce et al. (2016) did not propose any changes in standard deviations of NGA-W1 models due to unusually large between-event variability estimates. **This study provides a TR-adjusted standard deviation model that should be applied along with the median TR-Adjusted ASK14 and TR-Adjusted CY14 models.** This time, the model developers have more confidence in the between-event variability estimates, since the results are quite consistent with current literature (e.g. Cagnan and Akkar, 2019).
e. Recent studies correlate the between-event variability with the stress drop and the depth of the earthquake. Regional differences in stress drop parameter may be a part of inconsistency in Z_{TOR} scaling and this assumption calls for the evaluation of spatial distribution of event terms. Based on the analysis results, five source domains are defined as Marmara, Western Anatolia, Southwestern Anatolia, Hatay-Maras Block and Eastern Anatolian Plateau. For each source domain, region-specific event terms and region-specific between-event aleatory variability models are developed and presented at Chapter 3.
f. If the seismic source of interest falls into one of these domains, **the region-specific tau-model should be combined with the region-specific median TR-Adjusted ASK14 and TR-Adjusted CY14 models for PSHA and in other deterministic applications.**
g. The within-event residuals and their variability are analyzed carefully to capture systematic site and path effects. The site terms and within-event standard deviations (a.k.a. the single-station sigma) are calculated for each recording station. The phi-models developed in this study for repeatable site effects are in good agreement with the findings of Cagnan and Akkar (2019).

Therefore, **this study also provides a TR-adjusted phi-model that should be applied along with the median TR-Adjusted ASK14 and TR-Adjusted CY14 models to be used in PSHA calculations and deterministic applications**.

h. Rose diagrams given in Chapter 4 clearly shows that path effects (from one path range from a particular source to a group of stations) are mapped into the site terms for some of the selected station groups. Therefore, **estimated site terms and single station sigma values should be used with caution until these repeatable path effects are separated from the site effects**. This separation process requires significant computational resources and is out of the scope of this study.

5.1. Application of Proposed GMMs and Aleatory Variability Models

This section presents three different application examples for the proposed TR-specific, region-specific and station-specific median and aleatory variability models. Due to the complexity of integrating fully non-ergodic GMMs in the PSHA software, deterministic examples that combine a single source with a single site are provided. For this purpose, three different earthquakes in three different domains and one recording station for each event are selected. For the sake of simplicity, only the TR-specific, region-specific and station-specific ASK14 GMMs are used in examples. For each case, four scenarios are considered:

- **Original**: Median±1sigma predictions based on standard deviations of original ASK14 model are provided in panel (b) of each figure.
- **TR-specific ASK14:** Median±1sigma predictions of TR-adjusted ASK14 model using TR-specific tau (τ) and TR-specific phi (φ) values are provided in panel (c) of each figure. This case represents the application in Turkey for anywhere out of the five source domains with unknown single-station sigma.
- **Region-specific TR-adjusted ASK14:** Median±1sigma predictions of region-specific TR-adjusted ASK14 model using region-specific tau (τ) and TR-specific phi (φ) values are provided in panel (d) of each figure. This

scenario represents the application in Turkey within any of the five domains with unknown single-station sigma.

- **Region-and-station-specific TR-adjusted ASK14:** Median±1sigma predictions of region-specific TR-adjusted ASK14 model using region-specific tau (τ) and station-specific phi (φ) values are provided in panel (e) of each figure. This scenario represents the application in Turkey within any of the five source domains with known single-station sigma.

The first example is the well-known Kovancılar Earthquake ($M_w = 6.1$, occurred on 8th March 2010) and the selected station for this event is Bingöl Station (ID#1201, $V_{s30} = 529\ m/s$). Both the station and the earthquake are located in Region #5 (East Anatolian Plateau) as shown in Figure 5.1(a). Panels (b-e) of Figure 5.1 provide the four application scenarios described above and include the recorded spectral accelerations for comparison.

Regionalization of ASK14 GMM for Turkey (Figure 5.1(c)) resulted in a decrease in median values compared to the original model (Figure 5.1(b)) because of the adjustments applied to the median model. According to Figure 5.1(c), the recording is slightly above the median predictions at short periods and close to the 84th percentile on longer periods. On the other hand, there is a clear increase in total sigma due to the use of TR-specific τ and φ models. Removing the systematic source effects and adding the region-specific between event terms to the median (Figure 5.1(d)) led to a further decrease in the median predictions up to T=1s, as the events in Region#5 had a negative average event term that reaches up to zero after T≈1s. In comparison to Figure 5.1(c), the total standard deviation is decreased when the region-specific $\tau - model$ is utilized. Applying calculated site terms and single station sigma values resulted in a change in the spectral shape and larger standard deviations at longer periods. The total sigma increased due to the use of station-specific φ value, which represents the aleatory variability in site response for this station. The actual spectral accelerations lie within ±1 sigma range for all cases, but

the best match is accomplished with the TR-adjusted ASK14 at shorter periods and with region-and-station-specific TR-adjusted ASK14 at longer periods.

The recording from recent Samos Earthquake ($M_w = 7.0$, 30th October 2020) from Konak Station ID#3518 ($V_{s30} = 298$) is used as the second example. The station and the earthquake are located in Region#2 (Western Anatolia) as shown in Figure 5.2(a). Panels (b-e) of Figure 5.2 provide the four application scenarios described above and include the recorded spectral accelerations for comparison.

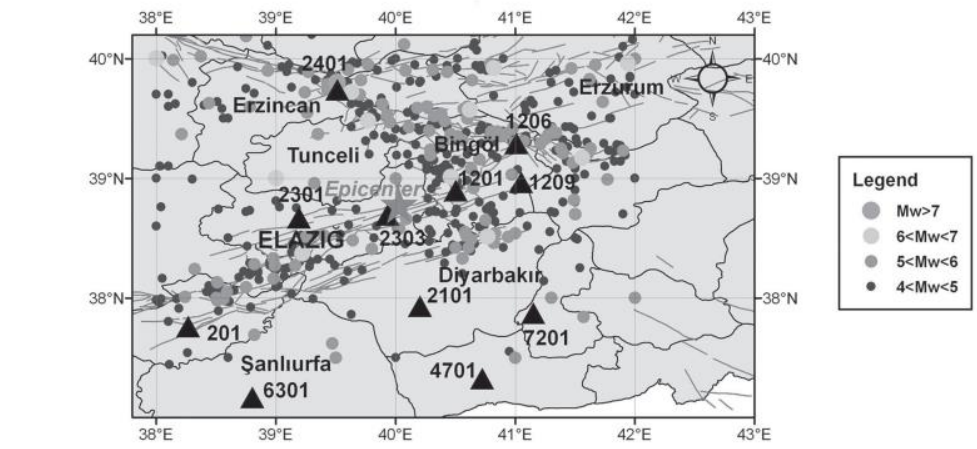

(a)

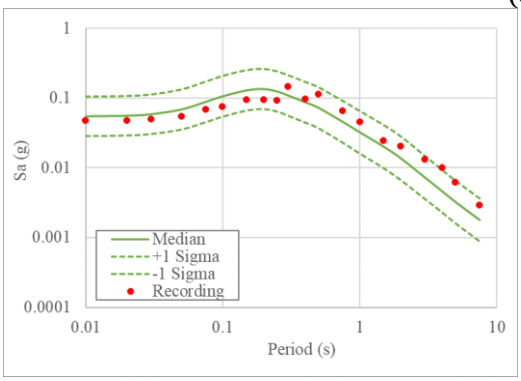

(b)

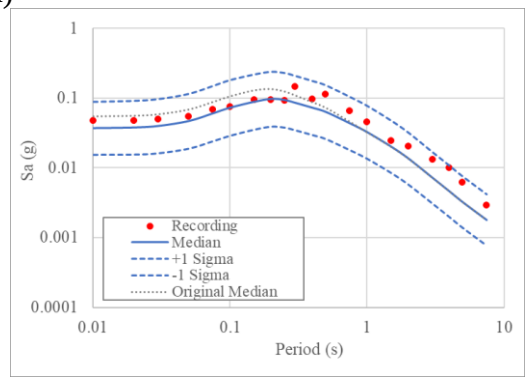

(c)

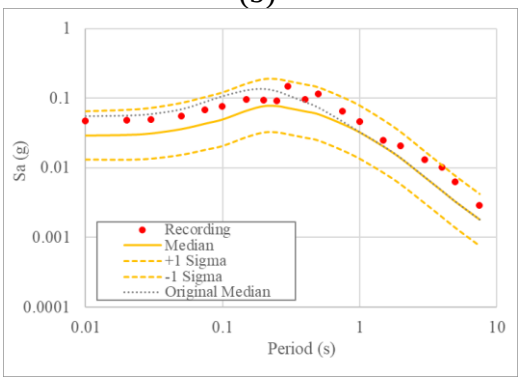

(d)

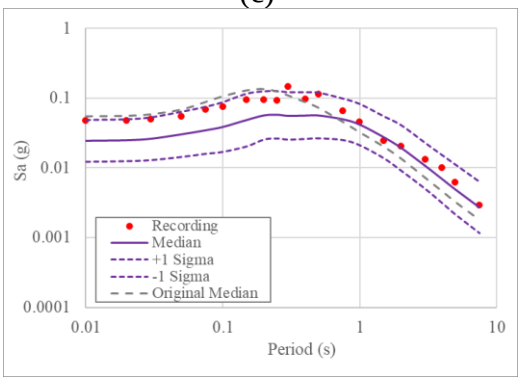

(e)

Figure 5.1: (a) The 2010 Kovancilar Earthquake and Station#1201 (taken form Akkar et al., 2010). Median±1sigma spectral accelerations by: (b) original ASK14, (c) TR-adjusted ASK14 model, and partially non-ergodic TR-adjusted ASK14 model after removing the systematic (d) source effects (e) source and site effects

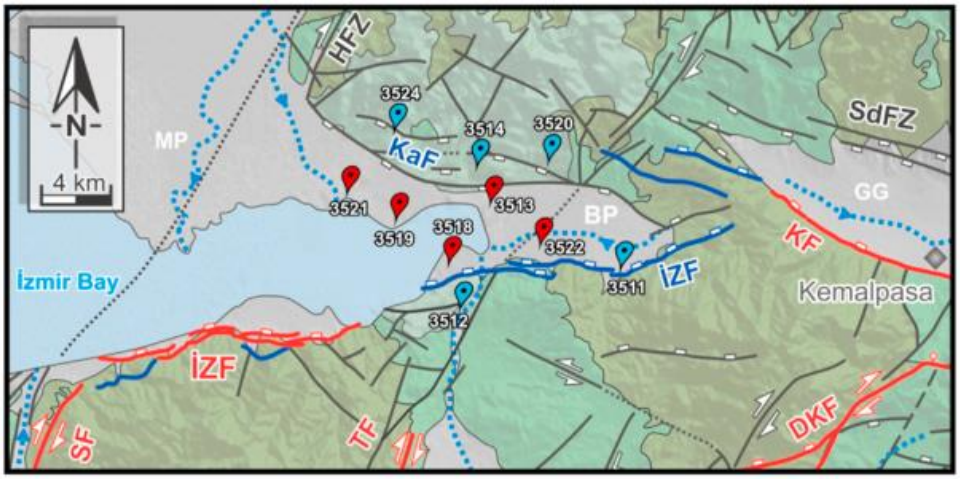

(a)

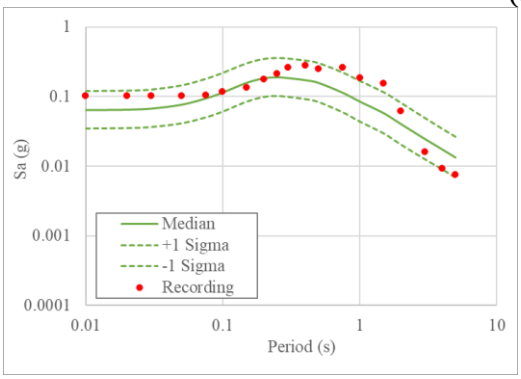

(b)

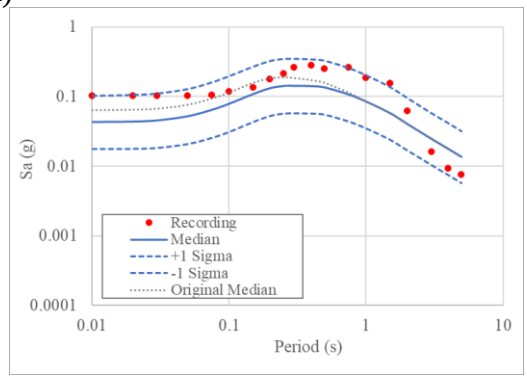

(c)

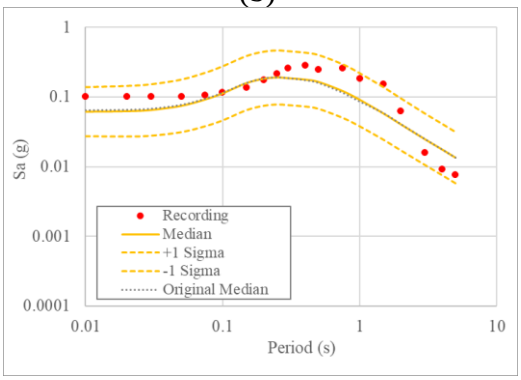

(d)

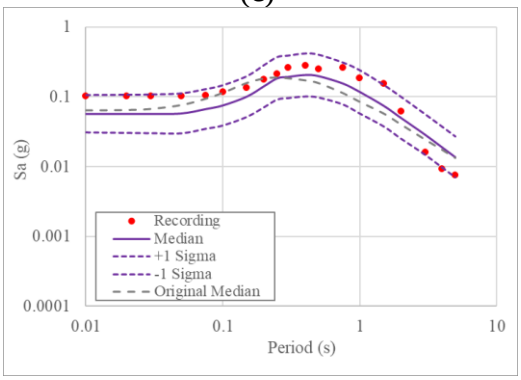

(e)

Figure 5.2: (a) The 2020 Samos Earthquake and Station#3518 (taken form Gulerce et al., 2022). Median±1sigma spectral accelerations by: (b) original ASK14 model, (c) TR-adjusted ASK14 model, and partially non-ergodic TR-adjusted ASK14 model after removing the systematic (d) source effects (e) source and site effects.

Similar to the first example the actual spectral accelerations are closer to the 84th percentile predictions in Figure 5.2(c), since the median predictions are reduced with the TR-specific adjustments. When the region-specific event terms are applied, the Western-Anatolia specific median estimates become very close to the original median estimates, but the median±1sigma band is enlarged (Figure 5.2(d)). The utilization of site terms and site-specific φ (Figure 5.2(e)) resulted in a better match with the actual recording. On the contrary to the first example, the site-specific φ value decreased the total standard deviation in this case.

The last example is the Silivri Earthquake ($M_w = 5.7$, occurred on 26th October 2019) recorded at the Silivri Station ID#3408 ($V_{s30} = 460\, m/s$). The station and the earthquake are located in Region#1 (Marmara) as shown in Figure 5.3(a). Panels (b-e) of Figure 5.3 provide the four application scenarios described above and include the original spectral values for comparison. For this event, the TR-specific adjustments (Figure 5.3 (c)) resulted in a significant deviation from the original model's median predictions (Figure 5.3(b)) since the contribution of Z_{TOR} scaling is bigger as compared to large magnitude events. It is notable that the region-specific source correction (Figure 5.3 (d)) made exactly the opposite effect and resulted in the median predictions that are almost equal to the original one. Finally, the site-term correction (Figure 5.3 (e)) reduced the median value extremely and the actual spectral accelerations are now around median+1sigma. The reason for the extreme site term, is that almost all the recordings from this station come from same direction and they are overestimated, which consequently led to a negative site term. This also shows the importance of systematic path effects.

5.2. Final Conclusive Remarks and Future Works

As shown with the three examples provided in this chapter, the regionalization of global GMMs or using partially non-ergodic approach does not always guarantee a reduction in the median estimations or standard deviations of the GMM. On the contrary, significantly high between-event variability in N-TSMD resulted in an increase in the total sigma when compared to the original ASK14 and

CY14 models. Regionalization of between-event variability and the region-specific event terms has reduced the median predictions and standard deviations in some regions but resulted in predictions similar to the original ASK14 predictions in others.

The ultimate goal of the non-ergodic GMMs is obviously to use in PSHA applications. However, the separation of systematic source, site and path effects from aleatory variability requires certain changes in a PSHA application. Systematic source, site and path effects should be this time included in the epistemic uncertainty. Only a few attempts (e.g. Abrahamson et al., 2019 created a non-ergodic GMM with 100 sets of coefficients to account for the newly introduced epistemic uncertainty) are made in the literature to include the emerging epistemic uncertainty; however, this issue should be studied carefully. Moreover, selected approach in this study, i.e., region-based approach does not enable neither prediction at new locations nor handling systematic path effects in a smooth way. The new emerging coordinate-based approaches offers a better base not only for these problems but also for the integration of non-ergodic GMMs in PSHA. This study provided a basis for the non-ergodic GMMs for Turkey but for the use in hazard calculations more studies are required in the future.

(a)

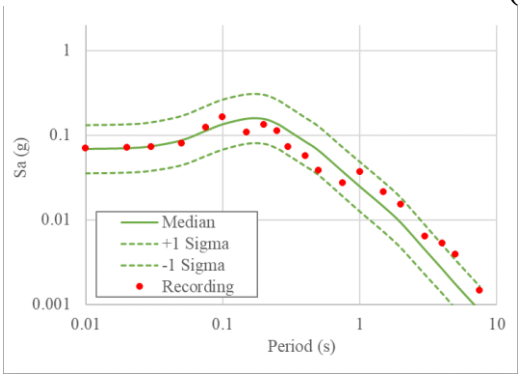

(b)

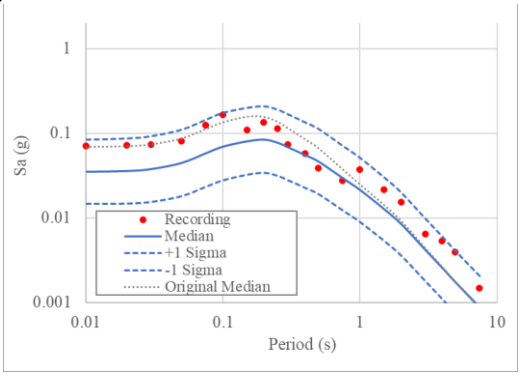

(c)

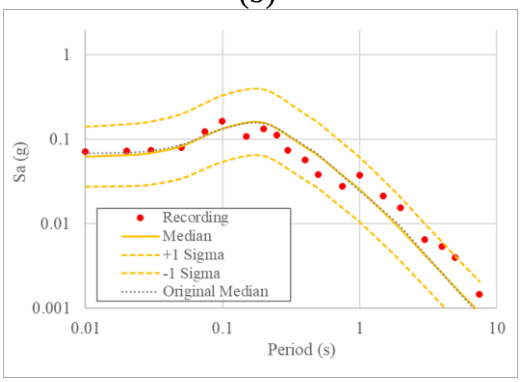

(d)

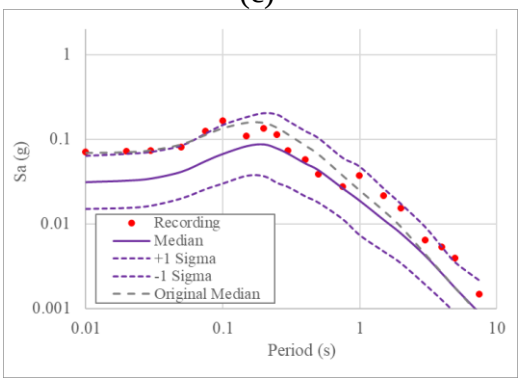

(e)

Figure 5.3: (a) The 2019 Silivri Earthquake and Station#3408 (taken form AFAD, 2019). Median±1sigma spectral accelerations by: (b) original ASK14 model, (c) TR-adjusted ASK14 model, and partially non-ergodic TR-adjusted ASK14 model after removing the systematic (d) source effects (e) source and site effects.

REFERENCES

Abrahamson, N.A., Gulerce, Z. (2022) Summary of the Abrahamson and Gulerce NGA-Sub ground-motion model for subduction earthquakes. Earthquake Spectra.

Abrahamson, N.A., Kuehn, N.M., Walling, M., & Landwehr, N. (2019). Probabilistic Seismic Hazard Analysis in California Using Nonergodic Ground Motion Models. Bulletin of the Seismological Society of America.

Abrahamson, N.A., Walter J. Silva, Ronnie Kamai (2014). Summary of the ASK14 Ground Motion Relation for Active Crustal Regions. Earthquake Spectra 2014; 30 (3): 1025–1055.

Akbaş B., Tetik T., Önder F.M., Sopacı E., Tanırcan G., Ozacar A.A., and Gulerce Z. (2022). The New Turkish Strong Motion Dataset (N-TSMD) for earthquake engineering applications. In preparation for Bulletin of Earthquake Engineering.

Akkar S, Kale Ö, Ansari A, Durgaryan R, Askan Gündoğan A, Hamzehloo H, Harmandar E, Tsereteli N, Waseem M, Yazjeen T, Yılmaz MT (2014a) EMME strong-motion database serving for predictive model selection to EMME ground-motion logic-tree applications. Second European conference on earthquake engineering and seismology, İstanbul, Abstract no. 3220

Akkar, Sinan & Cagnan, Zehra & Yenier, Emrah & Erdoğan, Özgür & Sandikkaya, M. Abdullah & Gülkan, Polat. (2010). The recently compiled Turkish strong motion database: Preliminary investigation for seismological parameters. Journal of Seismology. 14. 457-479.

Alipour, N. & Sandikkaya, M. Abdullah & Gulerce, Zeynep. (2020). Ground Motion Characterization for Vertical Ground Motions in Turkey—Part 1: V/H Ratio Ground Motion Models. Pure and Applied Geophysics. 177.

Anderson, J.G., & Brune, J.N. (1999). Probabilistic Seismic Hazard Analysis without the Ergodic Assumption. Seismological Research Letters, 70, 19-28.

Atik, L.A., Abrahamson, N.A., Bommer, J.J., Scherbaum, F., Cotton, F., & Kuehn, N.M. (2010). The Variability of Ground-Motion Prediction Models and Its Components. Seismological Research Letters, 81, 794-801.

Atkinson, G.M. (2006). Single-Station Sigma. Bulletin of the Seismological Society of America, 96, 446-455.

Baltay, Annemarie & Hanks, Thomas & Beroza, Gregory. (2013). Stable Stress-Drop Measurements and their Variability: Implications for Ground-Motion Prediction. The Bulletin of the Seismological Society of America. 103. 211-222.

Bayless, J., & Abrahamson, N.A. (2019). Summary of the BA18 Ground-Motion Model for Fourier Amplitude Spectra for Crustal Earthquakes in California. Bulletin of the Seismological Society of America.

Bommer, J.J., & Abrahamson, N.A. (2006). Why Do Modern Probabilistic Seismic-Hazard Analyses Often Lead to Increased Hazard Estimates? Bulletin of the Seismological Society of America, 96, 1967-1977.

Boore, David & Stewart, Jonathan & Seyhan, Emel & Atkinson, Gail. (2014). NGA-West2 equations for predicting PGA, PGV, and 5% damped PSA for shallow crustal earthquakes. NGA-West2 Equations for Predicting PGA, PGV, and 5% Damped PSA for Shallow Crustal Earthquakes. 30. 1057-1085.

Bozorgnia, Yousef & Ancheta, Timothy & Atkinson, Gail & Baker, Jack & Baltay, Annemarie & Boore, David & Campbell, Kenneth & Chiou, Brian & Darragh, Robert & Day, Steve & Donahue, Jennifer & Graves, Robert & Gregor, Nick & Hanks, Thomas & Idriss, I. & Kamai, Ronnie & Kishida, Tadahiro & Youngs, R.. (2014). NGA-West2 research project. Earthquake Spectra. 30.

Campbell, Kenneth & Bozorgnia, Yousef. (2014). Campbell-bozorgnia NGA-West2 horizontal ground motion model for active tectonic domains. NCEE 2014 - 10th U.S. National Conference on Earthquake Engineering: Frontiers of Earthquake Engineering.

Chiou, B. S. J., & Youngs, R. R. (2014). Update of the Chiou and Youngs NGA model for the average horizontal component of peak ground motion and response spectra. Earthquake Spectra, 30(3), 1117-1153.

Cotton, Fabrice & Archuleta, Ralph & Causse, Mathieu. (2013). What is Sigma of the Stress Drop?. Seismological Research Letters. 84.

Çağnan, Z., & Akkar, S. (2018). Assessment of Aleatory and Epistemic Uncertainty for Ground-Motion Intensity Measure Prediction in Turkey. Bulletin of the Seismological Society of America.

Dawood, H.M., & Rodriguez-Marek, A. (2013). A Method for Including Path Effects in Ground-Motion Prediction Equations: An Example Using the Mw 9.0 Tohoku Earthquake Aftershocks. Bulletin of the Seismological Society of America, 103, 1360-1372.

Douglas, J., & Aochi, H. (2016). Assessing Components of Ground-Motion Variability from Simulations for the Marmara Sea Region (Turkey). Bulletin of the Seismological Society of America, 106, 300-306.

Gulerce, Zeynep & Kargıoğlu, Bahadır. (2015). Turkey-Adjusted NGA-W1 Horizontal Ground Motion Prediction Models. Earthquake Spectra. 32.

Kaklamanos, James & Baise, Laurie & Boore, David. (2011). Estimating Unknown Input Parameters when Implementing the NGA Ground-Motion Prediction Equations in Engineering Practice. Earthquake Spectra. 27. 1219-1235.

Kale, Özkan & Akkar, Sinan & Ansari, Anooshiravan & Hamzehloo, Hosseyn. (2015). A Ground-Motion Predictive Model for Iran and Turkey for Horizontal PGA, PGV, and 5% Damped Response Spectrum: Investigation

of Possible Regional Effects. Bulletin of the Seismological Society of America. 105. 963-980.

Karasözen E, Nissen E, Büyükakpınar P, Cambaz MD, Kahraman M, Ertan EK, Abgarmi B, Bergman E, Ghods A, Özacar AA (2018) The 2017 July 20 Mw 6.6 Bodrum–Kos earthquake illuminates active faulting in the Gulf of Gökova, SW Turkey. Geophys J Int 214:185-199.

Ktenidou, O., Roumelioti, Z., Abrahamson, N.A., Cotton, F., Pitilakis, K., & Hollender, F. (2017). Understanding single-station ground motion variability and uncertainty (sigma): lessons learnt from EUROSEISTEST. Bulletin of Earthquake Engineering, 16, 2311-2336.

Kuehn, N.M., & Abrahamson, N.A. (2019). Spatial correlations of ground motion for non-ergodic seismic hazard analysis. Earthquake Engineering & Structural Dynamics, 49, 23 - 4.

Kuehn, N.M., Abrahamson, N.A., & Walling, M. (2019). Incorporating Nonergodic Path Effects into the NGA-West2 Ground-Motion Prediction Equations. Bulletin of the Seismological Society of America.

Landwehr, N., Kuehn, N.M., Scheffer, T., & Abrahamson, N.A. (2016). A Nonergodic Ground-Motion Model for California with Spatially Varying Coefficients. Bulletin of the Seismological Society of America, 106, 2574-2583.

Lanzano, G., Pacor, F., Luzi, L., D'Amico, M., Puglia, R., & Felicetta, C. (2017). Systematic source, path and site effects on ground motion variability: the case study of Northern Italy. Bulletin of Earthquake Engineering, 15, 4563-4583.

Lavrentiadis, G., Abrahamson, N.A., & Kuehn, N.M. (2021). A Non-Ergodic Effective Amplitude Ground-Motion Model for California.

Lin, P.S., Chiou, B.S., Abrahamson, N.A., Walling, M., Lee, C.T., & Cheng, C. (2011). Repeatable Source, Site, and Path Effects on the Standard Deviation

for Empirical Ground-Motion Prediction Models. Bulletin of the Seismological Society of America, 101, 2281-2295.

Luzi, L., Bindi, D., Puglia, R., Pacor, F., & Oth, A. (2014). Single-Station Sigma for Italian Strong-Motion Stations. Bulletin of the Seismological Society of America, 104, 467-483.

Morikawa, N., Kanno, T., Narita, A., Fujiwara, H., Okumura, T., Fukushima, Y., & Guerpinar, A. (2008). Strong motion uncertainty determined from observed records by dense network in Japan. Journal of Seismology, 12, 529-546.

Oth, A., Miyake, H., and Bindi, D. (2017), On the relation of earthquake stress drop and ground motion variability, J. Geophys. Res. Solid Earth, 122, 5474– 5492.

Rodriguez-Marek, A., Montalva, G.A., Cotton, F., & Bonilla, F. (2011). Analysis of Single-Station Standard Deviation Using the KiK-net Data. Bulletin of the Seismological Society of America, 101, 1242-1258.

Sandikkaya, M. Abdullah. (2016). Effects of low magnitude records on ground-motion prediction equations: A preliminary study for Turkey. 37. 237-252.

Satoh, Toshimi & Okazaki, Atsushi. (2016). Relation Between Stress Drops and Depths of Strong Motion Generation Areas Based on Previous Broadband Source Models for Crustal Earthquakes in Japan.

Scherbaum, F., Delavaud, É., & Riggelsen, C. (2009). Model Selection in Seismic Hazard Analysis: An Information-Theoretic Perspective. Bulletin of the Seismological Society of America, 99, 3234-3247.

Strasser, F.O., Abrahamson, N.A., & Bommer, J.J. (2009). Sigma: Issues, Insights, and Challenges. Seismological Research Letters, 80, 40-56.

Strasser, Fleur & Bommer, Julian. (2009). Sigma: Issues, Insights, and Challenges. Seismological Research Letters - SEISMOL RES LETT. 80. 40-56.

T.C. İçişleri Bakanlığı Afet ve Acil Durum Yönetimi Başkanlığı, 2019. 26 Eylül 2019 Marmara Denizi, Silivri Açıkları (İstanbul) Mw 5.8 Depremine İlişkin ön Değerlendirme Raporu

Villani, M., & Abrahamson, N.A. (2015). Repeatable Site and Path Effects on the Ground-Motion Sigma Based on Empirical Data from Southern California and Simulated Waveforms from the CyberShake Platform. Bulletin of the Seismological Society of America, 105, 2681-2695.

Wald, David & Allen, Trevor. (2007). Topographic Slope as a Proxy for Seismic Site Conditions and Amplification. Bulletin of the Seismological Society of America. 97. 1379-1395.

Zafarani, H., & Soghrat, M.R. (2017). Single-Station Sigma for the Iranian Strong Motion Stations. Pure and Applied Geophysics, 174, 4077-4099.

APPENDICES

A. Site Terms and Site-Corrected Within-Event Standard Deviations

ASK14

Station ID	Lat	Long	T=0.01s		T=0.2s		T=1s		T=2s	
			$\delta S2S_s$	$\varphi_{SS,s}$	$\delta S2S_s$	$\varphi_{SS,s}$	$\delta S2S_s$	$\varphi_{SS,s}$	$\delta S2S_s$	$\varphi_{SS,s}$
0118	37.0362	35.3184	-0.6907	0.5765	-0.7025	0.5228	0.4762	0.4934	0.7418	0.4882
0120	36.7701	35.7901	-0.7144	0.4076	-0.4491	0.4253	-0.1789	0.5652	-0.2396	0.6968
0122	37.4339	35.8202	-0.3778	0.7777	-0.1926	0.7682	-0.5858	0.5978	-0.9773	0.553
0126	37.5455	35.3919	-0.451	0.6918	-0.1015	0.6598	-0.0535	0.3974	-0.3392	0.3415
0201	37.7612	38.2674	0.377	0.3809	0.2845	0.4647	0.1194	0.3716	0.6552	0.4195
0204	38.029	39.0347	0.0647	0.5209	0.0026	0.6205	0.2192	0.4454	0.0687	0.5429
0205	37.7918	38.616	-0.602	0.5031	-0.656	0.4706	0.2169	0.3795	0.5234	0.3846
0207	38.0323	38.2476	-0.073	0.4136	0.1714	0.5614	-0.4787	0.4389	-0.3896	0.402
0208	37.7869	37.6528	-0.3597	0.4626	-0.2682	0.4872	-0.1223	0.5338	-0.0923	0.6378
0209	37.5776	38.4825	0.6812	0.5325	0.3547	0.575	-0.2405	0.3898	-0.0173	0.3875
0210	37.7863	38.2544	0.047	0.4835	-0.0354	0.5604	-0.3215	0.3655	0.0735	0.3674
0212	38.0277	38.62409	-1.0739	0.5063	-1.2923	0.4688	-0.7049	0.4568	-0.7405	0.4704
0213	37.79667	37.92957	0.4696	0.4556	0.7352	0.442	0.993	0.4464	0.3965	0.5067
0302	38.0599	30.1537	-0.123	0.5308	-0.4545	0.6635	0.1359	0.456	0.3721	0.4854
0401	39.7198	43.0164	-0.23	0.5854	-0.2161	0.4876	-0.4024	0.4711	-0.2972	0.3095
0403	39.7989	42.6801	0.2762	0.4339	0.2527	0.4821	0.4425	0.5434	0.4525	0.4821
0404	39.5388	42.7725	0.3546	0.6339	0.5605	0.5527	0.2781	0.4003	-0.049	0.4857
0603	39.5583	33.1186	-0.3838	0.4522	-0.3493	0.5364	-0.4636	0.3805	-0.3831	0.307
0617	40.4569	32.6319	0.1716	0.4157	0.477	0.4037	-0.2135	0.4143	-0.1202	0.2926
0619	39.9055	32.7571	-0.0157	0.5219	-0.267	0.4839	-0.1671	0.617	-0.5489	0.4603
0621	40.2294	33.0289	0.4832	0.3098	0.503	0.303	0.3668	0.4438	0.7507	0.2644
0705	36.1951	29.6474	-0.1556	0.6223	-0.0645	0.5551	0.8652	0.5854	0.4755	0.5943
0712	36.3022	30.148	0.345	0.8496	0.2857	0.8893	0.6158	0.6226	0.0645	0.6118
0716	36.2685	29.4128	-0.5499	0.4707	-0.4578	0.3603	0.0847	0.4794	-0.0479	0.502
0904	37.8572	28.0503	-0.364	0.3441	-0.267	0.4064	-0.0956	0.3684	-0.0859	0.3583
0905	37.86	27.265	-0.1099	0.5159	-0.0341	0.5264	-0.0247	0.5237	-0.3463	0.4261
0910	37.8455	27.7996	0.0871	0.4123	-0.0521	0.3914	0.306	0.4458	0.521	0.403
0911	37.7616	27.3921	-0.2074	0.4077	-0.1352	0.4369	-0.0563	0.489	-0.2733	0.4748
0912	37.9739	28.746	-0.1304	0.5045	-0.0972	0.5472	0.038	0.4573	0.0151	0.3544
0913	37.9115	28.4654	-0.132	0.3857	-0.1113	0.4463	0.1434	0.4859	0.1677	0.3823
0914	37.9133	28.3431	0.4898	0.2875	0.4263	0.3536	0.745	0.3239	0.8801	0.39
0915	37.8841	28.1506	0.2748	0.4259	0.3579	0.4889	0.7222	0.4962	0.821	0.3984
0916	37.8572	28.0503	-0.1885	0.3545	-0.122	0.3999	-0.0333	0.3299	0.2984	0.3415
0917	37.6052	28.0584	0.1389	0.4263	0.1517	0.4776	0.7859	0.4354	0.19	0.2813
0918	37.3697	27.2643	-0.2865	0.8077	-0.1914	0.7959	0.511	0.8291	0.5219	0.8784
0919	37.5595	27.8355	0.3479	0.4699	0.8211	0.4776	0.16	0.4409	0.0727	0.3288
0920	37.5604	27.3749	-0.5639	0.4553	-0.3332	0.4424	-0.0808	0.5589	-0.0138	0.4388
0921	37.8747	27.5922	0.09	0.3596	-0.0079	0.3759	0.6897	0.4543	0.5616	0.3434
0922	37.8537	27.7082	0.3757	0.8523	0.2623	0.8994	0.7785	0.9103	0.7675	0.8637
1001	39.65	27.8569	0.1894	0.6406	0.4977	0.821	-0.0113	0.4118	-0.042	0.2677

Station ID	Lat	Long	T=0.01s		T=0.2s		T=1s		T=2s	
			$\delta S2S_s$	$\varphi_{SS,s}$	$\delta S2S_s$	$\varphi_{SS,s}$	$\delta S2S_s$	$\varphi_{SS,s}$	$\delta S2S_s$	$\varphi_{SS,s}$
1003	39.655	27.862	0.4782	0.9529	0.794	0.9729	0.0225	0.9155	0.1896	1.0576
1005	39.3113	26.686	0.1832	0.891	0.1732	0.9986	-0.8166	0.5944	-0.9111	0.5664
1006	40.3319	27.9966	0.2228	0.4258	0.1583	0.5202	0.0907	0.602	0.107	0.7068
1008	39.3979	28.1273	-0.0209	0.528	-0.2099	0.6527	-0.9276	0.5379	-0.8862	0.388
1009	39.578	28.6323	-0.4133	0.4702	-0.3641	0.5552	-0.5456	0.6121	-0.4855	0.5497
1011	40.336	27.861	0.2272	0.5439	0.1956	0.626	-0.1463	0.5875	-0.3797	0.5538
1013	39.5895	27.0192	-0.117	0.5148	-0.2736	0.6614	-0.8836	0.5885	-1.0765	0.5204
1014	40.114	27.6424	-0.2608	0.5072	-0.4396	0.6316	-0.3274	0.5472	0.1133	0.6838
1015	39.2395	28.1714	-0.6476	0.6075	-0.9592	0.6846	-0.4464	0.5833	-0.9211	0.4482
1016	39.3804	27.6544	0.0297	0.469	0.143	0.5133	0.2522	0.4894	0.3202	0.4124
1017	39.6497	27.8572	0.4337	0.4735	0.6621	0.5111	0.4474	0.4628	0.4739	0.3317
1018	40.4093	27.7878	-0.1499	0.6548	-0.0274	0.7032	0.012	0.6774	-0.1674	0.5952
1019	39.498	26.9753	0.4995	0.431	0.5157	0.5501	-0.4183	0.5715	-0.3987	0.6828
1020	39.9171	28.1641	0.7361	0.5454	0.4819	0.6316	-0.1484	0.495	-0.246	0.4419
1021	39.7474	27.5762	0.056	0.4736	0.2311	0.5831	-0.3239	0.5439	-0.3092	0.4233
1022	39.5817	27.4936	0.28	0.4717	-0.0941	0.5956	0.2276	0.6241	0.243	0.5697
1023	39.6825	28.1666	0.2947	0.5351	0.3208	0.6554	0.3514	0.6237	-0.1621	0.5249
1024	40.0475	27.974	0.5473	0.4705	0.3171	0.5085	0.1971	0.5471	-0.1087	0.4029
1026	39.38445	26.83862	-0.3079	0.507	-0.5768	0.5322	-0.5552	0.5255	-0.66	0.4611
1027	39.57383	26.7422	0.23	0.4691	0.3193	0.5324	-0.2647	0.4746	-0.28	0.4528
1028	39.5855	26.92303	0.4333	0.406	0.4923	0.4613	-0.087	0.5239	-0.2151	0.4439
1101	40.1411	29.9774	-0.008	0.557	0.1884	0.5719	0.4648	0.5147	0.2054	0.3334
1102	39.9043	30.0529	0.033	0.4671	0.3183	0.4668	-0.0124	0.2878	-0.3961	0.3277
1201	38.8971	40.5032	-0.1903	0.506	-0.398	0.578	0.3348	0.335	0.3594	0.4557
1206	39.2935	41.0088	0.1081	0.7879	0.0437	0.7909	0.3716	0.6252	0.2287	0.4903
1210	38.7501	40.5593	-0.1338	0.6387	0.0402	0.6377	-0.6014	0.5234	-0.5002	0.4438
1211	38.9662	41.0504	0.3185	0.4045	0.2361	0.4432	0.0104	0.4783	-0.2519	0.3433
1212	39.4337	40.5477	0.1457	0.8875	0.2057	0.8824	0.4695	0.6942	0.2592	0.4564
1213	39.231	40.4774	-0.0936	0.4778	-0.164	0.5655	0.474	0.3804	0.5586	0.4072
1215	38.83498	40.55687	0.2612	0.5232	0.13	0.5234	-0.0063	0.4326	0.0025	0.4295
1302	38.4744	42.1591	0.5088	0.5703	0.6852	0.5966	0.2656	0.376	-0.3896	0.361
1303	38.7998	42.7631	-0.3438	0.4303	-0.3901	0.5168	-0.2267	0.3855	-0.0996	0.3484
1304	38.5031	42.281	0.1424	0.3969	-0.0709	0.4393	-0.3981	0.3613	-0.8418	0.3378
1305	38.58025	42.02169	0.0349	0.6793	0.1003	0.5769	-0.3768	0.3713	-1.0391	0.2838
1401	40.7457	31.6073	0.6692	0.6443	0.5206	0.6675	0.701	0.4287	0.5026	0.3664
1409	40.717	32.0636	0.2658	0.543	0.2136	0.4323	0.1667	0.3402	0.1002	0.165
1410	40.7711	32.037	-0.5567	0.6238	-0.595	0.57	-0.2931	0.3479	-0.2834	0.292
1411	40.6846	31.6175	-0.393	0.6527	-0.8365	0.4744	-0.6875	0.3442	-0.7466	0.1932
1502	37.7035	30.2208	-0.5782	0.6997	-0.7884	0.7173	-1.3673	0.5946	-0.9633	0.6017
1505	37.3161	29.779	-0.3948	0.6358	-0.6354	0.6234	-0.1882	0.5053	-0.1112	0.4312
1506	37.1472	29.5095	-0.5236	0.5811	-0.6019	0.6118	-0.3139	0.5138	-0.6004	0.4884
1507	37.4942	30.1336	-0.6537	0.6361	-0.8579	0.5479	0.2571	0.5796	0.6439	0.5067
1508	37.0363	29.8214	-0.8368	0.6176	-1.1393	0.592	-0.3305	0.6225	0.1706	0.4455
1606	40.363	29.1221	0.6956	0.5007	0.7364	0.5486	-0.1444	0.1031	-0.0447	0.2191
1607	40.3944	29.098	0.4443	0.3368	0.4127	0.3954	1.2071	0.3778	1.4359	0.5909
1610	40.0671	29.5088	0.3683	0.3829	0.4338	0.4211	0.1765	0.3737	0.1459	0.3129

Station ID	Lat	Long	T=0.01s		T=0.2s		T=1s		T=2s	
			$\delta S2S_s$	$\varphi_{SS,s}$	$\delta S2S_s$	$\varphi_{SS,s}$	$\delta S2S_s$	$\varphi_{SS,s}$	$\delta S2S_s$	$\varphi_{SS,s}$
1611	40.4292	29.7168	0.0051	0.369	-0.3343	0.3602	0.5407	0.2868	0.842	0.6481
1613	39.9151	29.2317	0.5171	0.5295	0.5408	0.6188	-0.048	0.5686	-0.5247	0.507
1614	40.0347	28.3939	0.6095	0.6611	0.3743	0.9257	-0.1305	0.7332	0.0137	0.4976
1618	40.351	28.9282	0.278	0.5098	0.0189	0.6629	-0.8574	0.6361	-0.911	0.3977
1619	40.4224	29.2907	0.1883	0.4726	0.1764	0.4631	0.6016	0.4509	1.0586	0.5094
1620	40.1824	29.1296	-0.0838	0.4652	0.0332	0.4578	0.3189	0.4846	0.4338	0.3376
1621	40.2269	28.9756	-0.0817	0.5163	-0.0602	0.5466	0.3477	0.3751	0.5976	0.4359
1623	40.2654	29.0334	0.4313	0.6615	0.5327	0.6856	0.8008	0.6539	0.7816	0.5222
1624	40.177	29.0567	0.0444	0.379	0.419	0.5225	0.1372	0.4631	0.0575	0.5197
1626	40.2403	28.9824	0.2669	0.4762	0.2526	0.5128	0.8491	0.2544	0.8838	0.4623
1627	40.2257	29.0752	0.2988	0.4031	0.0384	0.3732	0.7121	0.3789	0.9056	0.5068
1628	40.2734	29.0959	0.264	0.4615	0.5066	0.4807	0.0914	0.4052	-0.1161	0.2575
1629	40.4254	29.1666	0.6032	0.4415	0.5801	0.5502	0.8327	0.5275	0.4224	0.3055
1630	40.363	29.1221	0.6894	0.6579	0.7157	0.6743	0.0025	0.4806	0.0836	0.7593
1631	40.4865	29.3081	0.4324	0.4589	0.8342	0.442	-0.3742	0.4999	-0.3841	0.4929
1633	40.2147	28.3632	0.137	0.4969	0.1243	0.4863	0.2088	0.5381	0.372	0.5871
1634	39.7763	28.8821	0.3613	0.3291	-0.0696	0.3704	-0.5326	0.4985	-0.9577	0.5596
1635	40.4497	29.2587	0.239	0.4454	0.1082	0.5036	-0.6109	0.4789	-0.1633	0.2173
1636	40.2171	29.1946	0.2982	0.3631	0.4352	0.4917	0.1926	0.5201	0.3022	0.2057
1637	40.4763	29.0946	0.6811	0.2897	0.497	0.4011	1.1677	0.2887	0.27	0.2565
1638	40.3612	29.0333	0.2627	0.3515	0.6007	0.3702	0.5577	0.3699	0.3849	0.3319
1639	40.3776	29.5418	0.3722	0.3228	0.7977	0.3724	0.9381	0.4587	0.9264	0.443
1640	39.9112	28.9868	0.075	0.3934	0.3302	0.4955	-0.3074	0.42	-0.5214	0.2629
1642	40.410343	29.179435	0.1049	0.383	0.3951	0.3947	0.0909	0.3841	0.2754	0.143
1643	40.15546	29.05457	0.7403	0.4887	1.1329	0.5078	0.7834	0.2978	0.3895	0.2464
1644	40.17834	29.10741	0.4535	0.2981	0.8463	0.4559	0.8874	0.2441	0.8814	0.2004
1645	40.17828	29.06555	0.5174	0.433	1.0055	0.4811	0.5343	0.3215	0.5882	0.2397
1646	40.209078	28.968037	0.0529	0.5095	0.0357	0.5905	0.5518	0.4949	0.7357	0.5222
1647	40.251462	28.964	0.1661	0.5043	0.339	0.5812	0.4436	0.3561	0.8227	0.416
1648	40.255225	28.980285	-0.0384	0.445	-0.2621	0.3056	0.1792	0.318	0.5175	0.3231
1649	40.265783	29.095913	0.1805	0.2272	0.0344	0.3203	0.3317	0.3315	-0.1734	0.2131
1650	40.206197	29.05789	0.5419	0.4086	0.469	0.3628	1.0699	0.2637	0.9555	0.1644
1651	40.205487	29.089303	0.3319	0.7314	0.3499	0.713	0.87	0.3365	0.9474	0.427
1652	40.188565	29.139033	-0.1721	0.5242	-0.1532	0.5557	0.2744	0.4062	0.4735	0.2267
1653	40.415365	29.098645	0.3424	0.2475	0.2422	0.3094	0.7806	0.2094	0.68	0.2159
1701	40.1415	26.3995	-0.0616	0.6007	-0.1646	0.6851	0.174	0.4848	-0.1262	0.4679
1703	40.2318	27.2629	-0.443	0.5913	-0.6461	0.5505	0.1312	0.5144	0.3537	0.5941
1704	39.7739	26.3456	0.1075	0.6539	0.1641	0.7617	0.1718	0.4758	-0.0585	0.4684
1707	39.9292	27.2591	0.1096	0.4581	0.1587	0.5066	0.3947	0.4775	0.3391	0.4311
1710	40.4233	26.6672	0.3764	0.6208	0.2588	0.6571	0.0353	0.5277	0.1765	0.4509
1711	40.1908	25.9078	0.1222	0.5686	0.2682	0.6535	-0.2091	0.6578	-0.3163	0.5548
1712	40.404	27.3035	0.5958	0.4771	1.2716	0.57	-0.1412	0.5396	-0.0425	0.6133
1713	40.1622	26.4117	0.005	0.5211	0.2288	0.6811	0.0045	0.4993	0.2264	0.4255
1714	40.1129	26.4221	-0.1383	0.6552	-0.0125	0.8121	0.0625	0.597	0.242	0.5048
1715	40.3632	26.6923	0.0981	0.5436	-0.2308	0.5731	0.6282	0.4496	0.2581	0.4006
1716	39.5997	26.4076	0.7679	0.4536	0.6841	0.4746	-0.2632	0.4398	-0.0504	0.4631

Station ID	Lat	Long	T=0.01s		T=0.2s		T=1s		T=2s	
			$\delta S2S_s$	$\varphi_{SS,s}$	$\delta S2S_s$	$\varphi_{SS,s}$	$\delta S2S_s$	$\varphi_{SS,s}$	$\delta S2S_s$	$\varphi_{SS,s}$
1717	40.1818	26.3578	-0.0512	0.6001	-0.1339	0.7112	0.084	0.4785	-0.137	0.406
1718	39.8133	26.5862	-0.559	0.6088	-0.5834	0.6572	-0.134	0.5524	-0.0036	0.3584
1719	40.0293	27.05	1.059	0.4843	1.1896	0.5786	0.6521	0.4857	0.3665	0.4563
1720	39.5288	26.1206	0.2692	0.5267	0.3654	0.6984	-0.0589	0.4415	0.1661	0.4232
1721	39.5435	26.1905	0.6355	0.5529	0.6384	0.4927	0.1525	0.4792	-0.288	0.3772
1722	40.1974	25.9034	-0.0992	0.6042	-0.056	0.7697	-0.5852	0.5792	-0.3279	0.6269
1724	39.51288	26.25777	-0.0296	0.3443	0.1822	0.4476	-0.0954	0.4299	0.1837	0.4438
1802	40.6083	33.6104	-0.4917	0.4833	-0.5559	0.4977	-0.2771	0.4015	-0.1391	0.2249
1803	40.8149	32.8834	0.2356	0.806	0.0648	0.4939	-0.1338	0.4194	-0.0939	0.1144
1804	40.6124	33.0822	-0.2877	0.4049	-0.4537	0.4501	0.0623	0.3855	0.1706	0.3278
1805	40.9311	33.6232	-0.0414	0.3684	0.0147	0.5015	0.025	0.3836	0.0921	0.2606
1806	40.601	33.6019	-0.0977	0.4534	0.1515	0.4154	0.3543	0.3047	0.3536	0.389
1807	40.8435	33.2585	-0.2622	0.5466	-0.2151	0.5076	0.3129	0.2584	0.3027	0.2199
2002	37.8125	29.1111	-0.1062	0.3592	-0.2266	0.3609	0.2993	0.4129	0.525	0.3349
2007	37.9325	28.9229	0.235	0.2588	0.147	0.3063	0.3546	0.3012	0.3796	0.3907
2009	37.9134	29.038	-0.1012	0.4623	-0.27	0.4469	0.0796	0.4233	0.3947	0.3354
2011	37.7372	29.1006	-0.0976	0.612	0.1545	0.6108	-0.5219	0.4221	-0.5011	0.4164
2012	37.7781	29.0843	0.166	0.678	0.2083	0.5945	0.302	0.4147	0.5197	0.2846
2013	38.0448	28.8336	-0.2478	0.5738	-0.3674	0.6037	-0.0749	0.4449	-0.3016	0.3956
2014	37.0741	29.3464	-0.3091	0.4482	-0.2729	0.4844	0.0999	0.4354	-0.1931	0.4066
2015	37.9255	28.9288	0.3125	0.4866	0.1331	0.4956	-0.073	0.3281	0.305	0.347
2016	37.8044	29.24	0.1098	0.5962	0.3562	0.6432	0.6424	0.4242	0.9113	0.3233
2017	37.4335	29.3502	0.4057	0.5544	0.0653	0.5439	0.1091	0.4479	0.0943	0.4642
2018	37.233	28.8948	-0.1701	0.4907	-0.2856	0.4954	0.7711	0.3903	0.6872	0.3429
2019	37.442	28.8438	0.0186	0.3335	0.1482	0.3418	0.0624	0.5105	0.228	0.4526
2020	37.5711	29.0694	0.1084	0.4919	0.3905	0.3714	-1.1352	0.3331	-0.9661	0.329
2024	38.0868	29.3954	-1.0159	0.5478	-0.8067	0.5357	-1.0366	0.3857	-0.9682	0.3547
2025	38.2957	29.7366	-0.0303	0.4728	-0.2833	0.5605	0.1537	0.4533	0.4515	0.5247
2101	37.9309	40.2028	0.747	0.6273	1.0363	0.6105	0.3942	0.4186	0.6883	0.415
2104	38.2644	39.759	-0.3347	0.4297	-0.3271	0.4608	0.2551	0.2997	0.1785	0.478
2105	38.3581	40.0713	-0.7808	0.4644	-0.8938	0.518	-0.4329	0.3591	-0.3105	0.458
2106	38.4616	40.647	-0.0353	0.5602	-0.0034	0.5996	-0.0904	0.45	-0.1614	0.403
2107	38.1459	39.4838	-0.2384	0.6656	-0.0678	0.6519	-0.1699	0.553	-0.1292	0.3706
2201	40.7245	26.0873	0.1521	0.509	0.1293	0.5943	0.2842	0.6939	0.3179	0.5157
2202	41.6705	26.5859	0.3595	0.6948	0.5814	0.7225	0.1478	0.5871	0.0924	0.4499
2203	40.8681	26.6319	0.0106	0.427	0.2402	0.5838	-0.0294	0.7413	-0.0078	0.7154
2204	41.2932	26.6899	0.499	0.299	0.4164	0.2562	-0.0212	0.4466	0.1773	0.4187
2301	38.6704	39.1927	0.0688	0.5272	-0.193	0.5735	0.3068	0.4585	0.3127	0.4956
2302	38.3923	39.6754	-0.4266	0.6856	-0.3097	0.7229	0.0139	0.4099	0.1057	0.4372
2304	38.721	39.8629	-0.3254	0.7265	-0.2365	0.6999	-0.4223	0.35	-0.2389	0.5171
2305	38.7278	40.131	-0.6794	0.7831	-0.3349	0.7268	-0.3181	0.4135	-0.3578	0.372
2306	38.9595	40.0393	-0.3317	0.7281	-0.3585	0.7881	-0.0529	0.3952	-0.2841	0.4598
2307	38.6958	39.932	-0.6891	0.5678	-0.9647	0.6065	-0.2209	0.3319	-0.1773	0.4172
2308	38.4506	39.3102	0.1066	1.0406	-0.0328	1.0479	0.7118	0.7017	0.7404	0.5464
2309	38.7983	38.7273	0.7709	0.9238	0.2127	0.5864	-0.4105	0.4413	-0.4725	0.5386
2401	39.7418	39.5115	-0.5535	0.4286	-0.6893	0.5516	-0.5516	0.3378	-0.2382	0.3584

Station ID	Lat	Long	T=0.01s		T=0.2s		T=1s		T=2s	
			$\delta S2S_s$	$\varphi_{SS,s}$	$\delta S2S_s$	$\varphi_{SS,s}$	$\delta S2S_s$	$\varphi_{SS,s}$	$\delta S2S_s$	$\varphi_{SS,s}$
2404	39.9063	38.7706	-0.2365	0.3573	-0.3554	0.3328	0.171	0.3765	0.2192	0.4636
2407	39.7767	40.3911	-0.1682	0.7272	-0.2979	0.6507	-0.1921	0.5038	-0.1885	0.4073
2408	39.6019	39.0345	0.1988	0.3294	0.0078	0.3007	0.5454	0.2796	0.1175	0.3548
2409	39.2808	38.4911	0.5644	0.4819	0.9551	0.5002	-0.0706	0.3373	-0.0914	0.3427
2411	39.9702	40.0209	-0.5047	0.7901	-0.7731	0.7066	-1.3354	0.5725	-1.28	0.4412
2412	39.592	39.6922	-0.3661	0.6126	-0.4496	0.4862	-0.1546	0.3799	-0.1911	0.4024
2413	39.8077	40.0386	0.342	0.5932	0.202	0.612	0.0375	0.4165	0.2103	0.3981
2414	39.7951	39.4186	-0.0313	0.3848	-0.005	0.4079	-0.2323	0.3285	-0.2922	0.3211
2415	39.461	38.5549	0.0049	0.3943	-0.0589	0.4361	0.035	0.3601	-0.2862	0.2856
2501	39.9032	41.262	0.0692	0.252	0.1234	0.2532	0.0037	0.2951	0.1325	0.3137
2508	39.9429	41.1102	-0.1297	0.4537	-0.3162	0.3091	-0.2628	0.3377	-0.0195	0.2292
2509	39.8733	41.2227	-0.3873	0.4805	-0.2918	0.4345	-0.1994	0.3868	-0.0618	0.3638
2510	40.3483	41.8626	-0.0304	0.5537	-0.2394	0.5404	-0.246	0.3928	-0.4578	0.2708
2511	39.9748	41.6723	0.2402	0.7683	-0.0013	0.789	-0.0086	0.2274	0.8481	0.4275
2513	39.3624	41.706	0.0837	0.4561	0.2124	0.5261	-0.3515	0.3002	-0.2455	0.3405
2516	39.6153	40.9756	0.2881	0.6428	-0.0113	0.6999	-0.4582	0.5176	-0.4874	0.2786
2518	39.9072	41.2774	-0.9194	0.9249	-0.8102	0.9396	-0.8771	0.5426	-0.9926	0.4574
2521	39.64607	41.509117	0.1456	0.5312	0.5554	0.5794	-0.1143	0.2373	0.0436	0.3807
2522	39.700493	42.14172	-0.1882	0.3286	-0.2364	0.4214	0.3982	0.3559	-0.2891	0.2096
2601	39.8137	30.5284	-0.1517	0.4713	-0.4536	0.4622	-0.232	0.3883	0.2592	0.8551
2602	39.7893	30.4973	-0.2645	0.1725	-0.4407	0.2922	0.1355	0.2591	0.635	0.4252
2604	39.7733	30.5101	0.0555	0.2371	0.1872	0.3371	0.28	0.2341	-0.107	0.3869
2606	39.7487	30.4958	0.258	0.2798	0.6716	0.3609	-0.2912	0.3634	-0.1547	0.2986
2607	39.8175	30.146	-0.6636	0.3601	-0.6236	0.4067	-0.1876	0.2221	0.0612	0.4888
2610	39.822	30.4216	-0.05	0.2616	0.1726	0.3365	0.408	0.2988	-0.2288	0.2025
2611	39.7883	30.443	-0.1582	0.2123	-0.1044	0.3403	-0.0535	0.2588	0.3764	0.2574
2612	39.7713	30.4017	-0.503	0.4189	-0.4713	0.4351	-0.3885	0.3231	-0.6077	0.3953
2613	39.7936	30.5397	-0.04	0.3333	0.1056	0.3371	-0.3089	0.269	-0.1134	0.3426
2615	39.7403	30.6521	0.0074	0.3344	0.025	0.3257	0.408	0.3463	0.7953	0.2658
2616	39.7063	30.6189	-0.4847	0.2656	-0.2584	0.2608	-0.5823	0.3245	-0.3118	0.2932
2703	37.058	37.35	0.499	0.5331	0.7712	0.6811	0.6347	0.4029	0.6165	0.4144
2704	37.0088	37.8022	0.7117	0.5192	0.9799	0.6308	0.5902	0.446	0.527	0.3819
2705	37.0118	36.6206	0.5072	0.34	0.7474	0.5591	0.1478	0.5625	0.1249	0.3394
2707	36.9309	36.5738	0.1127	0.4448	0.0737	0.5642	0.2283	0.79	-0.0722	0.6465
2708	37.0993	36.6484	0.8025	0.3574	0.8481	0.3998	0.2048	0.4465	0.0611	0.1295
2709	37.1285	36.6705	-0.1583	0.2139	-0.0882	0.2949	-0.1703	0.4405	-0.2372	0.3652
2710	37.43291	37.68658	0.7931	0.4207	0.647	0.4917	-0.4285	0.2836	-0.5715	0.2996
2711	37.31736	37.56036	0.374	0.5598	0.3246	0.4676	-0.1813	0.3735	-0.0719	0.3779
2902	40.1244	39.4366	-0.2411	0.5972	-0.2834	0.7401	0.1104	0.5223	-0.0205	0.6209
2903	40.2084	39.6586	-0.3146	0.6287	-0.6019	0.6621	0.1497	0.426	0.0161	0.2875
2904	40.1908	39.1185	-0.4127	0.5915	-0.6055	0.5742	-0.0244	0.3626	0.1536	0.4106
3112	36.588	36.1477	-0.7532	0.6504	-1.2832	0.6692	0.0051	0.43	-0.167	0.3312
3113	36.5775	36.155	-0.3562	0.3946	-0.57	0.4718	-0.3483	0.472	0.0044	0.3004
3114	36.567	36.1514	-0.4902	0.4133	-0.6425	0.4334	0.0987	0.4425	-0.3106	0.3674
3115	36.5463	36.1646	-0.1412	0.3696	0.0129	0.3636	0.0979	0.3755	-0.2514	0.3487
3118	36.5821	36.1849	0.6245	0.3787	0.628	0.4546	-0.1314	0.4055	-0.414	0.4168

Station ID	Lat	Long	T=0.01s		T=0.2s		T=1s		T=2s	
			$\delta S2S_s$	$\varphi_{SS,s}$	$\delta S2S_s$	$\varphi_{SS,s}$	$\delta S2S_s$	$\varphi_{SS,s}$	$\delta S2S_s$	$\varphi_{SS,s}$
3119	36.5753	36.1681	-0.1754	0.401	-0.2885	0.4395	-0.7283	0.4908	-1.001	0.297
3120	36.5892	36.2057	0.4242	0.365	0.5057	0.4545	-0.4827	0.4376	-0.4009	0.333
3121	36.6641	36.2183	0.3738	0.5961	0.1276	0.6129	-0.7399	0.5463	-0.366	0.6813
3123	36.2142	36.1597	-0.041	0.5434	0.1159	0.492	0.7726	0.5259	0.5441	0.5029
3125	36.2381	36.1326	0.1807	0.3246	0.3227	0.4515	0.5284	0.6137	0.2941	0.5972
3126	36.2202	36.1375	0.7026	0.4524	0.4747	0.4456	0.5266	0.4629	0.4772	0.6643
3127	36.21	36.1353	0.6912	0.4341	0.8688	0.4321	0.4686	0.5394	0.2973	0.539
3130	36.1792	36.145	0.4658	0.284	-0.1098	0.3773	0.278	0.6399	0.023	0.3666
3132	36.2067	36.1716	-0.2129	0.3571	-0.3449	0.4869	0.2212	0.6989	-0.1471	0.5296
3133	36.2432	36.5736	-0.2659	0.2204	-0.2851	0.3301	-0.198	0.7691	-0.1393	0.6895
3134	36.8276	36.2049	-0.1604	0.5475	-0.3952	0.5406	-0.4681	0.2329	-0.6105	0.3594
3135	36.4089	35.8831	-0.174	0.5003	-0.1787	0.4772	-0.1412	0.5111	-0.0497	0.4408
3137	36.6929	36.4885	-0.2689	0.4619	0.1361	0.5774	0.186	0.5883	0.3053	0.3453
3138	36.8026	36.5112	0.227	0.4663	0.3508	0.447	0.211	0.7157	0.3536	0.6569
3141	36.3726	36.2197	0.2533	0.3367	0.3806	0.3851	-0.0474	0.3925	-0.2819	0.4359
3142	36.498	36.3661	-0.1725	0.293	-0.2235	0.2862	-0.5754	0.3309	-0.4627	0.3863
3143	36.8489	36.5571	0.0438	0.4857	-0.0802	0.4839	0.2081	0.5952	-0.2044	0.7317
3145	36.6454	36.4064	0.098	0.2649	-0.0013	0.3534	0.1863	0.5487	0.2172	0.3275
3201	38.1048	30.5576	-0.532	0.6349	-0.2419	0.699	-0.7054	0.6122	-0.5502	0.4543
3205	37.9302	30.2961	0.1888	0.7513	0.2484	0.788	0.0996	0.5538	0.1037	0.5211
3303	37.1659	34.6004	-0.3149	0.5655	-0.2069	0.5774	0.3655	0.3525	-0.0265	0.3078
3405	40.9111	29.1567	0.3359	0.6892	0.4738	0.735	-0.2046	0.5776	-0.4424	0.3818
3407	41.0582	29.0095	0.0825	0.5983	0.2195	0.7554	-0.4129	0.7292	-0.6194	0.3856
3408	41.0734	28.2557	-0.7054	0.5171	-0.6339	0.6166	-0.2968	0.709	-0.1304	0.5406
3410	41.1719	29.6082	0.951	0.4603	1.0797	0.5602	0.4608	0.4618	0.832	0.7112
3411	41.0119	28.9761	0.1554	0.7912	0.0048	0.8775	-1.0436	0.7637	-1.1903	0.6396
3412	41.0206	28.5782	0.0059	0.7287	-0.3925	0.9703	-0.1805	0.7892	-0.358	0.6798
3413	41.0943	28.9482	-0.0783	0.5961	-0.0321	0.7857	-0.8591	0.6221	-0.8232	0.4353
3415	41.0273	28.7585	0.9115	0.6898	0.8027	1.0005	0.027	0.7563	-	-
3416	40.9747	28.8364	-0.4645	0.5593	-0.3148	0.6911	-0.0928	0.7015	0.2069	0.5718
3417	40.9547	29.2563	0.1723	0.4296	0.5766	0.3273	-0.1036	0.5475	-0.5134	0.689
3419	41.061	29.358	0.7453	0.4326	0.6925	0.4662	-0.28	0.4462	-0.8587	0.384
3502	38.4551	27.2267	0.0062	0.3734	-0.1472	0.3633	-0.0424	0.3877	-0.1993	0.3059
3503	39.0739	26.8883	0.0262	0.508	0.0693	0.5282	0.1564	0.5711	-0.3817	0.498
3506	38.3944	27.0821	-0.3238	0.3712	-0.0235	0.4554	-0.1246	0.4025	-0.2037	0.3359
3508	39.0883	27.3747	-0.0261	0.3906	0.3025	0.3993	-0.1135	0.5098	-0.1084	0.5104
3509	38.2157	27.9645	0.1579	0.4617	0.0393	0.5695	0.2519	0.3976	0.7497	0.329
3510	38.409	27.043	0.1015	0.5531	0.2836	0.5765	-0.1897	0.4611	-0.3056	0.3848
3511	38.4213	27.2563	-0.1794	0.3519	0.0876	0.3929	-0.1153	0.4092	-0.1808	0.4543
3512	38.4009	27.1516	0.1185	0.4162	-0.1804	0.4462	-0.4872	0.3764	-0.7216	0.3398
3513	38.4584	27.1671	-0.2937	0.5223	-0.6389	0.4499	-0.0171	0.4709	-0.032	0.4555
3514	38.4762	27.1581	-0.127	0.354	0.0833	0.3681	0.1363	0.3997	0.2691	0.3759
3515	38.4649	27.094	-0.6477	0.4092	-1.1681	0.4107	-0.4949	0.4159	-0.604	0.4119
3516	38.3706	26.8907	-0.0929	0.4035	0.052	0.4643	0.035	0.4412	-0.2378	0.3521
3517	38.3756	27.1936	-0.6902	0.4088	-0.7028	0.4935	0.2108	0.3174	0.3271	0.2678
3518	38.4312	27.1435	-0.0708	0.3584	-0.2256	0.3942	0.1441	0.3839	0.2833	0.3393

Station ID	Lat	Long	T=0.01s		T=0.2s		T=1s		T=2s	
			$\delta S2S_s$	$\varphi_{SS,s}$	$\delta S2S_s$	$\varphi_{SS,s}$	$\delta S2S_s$	$\varphi_{SS,s}$	$\delta S2S_s$	$\varphi_{SS,s}$
3519	38.4525	27.1112	-0.2032	0.3681	-0.5096	0.4209	-0.2357	0.3876	-0.033	0.4151
3520	38.478	27.2111	-0.1914	0.359	0.0411	0.3914	0.3183	0.3662	0.3846	0.3815
3521	38.4679	27.0764	-0.1792	0.451	-0.5813	0.426	0.2108	0.385	0.0721	0.3794
3522	38.4357	27.1987	-0.2311	0.3104	-0.4325	0.3574	-0.0258	0.3385	-0.1968	0.3323
3523	38.3282	26.7706	-0.0787	0.4055	-0.1146	0.3966	-0.0742	0.4221	0.1471	0.346
3524	38.4969	27.1073	-0.0278	0.3928	0.0711	0.4241	-0.3682	0.3761	-0.4358	0.4583
3525	38.3723	27.1084	0.1368	0.4318	0.3198	0.4912	0.1074	0.4393	-0.0512	0.3941
3526	38.5782	26.9795	-0.0022	0.5153	-0.1062	0.6552	0.1118	0.4997	0.302	0.456
3527	38.639	26.5128	-0.7424	0.4741	-1.0766	0.5514	-0.4817	0.5065	-0.5559	0.5337
3528	38.3039	26.3726	0.0671	0.4184	0.19	0.4814	0.1339	0.4911	0.1004	0.3894
3529	37.9443	27.3675	0.6564	0.4643	0.5168	0.5162	-0.1515	0.3311	-0.597	0.3732
3530	38.453	27.2244	-0.1739	0.4245	-0.3537	0.4138	0.1918	0.3885	-0.1591	0.3358
3531	38.2193	27.6457	-0.1289	0.4586	-0.3168	0.4974	-1.1038	0.5594	-1.1366	0.4381
3532	38.1591	27.3596	0.1934	0.4231	0.0892	0.447	0.5196	0.4843	0.3046	0.3726
3533	38.2572	27.1302	-0.1613	0.4426	-0.1693	0.4823	0.144	0.4451	0.207	0.3032
3534	38.6624	26.7586	0.4733	0.513	0.6132	0.5188	-0.4376	0.4789	-0.6331	0.4497
3535	38.7963	26.9632	-0.5452	0.4684	-0.5976	0.5128	-0.147	0.45	-0.1099	0.443
3536	38.1968	26.8384	0.0715	0.4745	0.3218	0.4985	0.6932	0.5125	0.25	0.3796
3537	39.1096	27.1706	-0.7288	0.4352	-0.701	0.4979	-0.3113	0.5458	0.0297	0.4454
3538	38.3187	27.1234	-0.0056	0.4223	0.0575	0.467	0.5208	0.3731	0.2934	0.389
3539	38.1023	27.7211	0.1848	0.525	-0.2066	0.4433	-0.7275	0.4034	-0.8421	0.3486
3701	41.0132	34.0367	0.2284	0.564	0.2574	0.547	-0.0531	0.3275	-0.0383	0.246
3702	41.4164	33.7969	-0.455	0.3051	-0.329	0.2976	0.1071	0.3178	0.019	0.2676
3703	41.2456	33.3284	-0.376	0.3463	-0.2169	0.4643	-0.659	0.2197	-0.7492	0.1471
3802	38.4781	36.5036	0.2958	0.3386	0.0575	0.3761	0.9384	0.3194	1.3058	0.379
3901	41.7377	27.2151	-0.0391	0.4743	0.1193	0.3855	0.0307	0.5432	-0.3113	0.6909
3902	41.3571	27.3248	-0.3005	0.6303	-0.2992	0.6253	0.0482	0.6264	0.1354	0.545
4104	40.6804	29.97	-0.6013	0.3416	-0.3017	0.444	-0.433	0.4257	-0.5796	0.478
4105	40.6744	29.9694	0.2198	0.4026	0.2103	0.3736	-0.4337	0.4322	-0.9843	0.3426
4106	40.7863	29.45	-0.3034	0.6708	0.0155	0.7815	-0.1733	0.4769	-0.094	0.5943
4107	40.7602	29.9324	-0.2497	0.6189	-0.4471	0.515	0.8453	0.4292	0.6688	0.4303
4108	40.7602	29.9329	1.0266	0.4735	1.0134	0.4135	1.6443	0.3222	1.3808	0.4018
4111	40.6844	29.5888	-0.0008	0.5154	0.0086	0.4406	0.0646	0.3799	-0.2061	0.3985
4112	40.7245	29.84	0.2991	0.5341	0.3765	0.4956	0.9022	0.4609	1.3252	0.5131
4113	40.7768	29.7335	-0.6403	0.6354	-0.521	0.6495	-1.2671	0.3032	-1.1573	0.2778
4115	40.7433	29.7802	-0.5056	0.3499	-0.6166	0.3303	-0.3023	0.4349	-0.0136	0.4428
4116	40.7196	29.8658	0.0508	0.4391	-0.2957	0.3812	0.2249	0.5307	0.453	0.5492
4117	40.6989	30.0267	-0.1092	0.3954	-0.1104	0.4419	0.0572	0.4098	-0.2296	0.458
4118	40.7216	30.0781	0.3976	0.4674	0.2663	0.453	0.5382	0.4934	0.5068	0.6412
4120	40.7676	30.0274	0.0322	0.411	0.0821	0.3945	0.2374	0.5608	-0.337	0.5285
4121	40.7228	29.9699	0.2074	0.4319	0.2508	0.4139	0.4478	0.5053	0.4896	0.5184
4122	40.7483	30.0263	-0.2205	0.4471	-0.3841	0.336	0.5359	0.4959	0.6313	0.5588
4126	40.7625	29.9149	0.1981	0.5433	0.0903	0.6121	-0.4014	0.6047	-0.7908	0.548
4301	39.4278	29.9916	0.4162	0.3157	0.5817	0.4631	0.303	0.3516	0.4016	0.4111
4304	38.9948	29.4004	0.0946	0.3812	-0.0326	0.5394	-0.1544	0.6152	0.1384	0.6145
4305	39.0928	28.9785	0.4648	0.5146	0.2978	0.5763	0.5916	0.5553	0.182	0.6859

Station ID	Lat	Long	T=0.01s		T=0.2s		T=1s		T=2s	
			$\delta S2S_s$	$\varphi_{SS,s}$	$\delta S2S_s$	$\varphi_{SS,s}$	$\delta S2S_s$	$\varphi_{SS,s}$	$\delta S2S_s$	$\varphi_{SS,s}$
4306	39.3361	29.2491	-0.1643	0.6191	-0.2249	0.6513	0.5332	0.6985	0.0736	0.481
4307	39.4053	30.0143	-0.081	0.493	0.0128	0.4862	0.1963	0.6283	0.4832	0.6683
4309	39.0928	28.9785	0.0166	0.5788	-0.1694	0.686	-0.0415	0.5596	-0.4625	0.4681
4310	39.5384	29.4939	0.019	0.5984	-0.0811	0.5268	0.4103	0.5972	0.5238	0.5944
4311	38.8524	29.9812	-0.1206	0.3878	-0.1247	0.4253	0.0554	0.3386	-0.0791	0.3352
4312	39.0578	30.1065	-0.4177	0.3854	-0.0303	0.3381	-1.4572	0.4194	-0.9003	0.4388
4313	39.196	29.62	0.1925	0.2636	0.2441	0.2839	0.3538	0.3717	0.1981	0.3345
4314	39.8063	29.6174	0.2316	0.3255	0.2501	0.379	0.3482	0.2665	0.4338	0.2513
4401	38.3489	38.335	-0.0403	0.536	-0.0428	0.5565	-0.1883	0.5551	-0.4734	0.5145
4404	38.1959	38.8739	-0.1187	0.6732	0.2332	0.6863	0.2339	0.5989	-0.0913	0.5062
4405	38.8107	37.9396	-0.2045	0.557	-0.1605	0.5069	-0.6033	0.3999	-0.6509	0.3941
4406	38.3439	37.9738	0.2452	0.5049	0.2285	0.4748	-0.0772	0.4577	-0.2261	0.404
4407	38.7807	38.2641	0.0763	0.6112	0.0601	0.4989	0.5952	0.3012	0.6336	0.3461
4408	38.0962	37.8873	-0.7069	0.4247	-0.5064	0.4332	-0.4641	0.4043	-0.6246	0.3242
4409	38.56063	37.49076	-0.8252	0.3315	-0.7264	0.3422	-0.9235	0.3404	-0.9687	0.3939
4410	38.86677	37.679	-0.1695	0.3455	-0.2145	0.4356	-0.2034	0.3239	-0.5523	0.3069
4411	39.049298	38.503368	-0.449	0.4692	-0.5744	0.617	-0.3401	0.3046	-0.578	0.2898
4412	38.59685	38.18385	-0.7435	0.4866	-0.7388	0.5262	-0.2454	0.455	-0.0289	0.4364
4501	38.6126	27.3814	-0.7133	0.5269	-0.6687	0.5399	-0.1579	0.5115	-0.0674	0.5129
4502	38.9112	27.8233	-0.3849	0.4588	-0.7475	0.4538	0.0405	0.4925	0.3214	0.5237
4503	38.3555	28.5143	-0.7383	0.4509	-0.8467	0.4701	-0.1292	0.4504	-0.0225	0.4843
4504	39.035	28.6481	0.58	0.4554	0.4802	0.4889	0.3483	0.6069	0.2294	0.4861
4505	38.9398	28.2836	0.1386	0.4675	0.2924	0.5301	0.6516	0.4629	0.6059	0.4732
4506	38.4831	28.1235	-0.0417	0.5778	-0.3183	0.758	-0.0648	0.5411	0.0983	0.4948
4507	38.5075	27.7061	0.0286	0.5152	-0.3095	0.6019	-0.4113	0.3893	-0.0109	0.4671
4508	38.7322	27.5574	-0.1154	0.6137	-0.2211	0.6153	-0.0994	0.4726	-0.0165	0.3908
4509	38.7075	27.9199	-0.3488	0.5196	-0.6055	0.6256	-0.5499	0.5449	-0.5878	0.4552
4510	38.5461	28.6431	0.2378	0.4057	0.1634	0.4545	-0.5333	0.5863	-1.0896	0.4627
4511	38.24	28.6912	-0.2905	0.5806	-0.4116	0.5579	-0.0679	0.5552	0.2057	0.5151
4512	38.7422	28.8652	-0.3901	0.3831	-0.5149	0.3532	-0.2359	0.3725	-0.1675	0.4034
4513	39.1892	27.6171	-0.2339	0.4803	-0.2225	0.6424	0.0993	0.5543	0.2064	0.5989
4610	38.2037	37.1977	0.3538	0.6054	0.1186	0.4971	0.707	0.5344	0.9537	0.6045
4611	37.7472	37.2843	0.433	0.6792	0.2816	0.4649	0.6321	0.5133	0.518	0.5271
4612	38.024	36.4819	0.3216	0.4542	0.2314	0.4645	0.7166	0.5046	-0.1843	0.5266
4613	37.5646	36.3576	-0.1211	0.512	-0.2076	0.5654	-0.5985	0.3812	-0.4798	0.3487
4614	37.4804	37.2898	0.832	0.474	0.7624	0.7103	0.3065	0.5974	0.3911	0.5935
4615	37.3868	37.138	-0.0087	0.631	0.1709	0.6426	-0.0676	0.4389	0.058	0.3741
4616	37.3755	36.8384	-0.0825	0.3715	0.0821	0.4357	-0.6757	0.4875	-0.6623	0.3886
4617	37.5855	36.8303	-0.405	0.4807	-0.1738	0.4037	0.293	0.4469	0.5217	0.4395
4618	37.6001	36.8723	-0.074	0.4361	0.1008	0.4067	0.1854	0.4477	0.1136	0.3519
4619	37.587	36.8662	-0.0842	0.3859	0.0799	0.4582	-0.0169	0.3598	0.0894	0.3982
4620	37.5857	36.8985	0.0623	0.3322	0.1024	0.4875	-0.3195	0.3471	0.1421	0.3779
4621	37.5935	36.9291	0.3063	0.4439	0.2146	0.5784	0.4533	0.4487	0.8976	0.53
4622	37.5843	36.9776	0.0031	0.4804	-0.1805	0.5243	0.6889	0.3635	0.6266	0.4087
4623	37.5692	36.934	0.0697	0.4695	0.1551	0.5153	0.7209	0.3764	0.7544	0.4176
4624	37.5361	36.9177	0.2005	0.4475	0.207	0.4308	0.2705	0.3117	0.0614	0.3507
4625	37.5387	36.9819	0.1593	0.346	0.1069	0.3587	0.4052	0.4547	0.1555	0.4228
4626	37.5753	36.9151	0.2713	0.372	0.0746	0.3371	0.7997	0.3246	0.6624	0.3438

Station ID	Lat	Long	T=0.01s		T=0.2s		T=1s		T=2s	
			$\delta S2S_s$	$\varphi_{SS,s}$	$\delta S2S_s$	$\varphi_{SS,s}$	$\delta S2S_s$	$\varphi_{SS,s}$	$\delta S2S_s$	$\varphi_{SS,s}$
4628	38.2412	36.9228	0.051	0.7338	-0.219	0.3859	-0.9697	0.4162	-1.2706	0.2975
4629	37.2874	36.7887	-0.0625	0.2719	-0.042	0.2304	-0.5659	0.326	-0.7873	0.2721
4630	37.3449	36.806	-0.1432	0.266	-0.233	0.4338	-0.9924	0.4318	-0.9002	0.2493
4631	37.9663	37.4277	0.1155	0.4054	0.3781	0.4165	-0.1703	0.4539	-0.3385	0.509
4632	37.256	36.7737	0.1147	0.4046	0.0726	0.2959	0.7805	0.506	-0.1021	0.2903
4701	37.3263	40.7237	0.8378	0.4578	1.2856	0.4914	0.3252	0.3089	0.28	0.4321
4801	37.2145	28.3561	-0.0394	0.3958	0.1927	0.4226	-0.1215	0.3345	-0.385	0.3972
4803	36.6264	29.124	0.4387	0.5371	0.1492	0.508	0.7961	0.526	-0.3423	0.491
4806	37.3025	27.7805	-0.0573	0.3113	-0.2426	0.3398	-0.3657	0.3718	-0.4034	0.3152
4807	37.3397	28.1369	-0.0805	0.4059	-0.0451	0.3843	-0.4118	0.3733	-0.2112	0.3496
4808	37.1392	28.2873	0.4602	0.5458	0.7242	0.4835	0.2105	0.4268	-0.0381	0.4203
4809	37.033	27.44	-0.0987	0.7018	0.0149	0.671	-0.1348	0.5568	-0.2305	0.5297
4810	36.8394	28.2448	-0.2184	0.4234	-0.1286	0.4671	-0.931	0.4535	-0.8692	0.4366
4811	36.9697	28.6868	0.1153	0.6298	0.1815	0.5489	-0.2343	0.424	-0.5708	0.4214
4812	36.7123	27.688	-0.6634	0.4946	-0.3494	0.5183	-0.7757	0.5328	-0.5318	0.4916
4814	37.3991	27.6567	-0.2237	0.5102	-0.4326	0.4107	-0.6148	0.3875	-0.4243	0.3288
4815	36.6886	28.046	-0.4448	0.5962	-0.8535	0.5546	-1.7448	0.4659	-1.6393	0.536
4816	36.7718	28.7986	-0.1396	0.5173	-0.3705	0.4935	0.0726	0.4352	-0.2051	0.4645
4817	37.2401	27.6031	0.22	0.7198	0.3897	0.6433	-0.1027	0.4065	0.0406	0.4201
4818	37.444	28.3575	0.0504	0.4204	0.5678	0.4284	-0.0424	0.3319	-0.1677	0.3758
4819	37.0313	27.9712	0.1676	0.4427	-0.1068	0.477	-0.0076	0.4565	-0.1317	0.4867
4820	36.6485	29.3543	-0.1929	0.7525	0.2999	0.6326	-0.3051	0.7007	-0.0919	0.5277
4821	37.1055	28.4139	0.2815	0.5715	0.0577	0.5346	0.8526	0.6182	0.2208	0.4258
4822	37.4417	27.646	0.9348	0.4136	1.0488	0.4256	0.0468	0.4092	-0.1386	0.4163
4823	37.4418	27.644	0.0951	0.684	0.2006	0.5105	-0.6704	0.3552	-0.6104	0.3873
4901	38.7611	41.5039	0.0533	0.5128	0.0286	0.501	-0.1411	0.4376	-0.312	0.4074
4904	38.7356	41.7742	0.0645	0.4512	-0.1264	0.4949	0.3835	0.3233	0.4372	0.3324
4905	39.1764	41.4455	0.144	0.5563	0.1741	0.5923	1.0231	0.4475	1.0173	0.4632
4906	39.1439	42.5308	0.1312	0.3493	-0.0434	0.4541	-0.0677	0.2478	0.3579	0.4353
5401	40.7362	30.3808	-0.1432	0.7815	-0.2312	0.5173	-0.5102	0.6515	-0.6409	0.6599
5403	40.6908	30.27	-0.0571	0.4826	-0.0365	0.4818	0.1143	0.4651	0.066	0.5393
5404	40.5191	30.2932	0.1678	0.5137	0.189	0.5412	0.6529	0.497	0.8512	0.7031
5405	40.7961	30.7352	-0.3595	0.7142	-0.3849	0.7036	0.2805	0.4398	0.5961	0.4145
5601	37.912	41.931	-0.1744	0.6466	-0.2612	0.6266	-0.0537	0.3439	0.0798	0.31
5802	39.8928	37.7479	-0.1547	0.3899	-0.1637	0.3108	-0.5239	0.3746	-0.3264	0.2988
5807	38.7245	37.2896	-0.1655	0.557	-0.338	0.5852	-0.3027	0.4003	-0.1694	0.263
5809	39.2308	37.3824	0.2922	0.4212	0.4432	0.4372	-0.0258	0.4075	0.2877	0.4223
5810	39.3704	38.1179	1.0359	0.5858	0.6925	0.6189	-0.6359	0.5098	-0.0771	0.6684
5812	40.088	38.3457	-0.2592	0.4448	-0.5006	0.3292	-0.0901	0.2432	0.4248	0.4554
5814	40.0618	38.6036	-0.5421	0.368	-0.3865	0.4496	-0.2371	0.2365	0.1102	0.3431
5816	39.86868	38.11835	0.3147	0.2613	0.3508	0.4421	0.0559	0.323	-0.1086	0.2647
5904	40.6149	27.1226	0.5989	0.5238	0.4456	0.6587	0.5246	0.4905	0.2851	0.4734
5906	40.9734	27.9316	-0.0668	0.6702	-0.3637	0.6795	-0.6427	0.5835	-1.0282	0.6261
5907	41.1607	27.7918	-0.6199	0.7875	-0.6239	0.8378	-0.1032	0.7133	0.0746	0.6423
5908	40.9821	27.5479	-0.0883	0.7982	-0.1059	0.8383	0.1029	0.8431	0.1453	0.6962
5910	40.9811	27.4861	0.8808	0.6024	0.7733	0.7576	0.2678	0.7704	0.6125	0.8889

Station ID	Lat	Long	T=0.01s		T=0.2s		T=1s		T=2s	
			$\delta S2S_s$	$\varphi_{SS,s}$	$\delta S2S_s$	$\varphi_{SS,s}$	$\delta S2S_s$	$\varphi_{SS,s}$	$\delta S2S_s$	$\varphi_{SS,s}$
5914	40.66825	27.24526	0.3557	0.6082	0.5336	0.5897	0.5544	0.6963	0.4868	0.7013
6201	39.0747	39.5347	-0.1235	0.7098	0.1198	0.7748	-0.1071	0.3779	-0.4351	0.2846
6202	39.486	39.8998	0.3087	0.6301	0.4146	0.7081	0.6519	0.4596	0.5063	0.5783
6302	37.2342	39.7509	1.1714	0.4183	1.5629	0.3676	0.8313	0.4792	1.0614	0.4142
6304	37.3651	38.5132	0.8743	0.58	0.9652	0.6973	-0.1535	0.5208	-0.3286	0.4891
6401	38.6726	29.404	-0.1947	0.4579	-0.2387	0.4699	-0.2251	0.5223	-0.2927	0.5538
6402	38.4076	28.9766	-0.3143	0.6348	-0.1629	0.6298	-0.048	0.5665	-0.5754	0.4479
6403	38.7361	29.7568	0.0017	0.5514	-0.0489	0.48	-0.0035	0.4653	0.0625	0.5755
6501	38.5035	43.4018	-0.0022	0.375	0.0282	0.3843	0.0088	0.3717	0.1156	0.4926
6505	39.135	43.9011	0.2306	0.8919	-0.0152	0.8882	-0.8302	0.5056	-0.5898	0.5076
6506	39.0196	43.338	0.5201	0.613	0.5475	0.6402	0.296	0.453	0.4682	0.3776
6507	38.2963	43.1198	-0.3372	0.6209	-0.2079	0.5638	-0.344	0.478	-0.7512	0.3735
6508	38.6573	43.9767	0.0393	0.6793	-0.17	0.7499	0.7154	0.4624	0.673	0.4068
6512	38.99	43.763	0.0775	0.3584	-0.0847	0.416	-0.1218	0.2507	-0.3781	0.3028
6513	38.4145	43.2682	-0.6306	0.3863	-0.6673	0.3895	0.1881	0.366	0.1572	0.44
6901	40.2623	40.2101	-0.8523	0.7651	-0.9453	0.8126	-0.6934	0.4519	-0.7275	0.3045
7101	39.8497	33.518	0.2114	0.6447	0.1108	0.6091	0.0024	0.5226	0.3739	0.4465
7103	39.9403	34.0327	0.2894	0.2433	0.4374	0.4604	0.1048	0.2022	0.02	0.3548
7301	37.523	42.4534	0.3847	0.3779	0.6707	0.3885	0.7527	0.4609	0.6084	0.3178
7706	40.5131	28.8266	0.247	0.4392	0.4837	0.4996	-0.1003	0.4989	-0.4744	0.554
7707	40.6381	29.0788	-0.0689	0.5271	-0.0958	0.567	0.2732	0.4558	-0.1273	0.406
7708	40.6576	29.2473	-0.1706	0.3417	-0.4218	0.3778	-0.0765	0.3599	-0.0864	0.4391
7709	40.5593	29.3259	0.1031	0.5288	0.3463	0.4788	0.566	0.483	0.3774	0.2807
7710	40.59	29.2668	0.0549	0.289	-0.0481	0.3651	-0.3418	0.4986	-0.4557	0.2521
7711	40.6594	29.3271	-0.2135	0.5707	-0.5733	0.5989	0.0215	0.4911	-0.0944	0.3181
7714	40.52275	28.88833	-0.1923	0.3429	-0.3246	0.3488	-0.869	0.4264	-0.7606	0.4149
7715	40.46296	28.97072	1.2661	0.4576	1.5293	0.3315	1.83	0.2375	1.1197	0.2202
7802	40.9563	32.5322	0.0461	0.4231	0.2445	0.4043	-0.3676	0.4016	-0.4843	0.3459
7901	36.7088	37.1123	0.9585	0.4898	0.7451	0.6044	0.0427	0.6484	0.0587	1.2003
8002	37.1916	36.562	-0.2195	0.5398	-0.4135	0.6528	-0.3258	0.4748	-0.6267	0.5687
8003	37.0842	36.2694	-0.6191	0.5681	-0.6896	0.5613	0.1066	0.3197	0.1903	0.5111
8004	37.3799	36.0976	0.2593	0.629	0.2381	0.6906	0.2607	0.5993	0.3657	0.5939
8105	40.9028	31.152	0.7016	0.8134	0.9151	0.7415	0.3619	0.5461	0.2331	0.4165
8108	40.8613	31.23	-0.2885	0.349	-0.1424	0.4939	-0.3736	0.42	-0.2065	0.4371
8109	40.781	31.0144	0.1796	0.6518	-0.1351	0.5291	0.5474	0.4816	0.5849	0.4844

CY14

Station ID	Lat	Long	T=0.01s		T=0.2s		T=1s		T=2s	
			$\delta S2S_s$	$\varphi_{SS,s}$	$\delta S2S_s$	$\varphi_{SS,s}$	$\delta S2S_s$	$\varphi_{SS,s}$	$\delta S2S_s$	$\varphi_{SS,s}$
0118	37.0362	35.3184	-0.6615	0.5718	-0.7877	0.5267	0.6085	0.4623	0.9114	0.4478
0120	36.7701	35.7901	-0.7291	0.4161	-0.4403	0.4014	-0.1781	0.5024	-0.2183	0.6397
0122	37.4339	35.8202	-0.3894	0.7583	-0.2009	0.7669	-0.5644	0.6069	-0.9632	0.4873
0126	37.5455	35.3919	-0.4421	0.6729	-0.1279	0.6771	-0.0642	0.4287	-0.3564	0.3691
0201	37.7612	38.2674	0.356	0.3774	0.3795	0.4274	0.1614	0.3647	0.7251	0.4281
0204	38.029	39.0347	0.0791	0.5288	0.0821	0.6229	0.3026	0.4222	0.1901	0.5434
0205	37.7918	38.616	-0.5842	0.5143	-0.6163	0.4512	0.2957	0.373	0.6246	0.397
0207	38.0323	38.2476	-0.046	0.4116	0.2069	0.5559	-0.4042	0.4513	-0.293	0.3738
0208	37.7869	37.6528	-0.3604	0.4724	-0.2782	0.4462	-0.1576	0.4905	-0.1151	0.5862
0209	37.5776	38.4825	0.6585	0.52	0.4017	0.5542	-0.2546	0.3688	-0.0107	0.3793
0210	37.7863	38.2544	-0.0204	0.4814	-0.0755	0.5391	-0.0313	0.3799	0.3098	0.3693
0212	38.0277	38.62409	-1.1223	0.492	-1.1582	0.4706	-0.6072	0.4617	-0.6147	0.497
0213	37.79667	37.92957	0.4953	0.4551	0.6658	0.4231	1.0752	0.4238	0.4851	0.4868
0302	38.0599	30.1537	-0.1265	0.5264	-0.3826	0.6916	0.0309	0.478	0.2043	0.4985
0401	39.7198	43.0164	-0.242	0.5687	-0.2051	0.5347	-0.4569	0.5368	-0.3776	0.373
0403	39.7989	42.6801	0.2873	0.4188	0.2045	0.5201	0.3762	0.55	0.3811	0.4573
0404	39.5388	42.7725	0.3626	0.6206	0.519	0.5722	0.2542	0.4224	-0.0842	0.4325
0603	39.5583	33.1186	-0.3661	0.448	-0.4062	0.5215	-0.5183	0.3594	-0.4655	0.29
0617	40.4569	32.6319	0.2183	0.4082	0.4798	0.4322	-0.2211	0.3741	-0.1068	0.2526
0619	39.9055	32.7571	-0.0263	0.5373	-0.2217	0.4426	-0.221	0.5748	-0.6273	0.4068
0621	40.2294	33.0289	0.4493	0.3004	0.5689	0.3236	0.4031	0.4476	0.8079	0.3008
0705	36.1951	29.6474	-0.1162	0.628	-0.2135	0.5418	0.982	0.5781	0.7418	0.604
0712	36.3022	30.148	0.3167	0.8461	0.2705	0.9035	0.4762	0.594	-0.1	0.5812
0716	36.2685	29.4128	-0.5314	0.4718	-0.5068	0.3439	0.1882	0.4538	0.0556	0.4756
0904	37.8572	28.0503	-0.36	0.3567	-0.2933	0.403	-0.0755	0.3522	-0.0397	0.3273
0905	37.86	27.265	-0.1275	0.5094	-0.0446	0.5324	-0.0812	0.4805	-0.3881	0.3799
0910	37.8455	27.7996	0.0652	0.4065	-0.0301	0.3983	0.2145	0.4405	0.4064	0.3763
0911	37.7616	27.3921	-0.2267	0.4089	-0.1167	0.4214	-0.1248	0.4544	-0.3414	0.4413
0912	37.9739	28.746	-0.1258	0.5123	-0.1301	0.5614	-0.0344	0.4441	-0.0513	0.3322
0913	37.9115	28.4654	-0.1478	0.3927	-0.1087	0.457	0.0609	0.4704	0.0812	0.3672
0914	37.9133	28.3431	0.4632	0.2892	0.4602	0.3505	0.6745	0.3152	0.7899	0.3816
0915	37.8841	28.1506	0.25	0.4267	0.3482	0.4932	0.6729	0.5135	0.7841	0.4215
0916	37.8572	28.0503	-0.1999	0.3585	-0.1457	0.3988	-0.1034	0.3392	0.2452	0.3476
0917	37.6052	28.0584	0.169	0.4287	0.0969	0.4983	0.7604	0.4534	0.1645	0.3015
0918	37.3697	27.2643	-0.2501	0.8059	-0.2262	0.8017	0.5136	0.8021	0.5258	0.8392
0919	37.5595	27.8355	0.3955	0.4706	0.6892	0.5087	0.253	0.4259	0.2271	0.345
0920	37.5604	27.3749	-0.5167	0.4567	-0.4361	0.4616	-0.0031	0.5634	0.0729	0.4155
0921	37.8747	27.5922	0.0752	0.3604	0.0019	0.3703	0.6215	0.4314	0.5031	0.3155
0922	37.8537	27.7082	0.3566	0.8449	0.2942	0.888	0.6972	0.9006	0.6711	0.8442
1001	39.65	27.8569	0.1883	0.6048	0.422	0.745	0.0413	0.3505	-0.009	0.269
1003	39.655	27.862	0.4917	0.9552	0.7303	0.956	-0.0108	0.8975	0.1689	1.0299
1005	39.3113	26.686	0.1837	0.9001	0.2145	0.9733	-0.7635	0.5259	-0.8082	0.4596
1006	40.3319	27.9966	0.217	0.4411	0.1626	0.4622	0.0569	0.5159	0.0776	0.5815
1008	39.3979	28.1273	-0.0577	0.5357	-0.1194	0.6002	-0.8881	0.4692	-0.8589	0.3244

Station ID	Lat	Long	T=0.01s		T=0.2s		T=1s		T=2s	
			$\delta S2S_s$	$\varphi_{SS,s}$	$\delta S2S_s$	$\varphi_{SS,s}$	$\delta S2S_s$	$\varphi_{SS,s}$	$\delta S2S_s$	$\varphi_{SS,s}$
1009	39.578	28.6323	-0.3869	0.4778	-0.3925	0.5054	-0.49	0.5475	-0.404	0.4756
1011	40.336	27.861	0.2185	0.5571	0.1776	0.5723	-0.2111	0.5347	-0.4728	0.4992
1013	39.5895	27.0192	-0.1478	0.5282	-0.1845	0.6181	-0.9064	0.5605	-1.1548	0.4921
1014	40.114	27.6424	-0.2784	0.5084	-0.4591	0.5881	-0.3532	0.4975	0.0721	0.6173
1015	39.2395	28.1714	-0.6848	0.6379	-0.8302	0.6326	-0.4126	0.5371	-0.924	0.3656
1016	39.3804	27.6544	0.0245	0.4671	0.155	0.5069	0.2902	0.4636	0.3912	0.364
1017	39.6497	27.8572	0.4766	0.4853	0.568	0.4864	0.4515	0.4314	0.4873	0.3519
1018	40.4093	27.7878	-0.113	0.6704	-0.1103	0.6609	-0.0206	0.6279	-0.2256	0.5231
1019	39.498	26.9753	0.502	0.4383	0.5207	0.5383	-0.3726	0.5303	-0.3244	0.6371
1020	39.9171	28.1641	0.7179	0.5603	0.4875	0.5919	-0.2161	0.4749	-0.3575	0.4096
1021	39.7474	27.5762	0.0752	0.4775	0.1891	0.5531	-0.2925	0.5009	-0.2786	0.3857
1022	39.5817	27.4936	0.2661	0.4839	-0.065	0.5416	0.2741	0.5527	0.3228	0.5021
1023	39.6825	28.1666	0.2846	0.5374	0.3359	0.6213	0.3589	0.564	-0.1487	0.4553
1024	40.0475	27.974	0.5364	0.4786	0.3062	0.4795	0.1398	0.5077	-0.1899	0.3673
1026	39.38445	26.83862	-0.3382	0.5163	-0.505	0.5082	-0.5572	0.4755	-0.6664	0.4076
1027	39.57383	26.7422	0.2604	0.4893	0.2483	0.5157	-0.2088	0.4704	-0.245	0.4374
1028	39.5855	26.92303	0.408	0.4235	0.5383	0.4367	-0.127	0.4944	-0.3001	0.3826
1101	40.1411	29.9774	0.0526	0.5316	0.0329	0.5629	0.5344	0.515	0.2538	0.2873
1102	39.9043	30.0529	0.0405	0.4663	0.2992	0.462	-0.0102	0.2869	-0.3627	0.3663
1201	38.8971	40.5032	-0.1846	0.4971	-0.4076	0.5901	0.3356	0.3455	0.3657	0.4029
1206	39.2935	41.0088	0.0622	0.7491	0.0977	0.8305	0.3579	0.683	0.2339	0.5313
1210	38.7501	40.5593	-0.1307	0.6395	0.0202	0.6656	-0.6103	0.5282	-0.5222	0.4158
1211	38.9662	41.0504	0.3279	0.4132	0.2387	0.4822	-0.0036	0.4502	-0.2737	0.2716
1212	39.4337	40.5477	0.1451	0.8444	0.1618	0.8963	0.5679	0.7272	0.3617	0.484
1213	39.231	40.4774	-0.0689	0.4551	-0.2079	0.6007	0.4857	0.4221	0.5723	0.4026
1215	38.83498	40.55687	0.2602	0.5135	0.1321	0.5317	-0.049	0.4295	-0.0487	0.4021
1302	38.4744	42.1591	0.5125	0.561	0.6469	0.64	0.2443	0.3726	-0.4026	0.4025
1303	38.7998	42.7631	-0.3503	0.4277	-0.3554	0.5207	-0.1307	0.3887	-0.012	0.3479
1304	38.5031	42.281	0.114	0.4021	-0.0083	0.4276	-0.4296	0.3844	-0.8964	0.4187
1305	38.58025	42.02169	-0.0208	0.6318	0.1223	0.6329	-0.4318	0.4184	-1.096	0.3547
1401	40.7457	31.6073	0.6248	0.5786	0.5204	0.7287	0.648	0.3042	0.4027	0.2493
1409	40.717	32.0636	0.261	0.5105	0.2166	0.4664	0.1584	0.3697	0.0364	0.1369
1410	40.7711	32.037	-0.578	0.6051	-0.5725	0.6052	-0.2887	0.2984	-0.2813	0.2303
1411	40.6846	31.6175	-0.4206	0.5702	-0.8062	0.5431	-0.8079	0.3211	-0.9549	0.2127
1502	37.7035	30.2208	-0.578	0.7234	-0.7158	0.7416	-1.3541	0.5876	-0.9412	0.5666
1505	37.3161	29.779	-0.4087	0.6371	-0.5771	0.6282	-0.177	0.5208	-0.0822	0.4244
1506	37.1472	29.5095	-0.5479	0.5605	-0.5384	0.6142	-0.3138	0.4798	-0.5844	0.4491
1507	37.4942	30.1336	-0.6429	0.6458	-0.8388	0.5603	0.2216	0.5745	0.6169	0.5248
1508	37.0363	29.8214	-0.8354	0.6062	-0.9898	0.603	-0.3675	0.5904	0.0763	0.3917
1606	40.363	29.1221	0.6741	0.4876	0.7936	0.5237	-0.0961	0.1064	-0.0078	0.2171
1607	40.3944	29.098	0.4314	0.335	0.4104	0.3778	1.2074	0.3405	1.4777	0.5294
1610	40.0671	29.5088	0.3398	0.3929	0.4936	0.3881	0.173	0.3639	0.1479	0.2819
1611	40.4292	29.7168	-0.0051	0.3637	-0.3051	0.3497	0.4812	0.2754	0.7517	0.5805
1613	39.9151	29.2317	0.5354	0.5346	0.513	0.5784	-0.0605	0.5061	-0.5162	0.3934
1614	40.0347	28.3939	0.5884	0.6779	0.4084	0.8842	-0.1907	0.6681	-0.0823	0.4403
1618	40.351	28.9282	0.2512	0.5195	0.0227	0.6246	-0.8843	0.583	-0.9226	0.3614

Station ID	Lat	Long	T=0.01s		T=0.2s		T=1s		T=2s	
			$\delta S2S_s$	$\varphi_{SS,s}$	$\delta S2S_s$	$\varphi_{SS,s}$	$\delta S2S_s$	$\varphi_{SS,s}$	$\delta S2S_s$	$\varphi_{SS,s}$
1619	40.4224	29.2907	0.2069	0.5093	0.1462	0.4179	0.534	0.3823	0.9988	0.4223
1620	40.1824	29.1296	-0.0818	0.4739	-0.0133	0.4185	0.2968	0.4305	0.3936	0.2869
1621	40.2269	28.9756	-0.0735	0.5325	-0.1035	0.5116	0.2881	0.32	0.5481	0.3376
1623	40.2654	29.0334	0.4124	0.6687	0.5211	0.632	0.7696	0.5594	0.7502	0.4437
1624	40.177	29.0567	0.1019	0.4065	0.2657	0.4631	0.1905	0.367	0.1288	0.3549
1626	40.2403	28.9824	0.2778	0.5217	0.204	0.4477	0.8128	0.1968	0.8443	0.3239
1627	40.2257	29.0752	0.2772	0.4284	0.0596	0.3631	0.6102	0.3142	0.7621	0.3997
1628	40.2734	29.0959	0.2893	0.4576	0.4332	0.4598	0.0505	0.3849	-0.2007	0.2396
1629	40.4254	29.1666	0.6034	0.4751	0.6265	0.5046	0.7427	0.466	0.195	0.3027
1630	40.363	29.1221	0.6533	0.6662	0.7381	0.6297	-0.0402	0.4443	0.0047	0.7843
1631	40.4865	29.3081	0.4253	0.4801	0.815	0.4128	-0.3987	0.468	-0.4229	0.4891
1633	40.2147	28.3632	0.1183	0.4881	0.1224	0.4467	0.1894	0.483	0.3579	0.5028
1634	39.7763	28.8821	0.3681	0.3257	-0.1217	0.3688	-0.5411	0.4727	-0.9505	0.5159
1635	40.4497	29.2587	0.3019	0.4248	0.0227	0.4802	-0.6809	0.4641	-0.2925	0.2328
1636	40.2171	29.1946	0.2797	0.3712	0.4192	0.4553	0.0876	0.4692	0.15	0.2534
1637	40.4763	29.0946	0.6971	0.3057	0.4755	0.3728	1.0646	0.2512	0.0967	0.2249
1638	40.3612	29.0333	0.3321	0.3623	0.484	0.3576	0.4806	0.3508	0.2849	0.3164
1639	40.3776	29.5418	0.441	0.3491	0.6665	0.3278	1.0046	0.4228	0.9471	0.4691
1640	39.9112	28.9868	0.0917	0.3986	0.2592	0.4678	-0.3689	0.4254	-0.6004	0.2503
1642	40.410343	29.179435	0.171	0.3867	0.3064	0.3834	0.0113	0.3693	0.1595	0.1609
1643	40.15546	29.05457	0.7866	0.4953	0.9815	0.478	0.8313	0.3011	0.4147	0.2644
1644	40.17834	29.10741	0.5003	0.3102	0.6807	0.4376	0.9225	0.2528	0.8982	0.2007
1645	40.17828	29.06555	0.5768	0.413	0.8334	0.4849	0.5345	0.3222	0.5717	0.2571
1646	40.209078	28.968037	0.0673	0.5187	-0.0297	0.5542	0.504	0.4522	0.6711	0.4777
1647	40.251462	28.964	0.1797	0.5142	0.2751	0.5387	0.391	0.3048	0.7688	0.3442
1648	40.255225	28.980285	-0.041	0.4539	-0.3036	0.3104	0.0933	0.2829	0.4261	0.2899
1649	40.265783	29.095913	0.1745	0.222	0.0005	0.3124	0.2398	0.3482	-0.2723	0.2301
1650	40.206197	29.05789	0.5353	0.4078	0.4197	0.3401	0.9798	0.2445	0.8649	0.148
1651	40.205487	29.089303	0.3247	0.7445	0.3196	0.6722	0.7735	0.2901	0.8442	0.3659
1652	40.188565	29.139033	-0.1567	0.5368	-0.2372	0.5171	0.2265	0.3846	0.3908	0.2618
1653	40.415365	29.098645	0.3713	0.2495	0.2071	0.3026	0.6445	0.214	0.5045	0.2317
1701	40.1415	26.3995	-0.067	0.6174	-0.0313	0.6185	0.1455	0.4216	-0.2015	0.3901
1703	40.2318	27.2629	-0.4699	0.6141	-0.6502	0.5336	0.0671	0.4805	0.28	0.5385
1704	39.7739	26.3456	0.099	0.6693	0.1721	0.7088	0.1848	0.4576	-0.0303	0.4415
1707	39.9292	27.2591	0.0896	0.4646	0.1578	0.4824	0.3526	0.4439	0.2999	0.391
1710	40.4233	26.6672	0.3605	0.6336	0.2962	0.6082	0.017	0.4819	0.168	0.3889
1711	40.1908	25.9078	0.1019	0.5806	0.3102	0.6028	-0.1549	0.6376	-0.2576	0.5068
1712	40.404	27.3035	0.6437	0.4865	1.1669	0.5373	-0.1526	0.5056	-0.081	0.5687
1713	40.1622	26.4117	0.0075	0.541	0.2189	0.6182	0.0505	0.465	0.2827	0.3997
1714	40.1129	26.4221	-0.1292	0.6823	-0.0234	0.7418	0.0655	0.52	0.2557	0.4308
1715	40.3632	26.6923	0.0917	0.5596	-0.1592	0.532	0.5477	0.4044	0.1157	0.3363
1716	39.5997	26.4076	0.7319	0.4582	0.7125	0.474	-0.2465	0.4328	-0.0114	0.4257
1717	40.1818	26.3578	-0.0802	0.5847	-0.0741	0.6869	0.0206	0.5163	-0.2562	0.4035
1718	39.8133	26.5862	-0.5619	0.6175	-0.5756	0.586	-0.1494	0.471	0.0035	0.3572
1719	40.0293	27.05	1.0549	0.4985	1.1506	0.5388	0.6793	0.4447	0.4031	0.399
1720	39.5288	26.1206	0.2941	0.5378	0.2888	0.6732	-0.0851	0.4637	0.1349	0.4231

Station ID	Lat	Long	T=0.01s		T=0.2s		T=1s		T=2s	
			$\delta S2S_s$	$\varphi_{SS,s}$	$\delta S2S_s$	$\varphi_{SS,s}$	$\delta S2S_s$	$\varphi_{SS,s}$	$\delta S2S_s$	$\varphi_{SS,s}$
1721	39.5435	26.1905	0.6294	0.5439	0.6326	0.5162	0.126	0.5248	-0.303	0.4574
1722	40.1974	25.9034	-0.0822	0.6123	-0.0464	0.7341	-0.5968	0.5736	-0.2854	0.5712
1724	39.51288	26.25777	-0.004	0.3528	0.0767	0.4321	-0.1462	0.4115	0.1256	0.3928
1802	40.6083	33.6104	-0.4768	0.4639	-0.537	0.5187	-0.1916	0.4226	-0.049	0.2475
1803	40.8149	32.8834	0.1563	0.7295	0.0933	0.5107	-0.1252	0.4325	-0.0621	0.1599
1804	40.6124	33.0822	-0.3517	0.4118	-0.3399	0.4609	0.0381	0.3638	0.1061	0.3188
1805	40.9311	33.6232	-0.0436	0.3605	0.0549	0.5175	0.0237	0.3847	0.1	0.2557
1806	40.601	33.6019	-0.049	0.4315	0.0839	0.4568	0.5016	0.3463	0.5132	0.4084
1807	40.8435	33.2585	-0.2514	0.5216	-0.3128	0.5449	0.5251	0.2854	0.681	0.1993
2002	37.8125	29.1111	-0.1086	0.3638	-0.2118	0.3713	0.2705	0.4215	0.5105	0.3393
2007	37.9325	28.9229	0.1903	0.2799	0.1757	0.3165	0.279	0.3268	0.2639	0.4251
2009	37.9134	29.038	-0.0898	0.4604	-0.2227	0.4852	-0.0371	0.4093	0.2285	0.2943
2011	37.7372	29.1006	-0.1792	0.6081	-0.015	0.6505	-0.1169	0.4257	-0.1363	0.3852
2012	37.7781	29.0843	0.1711	0.6761	0.1735	0.6451	0.2575	0.4489	0.465	0.3103
2013	38.0448	28.8336	-0.2536	0.5775	-0.3737	0.615	-0.1408	0.4304	-0.3629	0.3623
2014	37.0741	29.3464	-0.319	0.4291	-0.2206	0.485	0.0888	0.4083	-0.1845	0.3677
2015	37.9255	28.9288	0.2995	0.4996	0.228	0.5267	-0.1137	0.3443	0.2201	0.3742
2016	37.8044	29.24	0.1387	0.587	0.3179	0.6795	0.7595	0.4369	1.0397	0.3064
2017	37.4335	29.3502	0.3323	0.5006	0.1366	0.5696	0.0896	0.4358	0.0711	0.4533
2018	37.233	28.8948	-0.1564	0.4715	-0.3043	0.54	0.7799	0.3987	0.6924	0.3511
2019	37.442	28.8438	0.0431	0.3269	0.1394	0.3629	0.0914	0.4509	0.2606	0.3896
2020	37.5711	29.0694	0.1041	0.4785	0.4243	0.3885	-1.0818	0.3202	-0.919	0.2973
2024	38.0868	29.3954	-0.9843	0.5403	-0.8658	0.5677	-1.0666	0.3959	-1.0077	0.3365
2025	38.2957	29.7366	-0.0357	0.4885	-0.2154	0.6045	0.065	0.4802	0.3118	0.5408
2101	37.9309	40.2028	0.7507	0.6214	1.0114	0.6249	0.3602	0.417	0.6512	0.4188
2104	38.2644	39.759	-0.3204	0.4412	-0.2357	0.4787	0.3719	0.3099	0.3065	0.4805
2105	38.3581	40.0713	-0.7894	0.4626	-0.8643	0.5325	-0.4566	0.3734	-0.3171	0.451
2106	38.4616	40.647	-0.0286	0.5583	-0.0534	0.6039	-0.1514	0.4314	-0.2441	0.3863
2107	38.1459	39.4838	-0.2206	0.6841	-0.018	0.6717	-0.0997	0.5351	-0.023	0.3607
2201	40.7245	26.0873	0.1337	0.5254	0.1651	0.5615	0.3002	0.6473	0.3612	0.4681
2202	41.6705	26.5859	0.3744	0.6807	0.5183	0.7351	0.0446	0.6032	0.0028	0.4773
2203	40.8681	26.6319	0.0566	0.4412	0.1596	0.5389	0.0045	0.6818	0.0332	0.651
2204	41.2932	26.6899	0.5205	0.3111	0.3505	0.2519	-0.0768	0.4257	0.1355	0.3925
2301	38.6704	39.1927	0.0297	0.5286	-0.0798	0.606	0.3693	0.4569	0.3975	0.4548
2302	38.3923	39.6754	-0.3995	0.6787	-0.3056	0.7678	0.1905	0.4354	0.3195	0.464
2304	38.721	39.8629	-0.3341	0.7158	-0.2001	0.6984	-0.3969	0.3407	-0.2118	0.5136
2305	38.7278	40.131	-0.643	0.776	-0.4087	0.7402	-0.2185	0.4296	-0.2479	0.3703
2306	38.9595	40.0393	-0.3063	0.7062	-0.3715	0.8112	-0.0258	0.3805	-0.2581	0.4171
2307	38.6958	39.932	-0.7195	0.5603	-0.8865	0.6107	-0.2411	0.3423	-0.1786	0.3992
2308	38.4506	39.3102	0.0787	1.0011	0.0225	1.105	0.7279	0.7604	0.7901	0.5923
2309	38.7983	38.7273	0.8079	0.9155	0.2021	0.6053	-0.2663	0.4064	-0.3058	0.5144
2401	39.7418	39.5115	-0.5925	0.4225	-0.6422	0.5643	-0.5914	0.3707	-0.2923	0.3867
2404	39.9063	38.7706	-0.2228	0.351	-0.4152	0.3476	0.1067	0.4022	0.1116	0.4123
2407	39.7767	40.3911	-0.1849	0.7638	-0.1821	0.6815	-0.1403	0.5513	-0.1007	0.4687
2408	39.6019	39.0345	0.1781	0.3262	0.005	0.2944	0.4826	0.2761	0.0407	0.3399
2409	39.2808	38.4911	0.5922	0.4687	0.8765	0.5107	-0.013	0.3394	-0.0328	0.3357

Station ID	Lat	Long	T=0.01s		T=0.2s		T=1s		T=2s	
			$\delta S2S_s$	$\varphi_{SS,s}$	$\delta S2S_s$	$\varphi_{SS,s}$	$\delta S2S_s$	$\varphi_{SS,s}$	$\delta S2S_s$	$\varphi_{SS,s}$
2411	39.9702	40.0209	-0.5211	0.7456	-0.7271	0.752	-1.4191	0.6137	-1.3983	0.4838
2412	39.592	39.6922	-0.3528	0.6159	-0.5196	0.5375	-0.0215	0.43	-0.0233	0.4693
2413	39.8077	40.0386	0.3339	0.6006	0.2289	0.6718	0.0399	0.4754	0.1927	0.4403
2414	39.7951	39.4186	-0.0478	0.3904	-0.0053	0.4092	-0.3104	0.3386	-0.371	0.3534
2415	39.461	38.5549	-0.0064	0.3761	-0.0836	0.4499	-0.0484	0.3538	-0.382	0.2799
2501	39.9032	41.262	0.0726	0.2435	0.1703	0.2826	0.0409	0.2755	0.1975	0.3026
2508	39.9429	41.1102	-0.1258	0.4475	-0.1417	0.3651	-0.2762	0.3332	-0.0951	0.2201
2509	39.8733	41.2227	-0.3603	0.4855	-0.2664	0.4737	-0.1393	0.4412	0.0084	0.4224
2510	40.3483	41.8626	-0.0455	0.5245	-0.2273	0.5986	-0.3316	0.4351	-0.6422	0.2085
2511	39.9748	41.6723	0.2382	0.7501	-0.0094	0.798	-0.0554	0.1908	0.7974	0.424
2513	39.3624	41.706	0.0984	0.4431	0.2045	0.5613	-0.456	0.3023	-0.3484	0.3242
2516	39.6153	40.9756	0.2838	0.6539	0.0145	0.71	-0.4873	0.5165	-0.5281	0.3164
2518	39.9072	41.2774	-0.9146	0.9073	-0.775	0.9401	-0.8717	0.5435	-0.9753	0.4409
2521	39.64607	41.509117	0.1779	0.5358	0.5299	0.6138	-0.1017	0.2555	0.0677	0.3916
2522	39.700493	42.14172	-0.1697	0.32	-0.312	0.4299	0.2976	0.38	-0.4029	0.2467
2601	39.8137	30.5284	-0.1428	0.4675	-0.4478	0.4416	-0.3354	0.3696	0.1147	0.831
2602	39.7893	30.4973	-0.2764	0.1683	-0.4872	0.2939	0.069	0.2489	0.5983	0.4109
2604	39.7733	30.5101	0.0325	0.2341	0.1803	0.3362	0.2336	0.2142	-0.1546	0.3181
2606	39.7487	30.4958	0.2616	0.2672	0.6091	0.3528	-0.3688	0.3234	-0.2008	0.2629
2607	39.8175	30.146	-0.6582	0.3674	-0.6182	0.3985	-0.2609	0.1902	-0.0202	0.4459
2610	39.822	30.4216	-0.0559	0.2541	0.1404	0.3383	0.3265	0.3069	-0.2921	0.1998
2611	39.7883	30.443	-0.1609	0.1985	-0.099	0.3427	-0.1448	0.2156	0.2804	0.2496
2612	39.7713	30.4017	-0.4937	0.3989	-0.521	0.4496	-0.4878	0.3191	-0.7065	0.365
2613	39.7936	30.5397	-0.0531	0.3299	0.1396	0.3453	-0.3966	0.2603	-0.2296	0.3193
2615	39.7403	30.6521	0.0027	0.336	-0.0339	0.3236	0.3572	0.32	0.7776	0.2269
2616	39.7063	30.6189	-0.4769	0.2705	-0.3409	0.2614	-0.6525	0.3077	-0.3543	0.2425
2703	37.058	37.35	0.5458	0.5434	0.7012	0.6175	0.6534	0.3699	0.5905	0.3958
2704	37.0088	37.8022	0.76	0.5368	0.9114	0.5708	0.5892	0.3808	0.5209	0.3522
2705	37.0118	36.6206	0.5393	0.3557	0.6919	0.5253	0.179	0.5112	0.1157	0.2628
2707	36.9309	36.5738	0.1403	0.4399	0.032	0.5129	0.2056	0.7278	-0.125	0.5894
2708	37.0993	36.6484	0.8272	0.3543	0.8127	0.382	0.181	0.397	-0.0281	0.0863
2709	37.1285	36.6705	-0.1344	0.2159	-0.1194	0.3169	-0.1695	0.3914	-0.272	0.286
2710	37.43291	37.68658	0.7879	0.4048	0.6953	0.5043	-0.5918	0.3013	-0.8209	0.3121
2711	37.31736	37.56036	0.3786	0.5544	0.2847	0.477	-0.2994	0.3892	-0.2111	0.3676
2902	40.1244	39.4366	-0.2196	0.6138	-0.3324	0.7713	0.0782	0.5164	-0.0905	0.6317
2903	40.2084	39.6586	-0.334	0.612	-0.5943	0.7072	0.0923	0.4499	-0.0342	0.3027
2904	40.1908	39.1185	-0.4196	0.5874	-0.6449	0.5676	-0.0684	0.3478	0.0765	0.3817
3112	36.588	36.1477	-0.7836	0.6708	-1.1741	0.6213	-0.0193	0.362	-0.2088	0.2681
3113	36.5775	36.155	-0.3827	0.4187	-0.4479	0.4176	-0.375	0.4277	-0.0416	0.2917
3114	36.567	36.1514	-0.5157	0.4312	-0.5106	0.4006	0.0782	0.4096	-0.3356	0.3476
3115	36.5463	36.1646	-0.1518	0.3934	0.0382	0.3199	0.1301	0.3437	-0.1298	0.3556
3118	36.5821	36.1849	0.6054	0.3927	0.6652	0.4095	-0.1609	0.3834	-0.4279	0.399
3119	36.5753	36.1681	-0.1948	0.4091	-0.2578	0.4068	-0.7217	0.4458	-0.9935	0.2752
3120	36.5892	36.2057	0.4221	0.3783	0.5152	0.3936	-0.4789	0.4029	-0.6204	0.3238
3121	36.6641	36.2183	0.3466	0.6197	0.1953	0.557	-0.7682	0.4683	-0.4149	0.6159
3123	36.2142	36.1597	-0.0311	0.5512	0.1124	0.4694	0.786	0.4495	0.574	0.4133

Station ID	Lat	Long	T=0.01s		T=0.2s		T=1s		T=2s	
			$\delta S2S_s$	$\varphi_{SS,s}$	$\delta S2S_s$	$\varphi_{SS,s}$	$\delta S2S_s$	$\varphi_{SS,s}$	$\delta S2S_s$	$\varphi_{SS,s}$
3125	36.2381	36.1326	0.1819	0.3338	0.309	0.399	0.5139	0.5561	0.2975	0.5042
3126	36.2202	36.1375	0.6763	0.4374	0.5313	0.4128	0.5448	0.3913	0.5138	0.6037
3127	36.21	36.1353	0.6828	0.4348	0.9068	0.37	0.4935	0.4808	0.3397	0.4955
3130	36.1792	36.145	0.4538	0.2639	-0.1075	0.3199	0.2871	0.5402	0.0485	0.2368
3132	36.2067	36.1716	-0.2258	0.3577	-0.302	0.4503	0.2374	0.6159	-0.0955	0.4451
3133	36.2432	36.5736	-0.2786	0.2216	-0.282	0.3125	-0.2272	0.7184	-0.167	0.6274
3134	36.8276	36.2049	-0.2085	0.5357	-0.321	0.5396	-0.4194	0.2384	-0.5416	0.3518
3135	36.4089	35.8831	-0.1774	0.4969	-0.1633	0.4489	-0.1103	0.525	-0.0093	0.3896
3137	36.6929	36.4885	-0.2366	0.4669	0.1068	0.5337	0.2347	0.5566	0.3375	0.2475
3138	36.8026	36.5112	0.2589	0.4694	0.3092	0.4133	0.2041	0.6642	0.309	0.5677
3141	36.3726	36.2197	0.2352	0.3473	0.4126	0.3322	-0.0713	0.3588	-0.267	0.3815
3142	36.498	36.3661	-0.1699	0.2891	-0.2053	0.2848	-0.5077	0.3149	-0.4212	0.3359
3143	36.8489	36.5571	0.0455	0.4879	-0.0937	0.4535	0.1722	0.5315	-0.2638	0.6478
3145	36.6454	36.4064	0.1192	0.2729	-0.0419	0.3152	0.1836	0.4693	0.1517	0.2725
3201	38.1048	30.5576	-0.5053	0.6593	-0.295	0.7493	-0.7595	0.6355	-0.6034	0.4785
3205	37.9302	30.2961	0.2252	0.7647	0.1868	0.8299	0.0687	0.5971	0.0638	0.5485
3303	37.1659	34.6004	-0.2755	0.5541	-0.2937	0.6055	0.326	0.3505	-0.0633	0.3457
3405	40.9111	29.1567	0.2431	0.6857	0.1393	0.7095	-0.0432	0.513	-0.0732	0.3711
3407	41.0582	29.0095	0.1181	0.6155	0.1995	0.7318	-0.3408	0.677	-0.4761	0.3523
3408	41.0734	28.2557	-0.6604	0.5533	-0.6687	0.5373	-0.2288	0.6678	-0.031	0.4661
3410	41.1719	29.6082	0.9934	0.4463	0.9959	0.5586	0.4556	0.436	0.838	0.6584
3411	41.0119	28.9761	0.1474	0.8137	0.0543	0.843	-1.0039	0.7085	-1.1261	0.5263
3412	41.0206	28.5782	-0.0068	0.7429	-0.2848	0.9194	-0.1463	0.7426	-0.3312	0.6443
3413	41.0943	28.9482	-0.0546	0.6134	-0.0439	0.7479	-0.8201	0.5677	-0.7787	0.3454
3415	41.0273	28.7585	0.9009	0.7106	0.849	0.9621	0.002	0.7016	-	-
3416	40.9747	28.8364	-0.4367	0.586	-0.3165	0.6535	-0.0782	0.6775	0.2561	0.52
3417	40.9547	29.2563	0.11	0.4115	0.1812	0.3489	0.0138	0.5207	-0.1193	0.64
3419	41.061	29.358	0.7659	0.4682	0.6867	0.4478	-0.3353	0.4384	-0.8902	0.3322
3502	38.4551	27.2267	0.0084	0.383	-0.1351	0.3584	-0.0613	0.3751	-0.2218	0.3382
3503	39.0739	26.8883	0.0186	0.5148	0.2253	0.5013	0.157	0.5273	-0.4173	0.4442
3506	38.3944	27.0821	-0.2841	0.3703	-0.0952	0.465	-0.0457	0.3898	-0.1181	0.3227
3508	39.0883	27.3747	-0.0056	0.3899	0.2921	0.3853	-0.0468	0.4565	-0.022	0.4348
3509	38.2157	27.9645	0.1391	0.458	0.0719	0.552	0.2066	0.387	0.7068	0.3262
3510	38.409	27.043	0.0896	0.5458	0.3065	0.5943	-0.225	0.4559	-0.3275	0.3609
3511	38.4213	27.2563	-0.2094	0.3455	-0.0389	0.4097	0.1672	0.3808	0.1056	0.3888
3512	38.4009	27.1516	0.1042	0.4201	-0.1801	0.4443	-0.2753	0.3716	-0.5694	0.3142
3513	38.4584	27.1671	-0.3292	0.5257	-0.5284	0.4522	-0.0757	0.4668	-0.0903	0.4569
3514	38.4762	27.1581	-0.085	0.3547	0.0146	0.363	0.2504	0.3869	0.4048	0.3481
3515	38.4649	27.094	-0.6469	0.4147	-1.0004	0.4059	-0.5351	0.4128	-0.6979	0.3988
3516	38.3706	26.8907	-0.0934	0.4109	0.0364	0.4614	0.0533	0.4326	-0.1999	0.3466
3517	38.3756	27.1936	-0.6505	0.4096	-0.7389	0.4892	0.2832	0.3137	0.4199	0.2381
3518	38.4312	27.1435	-0.0884	0.3636	-0.1722	0.3975	0.1376	0.3848	0.2917	0.3187
3519	38.4525	27.1112	-0.2485	0.3731	-0.3524	0.4298	-0.3654	0.374	-0.1891	0.3884
3520	38.478	27.2111	-0.1626	0.356	-0.0633	0.4088	0.4744	0.3603	0.5518	0.3364
3521	38.4679	27.0764	-0.2193	0.4536	-0.4297	0.4286	0.1049	0.3746	-0.0574	0.3518
3522	38.4357	27.1987	-0.2424	0.3149	-0.3431	0.3634	-0.0361	0.326	-0.2238	0.3054

Station ID	Lat	Long	T=0.01s		T=0.2s		T=1s		T=2s	
			$\delta S2S_s$	$\varphi_{SS,s}$	$\delta S2S_s$	$\varphi_{SS,s}$	$\delta S2S_s$	$\varphi_{SS,s}$	$\delta S2S_s$	$\varphi_{SS,s}$
3523	38.3282	26.7706	-0.0803	0.3943	-0.1212	0.4071	-0.0859	0.4117	0.1723	0.326
3524	38.4969	27.1073	-0.0211	0.3929	0.0711	0.4282	-0.384	0.3643	-0.3911	0.421
3525	38.3723	27.1084	0.1786	0.4274	0.256	0.5036	0.1757	0.4409	0.0303	0.3804
3526	38.5782	26.9795	-0.0124	0.5033	0.0194	0.6574	0.0776	0.4866	0.2288	0.4268
3527	38.639	26.5128	-0.7664	0.4837	-0.9695	0.538	-0.5351	0.4627	-0.6562	0.4773
3528	38.3039	26.3726	0.0946	0.4216	0.1634	0.4912	0.1637	0.4555	0.1258	0.3619
3529	37.9443	27.3675	0.59	0.4493	0.5326	0.508	-0.1841	0.3039	-0.7052	0.3459
3530	38.453	27.2244	-0.1949	0.4316	-0.2867	0.4018	0.1752	0.3839	-0.1891	0.2906
3531	38.2193	27.6457	-0.147	0.4549	-0.2628	0.4812	-1.1386	0.528	-1.202	0.404
3532	38.1591	27.3596	0.1765	0.4219	0.0965	0.4414	0.4728	0.4675	0.2712	0.3372
3533	38.2572	27.1302	-0.1655	0.4364	-0.1687	0.4853	0.1396	0.4426	0.2291	0.2954
3534	38.6624	26.7586	0.4518	0.5049	0.6448	0.5036	-0.444	0.4444	-0.6181	0.4048
3535	38.7963	26.9632	-0.5538	0.4723	-0.5646	0.5027	-0.1276	0.425	-0.0534	0.4104
3536	38.1968	26.8384	0.1037	0.4658	0.1688	0.4979	0.8458	0.5042	0.6125	0.3781
3537	39.1096	27.1706	-0.7038	0.4394	-0.6945	0.4596	-0.2082	0.5027	0.1646	0.3991
3538	38.3187	27.1234	0.0195	0.4155	0.0149	0.4879	0.5244	0.3706	0.2843	0.3708
3539	38.1023	27.7211	0.1734	0.5248	-0.2109	0.4346	-0.7999	0.371	-0.9105	0.2988
3701	41.0132	34.0367	0.2029	0.5464	0.2608	0.5777	-0.0886	0.3145	-0.0723	0.1935
3702	41.4164	33.7969	-0.4253	0.3034	-0.4096	0.2784	0.0743	0.2906	-0.0332	0.2316
3703	41.2456	33.3284	-0.3714	0.3417	-0.1986	0.4982	-0.7021	0.2285	-0.7958	0.1474
3802	38.4781	36.5036	0.3089	0.3536	0.033	0.3705	0.7742	0.2901	1.0951	0.3788
3901	41.7377	27.2151	0.0135	0.4503	0.0189	0.3804	-0.0139	0.5781	-0.3976	0.6468
3902	41.3571	27.3248	-0.2823	0.6361	-0.3283	0.6046	-0.0326	0.6004	0.0544	0.4865
4104	40.6804	29.97	-0.5394	0.3342	-0.4114	0.4211	-0.3762	0.3987	-0.4906	0.439
4105	40.6744	29.9694	0.2121	0.4009	0.2134	0.3573	-0.4899	0.4138	-1.077	0.3289
4106	40.7863	29.45	-0.2652	0.6885	-0.0698	0.7469	-0.1689	0.4442	-0.0741	0.5844
4107	40.7602	29.9324	-0.2433	0.6274	-0.4591	0.4874	0.7842	0.3978	0.6145	0.3794
4108	40.7602	29.9329	1.0226	0.4744	0.9113	0.384	1.8061	0.2981	1.4739	0.3487
4111	40.6844	29.5888	-0.0082	0.5305	0.019	0.4115	0.0229	0.3348	-0.2502	0.3263
4112	40.7245	29.84	0.2997	0.5333	0.3588	0.4733	0.8633	0.4209	1.3106	0.4525
4113	40.7768	29.7335	-0.6465	0.6378	-0.5354	0.6576	-1.3378	0.3062	-1.2356	0.286
4115	40.7433	29.7802	-0.5012	0.3702	-0.5988	0.2879	-0.3732	0.38	-0.0967	0.3596
4116	40.7196	29.8658	0.0619	0.4289	-0.1899	0.3678	0.1389	0.496	0.3011	0.4885
4117	40.6989	30.0267	-0.1086	0.3927	-0.1075	0.4304	-0.0074	0.3925	-0.3051	0.4222
4118	40.7216	30.0781	0.4119	0.4697	0.3537	0.4367	0.4489	0.4726	0.3187	0.6133
4120	40.7676	30.0274	0.0237	0.405	0.1518	0.3529	0.172	0.5131	-0.4515	0.4918
4121	40.7228	29.9699	0.2057	0.433	0.2441	0.4101	0.3807	0.4657	0.4154	0.467
4122	40.7483	30.0263	-0.2326	0.4365	-0.3857	0.326	0.4918	0.477	0.5915	0.4992
4126	40.7625	29.9149	0.2043	0.5487	0.2028	0.5762	-0.441	0.583	-0.9266	0.5179
4301	39.4278	29.9916	0.4241	0.2981	0.6007	0.4989	0.2426	0.2895	0.3323	0.3447
4304	38.9948	29.4004	0.0894	0.396	-0.028	0.4893	-0.1771	0.5269	0.1328	0.505
4305	39.0928	28.9785	0.4151	0.5358	0.3315	0.5708	0.8175	0.609	0.4512	0.7623
4306	39.3361	29.2491	-0.1812	0.6399	-0.196	0.5946	0.5208	0.6347	0.0576	0.4233
4307	39.4053	30.0143	-0.0259	0.5258	-0.0716	0.4437	0.1078	0.5542	0.3878	0.5832
4309	39.0928	28.9785	-0.0244	0.5923	-0.0959	0.6638	-0.052	0.5075	-0.495	0.4286
4310	39.5384	29.4939	0.0397	0.6175	-0.1673	0.4655	0.385	0.4938	0.4799	0.4937

Station ID	Lat	Long	T=0.01s		T=0.2s		T=1s		T=2s	
			$\delta S2S_s$	$\varphi_{SS,s}$	$\delta S2S_s$	$\varphi_{SS,s}$	$\delta S2S_s$	$\varphi_{SS,s}$	$\delta S2S_s$	$\varphi_{SS,s}$
4311	38.8524	29.9812	-0.0779	0.3825	-0.1894	0.4379	-0.1042	0.3225	-0.2653	0.2787
4312	39.0578	30.1065	-0.3293	0.3924	-0.1461	0.3381	-1.5529	0.3871	-1.0201	0.3933
4313	39.196	29.62	0.2157	0.2649	0.1733	0.2691	0.2531	0.3302	0.1037	0.2874
4314	39.8063	29.6174	0.2803	0.331	0.1451	0.3727	0.2567	0.2526	0.3065	0.2512
4401	38.3489	38.335	-0.0539	0.5305	0.0535	0.5573	-0.0986	0.553	-0.3235	0.5119
4404	38.1959	38.8739	-0.2298	0.6537	0.0469	0.7012	0.4345	0.6069	0.4044	0.502
4405	38.8107	37.9396	-0.2191	0.5304	-0.155	0.5211	-0.5876	0.4045	-0.641	0.3924
4406	38.3439	37.9738	0.2719	0.494	0.221	0.4767	0.0332	0.4165	-0.0767	0.3555
4407	38.7807	38.2641	0.0797	0.589	0.0525	0.5134	0.6617	0.2923	0.716	0.3116
4408	38.0962	37.8873	-0.6822	0.4199	-0.5006	0.4375	-0.4258	0.3963	-0.5925	0.2943
4409	38.56063	37.49076	-0.8342	0.3325	-0.7283	0.344	-0.966	0.3242	-1.0068	0.3801
4410	38.86677	37.679	-0.1924	0.3394	-0.1946	0.4386	-0.265	0.298	-0.5994	0.3327
4411	39.049298	38.503368	-0.4561	0.461	-0.5436	0.6411	-0.3703	0.3179	-0.5906	0.2994
4412	38.59685	38.18385	-0.7725	0.4729	-0.6365	0.5396	-0.1944	0.463	0.0442	0.4315
4501	38.6126	27.3814	-0.7329	0.5363	-0.6227	0.4959	-0.1377	0.4607	-0.0201	0.4544
4502	38.9112	27.8233	-0.4918	0.4843	-0.6407	0.4427	0.101	0.4742	0.4076	0.4912
4503	38.3555	28.5143	-0.7555	0.4563	-0.8366	0.4446	-0.146	0.4422	-0.0252	0.4446
4504	39.035	28.6481	0.5758	0.4741	0.551	0.4776	0.4054	0.5539	0.3225	0.4344
4505	38.9398	28.2836	0.2046	0.4779	0.2259	0.5187	0.6651	0.4318	0.6294	0.4605
4506	38.4831	28.1235	-0.0682	0.5779	-0.2153	0.6987	-0.0295	0.4941	0.141	0.4562
4507	38.5075	27.7061	0.0067	0.5138	-0.254	0.583	-0.3804	0.3499	0.0449	0.3921
4508	38.7322	27.5574	-0.1534	0.5975	-0.0949	0.62	-0.089	0.4366	-0.0233	0.3551
4509	38.7075	27.9199	-0.3458	0.508	-0.6064	0.6239	-0.461	0.5158	-0.4846	0.4424
4510	38.5461	28.6431	0.2218	0.408	0.1952	0.4592	-0.5311	0.5862	-1.1161	0.4982
4511	38.24	28.6912	-0.3101	0.5884	-0.4068	0.5592	-0.1049	0.5194	0.1789	0.4606
4512	38.7422	28.8652	-0.4167	0.3902	-0.4702	0.3524	-0.2198	0.3733	-0.1277	0.4154
4513	39.1892	27.6171	-0.2884	0.5417	-0.1612	0.6043	0.1567	0.4637	0.2968	0.4788
4610	38.2037	37.1977	0.3053	0.606	0.1538	0.4719	0.6242	0.4925	0.8726	0.5538
4611	37.7472	37.2843	0.4597	0.6868	0.2144	0.4301	0.6288	0.4858	0.4897	0.4938
4612	38.024	36.4819	0.3126	0.4677	0.2838	0.4757	0.5968	0.4705	-0.4081	0.5123
4613	37.5646	36.3576	-0.1209	0.4891	-0.2239	0.544	-0.5515	0.3525	-0.4714	0.3459
4614	37.4804	37.2898	0.8563	0.4995	0.6983	0.6695	0.277	0.5324	0.3482	0.514
4615	37.3868	37.138	0.0021	0.6339	0.1287	0.6097	-0.1224	0.3777	-0.0072	0.3854
4616	37.3755	36.8384	-0.0666	0.3876	0.0736	0.401	-0.7556	0.4552	-0.8028	0.3511
4617	37.5855	36.8303	-0.3662	0.4979	-0.2316	0.369	0.25	0.3747	0.4714	0.3801
4618	37.6001	36.8723	-0.0264	0.4516	0.0247	0.3548	0.1708	0.3869	0.086	0.2914
4619	37.587	36.8662	-0.0715	0.3977	0.053	0.4048	-0.0206	0.2882	0.0869	0.3241
4620	37.5857	36.8985	0.0625	0.3449	0.0911	0.4344	-0.3275	0.281	0.1306	0.3106
4621	37.5935	36.9291	0.3469	0.4514	0.1637	0.5123	0.4887	0.3902	0.94	0.4693
4622	37.5843	36.9776	0.0238	0.4849	-0.2235	0.4855	0.5994	0.3062	0.5122	0.3438
4623	37.5692	36.934	0.0969	0.4812	0.102	0.4775	0.6793	0.3138	0.6972	0.356
4624	37.5361	36.9177	0.2011	0.4515	0.233	0.4012	0.1599	0.2543	-0.0926	0.3194
4625	37.5387	36.9819	0.1495	0.3675	0.0974	0.326	0.3	0.4088	0.0206	0.4001
4626	37.5753	36.9151	0.265	0.3917	0.0874	0.2901	0.7081	0.2696	0.5584	0.2988
4628	38.2412	36.9228	0.0333	0.7284	-0.0996	0.3826	-1.1121	0.393	-1.5021	0.2749
4629	37.2874	36.7887	-0.0747	0.2715	-0.0046	0.2206	-0.5626	0.2827	-0.8116	0.1864

Station ID	Lat	Long	T=0.01s		T=0.2s		T=1s		T=2s	
			$\delta S2S_s$	$\varphi_{SS,s}$	$\delta S2S_s$	$\varphi_{SS,s}$	$\delta S2S_s$	$\varphi_{SS,s}$	$\delta S2S_s$	$\varphi_{SS,s}$
4630	37.3449	36.806	-0.1433	0.2812	-0.2072	0.3685	-1.0571	0.3655	-0.9571	0.1407
4631	37.9663	37.4277	0.132	0.4107	0.3362	0.4059	-0.2231	0.4259	-0.4244	0.4897
4632	37.256	36.7737	0.1318	0.4307	0.0593	0.2698	0.7245	0.4247	-0.1807	0.2011
4701	37.3263	40.7237	0.9226	0.4897	1.1598	0.4835	0.2022	0.3015	0.1113	0.4329
4801	37.2145	28.3561	-0.0334	0.4012	0.2338	0.453	-0.0789	0.3488	-0.3146	0.3774
4803	36.6264	29.124	0.423	0.5233	0.2528	0.5061	0.7628	0.5128	-0.4036	0.4904
4806	37.3025	27.7805	-0.0978	0.3167	-0.1619	0.3769	-0.3673	0.3864	-0.4172	0.286
4807	37.3397	28.1369	-0.0393	0.4125	-0.0369	0.414	-0.3272	0.369	-0.1147	0.3317
4808	37.1392	28.2873	0.4284	0.5471	0.4947	0.5238	0.3501	0.4023	0.3446	0.3954
4809	37.033	27.44	-0.1354	0.6818	-0.0058	0.6906	-0.0638	0.5551	-0.1636	0.5009
4810	36.8394	28.2448	-0.2239	0.4153	-0.0688	0.4755	-0.9158	0.4321	-0.8273	0.4122
4811	36.9697	28.6868	0.0883	0.5797	0.2212	0.5799	-0.2496	0.4131	-0.5385	0.3672
4812	36.7123	27.688	-0.6565	0.4932	-0.3709	0.5134	-0.7177	0.4798	-0.4663	0.4254
4814	37.3991	27.6567	-0.1931	0.5164	-0.4568	0.4449	-0.5765	0.3502	-0.4026	0.3116
4815	36.6886	28.046	-0.4786	0.5839	-0.7171	0.5642	-1.7194	0.4522	-1.616	0.511
4816	36.7718	28.7986	-0.1582	0.5051	-0.2718	0.5	0.0188	0.4184	-0.2893	0.4655
4817	37.2401	27.6031	0.2255	0.6991	0.3259	0.6971	0.0368	0.406	0.1809	0.421
4818	37.444	28.3575	0.1025	0.4244	0.4266	0.462	0.0751	0.336	0.1176	0.3506
4819	37.0313	27.9712	0.1377	0.4466	0.0261	0.5068	-0.0563	0.4112	-0.2323	0.4386
4820	36.6485	29.3543	-0.1643	0.7413	0.2608	0.6431	-0.3121	0.7083	-0.1065	0.5385
4821	37.1055	28.4139	0.261	0.5757	0.1642	0.5489	0.7978	0.5895	0.1211	0.3867
4822	37.4417	27.646	0.9817	0.4096	0.9946	0.4572	0.0271	0.425	-0.1723	0.417
4823	37.4418	27.644	0.1298	0.6726	0.1584	0.5651	-0.6956	0.3494	-0.6572	0.3787
4901	38.7611	41.5039	0.0481	0.5265	0.0539	0.506	-0.1928	0.4101	-0.3612	0.4275
4904	38.7356	41.7742	0.0555	0.4441	-0.1355	0.5194	0.3044	0.349	0.3553	0.3614
4905	39.1764	41.4455	0.1715	0.5612	0.1668	0.6236	1.0222	0.4836	1.0165	0.5222
4906	39.1439	42.5308	0.109	0.3295	-0.0251	0.4495	-0.1071	0.2131	0.2957	0.405
5401	40.7362	30.3808	-0.159	0.7566	-0.2364	0.4846	-0.4995	0.578	-0.5875	0.585
5403	40.6908	30.27	-0.0635	0.4707	0.0257	0.4639	0.04	0.4121	-0.0463	0.4496
5404	40.5191	30.2932	0.1685	0.5004	0.1471	0.5315	0.6074	0.4426	0.8298	0.6223
5405	40.7961	30.7352	-0.3421	0.6857	-0.4451	0.7201	0.2208	0.3944	0.5613	0.3145
5601	37.912	41.931	-0.1822	0.6411	-0.2912	0.6381	-0.0638	0.3434	0.0428	0.3019
5802	39.8928	37.7479	-0.165	0.3999	-0.1408	0.3045	-0.6623	0.3789	-0.5192	0.2748
5807	38.7245	37.2896	-0.1893	0.5507	-0.2986	0.6199	-0.3186	0.3873	-0.2073	0.2602
5809	39.2308	37.3824	0.2907	0.4135	0.4517	0.4333	-0.135	0.3732	0.1755	0.3754
5810	39.3704	38.1179	1.0435	0.6037	0.7156	0.5666	-0.622	0.4396	-0.0801	0.6426
5812	40.088	38.3457	-0.2277	0.4688	-0.5404	0.3487	-0.2119	0.2405	0.2755	0.3805
5814	40.0618	38.6036	-0.5043	0.3791	-0.495	0.4738	-0.26	0.2541	0.0135	0.3039
5816	39.86868	38.11835	0.3516	0.2559	0.3025	0.4479	-0.1087	0.3214	-0.2979	0.2455
5904	40.6149	27.1226	0.6017	0.5383	0.5147	0.6177	0.4906	0.4742	0.2357	0.462
5906	40.9734	27.9316	-0.0794	0.6991	-0.2919	0.6398	-0.6968	0.562	-1.1567	0.5302
5907	41.1607	27.7918	-0.6255	0.799	-0.5945	0.8008	-0.1106	0.6873	0.093	0.5601
5908	40.9821	27.5479	-0.076	0.7958	-0.1492	0.7864	0.1396	0.8009	0.1685	0.624
5910	40.9811	27.4861	0.9019	0.6064	0.7207	0.6991	0.2726	0.7015	0.5999	0.7902
5914	40.66825	27.24526	0.3984	0.6109	0.4638	0.5521	0.5037	0.6479	0.4551	0.6585
6201	39.0747	39.5347	-0.1188	0.7069	0.1313	0.7896	-0.0889	0.364	-0.4056	0.2685

Station ID	Lat	Long	T=0.01s		T=0.2s		T=1s		T=2s	
			$\delta S2S_s$	$\varphi_{SS,s}$	$\delta S2S_s$	$\varphi_{SS,s}$	$\delta S2S_s$	$\varphi_{SS,s}$	$\delta S2S_s$	$\varphi_{SS,s}$
6202	39.486	39.8998	0.3158	0.5895	0.387	0.7451	0.6312	0.5044	0.4638	0.6447
6302	37.2342	39.7509	1.1857	0.4272	1.4417	0.3681	0.8663	0.4921	1.0846	0.457
6304	37.3651	38.5132	0.8487	0.5923	0.9775	0.6694	-0.2207	0.4832	-0.375	0.4269
6401	38.6726	29.404	-0.1844	0.4742	-0.2024	0.4897	-0.237	0.4837	-0.3259	0.4745
6402	38.4076	28.9766	-0.3016	0.6466	-0.2242	0.6258	-0.0993	0.5313	-0.6293	0.448
6403	38.7361	29.7568	0.0235	0.5443	-0.0698	0.527	-0.126	0.4109	-0.0841	0.5246
6501	38.5035	43.4018	-0.0285	0.3799	0.1025	0.3867	0.0781	0.3653	0.2115	0.5056
6505	39.135	43.9011	0.2038	0.8719	0.0569	0.9117	-0.7856	0.5103	-0.536	0.5364
6506	39.0196	43.338	0.4679	0.5792	0.6007	0.668	0.3268	0.5016	0.5099	0.4173
6507	38.2963	43.1198	-0.3324	0.5913	-0.2114	0.5799	-0.3138	0.5145	-0.7133	0.4169
6508	38.6573	43.9767	0.0461	0.6579	-0.1622	0.7645	0.8049	0.4891	0.7786	0.4373
6512	38.99	43.763	0.0314	0.3391	0.0048	0.439	-0.0839	0.278	-0.3085	0.3605
6513	38.4145	43.2682	-0.6086	0.4055	-0.6729	0.3988	0.2537	0.3605	0.2317	0.474
6901	40.2623	40.2101	-0.8357	0.7446	-0.9682	0.8617	-0.6908	0.4626	-0.7259	0.2481
7101	39.8497	33.518	0.2239	0.6088	0.1088	0.6373	0.0007	0.527	0.3873	0.4046
7103	39.9403	34.0327	0.3154	0.2606	0.3914	0.4075	0.0837	0.2137	-0.0405	0.2783
7301	37.523	42.4534	0.4178	0.3787	0.6365	0.4146	0.8505	0.4786	0.6966	0.3732
7706	40.5131	28.8266	0.2279	0.468	0.5153	0.448	-0.1538	0.4374	-0.6113	0.4386
7707	40.6381	29.0788	-0.1003	0.5286	-0.0814	0.5681	0.2482	0.4522	-0.1764	0.3929
7708	40.6576	29.2473	-0.1798	0.3353	-0.3078	0.3715	-0.1219	0.3436	-0.1895	0.4068
7709	40.5593	29.3259	0.1003	0.572	0.3326	0.4457	0.5549	0.4466	0.3492	0.2049
7710	40.59	29.2668	0.0442	0.3375	-0.0604	0.3408	-0.3706	0.4808	-0.4741	0.2444
7711	40.6594	29.3271	-0.22	0.563	-0.4664	0.5531	-0.0249	0.4468	-0.1956	0.2305
7714	40.52275	28.88833	-0.1299	0.3376	-0.4093	0.3325	-0.9632	0.4054	-0.8613	0.368
7715	40.46296	28.97072	1.3593	0.4539	1.3646	0.3294	1.8142	0.2333	1.0781	0.2032
7802	40.9563	32.5322	0.046	0.4215	0.2761	0.4155	-0.3278	0.3479	-0.4352	0.2649
7901	36.7088	37.1123	0.9624	0.4842	0.7286	0.5761	0.0115	0.5904	0.0394	1.0936
8002	37.1916	36.562	-0.2371	0.539	-0.3799	0.6073	-0.3183	0.4261	-0.6396	0.4924
8003	37.0842	36.2694	-0.6607	0.569	-0.6367	0.5351	0.1138	0.3164	0.2192	0.4965
8004	37.3799	36.0976	0.2154	0.6356	0.2721	0.6585	0.2811	0.5766	0.381	0.5718
8105	40.9028	31.152	0.7842	0.7997	0.7603	0.7641	0.4515	0.4573	0.2816	0.3573
8108	40.8613	31.23	-0.2565	0.3204	-0.1858	0.5369	-0.3428	0.3204	-0.2042	0.2854
8109	40.781	31.0144	0.2225	0.6304	-0.062	0.5454	0.4318	0.3991	0.405	0.3822